University of Stavanger

Faculty of Science and Technology

MASTER'S THESIS

Study program/ Specialization: **Offshore Technology, Subsea Technology**	**Spring semester, 2012** ~~Open~~ / **Restricted access**
Writer: **Tomy Nurwanto**	…… (Writer's signature)
Faculty supervisor: **Dr. Daniel Karunakaran, Ph.D (University of Stavanger)** External supervisor(s): **Dr. Daniel Karunakaran, Ph.D (Subsea 7 Norway)**	
Title of thesis: **COBRA Riser Concept for Ultra Deepwater Condition**	
Credits (ECTS): **30**	
Key words: COBRA, Uncoupled Riser, Ultra Deepwater, Santos Basin Central Cluster, Bidirectional Current, Strength Design, Fatigue Design	Pages: xvii +105 + enclosure: 74 Stavanger, 9th June 2012 Date/year

Frontpage for master thesis
Faculty of Science and Technology
Decision made by the Dean October 30th 2009

Abstract

Offshore ultra deepwater field is being promising as the future of oil and gas reserves. The advancement of technology in ultra deepwater has been leading Brazil into one of the promising offshore market. A Brazilian state-owned oil operator, Petrobras, confirms that 33% from their total exploration area are located at water depth below 1500 m (Salies, 2005). It can be seen that the future of oil and gas exploration and production lies in ultra deepwater.

The development of ultra deepwater field posed many challenges, in particular, on the selection of the riser concept. For ultra deepwater environment, the long suspended length of riser will significantly increase the vessel payload. High external hydrostatic pressure on the riser will increase the probability of collapse failure. Large dynamic motions of the vessel due to waves, and also large vessel offsets from wind, current and slow-drift motion yields potential buckling issues at the touch-down-point (TDP). In addition, potential fatigue problems due to vessel motions and soil-riser interactions also present at touch-down-point (TDP) area. Large current speed in deepwater field might also lead to vortex induced vibration (VIV) which eventually will contribute to significant fatigue damage for particular riser sections. By looking into these challenges, it is very important to select the most appropriate riser concept for the ultra deepwater field.

Catenary Offset Buoyant Riser Assembly (COBRA) as newly developed hybrid riser concept offers a solution to overcome the challenges in ultra deepwater field. In general, COBRA riser arrangement consists of a catenary riser section with a long-slender sub-surface buoyancy module on top which is tethered down to sea bed via two mooring lines. The catenary section from top of the sub-surface buoy is connected to the floater by a flexible jumper. This flexible jumper can effectively absorb the floater motions, which give significant improvements for both strength and fatigue performance on the overall system. As a hybrid riser concept, this concept offers cost effective solution by avoiding all the expensive bottom assemblies that normally needed for a hybrid riser concept.

This thesis focuses on COBRA riser concept for offshore Brazil ultra deepwater environment, specifically for Santos Basin Central Cluster region at 2200 m water depth. It is observed that there is common sudden change phenomenon on the current direction in Santos Basin area. In this thesis, the effect of bidirectional (2-directions) current is analyzed, and the comparison with unidirectional current is discussed thoroughly. The analyses are focused on the global strength design performance under extreme environmental load and global fatigue design performance of the riser due to wave induced and VIV induced.

This thesis captures detail analysis of COBRA base case configuration. In addition, further sensitivity studies from the base case riser arrangement are also presented. The parameter on sensitivity studies are determined based on possible alternative riser arrangements, i.e. locating the sub-surface buoyancy in deeper area, connecting the flexible jumper through the bottom section of the sub-surface buoyancy, and also alternative buoyancy tethers configurations on the seabed.

Based on detailed strength and fatigue analyses result, this thesis concludes that COBRA riser concept has a robust design and it is feasible for 2200 m water depth, in particular for

Santos Basin Cluster Region area. It is also shows COBRA riser concept has sufficient strength performance even for extreme bidirectional (2-directions) current.

Keywords: COBRA, Uncoupled Riser, Ultra Deepwater, Santos Basin Central Cluster, Bidirectional Current, Strength Design, Fatigue Design

Acknowledgment

This thesis work is part of the requirement to complete my Master of Science degree in Marine and Subsea Technology, Faculty of Science and Technology, University of Stavanger. The writing process is carried out with Subsea 7 Norway since January 2012 and was completed in early June 2012.

First of all, I would like to express my sincere gratitude to my supervisor, Dr. Daniel Karunakaran, Ph.D for giving me an opportunity to do my thesis work on ultra deepwater riser topic. For all of discussions, essential input, and his time to read and review my thesis, I would like to say many thanks. This is a new path for my career and it is an honor to work with him.

I would also thank to Subsea 7 colleagues who help me a lot during the writing process of this thesis. Special thanks to Heidi, Adedayo, Airindy and Iswan for the discussions. I would also thank to my colleagues in structural department for giving me an opportunity to work part-time while I'm doing my master study. My best gratitude goes to Haavard Haaskjold and Anton Skaar Stornes.

My best wishes to all of my friends from Indonesia: Sanggi, Sakti, Surya, Yahya, Hermanto, Whida, and Dani. Every great journey starts with a small step, and this is just another beginning of our journey in life.

I would also like to thank to my wife Astrid Kurniasari, and my cute daughter Athalya Aqeela Nurwanto, who always be patience on waiting for me to go back home. Their supports, love and prayers are my energy to finish this study. Good things happen in good time. Keep dreaming, don't stop believing, and do the actions.

Lastly, for both of my parents, Ikung, Tiyah, Atuk, Nenek, and all of my families in Indonesia, I would say my sincerely thank for all supports and prayers. Let's build our nation for better future.

Stavanger, 9th June 2012

Tomy Nurwanto

Nomenclature

Greek Characters

α_c	Parameter accounting for strain hardening and wall thinning
α_{fab}	Fabrication factor
γ_A	Load effect factor for accidental loads (vector or scalar)
γ_c	Resistance factor to account for special conditions
γ_E	Load effect factor for environmental load (vector or scalar)
γ_F	Load effect factor for functional loads (vector or scalar)
γ_m	Resistance factor to account for material and resistance uncertainties
γ_{SC}	Resistance factor to take into account the safety class (i.e. failure consequence)
$\zeta(t)$	Periodic function of irregular wave
$\zeta_{a1/3}$	Significant wave amplitude
ζ_{an}	n wave amplitude
ν	Poisson's ratio
ρ	Water density
ρ_i	Density of the internal fluid
σ^2_ζ	Variance of the water surface elevation
ω_p	Angular spectral frequency

Symbols

A	Cross section area
A_i	Internal cross-sectional area
A_ω	Normalizing factor
C_D	Drag coefficient
C_M	Inertia coefficient
D	Nominal outside diameter
$D_{100\text{-}yr}$	Maximum fatigue damage from 100 year current
$D_{10\text{-}yr}$	Maximum fatigue damage from 10 year current
$D_{1\text{-}yr}$	Maximum fatigue damage from 1 year current
D_b	Buoyancy diameter
deg	Degree
D_{fat}	Accumulated fatigue damage (Palmgren-Miner rule)
D_h	Hydrodynamic diameter
$D_{VIV\text{-}ST}$	Fatigue damage due to short term event VIV
f_0	Initial ovality
f_n	Force per unit length in normal direction
f_n	Natural frequency
f_s	Vortex shedding frequencies
f_t	Force per unit length in tangential direction
g	Acceleration of gravity
g(•)	Generalized load effect
h	Height
$H_{1/3}$	Significant wave height (H_s)

H_{min}	Distance between the lowest point of flexible jumper along the catenary configuration and its connection point at the sub-surface buoy
k	Characteristic dimension of the roughness on the body
KC	Keulegan Carpenter number
kg	kilogram
kN	kilo Newton
m	meter
$m_{0\zeta}$	Area under the spectral curve
$m_{1\zeta}$	First order moment (static moment) of area under the spectral curve
$m_{2\zeta}$	Second order moment (moment of inertia) of under the spectral curve
M_A	Bending moment from accidental loads.
M_E	Bending moment from environmental loads
M_F	Bending moment from functional loads
M_k	Plastic bending moment resistance
mm	millimeter
MN	Mega Newton
$m_{n\zeta}$	n^{th} order moment under spectral density
MPa	Mega Pascal
N_{cg}	Number of stress cycles necessary to increase the defect from the initial to the critical defect size
N_{NW}	Number of cycles which change in slope appears under SN curve
N_{tot}	Total number of applied stress cycles during service or to in-service inspection
p_b	Burst resistance
p_c	Resistance for external pressure (hoop buckling)
p_d	Design pressure; the maximum surface pressure during normal operations
p_e	External pressure
p_{el}	Elastic collapse pressure (instability) of a pipe
p_i	Internal (local) pressure
p_{ie}	External (local) pressure
p_{inc}	Incidental pressure; the surface pressure which unlikely to be exceeded during the life of the riser
p_{ld}	Local internal design pressure, defined by
p_{li}	Local incidental pressure
p_{min}	Minimum internal pressure
$p_p(t)$	Plastic collapse pressure
p_{pr}	Resistance against buckling propagation
R_e	Reynolds number
R_k	Generalized resistance (vector or scalar)
s	second
S(ω)	Spectral Density
S_0	Nominal stress range
S_A	Load effect from accidental loads (vector or scalar)
S_E	Load effect from environmental load (vector or scalar)
S_F	Load effect from functional loads (vector or scalar)
S_J (ω)	JONSWAP spectrum
S_P	Pressure loads
S_{PM} (ω)	Pierson-Moskowitz (PM) spectrum
S_{SW}	Stress at intersection of the two SN curves
S_t	Strouhal number

$S_\zeta(\omega)$	Wave energy spectrum
t	time
t_1	Minimum required wall thickness for a straight pipe without allowances
t_{corr}	Internal and external corrosion allowance
Te	tonne
T_{eA}	Effective tension from accidental loads
T_{eE}	Effective tension from environmental loads
T_{eF}	Effective tension from functional loads
t_{fab}	Absolute value of the negative tolerance taken from the material standard/specification of the pipe
T_k	Plastic axial force resistance
t_{nom}	Nominal wall thickness
T_p	Wave peak period
T_w	True wall tension
T_z	Wave zero-crossing wave period
U_M	free stream velocity amplitude of the oscillatory flow
$v_c(z)$	total current velocity at level z
$v_{c,tide}(0)$	tidal current velocity at the still water level
$v_{c,wind}(0)$	wind-generated current velocity at the still water level
z	distance from still water level, positive upwards

Abbreviations

ALS	Accidental Limit State
API	American Petroleum Institute
BSR	Buoyancy Supported Riser
COBRA	Catenary Offset Buoyant Riser Assembly
DFF	Design Fatigue Factor
DNV	Det Norske Veritas
DOF	Degree of Freedom
FE	Finite Element
FLS	Fatigue Limit State
FPSO	Floating Production Storage and Offloading
FPU	Floating Production Unit
FSHR	Free Standing Hybrid Riser
HRT	Hybrid Riser Tower
JONSWAP	Joint Operation North Sea Wave Project
LF	Low Frequency
LRFD	Load and Resistance Factor Design
MBR	Minimum Bending Radius
RAO	Response Amplitude Operator
SCF	Stress Concentration Factor
SCR	Steel Catenary Riser
SHRT	Single Hybrid Riser Tower
SLOR	Single Line Offset Riser
SLS	Serviceability Limit State
SLWR	Steel Lazy Wave Riser
SMYS	Specified Minimum Yield Stress

TDP	Touch Down Point
TLP	Tension Leg Platform
TSJ	Tapered Stress Joint
ULS	Ultimate Limit State
VIV	Vortex Induced Vibration
WF	Wave Frequency
WSD	Working Stress Design

Table of Contents

List of Table

List of Figures

1. Introduction

1.1 Background

Oil and gas industries are one of the most modern and high technological industries among the others. Their essential existences in global world activities are truly powerful and un-displaceable. Even though they are not renewable energy, but the energy supply is still highly demanded.

Offshore oil and gas development is relatively recent historically. The first well located offshore in the Gulf of Mexico was drilled in 1947 at Kerr-McGee's Ship Shoal block 32. It was 17 km from shore and in 6 m of water depth. (Palmer & King, 2004). Since then, the emerging of offshore oil and gas industries is growing drastically with high sophisticated technology. Not to mention, to attract and explore in deeper water.

In recent years, there has been an increasing trend towards ultra deepwater exploration. To date, Perdido platform is the world's deepest offshore drilling and production activity at 2450 m (8,000 feet) water depth (Shell, 2011). Located 320 kilometers from the Texas coast in Alaminos Canyon Block 857, this spar platform can handle 100,000 barrels of oil per day and 200 million standard cubic feet gas per day.

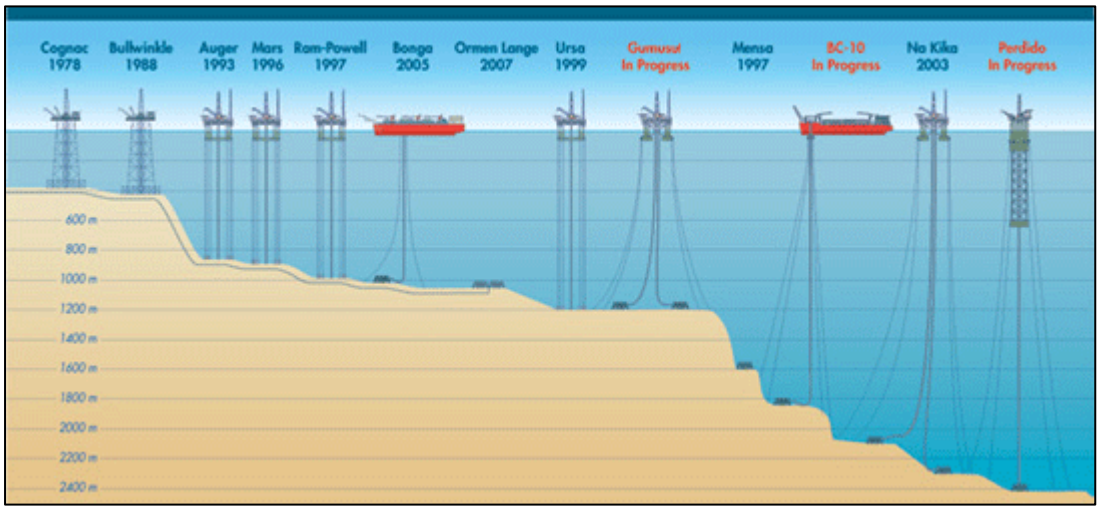

Figure 1.1 – Deepwater Milestones (Shell, 2011)

The advancement of technology in ultra deepwater has been leading Brazil into one of promising offshore market. According to GBI Researh (2010), Brazil's offshore crude oil reserves were 11,744.3 million barrels in 2008. Recent sub-salt discoveries (e.g. Tupi Field) have transformed Brazil into a country with one of the highest potential investment acreages globally. According to Saliés (2005), 33% from the total exploration area operated by Petrobras, a Brazilian state-owned oil operator, are at water depth below 1,500 m. In late 2011, the company confirms the discovery of oil and natural gas located in 2,313 m water depth of the Sergipe-Alagoas Basin offshore north east Brazil (MercoPress, 2011). This can be concluded that the future lies in ultra deepwater.

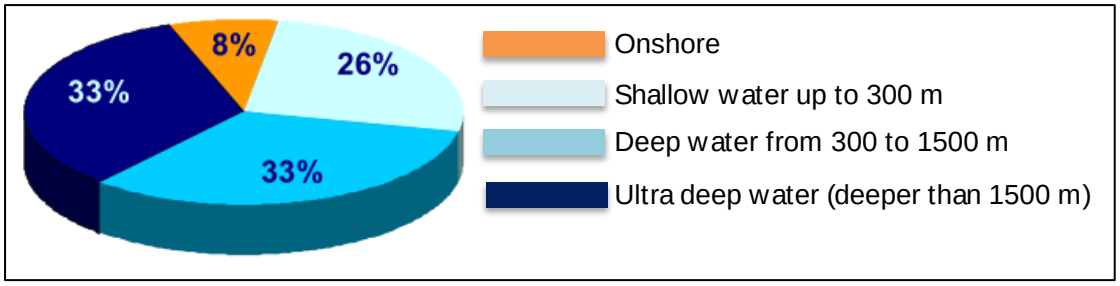

Figure 1.2 – Petrobras Brazilian Exploration Leases per Water Depth (Saliés, 2005)

Though ultra deepwater developments are being promising, there are a lot of challenges that is always become our interest, in particular, the selection of riser concept. Ultra deepwater riser selection is one of the major drivers in the evaluation of technical and feasibilities of a project. As the preliminary field layout and floating platform type are selected based on reservoir, drilling, and environmental conditions, the riser selection is interdependent compare to them. A proper floating platform motion will offer reliable riser behavior, while a robust riser configuration will have impact on less design constraints on the platform and eventually on the project execution (Shu et all, 2011).

In this thesis, many riser concepts will be discussed. Among of these, the newly developed Catenary Offset Buoyant Riser Assembly (COBRA) concept is selected as the main topic of this thesis, in particular for offshore Brazil ultra deepwater environment. In general, COBRA presents a combination between Steel Catenary Riser (SCR) at bottom section and flexible jumpers at top section, with a long and slender subsurface buoyancy module on top of SCR section on which it is tethered down to sea bed. The flexible jumper is connected to the host platform and can effectively absorb the platform motions. According to Karunakaran et al (2011), with this concept, it can improves both strength and fatigue performance of the riser system.

1.2 Purpose and Scope

The emerging ultra deepwater market in offshore Brazil and development study on the new riser concept are the key points on this thesis. This thesis looks into further COBRA riser concept optimizations with regards to offshore Brazil ultra deepwater conditions. This thesis will capture a base case study of COBRA and sensitivity study of the base case. Among of these are the sub-surface buoyancy position with regards to the water depth, the flexible jumper end-connection configurations, and the buoyancy tethers configurations on the sea bed.

A static and dynamic analysis will be performed in conjunction with the above mentioned cases. OrcaFlex software will mainly be used to study the topics. In addition, VIVANA software will be used for fatigue due Vortex Induced Vibration (VIV).

The scope of thesis will consist of:

- Chapter 2 gives review of general type of riser systems, challenges in ultra deepwater condition, and focus on the uncoupled riser system for ultra deepwater environment, including the COBRA riser concept.
- Chapter 3 provides the code checks that are used in riser design. The LRFD code based on DNV code is the main focus on this chapter.
- Chapter 4 gives the analysis methodology of the riser analysis, including some theoretical backgrounds that relevant on this thesis.

- Chapter 5 gives the design basis of the COBRA concept study. These include general overview of the riser system, design parameter, model overview, and also the design acceptance criteria
- Chapter 6 provides detail information of the COBRA concept base case study and correspondence response from the case. This includes static, dynamic, and fatigue responses.
- Chapter 7 demonstrates the sensitivity study from the base case configuration from Chapter 6. The sensitivity methods are mainly focused on the riser system configurations. At the end of this chapter, a discussion on comparison summary is presented.
- Chapter 8 gives the conclusion and recommendation from the study.

2. Ultra Deepwater Riser Overview

2.1 Introduction

The term riser in oil and gas industry can be defined as a portion of pipeline which extends from the sea floor to the surface and has a specific function to provide conduit(s) for the conveying of fluids between the seafloor equipment and the production host (Subsea1, 2012). While this definition is more into a production riser, there are also different definitions for drilling riser and completion/workover risers, which is not the focus on this thesis.

Moreover, API (2009) defines the general riser functions as below:

1. To conveys fluids between the wells and the floating production system.
2. To import, export, or circulate fluids between the floating production system and remote equipment or pipeline systems.
3. As guide drilling or workover tools and tubulars to and into the wells.
4. To support auxiliary lines.
5. To serve as, or be incorporated in a mooring element

The essential function of riser in oil and gas production has encouraged more professionals and researchers to study and develop new technology and new concept in order to achieve more reliable and cost effective riser system. As the offshore production getting deeper, it is become interest to study the applicability of the new riser concept in the ultra-deepwater condition.

In this chapter, the general riser system will be discussed, including challenges in ultra-deepwater environment conditions. Particular topic will be more focused on the uncoupled riser system, the advantage, and review on the COBRA riser concept.

2.2 Ultra Deepwater Challenges

As the industry moved into ultra-deepwater environment, the challenges that come with this trend are still evolving and require further development. When it comes to riser, some of the challenges are presented below.

2.2.1 Riser Weight

In ultra deepwater, the suspended length of riser is significantly long. This will increase the top-tension force. During service life, heavy riser weight will increase vessel payload. According to Howells and Hatton (1997), vessel payload may be 10 to 30% larger in nominal conditions and 50 to 100% larger in extreme storm conditions.

2.2.2 Sizing

External hydrostatic pressure will increase proportionally with the water depth. In ultra deepwater, high external hydrostatic pressure on the riser will increase the probability of collapse failure. As the key driver of the wall thickness design, collapse resistance in ultra deepwater condition normally required thicker riser section. Eventually, this will increase the cost development of the field.

2.2.3 Dynamic Response

Design of risers in harsh environment has been a great challenge. For ultra deepwater field, steel catenary risers (SCR) have been an attractive riser option. However, the application presents design challenges due to large motions of the vessel from waves. In addition, large vessel offsets from wind, current and slow-drift wave motions are also sum up the challenges. Due to large dynamic heave and surge motions, there are buckling issues at touch-down point (TDP), and also fatigue problems due to vessel motions and soil-riser interaction (Karunakaran et al., 2005).

Another challenge in ultra-deepwater application comes from large currents speed. For large currents speed, vortex induced vibration (VIV) is an important issue. VIV in ultra-deepwater risers gives significant fatigue damage. Normally, strakes along the critical area of riser are needed. In other hand, this will also increase drag forces.

2.2.4 Platform Motion

Riser arrangements to floating production system are mostly dependent on vessel drift offsets. For a tension leg platform (TLP) or spars with relatively small offsets, simple catenary risers may be adopted. However, as the water depth increase, the offsets increase accordingly and this impacted on more severe dynamic motions. Alternative riser arrangements such hybrid risers or wave catenaries configurations may be needed.

2.2.5 Installation

In ultra-deepwater conditions, a limitation on riser installation comes from tensioner capacity of the installations vessel. Moreover, in such extreme weather, the limitation might also come from the load capacity of abandonment and recovery winch.

In case of reeling method, the deformations introduced by this method may reduce collapse resistance and require greater wall thicknesses at increased water depth. Again, by using higher wall thickness will ultimately increase the overall weight of the riser.

Installation schedule is also taking important aspect. Greater water depth requires longer riser length, and hence it cost on longer installation schedule. The concept of uncoupled riser may save the installation time as the riser can be installed prior to the existence of the floater, in particular when more than a single riser is planned to be installed.

2.3 Review of Deepwater Riser System

In the riser system, particularly on the floating production system, the motions of the floater will have significant effect on the riser long-life performance. In vice versa, the riser presence will also give static and dynamic effect on the floater response. The floater, risers, and also the mooring system create a global system with complex response to environmental loading. All of this interaction effects is called coupling effects. Types of risers that are influenced by this effect are normally called as coupled riser system. According to Chakrabati (2005), for some systems, the coupling effects may magnify the extreme hull/floater responses.

Recent year's riser system development has been technically-proven for de-coupling the floater platform motions. These riser systems type are mainly developed for hybrid riser system. Among of these are single-line offset riser (SLOR), grouped single-line offset riser (Grouped SLOR), and recent new variant from the original concept of catenary bundle riser for single riser, which is called catenary offset buoyant riser assembly (COBRA).

The following figure shows the classification of deepwater riser system.

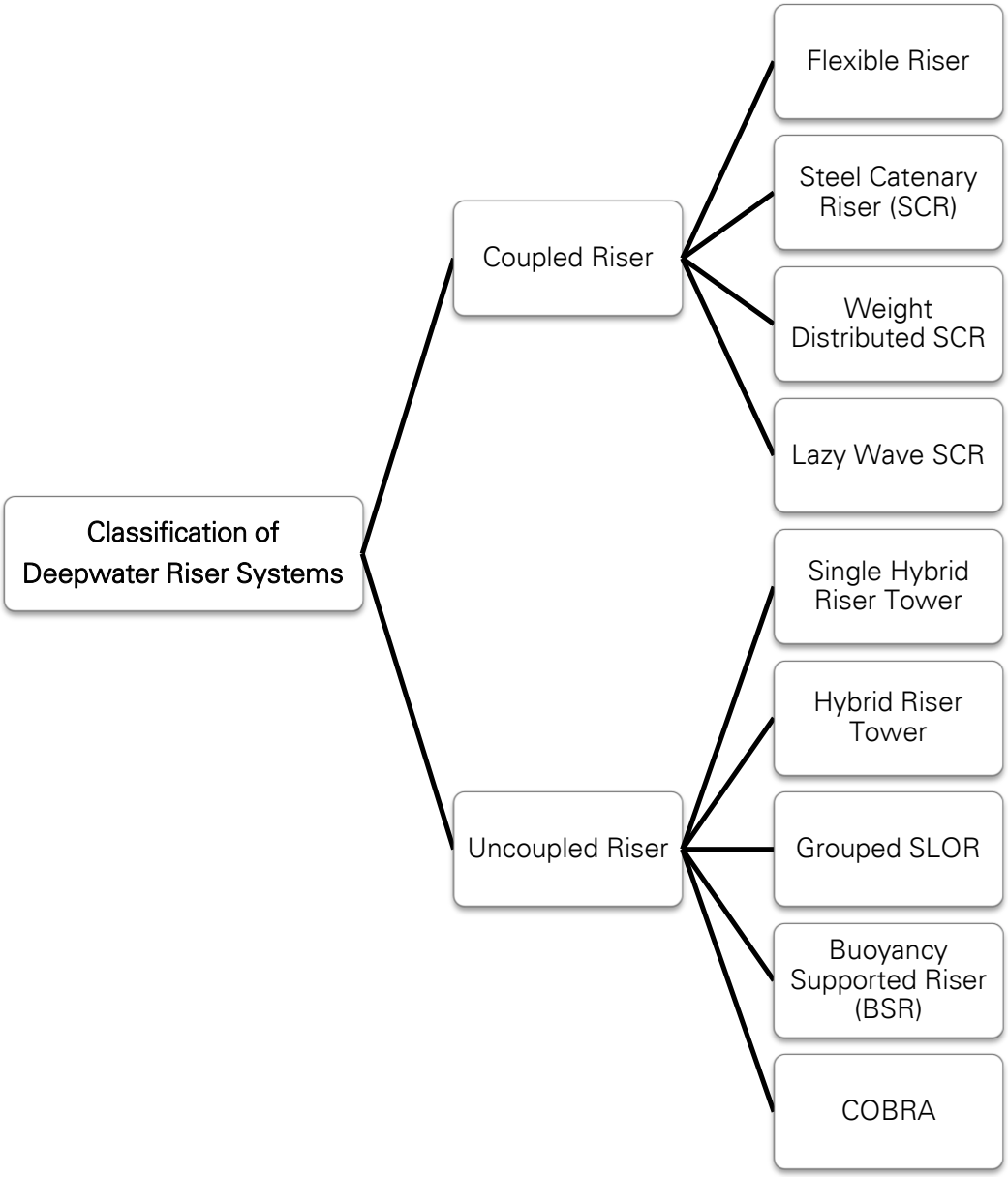

Figure 2.1– Classification of Deepwater Riser Systems

2.3.1 Coupled Riser

Coupled riser systems can be differentiated into two types of riser system configurations, i.e. flexible risers and steel catenary risers (SCR). The following sections provide the general descriptions of flexible riser and steel catenary risers.

2.3.1.1 Flexible Riser

According to API (2009), the definition of flexible pipe is an assembly of a pipe body and end fittings where the pipe body is composed of a composite of layered materials that form a pressure-containing conduit and the pipe structure allows large deflections without a significant increase in bending stresses. Moreover, API defines flexible riser as a flexible pipe connecting a platform/buoy/ship to a flowline, seafloor installation, or another platform where the riser may be freely suspended (free, catenary), restrained to some extent (buoy, chains), totally restrained or enclosed in a tube (I-or J-tubes).

There are two types of flexible pipes, i.e. bonded and unbonded flexible riser. Bonded riser using different layers of fabric, elastomer, and steel, and these are bonded together through a vulcanization process. This type of pipe is only used in short sections such as jumpers (Bai et al, 2005). While unbonded flexible riser is a multi-layered composite wall pipe with particular characteristic of having low bending stiffness combined with high axial tensile stiffness. The size range of this type is from 2" to 19". The typical internal pressure rating is in the order of 70 to 700 bar (1000-10000 psi) depending upon the pipe size, water depth, and its function. The fluid temperature inside the pipe may be transported with the temperature up to 130° Celcius.

Several concepts of flexible riser were developed since late of 1970s. Starting in relative benign weather conditions, the further advanced in flexible pipe technology makes flexible riser significantly grows in the market and has been widely used in the harsh environment of various fields.

Free Hanging Catenary Flexible Riser

Free hanging catenary riser is the simplest configuration of flexible riser. For installation, the riser is simply lifted off or lowered down to the seabed. By this simple method, it requires less subsea infrastructure, and hence can reduce the installation cost.

However, as it free hanging to the floater, it has direct severe loading from the floater motions. Depending on the floater type and its motion behavior, in general case, this configuration has high concentrated stress from the compression buckling on the touch down point (TDP). When it comes to deepwater or ultra-deepwater field, the top tension riser is extremely high due to the self-weight of the riser itself, as well as the combination from the self-weight and environmental loads.

Lazy Wave and Steep Wave Flexible Riser

In general, the main difference between wave-type configurations and free hanging type of flexible riser configurations is their ability to reduce the effect of floater motions at the touch down point (TDP) of the riser. In this type, the buoyancy modules which clamped into the riser are introduced. They are made from syntactic foam with specific material property that has low water absorption.

During the lifetime of the production, the changing of internal pipe fluid density might happen. This may cause some changes on the lazy wave riser configuration. While the steep wave riser configurations require subsea base and subsea bend stiffeners, but this type of configurations are able to maintain their configuration.

In ultra-deepwater condition, a major FPSO turret designer has estimated that the maximum practical depth for lazy-wave flexible riser to a disconnectable turret is around 1500 m, depending on the number of lines and lateral current velocity (Shotbolt, 2009).

Lazy S and Steep S Flexible Riser

Compared to the wave-type configurations, this lazy S and steep S configurations are using buoy system that either a fixed buoy that designed with a fixed structure support at the seabed, or a buoyant buoy which is tethered by mooring system that made by fiber ropes or steel chain. The buoys are often constructed as large horizontal tubes or cylinders. The advantage of using this buoyancy system is that the tethered mid-water buoy can maintain the lower section part and touch-down point almost static. In addition, it also can facilitate multi-line flexible risers.

Normally, these type of configurations require complex installations method and used when the wave-type configurations are not suitable for the designation field. However, in a 2001 survey of 277 flexible risers operating in the North Sea and West of Sheetlands offshore area showed that approximately 50% were arranged in the lazy S-configuration (Shotbolt, 2009).

Pliant Wave Flexible Riser

Pliant wave riser configuration or tethered wave configuration is similar to steep wave configurations, except that the tension force occurred at touch-down point on the riser is transferred to the subsea anchors. As the anchors control the tension forces, the riser configurations will tend to be more stable, and hence any changes on the inner pipe fluid density would not be a significant issue.

One of the main advantages of this type of configuration is the floater can be positioned directly above the well on the seabed, which make it possible to do the well interventions throughout the floater itself.

2.3.1.2 Steel Catenary Riser

Steel Catenary Riser (SCR) is another riser concept options instead of flexible riser. SCR is a single pipe suspended from the surface support facilities in a catenary shape, which lies on the seabed and either continues directly into the horizontal flowline or connects to it mechanically. The interface with the floater consists of a hang-off structure and a flex or taper joint to absorb the dynamic moment variations which generated by the motions of the floater. The interface with the seabed is dynamic, as the touch-down-point (TDP) can move both axially and laterally along the seabed (Alliot at all, 2005).

Several key aspects in the SCR plays significant role in the design consideration and also the fabrication. Cycling expansion loads along the pipe combined with the dynamic seabed interface makes SCR as a fatigue-dominated structure type. The hydrodynamic loads from waves and currents, including those generated from vortex induced vibrations (VIV) also drives the design, dictating the choice of material for the riser structure and driving the high quality welding requirements for the fabrication process.

As the exploration and development of oil and gas trend expanded to deepwater and ultra-deepwater area, many new floating production systems are developed with concern on the development cost. SCR has the advantages of low manufacturing cost, resistance of high temperature and high pressure, and widely used in the development of deepwater oil and gas fields (Duan et al, 2011). However, according to Bai et al (2005), the design, welding, installations challenges associated with SCR in ultra-deepwater floating production are primarily related to:

- SCR hang-off tensions. For ultra-deepwater SCRs, the water depth alone will give significant role in determining the hang-off tension. This large tension will resulted in high von Mises stress near hang-off location. In addition, the large hang-off loads at the floater facility require more supporting structural steel at the riser porch.
- SCR touchdown zone effective compression. The SCR touchdown zone motion response is coupled to the hang-off motion response included by the hull motions. During storm or hurricanes, the floater/vessel heave motions can cause effective bottom compression in the SCR touchdown zone. This effect may cause upheaval/lateral buckling of the SCRs on the seabed, and eventually would give high risk on the integrity of the pipe.

- SCR touchdown zone stress. Stress in this zone might result in yielding and low-cycle fatigue issues.

2.3.1.3 Weight Distributed SCR

To accommodate buckling issues at TDP region due to large heave and surge motions, and also the fatigue problems, Karunarakan et al. (2005) offers an alternative solution for SCR concept that called Weight Distributed SCR. The solution offers an SCR concept with varying weight along the riser and with lightest possible cross sections in the touch down zone. It is achieved by using well qualified ballast elements that are attached at certain sections of SCR. This concept enhances the applicability of SCRs to harsher environment by reducing the stresses around TDP, and hence also enhancing the fatigue performance. This concept can be fabricated and installed in the same way as traditional SCRs.

The following figure shows the schematic of Weight Distributed SCR.

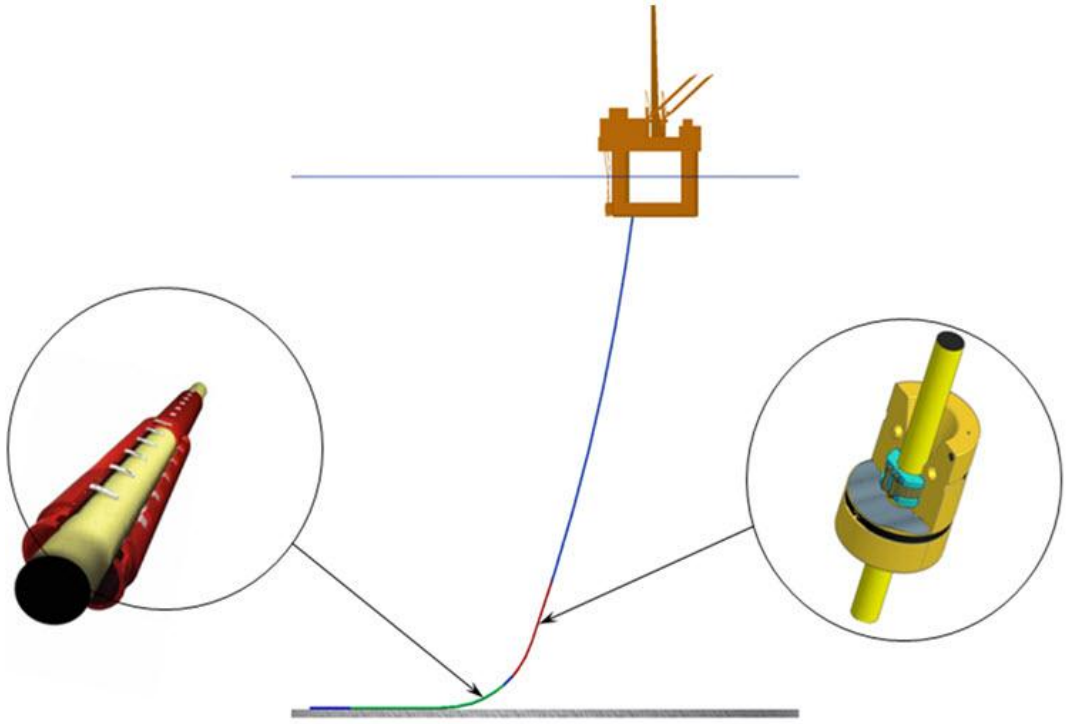

Figure 2.2 – Schematic of Weight Distributed SCRs (Karunakaran, 2010)

2.3.1.4 Lazy Wave SCR

Another type of SCR configuration is called Steel Lazy Wave Risers (SLWR). Similar like lazy wave configuration in flexible riser, the aim of using this kind of configuration is to reduce the effect of floater motions at touch-down-point (TDP). As mentioned earlier, typical key issues from SCR configuration are the dynamic seabed interface that may cause fatigue problem, and also the riser payload.

Steel Lazy Wave Risers (SLWR) offers solutions to improve fatigue performance and also reduce payload. These are issues often occurs when applying steel catenary risers on an FPSO turret in ultra deepwater (Sarkar, 2010). The first SLWR was installed in BC-10 offshore Brazil, located in 1800 m water depth. In this riser configuration, buoyancy elements were attached to the riser in the sagbend region near the touch down point. The purpose is to provide better compliance of the riser to FPSO motion responses in harsh environment conditions, and thereby improving the fatigue performance.

The following figure shows the Lazy Wave SCR arrangement.

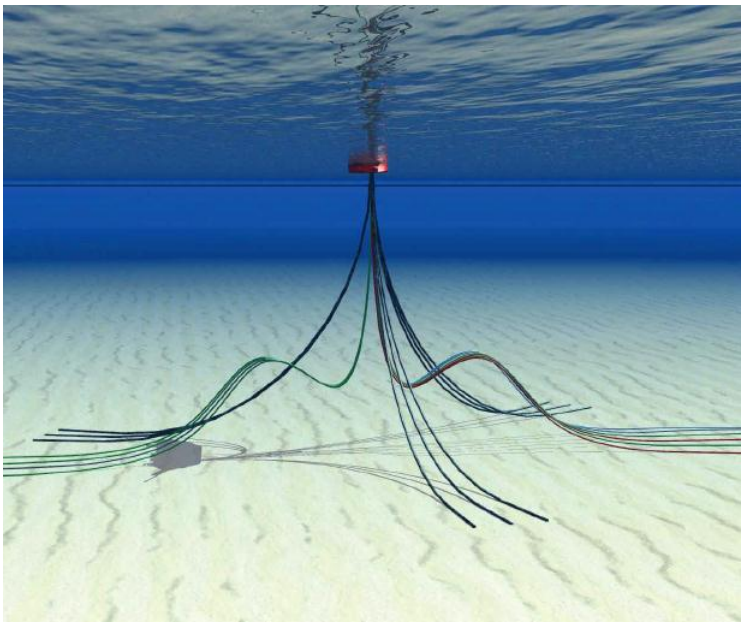

Figure 2.3 – Lazy Wave SCR (courtesy of Subsea 7, 2012)

Some challenges for SLWR concept are high requirement for the development of a detailed subsea layout description, installation sequence when all the heavy buoyancies are attached to the SCR, high specification welds.

2.3.2 Uncoupled Riser

In recent deepwater and ultra deepwater field developments, uncoupled riser systems have been applied as feasible concept and the demand is increasing along with more advanced riser technology. The following sections provide the general descriptions of some type of uncoupled riser system as described in Figure 2.1.

2.3.2.1 Single Hybrid Riser Tower

The first concept of single hybrid riser tower was come from the drilling technology that assembled the riser bundle with adequate buoyancy from a drilling rig. The riser tower foot and spools were connected to subsea base manifold and flexible jumpers at the top were connected to the rig. This concept was first installed in 1988 by Placid on the Green Canyon field block 29, where was then upgraded and reinstalled in the deeper Garden Bank field by Enserch in 1994. During that time, this concept was proved to be cost effective and well adapted to operate in the Gulf of Mexico (Alliot and Legras, 2005).

Recent field that has been used this concept is Roncador P-52 Oil Export System, located at 1800 m water depth. It combines a single rigid steel pipe with flexible pipe. It consists of a single near vertical pipe that connected to a foundation system at seabed. The riser is tensioned by means of a buoyancy can. This buoyancy can is connected to the top of the riser through a segment of chain, and it is located below the sea level. In this case, it is located beyond the influence of of wave and high current. A gooseneck assembly is also located at top of the riser. A flexible jumper connects the FPU and the riser through the gooseneck, and it decouples the vertical part of riser from the vessel motions.

The following figure shows some example of single hybrid riser tower arrangement, taken from Roncador P-52 field.

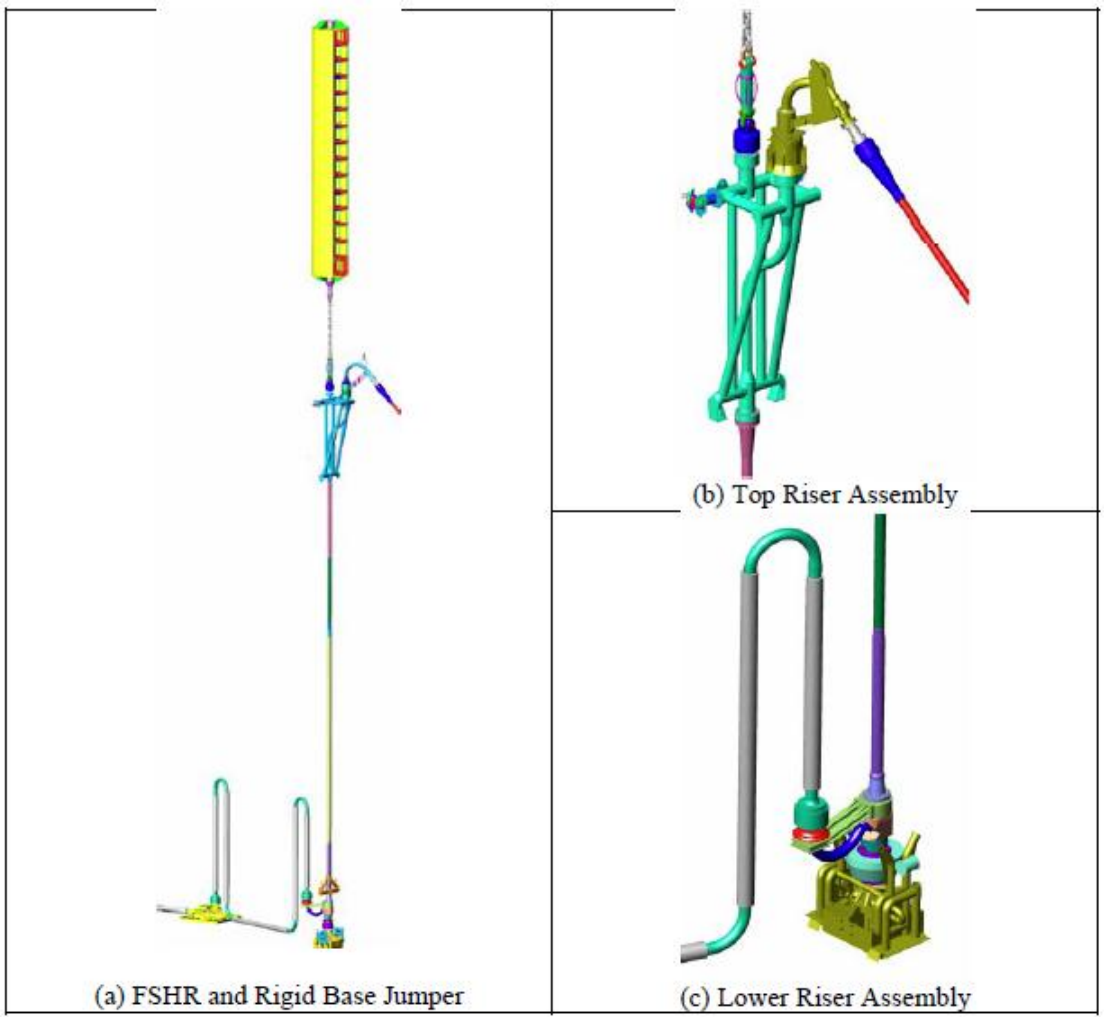

Figure 2.4 – Single Hybrid Riser Tower General Arrangement (Marques et al., 2008)

According to Marques et al. (2008), this concept has a reduced dynamic response, as a result of significant motion decoupling between the riser tower and the vessel motion. The vessel interface loads are small when compared with flexible pipe or SCRs configurations. In addition, there are possible cost savings on this concept with regards to the consideration that the riser can be installed prior to the installation of the Floating Production Unit (FPU).

2.3.2.2 Hybrid Riser Tower

Hybrid Riser Towers are one of the deepwater riser types that offer benefits in terms of flow assurance, thermal performance, and also robust field layout. The riser configuration consists of a riser tower bundle, with a buoyancy tank connected at top of the riser tower which maintains tension in the structure. The tower bundles several risers and anchored to the seabed. The tower is connected to FPSO via flexible jumpers, and it is connected to seabed flowlines termination assemblies via spools. The bottom part of tower is fixed to the riser base foundation via a flexible joint.

BP's Greater Plutonio field is one example of the field that has been used hybrid riser tower (HRT) concept. According to Louvety et al. (2009), the Greater Plutonio HRT is believed to be the largest installed in the world today, where it conveys all production and injection fluids from five operated fields on site. Another field that has been used this concept is Girassol

field in Angola, West Africa. Compared to Greater Plutonio HRT, Girassol field is transporting the oil production through three towers.

The following figure shows the HRT arrangement taken from Girassol field.

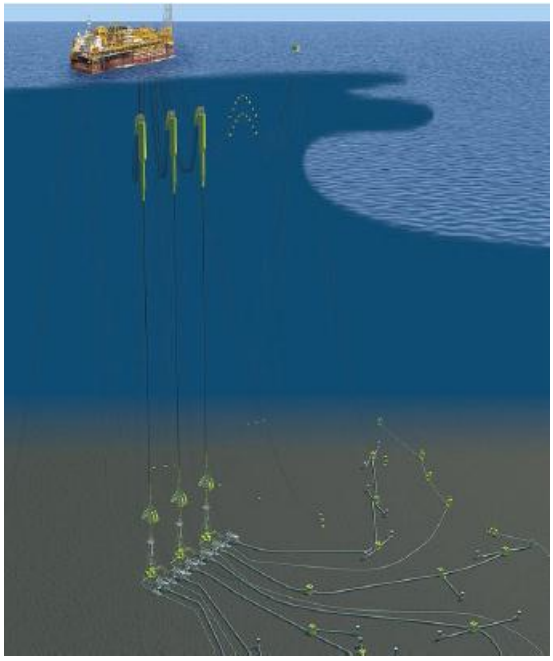

Figure 2.5 – Girassol HRT (Legras, 2011)

In general, hybrid riser tower (HRT) concept has several advantages (Louvety et al., 2009):

- Compact field layout: simple and tidy field layout as all risers are gathered in one single bundle. This concept reduces the issues of clashing between risers and allows leaving room for future developments.
- Reduced loads on the FPSO: As the bundled risers weight and part of the flexible catenary is supported by the buoyancy tank, the FPSO loads are reduced. This also reduces the associated structural reinforcements needed in the FPSO hull.
- Cost effectiveness: this concept offers competitive cost against other concepts like flexible riser, Single Hybrid Riser and Steel Catenary Risers.
- Installation: the towing and upending of the riser tower do not require mobilization of heavy lifting/laying vessels
- Local content: the production and fabrication of the bundle and bottom assembly of the riser tower contributes to the development of the country.

2.3.2.3 Grouped SLOR

The SHRT concept, which has similar concept with Single Line Offset Riser (SLOR) that developed by 2H, offers an attractive solution due to its excellent fatigue performance and ability for pre-installation. However, recent field developments that require larger riser numbers and the need for tiebacks to existing development pose some problems to this concept. Firstly, the field layout challenge is mainly as a result of its large deflections due to the current loading. This requires each SLOR arrangement to have a large spatial clearance with the adjacent SLOR, mooring line, or umbilical. Secondly, when it comes to the maximum number of SLORs and jumpers connection that can be accommodated, this limitation on the field layout space might give insufficient facility for the initial and future project requirements (Dale et al., 2007).

In order to meet the riser requirements on large offshore development, 2H Offshore and Subsea 7 have developed the new hybrid riser concept, called Grouped SLOR. This concept is a variant of SLOR and COR design which incorporates a guide frame connecting between 2 or more risers (typically 4-6), constraining them to move separately. This concept facilitates a large number of lines in close proximity but capable in maintaining the distance between adjacent lines, hence removes the clashing issues. This makes the installation, inspection, and maintenance, including removal and reinstallation procedure easier. Typical of Grouped SLOR arrangement is shown in Figure 2.6.

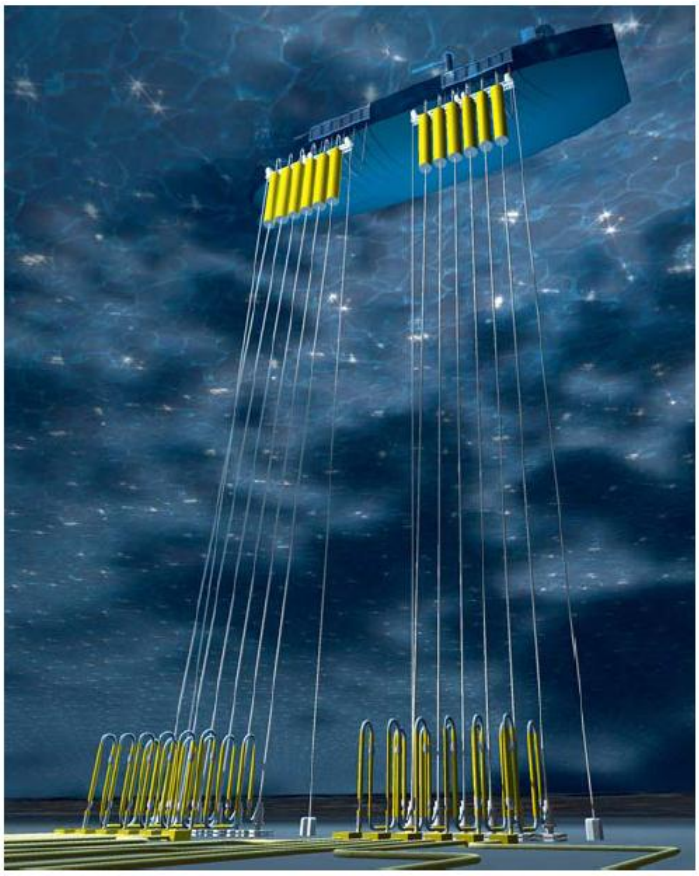

Figure 2.6 – Grouped SLOR with 6 Riser Arrangement (Karunakaran et al., 2007)

According to Karunakaran et al. (2007), the main modification of each individual SLOR in the Grouped SLOR concept is located at the elongated large diameter upper stem between the top of the aircan and the gooseneck connector. This element is used to guide the riser at the guide frame elevation. The aircans are typically 5-6 m in diameter, and the length depends on the water depth and required overpull. The gooseneck is designed to be removed and attached after the SLOR and guide frame have been installed, in which allows the flexible jumper to pass over the top of the guide frame.

In addition to the upper stem configuration, the guide frame is the component that differentiates the Grouped SLOR from the standalone SLOR design. Fabricated from steel tubulars in a truss arrangement, this guide frame is easy to install. Due to its light weight, it can be installed using a standard vessel. The frame connection to seabed is using spiral strand steel tethers. The tethers are then restrained to the mudline by using suction piles. Buoyancy tanks arrangement is welded to this guide frame in order to maintain the pulling tension at the base of each tether at all times. A typical guide frame that used in the Grouped SLOR arrangement is shown in Figure 2.7.

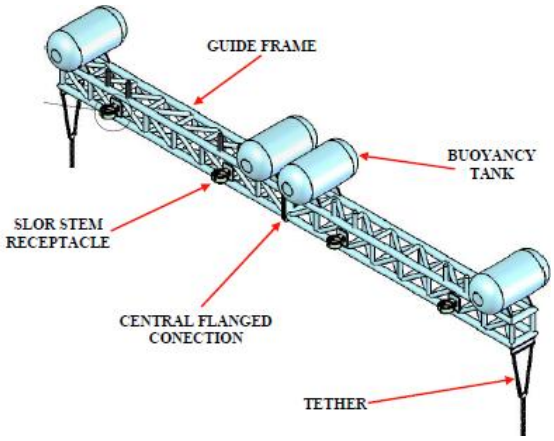

Figure 2.7 – Guide Frame in Grouped SLOR (Karunakaran et al., 2007)

2.3.2.4 Buoyancy Supported Riser (BSR)

By definition, the Buoyancy Supported Riser (BSR) is a system composed of a submersible buoy, anchored at the sea bottom by a certain number of tethers. As an intermediate floating element, the buoy connects the U-shape flexible jumpers to the SCR in which laying towards the seabed in catenary shape. General schematic of the system is shown in Figure 2.8.

The subsurface buoy concept was initially developed in 1996 by Deepstar JIP, in coordination with Texaco. During that time, the buoy was using H shape structure. In 1998, Petrobras had performed several studies and developed new rectangular ring buoy as the best solution to solve the H shape buoy problems. In 2002, the concept was finalized in 1800 m water depth, sustaining 19 risers (Franciss, 2005).

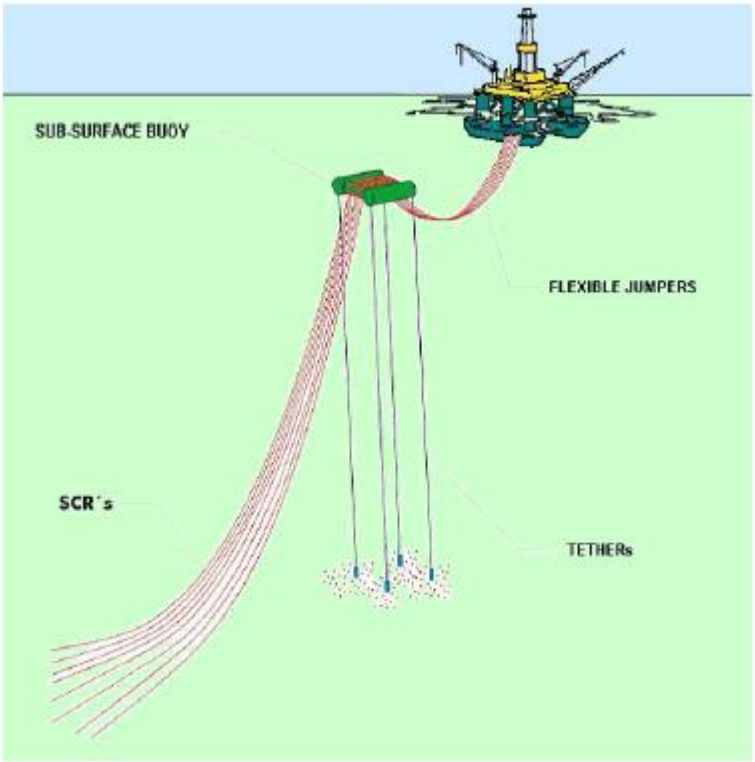

Figure 2.8 – General Schematic of SCR supported by sub-surface buoy (Francis, 2005)

According to Franciss (2005), this concept offers several advantages, i.e.:

- Ability to uncouple the movement of the riser system, hence giving the independency to choose the best option for the floater production platform;
- Reduction of the top loads due to intermediate buoy design;
- Possibility to install almost 90% of the total SCR independently of the arrival of the floater and its correspondent mooring system;
- Reduction of pull-in and pull-out system at the floater for the flexible jumpers;
- Increase the technicall feasibility window of the SCR in free-hanging configuration;
- The jumpers can be installed or replaced using conventional vessels due to smaller loads.

2.3.2.5 COBRA

Among the alternative concept of the uncoupled riser systems mentioned in the previous sections, a new uncoupled riser system has been developed and it is called Catenary Offset Buoyant Riser Assembly (COBRA). COBRA consists of a catenary riser section with a long, slender buoyancy module on top of bottom catenary section, which is tethered down to the seabed via two mooring lines. The top of catenary riser section is connected to the floater by a flexible jumper. This flexible jumper can absorb the floater motions, which give improvement both strength and fatigue performance on the overall system. The sub-surface buoy is positioned at particular water depth in order to reduce the surface wave and current effect, and anchored to a single suction pile on the seabed. Typical COBRA riser arrangement is shown in the following figure.

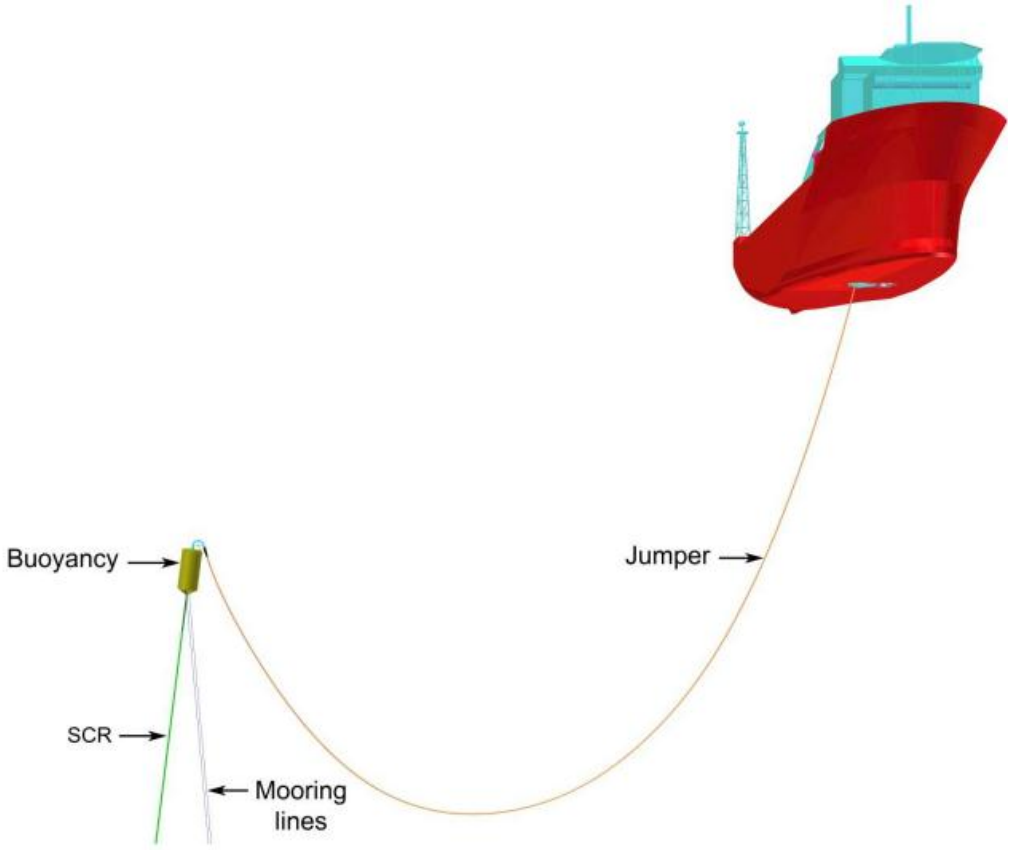

Figure 2.9 – COBRA Riser Arrangement (Karunakaran et al, 2011)

According Karunakaran et al. (2011), this concept offers advantages of the SCR and the Single Hybrid Riser Tower. Compared to SCR, this concept has excellent dynamic performance with less or no fatigue response. Compared to Single Hybrid Riser Tower, this concept avoids all the expensive bottom assembly, foundation, and bottom connections which in general needed for Single Hybrid Riser Tower concept. In addition, since the platform motions are un-coupled and hence give very small fatigue impact on the SCR part, there is a possibility that the riser can be designed using pipeline class welds (e.g. F1 class), where such material like BuBi pipe can be used for this SCR section.

In this thesis, COBRA riser concept is the main topic discussion, in particular for ultra deepwater condition in 2200 m water depth, located in Santos Basin Central Cluster region. A COBRA Base Case configuration will be presented, and detail discussion on strength and fatigue design analyses will be followed accordingly. In addition, sensitivity studies based on the Base Case configuration result will be also presented to study the effect on other possible alternative configuration solutions.

3. Design Code for Riser

3.1 Introduction

Any type of riser that will be implemented in the oil and gas field shall be designed according to standardized design codes. The fundamental design requirements are to make the riser fit for use on the intended conditions and periods, capable to sustain all foreseeable load effects and other influences likely to occur during the service life, and have adequate durability in relation to maintenance cost (DNV, 2010).

In general, there are two methods that commonly used as the basis criteria in structural design. One method is referred to as Working Stress Design (WSD), in which adopted a single safety factor for each limit state to account the influence of uncertainty. In riser design, WSD method is provided in API-RP-2RD. Another method is referred to as Load and Resistance Factor Design (LRFD) where partial safety factor is accounted for each load effect and resistance. In riser design, LRFD method is provided in DNV-OS-F201.

According to DNV (2010), the LRFD method allows for a more flexible and optimal design with uniform safety level and is considered superior to the WSD method. Writing in this chapter is focused on the LRFD method and mainly based on DNV-OS-F201.

3.2 Design Principles

The basic design principles of riser is rooted to the safety philosophy, where all activities involved with regards to the design are safe and conducted with due regard to public safety and protection of the environment. All phase from conceptual development until the abandonment shall establish the safety objective, e.g. covered the principle on reducing of any hazardous impact to as low as reasonably practicable (ALARP principle).

According to DNV (2010) Section 2, B600, the structural safety of the riser is ensured by use of a safety class methodology, where the riser system shall be classified into one or more safety classes based on the failure consequences. This gives the possibility of the riser to be design with different safety requirements, depending on which class that the riser belongs. The classification of safety classes is given in the following table:

Classification of safety classes

Safety Class	Definition
Low	Where failure implies low risk of human injury and minor environmental and economic consequences.
Normal	For conditions where failure implies risk of human injury, significant environmental pollution or very high economic or political consequences.
High	For operating conditions where failure implies high risk of human injury, significant environmental pollution or very high economic or political consequences.

Table 3.1 – Classification of safety classes (DNV-OS-F201 Section 2-B204, 2010)

In general, all the riser system, including the pipe and interfaces, details, and other components, shall apply to the basic design principles. According DNV (2010), Section 2 B602, these basic design principles are:

- the riser system shall satisfy functional and operational requirements as given in the design basis.
- the riser system shall be designed such that an unintended event does not escalate into an accident of significantly greater extent than the original event;
- permit simple and reliable installation, retrieval, and be robust with respect to use;
- provide adequate access for inspection, maintenance, replacement and repair;
- the riser joints and components shall be made such that fabrication can be accomplished in accordance with relevant recognized techniques and practice;
- design of structural details and use of materials shall be done with the objective to minimize the effect corrosion, erosion, and wear;
- riser mechanical components shall, as far as practicable, be designed "fail safe". Consideration is to be given in the design to possible early detection of failure or redundancy for essential components, which cannot be designed according to this principle;
- the design should facilitate monitoring of its behavior in terms of tension, stresses, angles, vibrations, fatigue cracks, wear, abrasion, corrosion, etc.

In Load and Resistance Factor Design (LRFD) method, the fundamental principle is to verify that factorized design load effects do not exceed factored design resistance for any of the considered limit states. The design load effects are differentiated between:

- pressure load effect
- functional load effects
- environmental load effects
- accidental load effects

where more details on these type is given in the section 3.3.

The general LRFD safety format can be expressed as:

$$g(Sp; \gamma_F \cdot S_F; \gamma_E \cdot S_E; \gamma_A \cdot S_A; R_K; \gamma_{SC}; \gamma_m; \gamma_C; t) \leq 1 \qquad \textbf{(3.1)}$$

where

$g(\bullet)$	=	the generalized load effect, g(•) <1 implies a safe design andg(•)>1 implies failure
S_P	=	Pressure loads
S_F	=	Load effect from functional loads (vector or scalar)
S_E	=	Load effect from environmental load (vector or scalar)
S_A	=	Load effect from accidental loads (vector or scalar)
γ_F	=	Load effect factor for functional loads (vector or scalar)
γ_E	=	Load effect factor for environmental load (vector or scalar)
γ_A	=	Load effect factor for accidental loads (vector or scalar)
R_k	=	Generalised resistance (vector or scalar)

γ_{SC} = Resistance factor to take into account the safety class (i.e. failure consequence)

γ_m = Resistance factor to account for material and resistance uncertainties

γ_c = Resistance factor to account for special conditions

t = time

3.3 Design Loads

According to DNV (2010) Section 3, the loads and deformations are defined into four groups as follows:

- pressure (P) loads,
- functional (F) loads
- environmental (E) loads,
- accidental (A) loads.

The following table describes the example on above list.

Examples of categorization of loads[1)]

F-loads	E-loads	P-loads[7)]
Weight and buoyancy[6)] of riser, tubing, coatings[6)], marine growth[2)], anodes, buoyancy modules, contents and attachments Weight of internal fluid Applied tension for top-tension risers Installation induced residual loads or pre-stressing Pre-load of connectors Applied displacements and guidance loads, including active positioning of support floater Thermal loads Soil pressure on buried risers Differential settlements Loads from drilling operations Construction loads and loads caused by tools	Waves Internal waves and other effects due to differences in water density Current Earthquake[4)] Ice[3)] Floater motions induced by wind, waves, and current, i.e.: - Mean offset including steady wave drift, wind and current forces - Wave frequency motions - Low frequency motions	External hydrostatic pressure Internal fluid pressure: hydrostatic, static and dynamic[5)] contributions, as relevant Water levels

Notes:

1) Accidental loads, both size and frequency, for a specific riser and floater may be defined by a risk analysis.
2) For temporary risers, marine growth can often be neglected due to the limited duration of planned operations.
3) Ice effects shall be taken into account in areas where ice may develop or drift.
4) Earthquake load effects shall be considered in the riser design for regions considered being seismically active.
5) Slugs and pressure may introduce global load effects for compliant configurations.
6) Include also absorbed water.
7) Possible dynamic load effects from P-loads and F-loads shall be treated as E-loads, e.g. slug flow.

Table 3.2 – Examples of categorization of loads (DNV-OS-F201 Section 3-A301, 2010)

3.4 Limit States Design

DNV (2010) provides four categories for the limit states group, i.e. SLS, ULS, ALS, and FLS. The general descriptions of these categories are:

- Serviceability Limit State (SLS): the riser must be able to remain fit during the service period and operate properly.
- Ultimate Limit State (ULS): the riser must remain intact and avoid rupture, but not necessary be able to operate, and corresponds to the maximum resistance to peak design loads with 10^{-2} annual exceedence probability.
- Accidental Limit State (ALS): the riser must remain intact and avoid rupture, but not necessary be able to operate, and corresponds to infrequent accidental loads (e.g. dropped object, explosion, etc.).
- Fatigue Limit State (FLS): the riser must be able to remain fit to function during its service life due to accumulated excessive fatigue crack growth or damage under cyclic loading.

These categories will be discussed in more detail in the next section.

For each limit states, there are different types of load effect factors and resistance factors. The load effect factors are also determined based on the design loads (refer to Section 3.3). In other hand, the resistance factors are also determined based on the safety class as described in Table 3.1.

The formula for characteristic bending moment, according to DNV (2010), is

$$M_d = \gamma_F \cdot M_F + \gamma_E \cdot M_E + \gamma_A \cdot M_A \qquad \textbf{(3.2)}$$

where

M_F = Bending moment from functional loads

M_E = Bending moment from environmental loads

M_A = Bending moment from accidental loads.

For effective tension, the characteristic load is given as

$$T_{ed} = \gamma_F \cdot T_{eF} + \gamma_E \cdot T_{eE} + \gamma_A \cdot T_{eA} \qquad \textbf{(3.3)}$$

where

T_{eF} = Effective tension from functional loads

T_{eE} = Effective tension from environmental loads

T_{eA} = Effective tension from accidental loads.

The effective tension T_e is given below:

$$T_e = T_W - p_i A_i + p_e A_e \qquad \textbf{(3.4)}$$

where

T_w = True wall tension (i.e. axial stress resultant found by integrating axial stress over the cross section

p_i = Internal (local) pressure

p_{ie} = External (local) pressure

A_i = Internal cross-sectional area

According to DNV (2010), the load effect factors shall be used wherever the design load effect is referred to for all limit states and safety class. Several load effect factors based on the limit states and design loads are given in the following table.

Load effect factors			
Limit State	F-load effect	E-load effect	A-load effect
	γ_F	γ_E	γ_A
ULS	1.1 [1)]	1.3 [2)]	NA
FLS	1.0	1.0	NA
SLS & ALS	1.0	1.0	1.0

Notes:
1) If the functional load effect reduces the combined load effects, γ_F shall be taken as 1/1.1.
2) If the environmental load effect reduces the combined load effects, γ_E shall be taken as 1/1.3.

Table 3.3 – Load Effect factors (DNV-OS-F201 Section 5-B201, 2010)

According to DNV (2010), the applicable resistance factors are:

- Safety class factor γ_{SC}: based on the actual safety class (refer to Table 3.1), to account for the failure consequence.
- Material resistance factor γ_M: based on the limit state conditions, to account for material and resistance uncertainties.
- A condition factor γ_C: to account for special conditions specified explicitly at different limit states where applicable

The following tables give the correspondence resistance factor:

Safety class resistance factor γ_{SC}		
Low	Normal	High
1.04	1.14	1.26

Table 3.4 – Safety class resistance factor (DNV-OS-F201 Section 5-C102, 2010)

Material resistance factor γ_M	
ULS & ALS	SLS & FLS
1.15	1.0

Table 3.5 – Material resistance factor (DNV-OS-F201 Section 5-C102, 2010)

3.4.1 Ultimate Limit State

Per definition, the Ultimate Limit State (ULS) condition shall be able to resist the loads with 10^{-2} annual exceedence probability. According to DNV (2010), typical limit states for the riser system on this category are:

- Bursting
- Hoop buckling (collapse)

- Propagating buckling
- Gross plastic deformation and local buckling
- Gross plastic deformation, local buckling and hoop buckling
- Unstable fracture and gross plastic deformation
- Liquid tightness
- Global buckling

Bursting

The internal overpressure on the pipe may cause the bursting failure. During the operation, the internal pressure is dominating the load that occurs on the riser pipe. DNV (2010) provides the formula to check the bursting condition as below:

$$(p_{li} - p_e) \leq \frac{p_b(t_1)}{\gamma_m \cdot \gamma_{SC}} \quad \textbf{(3.5)}$$

where:

p_{li} = local incidental pressure, that is the maximum expected internal pressure with a low annual exceedence probability, and defined by

$$p_{li} = p_{inc} + \rho_i \cdot g \cdot h \quad \textbf{(3.6)}$$

with

p_{inc} = incidental pressure; the surface pressure which unlikely to be exceeded during the life of the riser

ρ_i = the density of the internal fluid

g = the acceleration of gravity

h = the height difference between the actual location and the internal pressure reference point

p_e = external pressure

p_b = burst resistance, defined by

$$p_b(t) = \frac{2}{\sqrt{3}} \cdot \frac{2 \cdot t}{D - t} \cdot min\left(f_y; \frac{f_u}{1.15}\right) \quad \textbf{(3.7)}$$

where:

D = nominal outside diameter

f_y = yield strength of material

f_u = tensile strength of material

Normally, the local incidental pressure, p_{li} is taken 10% higher than the design pressure, p_d, i.e.:

$$p_{li} = p_{ld} + 0.1 \cdot p_d \quad \textbf{(3.8)}$$

where:

p_{ld} = local internal design pressure, defined by

$$p_{ld} = p_d + \rho_i \cdot g \cdot h \quad \textbf{(3.9)}$$

and

p_d = design pressure; the maximum surface pressure during normal operations

The nominal wall-thickness of the pipe is given by:

$$t_{nom} = t_1 + t_{corr} + t_{fab} \quad \textbf{(3.10)}$$

where:

t_{corr} = internal and external corrosion allowance

t_{fab} = absolute value of the negative tolerance taken from the material standard/specification of the pipe

The minimum required wall-thickness for a straight pipe without allowances and tolerance is given by:

$$t_1 = \frac{D}{\frac{4}{\sqrt{3}} \cdot \frac{min\left(f_y; \frac{f_u}{1.15}\right)}{\gamma_m \gamma_{SC} (p_{li} - p_e)} + 1} \quad \textbf{(3.11)}$$

Hoop Buckling (Collapse)

In addition to internal pressure, pipe members also experienced the external pressure. According to DNV (2010), this pressure shall be designed to the following condition:

$$(p_e - p_{min}) \leq \frac{p_c(t_1)}{\gamma_{SC} \cdot \gamma_m} \quad \textbf{(3.12)}$$

where:

p_{min} = a minimum internal pressure

$p_c(t)$ = the resistance for external pressure (hoop buckling) , given by

$$\left(p_c(t) - p_{el}(t)\right) \cdot \left(p_c^2(t) - p_p^2(t)\right) = p_c(t) \cdot p_{el}(t) \cdot p_p(t) \cdot f_0 \cdot \frac{D}{t} \quad \textbf{(3.13)}$$

where:

$p_{el}(t)$ = the elastic collapse pressure (instability) of a pipe, given by

$$p_{el}(t) = \frac{2 \cdot E \cdot \left(\frac{t}{D}\right)^3}{1 - \vartheta^2} \quad \textbf{(3.14)}$$

$p_p(t)$ = the plastic collapse pressure, given by

$$p_{p(t)} = 2\frac{t}{D} \cdot f_y \cdot \alpha_{fab} \quad \textbf{(3.15)}$$

α_{fab} = fabrication factor (given in Table 5-7, DNV 2010)

f_0 = initial ovality, given by

$$f_0 = \frac{D_{max} - D_{min}}{D} \quad \textbf{(3.16)}$$

Propagating Buckling

The local buckle phenomenon shall be maintained as a local effect and this should not lead to successive hoop buckling of neighboring pipe. Propagation is initiated by a combination of bending and pressure. Once started, the buckle can propagate at a lower pressure (Karunakaran, 2011). According to DNV (2010), the following term is required to check the propagating buckling:

$$(p_e - p_{min}) \leq \frac{p_{pr}}{\gamma_c \cdot \gamma_m \cdot \gamma_{SC}} \quad \textbf{(3.17)}$$

where:

γ_c = 1.0 if no buckle propagation is allowed, 0.9 if buckle is allowed to travel a short distance

p_{pr} = the resistance against buckling propagation, given by

$$p_{pr} = 35 \cdot f_y \cdot \alpha_{fab} \cdot \left(\frac{t_2}{D}\right)^{2.5} \quad \textbf{(3.18)}$$

where:

t_2 = t_{nom} - t_{corr}

Combined Loading Criteria

The equation for designing pipe members subjected to bending moment, effective tension, and net internal overpressure shall be satisfy to (DNV, 2010):

$$\{\gamma_{SC} \cdot \gamma_m\}\left\{\left(\frac{|M_d|}{M_k} \cdot \sqrt{1 - \left(\frac{p_{ld} - p_e}{p_b(t_2)}\right)^2}\right) + \left(\frac{T_{ed}}{T_k}\right)^2\right\} + \left(\frac{p_{ld} - p_e}{p_b(t_2)}\right)^2 \leq 1 \quad \textbf{(3.19)}$$

where:

M_d = design bending moment (refer to eq. (3.2))

T_{ed} = design effective tension (refer to eq. (3.3))

p_{ld} = local internal design pressure (refer to eq. (3.9))

p_e = local external pressure

p_b = burst resistance (refer to eq. (3.7))

M_k = plastic bending moment resistance, given by:

$$M_k = f_y \cdot \alpha_c \cdot (D - t_2)^2 \cdot t_2 \quad \textbf{(3.20)}$$

T_k = plastic axial force resistance, given by:

$$T_k = f_y \cdot \alpha_c \cdot \pi \cdot (D - t_2) \cdot t_2 \quad \textbf{(3.21)}$$

where:

α_c = a parameter accounting for strain hardening and wall thinning, given by

$$\alpha_c = (1-\beta) + \beta \cdot \frac{f_u}{f_y} \quad \textbf{(3.22)}$$

$$\beta = \begin{cases} (0.4 + q_h) & \text{for } D/t_2 < 15 \\ (0.4 + q_h)(60 - D/t_2)/45 & \text{for } 15 < D/t_2 < 60 \\ 0 & \text{for } D/t_2 > 60 \end{cases}$$

$$q_h = \begin{cases} \dfrac{(p_{ld} - p_e)}{p_b(t_2)} \dfrac{2}{\sqrt{3}} & \text{for } p_{ld} > p_e \\ 0 & \text{else} \end{cases}$$

For pipe members subjected to bending moment, effective tension, and net external overpressure, the following equation shall be satisfied (DNV, 2010):

$$\{\gamma_{SC} \cdot \gamma_m\}^2 \left\{ \left(\frac{|M_d|}{M_k} \right) + \left(\frac{T_{ed}}{T_k} \right)^2 \right\} + \{\gamma_{SC} \cdot \gamma_m\}^2 \left(\frac{p_e - p_{min}}{p_c(t_2)} \right)^2 \leq 1 \quad \textbf{(3.23)}$$

where:

$p_c(t_2)$ = hoop buckling capacity (refer to eq. (3.13))

3.4.2 Fatigue Limit State

The Fatigue Limit State is presented in order to check the structure for the correspondence cyclic load that imposed during entire service life. The structure shall have an adequate fatigue life. The fatigue assessment methods may be categorized into (DNV, 2010):

- Methods based on S-N curves
- Methods based on fatigue crack propagation

S-N curves

According to DNV (2010), the fatigue criterion that shall be satisfied based on S-N curves method is:

$$D_{fat} \cdot DFF \leq 1.0 \quad \textbf{(3.24)}$$

where:

D_{fat} = Accumulated fatigue damage (Palmgren-Miner rule)

DFF = Design fatigue factor, refer to Table 3.6.

Design Fatigue Factor, DFF

Safety Class		
Low	Normal	High
3.0	6.0	10.0

Table 3.6 – Design Fatigue Factor (DNV-OS-F201, 2010)

Fatigue Crack Propagation

Fatigue crack growth life shall be designed and inspected to satisfy the following criterion (DNV, 2010):

$$\frac{N_{tot}}{N_{cg}} \cdot DFF \leq 1.0 \qquad \textbf{(3.25)}$$

where:

N_{tot} = total number of applied stress cycles during service or to in-service inspection

N_{cg} = Number of stress cycles necessary to increase the defect from the initial to the critical defect size

DFF = Design fatigue factor (refer to Table 3.6)

3.4.3 Accidental Limit State

Accidental Limit State is a limit state due to accidental loads where the riser may be subjected to abnormal conditions, incorrect operation or technical failure, and typically results from unplanned occurrences (DNV, 2010). The loads may be categorized into:

- Fires and explosions
- Impact/collisions
- Hook and snag loads
- Failure of support system, e.g. loss of buoyancy, loss of mooring line, etc.
- Failures due internal overpressure, e.g. failure of well tubing or packers, well kill, etc.
- Earthquake, tsunamis, iceberg.

A simplified design check with respect to accidental load may be performed as described in table below.

Simplified Design Check for Accidental loads

Prob. of occurrence	Safety Class Low	Safety Class Normal	Safety Class High
$>10^{-2}$	Accidental loads may be regarded similar to environmental loads and may be evaluated similar to ULS design check		
$10^{-2} – 10^{-3}$	To be evaluated on a case by case basis		
$10^{-3} – 10^{-4}$	$\gamma_c = 1.0$	$\gamma_c = 1.0$	$\gamma_c = 1.0$
$10^{-4} – 10^{-5}$		$\gamma_c = 0.9$	$\gamma_c = 0.9$
$10^{-5} – 10^{-6}$	Accidental loads or events May be disregarded		$\gamma_c = 0.8$
$< 10^{-6}$			

Table 3.7 – Simplified Design Check for Accidental Loads (DNV-OS-F201, 2010)

3.4.4 Serviceability Limit State

Serviceability Limit States are associated with determination of acceptable limitations to normal operation. DNV (2010) defines for the global riser behavior, the serviceability limit states behavior associated with the limitations of deflections, displacements, and rotation or ovalisation of the riser pipe.

Ovalisation Limit due to bending

Riser shall not be subjected to excessive ovalitation. Thus, in order to prevent premature local buckling, the flattening due to bending together with the out-of-roundness tolerance from fabrication of the pipe shall be limited to (DNV, 2010):

$$f_0 = \frac{D_{max} - D_{min}}{D_o} \leq 0.03 \qquad \textbf{(3.26)}$$

Riser Stroke

The term 'stroke' means the travel of the tensioner, where a top tensioner shall maintain constant tension on the riser in order to limit bending, and this tensioner shall continue to pull as the riser and the floater move vertically relative to each other. Due to this regard, the riser system shall be designed to have sufficient stroke such that damages to riser, components, and equipment are avoided (DNV, 2010).

Examples of SLS for production risers

Table below show some example of serviceability limit state (SLS) for production risers with surface tree (refer to Table 5-15 Section 5, DNV 2010):

Examples of SLS for production risers with surface tree

Component	Function	Reason for SLS	Comment
Riser installation	Running and retrieving the riser	A weather limitation would be set to avoid riser interference	Usually run on guide-wires in close proximity to other risers
Riser stroke	Limit the frequency of bottom-out	The tensioner may be designed for bottom-out	Energy absorption criteria shall be specified
	Limit the design requirements for the jumper from the surface tree to the topside piping	The tensioner may be designed for bottom-out	Energy absorption criteria shall be specified

Table 3.8 – Examples of SLS for production risers with surface tree (DNV-OS-F201, 2010)

4. Analysis Methodology

4.1 Introduction

This chapter will cover the general summary of theoretical background related to riser analysis concept and analysis methodology that is used in this thesis work. The analysis methodologies are in accordance with DNV-OS-F201 (2010).

4.2 Waves

The basic understanding of wave is important in order to design and analyze riser, whether during installation or operation. In general, two basic approaches are captured in order to consider the wave as environmental design load. One can consider the single wave method in which the design wave is presented by a wave period and a wave height. The other method is by considering the wave spectrum.

The single wave method is normally used in order to analyze the maximum (or extreme) wave height that might occur during certain period of time. It is quite simple and easy to determine the responses due to this method. A regular (linear and non-linear) wave is commonly used for this method. This method will not be discussed in detail on this thesis work.

The wave spectrum method is used to represent the actual sea-state condition at the site under consideration. A suitable wave spectrum model is normally chosen to represent an appropriate density distribution of the sea waves at the particular site.

Nowadays, engineers will tend to choose one of the theoretical spectrum models which are available (e.g Pierson-Moskowitz Spectrum, Bretschneider Spectrum, JONSWAP Spectrum, etc). However, the most suitable spectrum is a measured design wave spectrum at the site, even though the data is not always available (Chakrabarti, 1994).

The wave spectrum method will be discussed in more detail in Section 4.2.1. The following section will describe the basic type of waves and further discussion on the wave spectrum analysis.

The term regular wave refers to a unidirectional train of waves with constant amplitude and frequency. The result becomes the wave with typically of constant length. Linear wave is defined as the regular wave with small steepness, where wave steepness is the ratio of wave amplitude and wave length. It is also can be easily pictured as a sinusoidal function wave.

Non-linear wave is described as a regular wave with greater steepness. It has more peaked at the crest and flatter in the troughs. In addition, the valid description of the profile requires non-linear solutions of the relevant equations. Some example of the linear and non-linear waves is shown in the following figure.

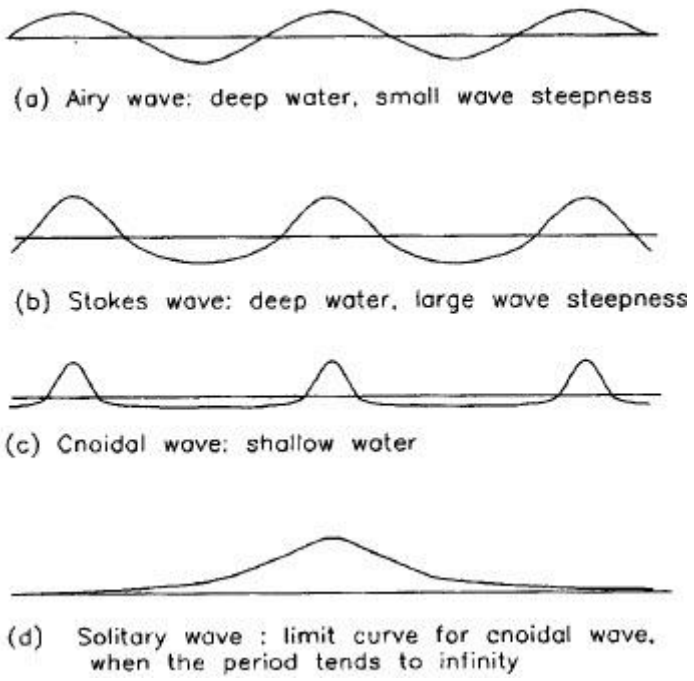

Figure 4.1 – Wave Profiles (after Le Mehaute, 1976)

As mentioned, the linear and non-linear wave relates mostly to model and analyze the extreme wave condition.

Even though that this regular wave, either linear or non-linear, is not really represent the actual sea environment, but they have significant importance as the basis for generating the wave spectrum method analysis. The linear wave can be combined by linear superposition to compose realistic models of actual sea condition in terms of energy spectra. The energy spectra curve, which is a function of spectral density $S(\omega)$ and frequency, can be translated into a time history of complete wave motion including the subsurface kinematics by linear superposition of the components with random phase differences. This concept can be extended to directional spectra where the energy density is then a function of $S(\omega,\theta)$ of frequency and directions.

Waves in the real ocean sea environment are commonly referred as random or irregular waves. These waves are composed of random waves with different wave heights and wave periods, and best modeled in terms of energy spectrum. The spectrum gives the distribution of wave energy among different wave frequencies or wave lengths on the sea surface.

4.2.1 Wave Energy Spectrum

As mentioned, the wave energy spectrum may best describe the random (irregular) wave that represents the real ocean wave. In order to develop the wave energy spectrum, the principle of linear superposition may applied by using a Fourier series method.

Fourier showed that periodic function of $\zeta(t)$ can be represented over the interval $-T/2 < t < T/2$ as the sum of an infinite series of sine and cosine functions with harmonic wave frequencies.

A time history of irregular wave can be shown in the following figure

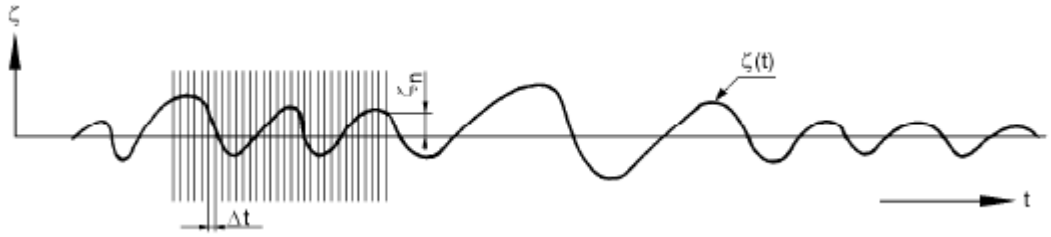

Figure 4.2 – Irregular Time History Wave (Journée and Massie, 2001)

The total long period can be defined as $\tau = N \cdot \Delta t$. For each time shift Δt, the amplitudes ζ_{a_n} might have different value. According to Journée and Massie (2001), a mean square value of ζ_{an} can be found by $\overline{\zeta^2}_{a_n}$.

The variance of the water surface elevation $\sigma^2{}_\zeta$ can be expressed as

$$\sigma^2{}_\zeta = \sum_{n=1}^{N} \frac{1}{2} \zeta_{a_n}^2 \qquad (4.1)$$

Thus, the wave amplitude ζ_{a_n} can be expressed by a wave spectrum $S_\zeta(\omega_n)$

$$S_\zeta(\omega_n) \cdot \Delta\omega = \sum_{\omega_n}^{\omega_n+\Delta\omega} \frac{1}{2} \zeta_{a_n}^2(\omega) \qquad (4.2)$$

where Δω is a constant difference between two successive frequencies.

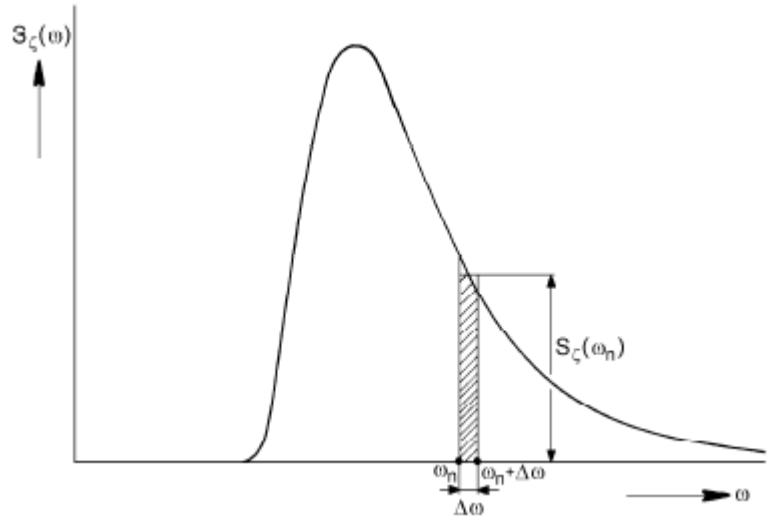

Figure 4.3 – Definition of Spectral Density (Journée and Massie, 2001)

Considering Δω → 0, the above equation becomes

$$S_\zeta(\omega_n) \cdot d\omega = \frac{1}{2} \zeta^2{}_{a_n} \qquad (4.3)$$

where it defines the definition of the wave energy spectrum $S_\zeta(\omega)$, and the variance $\sigma^2{}_\zeta$ can be expressed as

$$\sigma^2{}_\zeta = \int_0^\infty S_\zeta(\omega_n) \cdot d\omega \qquad (4.4)$$

Using statistics, the above equations implied to particular wave parameters that is significantly important.

Denotes m as a moment, then $m_{n\zeta}$ denotes the nth order moment given by

$$m_{n\zeta} = \int_0^\infty \omega^n \cdot S_\zeta(\omega_n) \cdot d\omega \qquad (4.5)$$

where $m_{0\zeta}$ is the area under the spectral curve (as defined as variance $\sigma^2{}_\zeta$), $m_{1\zeta}$ is the first order moment (static moment) of this area, and $m_{2\zeta}$ is the second order moment (moment of inertia) of this area.

The relation of these equations to the wave amplitude and height are:

$\zeta_{a_{1/3}} = 2 \cdot \sqrt{m_{0\zeta}}$ = significant wave amplitude

$H_{1/3} = 4 \cdot \sqrt{m_{0\zeta}}$ = significant wave height

and the characteristic wave periods can be defined from the spectral moments

$m_{1\zeta} = \omega_1 \cdot m_{0\zeta}$ where ω_1 is spectral centroid

$m_{2\zeta} = {\omega_2}^2 \cdot m_{0\zeta}$ where ω_2 is spectral radius of inertia

as follows:

$T_z = 2\pi \cdot \sqrt{\frac{m_{0\zeta}}{m_{2\zeta}}}$ = mean zero-crossing wave period

4.2.2 Pierson-Moskowitz Spectrum

Pierson and Moskowitz (1964) assumed that if the wind blew steadily for a long time and over a large area, it will result as an equilibrium condition with the waves. The terms "long time" here is roughly ten-thousand wave periods, and the terms "large area" is roughly five-thousand wave lengths on a side. This is the concept of a fully developed sea. The measurement of waves was made by accelerometers on British weather ships in the north Atlantic. (Stewart, 2008)

According to DNV (October 2010), The Pierson-Moskowitz (PM) spectrum $S_{PM}(\omega)$ is given by:

$$S_{PM}(\omega) = \frac{5}{16} \cdot {H_s}^2 {\omega_p}^4 \cdot \omega^{-5} exp\left(-\frac{5}{4}\left(\frac{\omega}{\omega_p}\right)^{-4}\right) \qquad (4.6)$$

where $\omega_p = 2\pi/T_p$ is the angular spectral frequency.

4.2.3 JONSWAP Wave Spectrum

In 1968 and 1969, an extensive wave measurement program known as Joint Operation North Sea Wave Project (JONSWAP) was carried out in over 100 miles line in the North Sea, starting from the Sylt Island. The analysis of measurement data resulted in a spectrum formulation for a fetch-limited wind generated seas. The description of the waves generated by local wind fields was proven with it (Felisita, 2009).

According to DNV (October 2010), the JONSWAP spectrum S_J (ω), which is formulated as a modification of the Pierson-Moskowitz spectrum, is given by:

$$S_J(\omega) = A_\omega S_{PM}(\omega)\gamma^{exp\left(-0.5\left(\frac{\omega-\omega_p}{\sigma\,\omega_p}\right)^2\right)} \quad (4.7)$$

where:

A_ω = 1-0.287 ln(γ) is a normalizing factor

$S_{PM}(\omega)$ = Pierson-Moskowitz spectrum

σ = spectral width parameter

σ = σ_a for ω < ω_p (for average value, σ_a = 0.07)

σ = σ_b for ω > ω_p (for average value, σ_b = 0.09)

γ = non-dimensional peak shape parameter, should be taken as

$\gamma = 5$ for $T_p/\sqrt{H_s} \leq 3.6$

$\gamma = \exp(5.75 - 1.15\frac{T_p}{\sqrt{H_s}})$ for $3.6 < T_p/\sqrt{H_s} < 5$

$\gamma = 1$ for $5 < T_p/\sqrt{H_s}$

4.3 Current

The current at the sea surface is mainly introduced by the wind effect on the water, variation of atmospheric pressure and tidal effects. Early years on offshore development believes that the currents was not exist below a water depth of about 1000 m. However, in recent days, it is recognized that a number of classes of currents exist in the deep waters, and some are known to extend to large depths. Examples of these classes of currents are tropical cyclones such as hurricanes, extra-tropical cyclones, and cold air outbreaks and currents arising from major surface circulation features (Chakrabarti, 1994).

The most common categories ocean currents are (DNV, 2010):

- Wind-generated currents, where the currents are caused by wind stress and atmospheric pressure gradient throughout a storm
- Tidal currents, where the currents are regular, following the harmonic astronomical motions of the planets, and generally weak in deep water, but are strengthened by shoreline configurations.
- Circulational currents, where the currents are steady, large-scale currents of the general oceanic circulation (i.e. the Gulf Stream in the Atlantic Ocean).
- Loop and eddy currents, where the currents can penetrate deeply in the water column.
- Solition currents, where the currents occur due to internal waves generated by density gradients.
- Longshore currents (littoral current), where the currents normally occur in coastal regions, and it runs parallel to the shore as a result of waves breaking at an angle on the shore.

DNV (2010) implies that the significant effects of current in the design of any offshore structures or pipeline riser should be considered. Among of these effects are:

- Large steady excursions and slow drift motions of moored platforms
- Drag and lift forces on submerged structures

- Rise to vortex induced vibrations on slender structural elements, and vortex induced motions on large volume structures
- Changing in wave height and wave period due to interaction between strong currents and waves
- Seabed scouring around bottom mounted structures

The current velocity may be modelled as a simple power law (assuming uni-directional current) when the field current measurements are not available. The total current velocity should be taken as the vector sum of each current component (i.e. wind generated, tidal, etc.) as below:

$$v_c(z) = v_{c,wind}(z) + v_{c,tide}(z) + v_{c,circ}(z) + \cdots \quad (4.8)$$

where:

$$v_{c,wind}(z) = v_{c,wind}(0)\left(\frac{d_0 + z}{d_0}\right) for - d_0 \le z \le 0 \quad (4.9)$$

$$v_{c,tide}(z) = v_{c,tide}(0)\left(\frac{d + z}{d}\right)^{\alpha} for\ z \le 0 \quad (4.10)$$

where:

$v_c(z)$ = total current velocity at level z

z = distance from still water level, positive upwards

$v_{c,tide}(0)$ = tidal current velocity at the still water level

$v_{c,wind}(0)$ = wind-generated current velocity at the still water level

d = water depth to still water level (taken positive)

d_0 = reference depth for wind generated current, d_0 = 50 m

α = exponent (typically = 1/7)

4.4 Floater Motions

A floater in the open sea is always encountered by the wind, wave and current. The motion response due to these environmental conditions can be divided into 6 degrees of freedom (DOF), as they are translational motions and rotational motions.

The translational motions are:

- Sway motion
- Surge motion
- Heave motion

In addition, the rotational motions are:

- Roll motion
- Pitch motion
- Yaw motion

The following figure shows the translational and rotational motions.

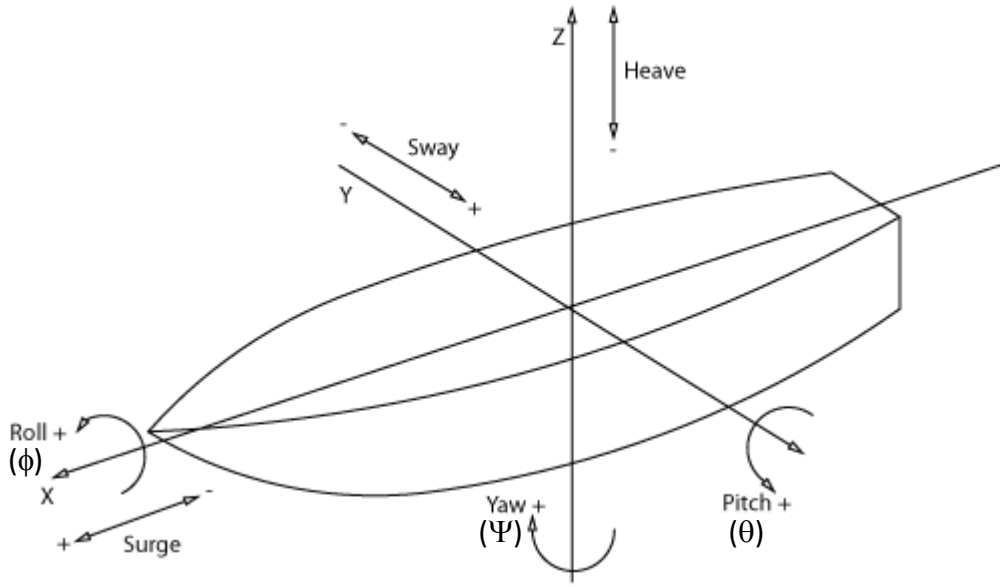

Figure 4.4 – Floater Motions in Six Degrees of Freedom (AT-Marine Oy, 2010)

To explain the relationship between waves and floater motion, consider the following figure that shows the three components in a block diagram, i.e. waves input, floating structure, and motions output.

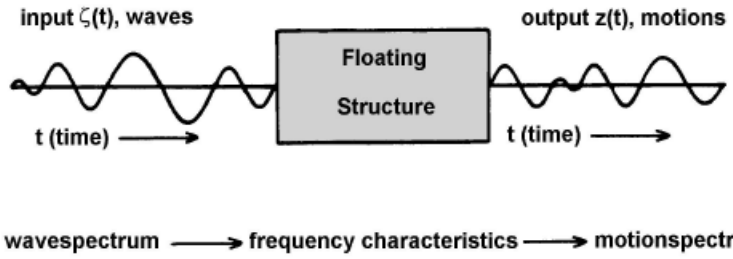

Figure 4.5 – Relation between Floater Motions and Waves (Journée and Massie, 2001)

The input for a linear characteristic from the system as shown above is coming from a random irregular wave, which the energy distribution over the wave frequencies is known (wave energy spectrum, refer to Section 4.2.1). The frequency characteristics from the floating structure can be found from model experiments of detail computations. The output of the system is motion of the floating structure. This floating structure motion has an irregular behavior just as the wave that causes the motion.

According to Journée and Massie (2001), in many cases, the ship motions have mainly a linear behavior. This means that the ratio between motion amplitudes and wave amplitudes at each frequency, and also the phase shifts between the motions and the waves, are constant. As the result, the resulting motions in irregular waves can be obtained by adding together results from regular waves of different amplitudes, frequencies and possibly propagation directions. By knowing the wave energy spectra and frequency characteristic response of the ship, the response spectra can be found.

Floater motions and floater offset constitute a source of both static and dynamic loading on the riser. The types of floater offset that normally considered are:

- Static (nominal) offset – mean offset due to average wave, wind, and current load

- Near offset – the floater is displaced along the plane of the riser towards the riser-seabed connection
- Far offset – the floater is displaced along the plane of the riser away from the riser-seabed connection
- Cross offset – the floater is displaced perpendicular to the plane of the riser

There are two terms of floater motions characteristic, i.e. wave frequency (WF) motion and low frequency (LF) motion. According to DNV (2010), the definitions of both terms are:

- WF (Wave Frequency) motion : the motions that are a direct consequence of first order wave forces acting on the floater, causing the platforms to move at periods typically between 3-25 seconds.
- LF (Low Frequency) motion : motion response at frequencies below wave frequencies at, or near surge, sways, and yaw eigen periods for the floater (second order wave forces). LF motions typically have periods ranging from 30 to 300 seconds.

The WF floater motions are usually given as RAO's.

4.5 RAO

Response Amplitude Operator (RAO) is a dimensionless parameter to generate the response spectrum from the energy spectrum. It is also often called as a transfer function. For a floater which encountered by irregular wave, the vessel response spectrum of motion for each degree of freedom (e.g. heave, roll, etc.) can be found by using the transfer function for each individual motion and the wave energy spectrum.

The equation of wave energy spectrum is already defined in equation (4.3) as

$$S_\zeta(\omega_n) \cdot d\omega = \frac{1}{2}\zeta_a^2(\omega) \qquad (4.11)$$

The energy spectrum, for example, of the heave response z(ω,t) can be defined by:

$$\begin{aligned} S_z(\omega_n) \cdot d\omega &= \frac{1}{2} z_a^2(\omega) \\ &= \left|\frac{z_a}{\zeta_a}(\omega)\right|^2 \cdot \frac{1}{2}\zeta_a^2(\omega) \\ &= \left|\frac{z_a}{\zeta_a}(\omega)\right|^2 \cdot S_\zeta(\omega) \cdot d\omega \end{aligned} \qquad (4.12)$$

Hence, the heave response spectrum can be found by using the transfer function of the motion and the wave energy spectrum by:

$$S_z(\omega) = \left|\frac{z_a}{\zeta_a}(\omega)\right|^2 \cdot S_\zeta(\omega) \qquad (4.13)$$

where:

$z_a(\omega)$ = heave amplitude

$\zeta_a(\omega)$ = wave amplitude

$S_\zeta(\omega)$ = wave energy spectrum

The following figure shows an example of heave response spectrum taken from a container ship which sailing in head waves with significant wave height of 5.0 m and period of 6.0 s.

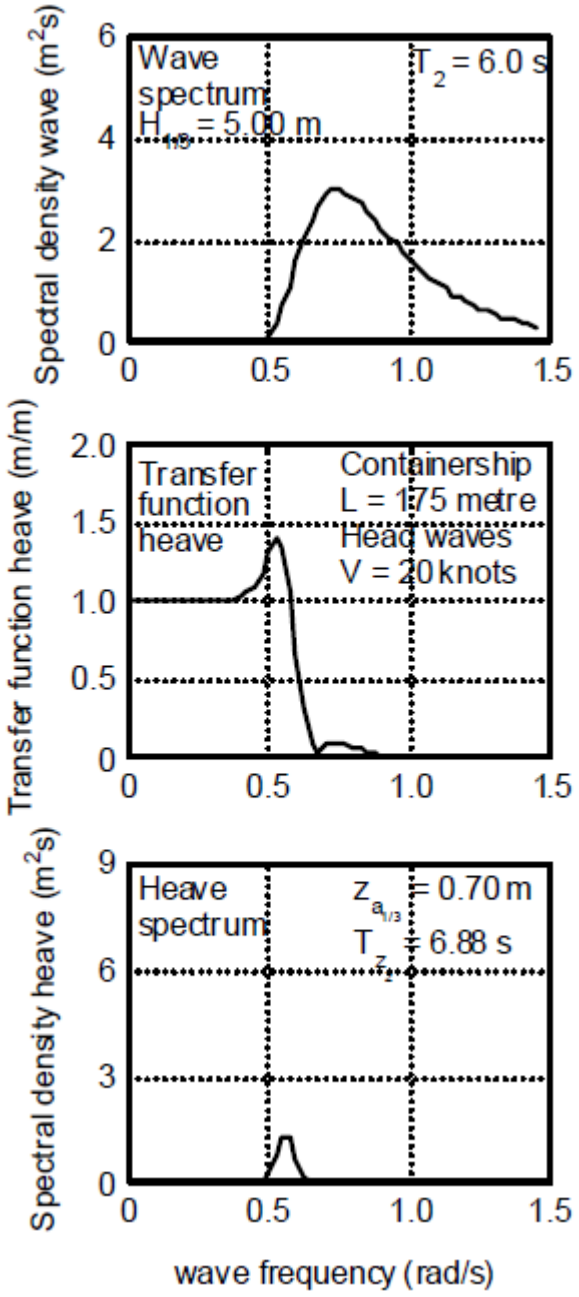

Figure 4.6 – Example of Wave Energy Spectrum, RAO (Transfer Function) of Heave, and Heave Energy Spectrum (Journée and Massie, 2001)

4.6 Hydrodynamic Load Effect

The hydrodynamic load effect on riser can be expressed by the Morison equation in terms of relative fluid-structure velocities and accelerations. The component includes hydrodynamic load in normal pipe and tangential pipe directions. For circular cross-section, the Morison equation can be expressed as (DNV, 2010):

$$f_n = \frac{1}{2}\rho C_D^n D_h |v_n - \dot{r}_n|(v_n - \dot{r}_n) + \rho\frac{\pi D_b^2}{4} C_M^n \dot{v}_n - \rho\frac{\pi D_b^2}{4}(C_M^n - 1)\ddot{r}_n \quad (4.14)$$

$$f_t = \frac{1}{2}\rho C_D^t D_h |v_t - \dot{r}_t|(v_t - \dot{r}_t) + \rho\frac{\pi D_b^2}{4} C_M^t \dot{v}_t - \rho\frac{\pi D_b^2}{4}(C_M^t - 1)\ddot{r}_t \quad (4.15)$$

where:

f_n = force per unit length in normal direction

f_t = force per unit length in tangential direction

ρ = water density

D_b = buoyancy diameter (i.e. equivalent diameter for description of resulting buoyancy on a general riser cross section)

D_h = hydrodynamic diameter

$v_n, \dot{v}_n$ = fluid velocity and acceleration in normal direction

$\dot{r}_n, \ddot{r}_n$ = structural velocity and acceleration in normal direction

C_D^n, C_M^n = drag and inertia coefficients in normal direction

$v_t, \dot{v}_t$ = fluid velocity and acceleration in tangential direction

$\dot{r}_t, \ddot{r}_t$ = structural velocity and acceleration in tangential direction

C_D^t, C_M^t = drag and inertia coefficients in tangential direction

The above drag and inertia coefficients are dependent on several parameters, i.e.:

- Body shape;
- Reynolds number (Re = UD/ν), where U is the free stream velocity, D is the diameter of object considered, and ν is the kinematic viscosity;
- Keulegan Carpenter number KC = U_MT/D, where U_M is the free stream velocity amplitude of the oscillatory flow, and T is the period of oscillation;
- Roughness ratio k/D, where k is the characteristic dimension of the roughness on the body;
- Reduced velocity U/f_nD, where f_n is the natural frequency of the riser
- Relative current number U_c/U_M, where U_c is the current velocity

Considering the above mentioned parameters, it is obvious that the hydrodynamic loading according to the Morison formulation is a major source to nonlinearities in the response characteristic of slender structures, as also implied by DNV (2010).

4.7 Soil-Riser Interaction

Soil condition at the seabed plays important role in riser design, especially in fatigue damage. At touch down point (TDP) region of the riser, out-of-plane motions will occur as a consequence of oscillatory forces caused by transverse wave acting on the free hanging part of the riser. Depending on the stiffness and friction of the seafloor, out-of-plane bending stresses will be more or less concentrated in this TDP region when the riser is subjected to oscillatory motion. The pipe-soil interaction is commonly modeled by use of friction coefficient (sliding resistance) and linear springs (elastic soil stiffness) (Bai, 2005).

4.8 Global Analysis

In riser analysis, the purpose of performing the global analysis is to capture the overall responses from the rises system. These responses come from static and dynamic structural behavior in such particular environmental loading condition. From DNV (2010), the global response quantities can be grouped into four main categories, i.e.:

- Cross-sectional forces, e.g. effective tension, bending moments, torsional moment
- Global riser deflections, e.g. curvature, elongation, angular orientation
- Global riser position, e.g. co-ordinates, translations, distance to other structures, position of touch-down point (TDP) on seafloor, etc.
- Support forces at termination on rigid structures

A finite element approach is normally considered for global riser system analysis. It is strongly required to understand the basic modelling parameter in order to generate accurate result, e.g. regular or irregular loading due to waves and floater motions, current modelling, hydrodynamic parameter, special components modelling (buoyancy module, hinges, etc.), seafloor contact formulations, etc.

4.8.1 Static Analysis

The first step in global riser analysis is a static analysis. This step is required in order to develop further analysis, such as eigenvalue and dynamic analyses. The purpose of the static analysis is to establish the static equilibrium configuration due to static loading for given locations of riser terminations to rigid structures (e.g. terminations to floater and seafloor). There are four basic static loading components according to DNV (2010). These loading components are explained below:

1. Volume forces
   Static profile equilibrium on volume forces basis can be derived by simplified the calculations based on the effective tension and effective weight (Barltrop, 1998). The following figure shows the equilibrium state from a segment of curved pipe under the combined effects of tension, hydrostatic, and internal fluid pressure, where the expression can be equated to equilibrium by the considering equal and opposite pressure over the end faces of the segment.

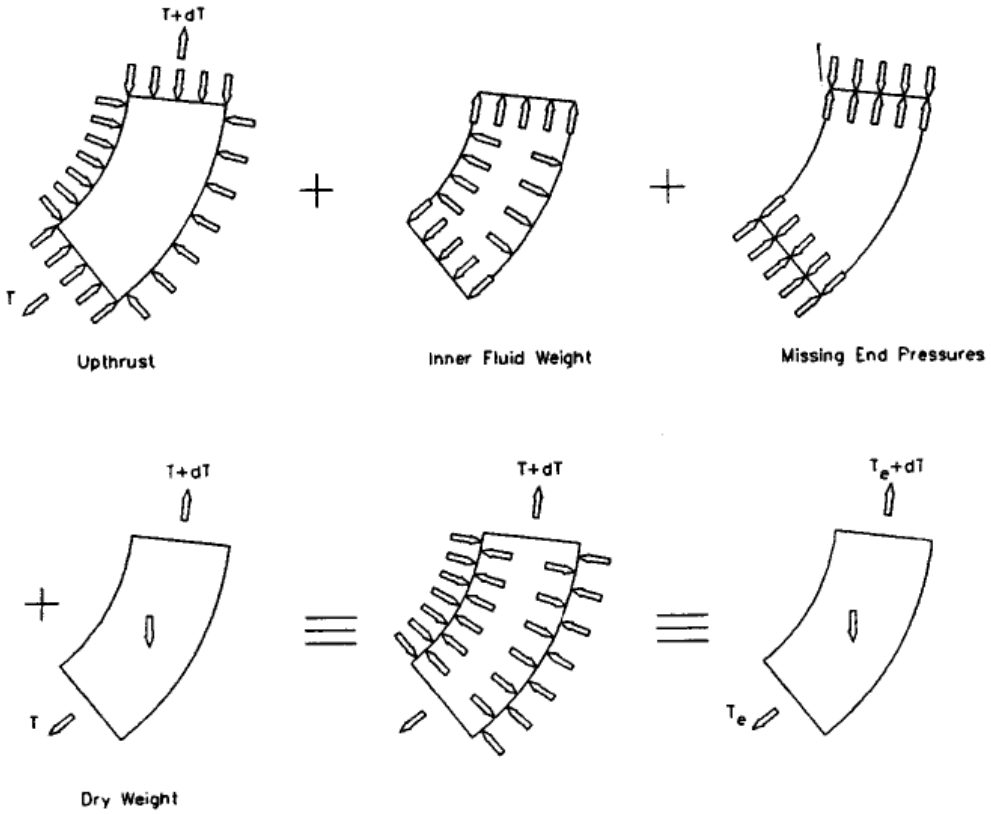

Figure 4.7 – Effective Weight and Tension (Barltrop, 1998)

The derivation formula for the effective weight and tension based on above figure are as follow:

$$W_{eff} = \gamma_s A_s + \gamma_i A_i - \gamma_o A_o \qquad (4.16)$$

$$T_{eff} = T_i + P_o A_o - P_i A_i - \rho_i U_i^2 A_i \qquad (4.17)$$

where:

γ	=	weight density
A	=	area
P	=	pressure
T	=	tension
ρ	=	mass density
U	=	flow velocity

i	=	subscripts for 'internal'
o	=	subscripts for 'external'
s	=	subscripts for 'structural'
t	=	subscripts for 'true'

2. Specified forces
   During installation or operating condition, specified tension forces are normally applied on top of the riser section, in order to keep the riser under particular tension state, and to avoid compression force which might lead to buckling. This additional force should also be accounted for the static equilibrium condition.

3. Prescribed displacements
   The prescribed displacements are used in order to simulate the static equilibrium condition from a stress-free condition (e.g. as laid condition) into a specified position. Some example on this case is a pull-in analysis during riser installation, where a riser that has been laid on the seabed is going to be connected to the wellhead.

4. Displacement dependent forces (current loading)
   Some example of displacement dependent forces is current load. In order to determine the final static equilibrium conditions, it is important to see the relative magnitude effect of current load in comparison to the effective weight of the riser. The steady current will induce the drag forces on the riser, and on the sub-surface buoyancy (if any). The result will show whether or not the current has a significant effect on the static configuration.

4.8.2 Eigenvalue Analysis

To avoid the so called 'resonance effect' due to dynamic response of the structure, it is important to check the modes (and correspondent frequencies) of the riser system. The purpose of eigenvalue analysis is to calculate the natural frequencies of the structure and the corresponding stress due to associated mode shapes. This analysis is normally performed as the first step prior to the dynamic analysis.

In case for Vortex Induced Vibration (VIV), eigenvalues analysis of the structure is very important. On each eigen frequencies on each mode shapes of the structure that close to the vortex shedding frequency, the structure might be excited and start to vibrate. The vibration amplitudes create cyclic loads that lead to fatigue damage on the structure.

4.8.3 Dynamic Analysis

The floater motions, station-keeping system such as mooring system and the risers creates a complex dynamic response to the environmental loading from wind, waves and current. Nonlinearities arise with respect to geometric stiffness, hydrodynamic loads, materials and riser components contact interfacing with other components. Common methods to analyze these nonlinearities are frequency domain analysis and time domain analysis.

4.8.3.1. Frequency Domain Analysis

According to DNV (2010), this method is based on linearization of stiffness, damping, inertia, and external forces at static equilibrium position (i.e. structural and load linearization). For irregular analysis, a stochastic linearization for combined wave/current loading is required.

The structural response will be represented by a spectrum, which means that the statistical properties of the response are known, and the response process (time history) will always be Gaussian. Consequently, non-symmetric response i.e. due to non-symmetric wave loading close to mean water level, cannot be correctly described (Larsen, 1987).

4.8.3.2. Nonlinear Time Domain Analysis

DNV (2010) describes this method as a step by step numerical integration of the incremental dynamic equilibrium equations based on Newton-Raphson method. A good representation of the riser system's characteristics non-Gaussian response will be resulted as the consequence of the nonlinear approach on all nonlinear effects.

According to Larsen (1987), wave loads can be better described in this method compared to the frequency domain method. However, this statement is valid only for such effect, e.g. the unsymmetrical effect when current and waves are combined, variation of wet surface (load area) of the riser due to varying sea surface elevation in waves, the fact that a specific riser cross section will move and hence not stay in a position where wave induced velocities and accelerations can be calculated independently of riser displacements, non-linear wave theories.

4.8.4 Coupled/Uncoupled Analysis

Floater, risers, and station keeping system (mooring lines) are resulting in a complex dynamic system respond when they interact with the environmental loads. Moreover, current loading and damping influences due to slender structures attaced to the floater (i.e. riser, tethers, and mooring lines) may significantly influence the LF floater motions, in particular in deep water condition. As the consequence, it is important to determine the coupling effects when deriving the floater motion response as well as the riser response.

According to DNV (2010), the combined irregular wave frequency (WF) and low frequency (LF) environmental loading should be considered in riser analysis if riser dynamics is significantly influenced by low frequency excitation. This can be achieved by consistently representing the fully coupled analysis where the floater force model is introduced in a detailed Finite Element (FE) model of the complete slender structure system including all mooring lines and risers. However, DNV (2010) implies that this method requires substantial computational efforts and therefore should be considered as a tool for final verification purposes.

In order to capture the coupling effect with such a computational efficiency, the floater motion and slender structure analyses are then carried out separately. This is called un-coupled analysis. The first step is always a floater motion analysis, which is then applied as loading in terms of forced boundary displacements in subsequent slender structure analysis (i.e. individual riser or mooring line analysis).

In this thesis work, the un-coupled floater motion analysis is considered. The WF floater motions are considered as dynamic excitation using floater RAO transfer function, while LF floater motions are accounted for by an additional representative floater offset. The slender structure is consequently assumed to respond quasi-statically to LF floater motions.

4.9 Time Domain Fatigue Analysis

According to DNV (2010), the fatigue analysis should be based on S-N data, determined by fatigue testing of the considered welded detail, and the linear damage hypothesis. The stress range may be found by deterministic or spectral analysis. The determination of stress history shall consider the dynamic effects. This stress history can be defined as expected number of cycles at each stress range level during the predicted life span, and the practical application of this is to establish a long term stress range history that is on the safe side.

The basic fatigue capacity is given in terms of S-N curves, where S is a given constant stress range, and N is the number of stress cycle to failure. The expression of this S-N curve is given as

$$N = \bar{a}S^{-m} \qquad (4.18)$$

or equivalently:

$$\log(N) = \log(\bar{a}) - m\log(S) \tag{4.19}$$

where:

$\bar{a}$ and m are empirical constant established by experiments.

The stress range to be applied in fatigue damage calculation is given as:

$$S = S_0 \cdot SCF \cdot \left(\frac{t_3}{t_{ref}}\right)^k \tag{4.20}$$

where:

S_0 = Nominal stress range

SCF = Stress Concentration Factor

$\left(\frac{t_3}{t_{ref}}\right)^k$ = Thickness correction factor, where this factor applies for pipes with a wall thickness t_3 greater than a reference wall thickness, t_{ref} = 25 mm.

Bilinear (two-slope) S-N curves in log-log scale are also frequently applied for representation of the experimental fatigue data:

$$N = \begin{cases} \overline{a_1} S^{-m_1} & \text{for } S > S_{SW} \\ \overline{a_2} S^{-m_2} & \text{for } S \leq S_{SW} \end{cases} \tag{4.21}$$

where:

S_{SW} is the stress at intersection of the two SN curves given by:

$$S_{SW} = 10^{\left(\frac{\log(\overline{a_1}) - \log(N_{SW})}{m_1}\right)} \tag{4.22}$$

and N_{NW} is the number of cycles which change in slope appears. The typical Log (N_{SW}) is 6-7. The following figure shows the basic definitions for two-slope SN-curves.

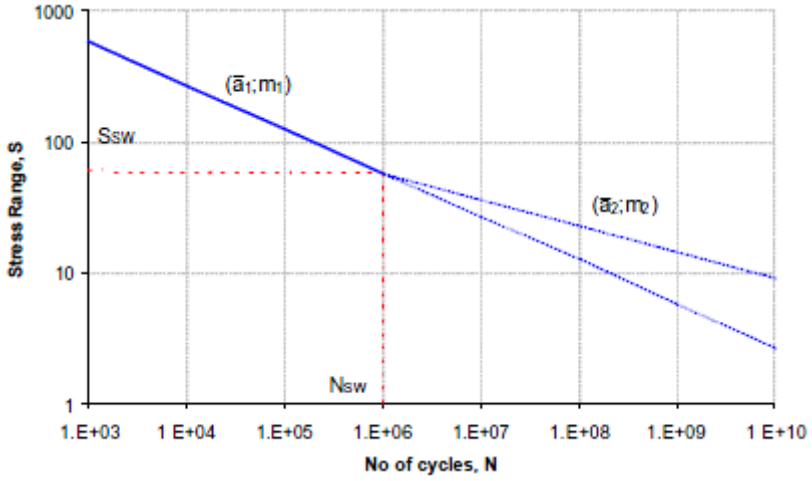

Figure 4.8 – Basic definitions for two-slope SN-curves (DNV-OS-F201, 2010)

The accumulation of fatigue damage from stress cycles is adopting the Miner-Palmgren rule as below:

$$D = \sum_i \frac{n(S_i)}{N(S_i)} \qquad (4.23)$$

where:

$n(S_i)$ is the number of stress cycles with range Si and $N(S_i)$ is the number of stress cycles to failure as mentioned in eq. (4.24).

There are three different contributions to fatigue damage that should be assessed, i.e. the wave-induced, the low-frequency, and the vortex-induced-vibration (VIV) stress cycles.

The procedures for calculating fatigue damage contributions for wave and low-frequency fatigue damage are (DNV, 2010):

- Divide the wave environment scatter diagrams into a number of representative blocks
- Select a single sea-state to represent all the sea-states within the block. This representative sea-state has the highest occurrence within the block.
- Calculate the fatigue damage within each simulation using rain-flow counting procedure and weight that with the probability of each block
- Sum-up the fatigue damage over all the blocks and obtain the fatigue damage for that direction
- Repeat the same procedure for other directions and sum-up the total fatigue damage by applying directional probabilities
- The predicted fatigue life is the reciprocal of this cumulative damage rate.

The VIV fatigue analysis is based on VIVANA theory manual developed by Norwegian Marine Technology Research Institute (Marintek). The analysis procedure is outlined as follow (Marintek, 2005):

- Static analysis
  Find the static shape configuration of the riser based on the defined boundary condition.
- Eigenvalue analysis
  Calculate the eigenfrequencies and corresponding mode shapes of the structure. In this step, added mass is initially applied as for non-responding riser in still water.
- Identification of possible and dominating excitation frequencies
  Based on the calculated eigenfrequencies, a complete set of possibly active eigenfrequencies is observed. Since the added mass will differ under VIV condition, iteration should be performed for each frequency candidate in order to find a set of possible response frequencies. The set of these frequencies are then associated to an excitation zone. The dominating response frequency among the others is then captured.
- Analysis of the response at the dominating frequency
  Calculate the dynamic response of the dominating frequency from the previous step. The analysis applies an iteration that shall converge for non-linear models for any excitation and damping. The local response amplitude and phase are considered in this iteration.
- Post-processing
  The post-processing includes the calculation of fatigue damage based on the relevant S-N curve. Sum-up the fatigue damage over the long-term current distribution for various velocities and direction.

5. Design Basis

5.1 Introduction

This chapter gives detailed descriptions about the design basis and design parameter of the COBRA riser concept that is considered in this thesis work.

5.2 System Overview

Catenary Offset Buoyant Riser Assembly (COBRA) consists of a catenary riser section with a long, slender buoyancy module on top which is tethered down to sea bed. The top of the catenary riser section is connected to the host platform by flexible jumper.

The general COBRA riser arrangement is shown in the following figure.

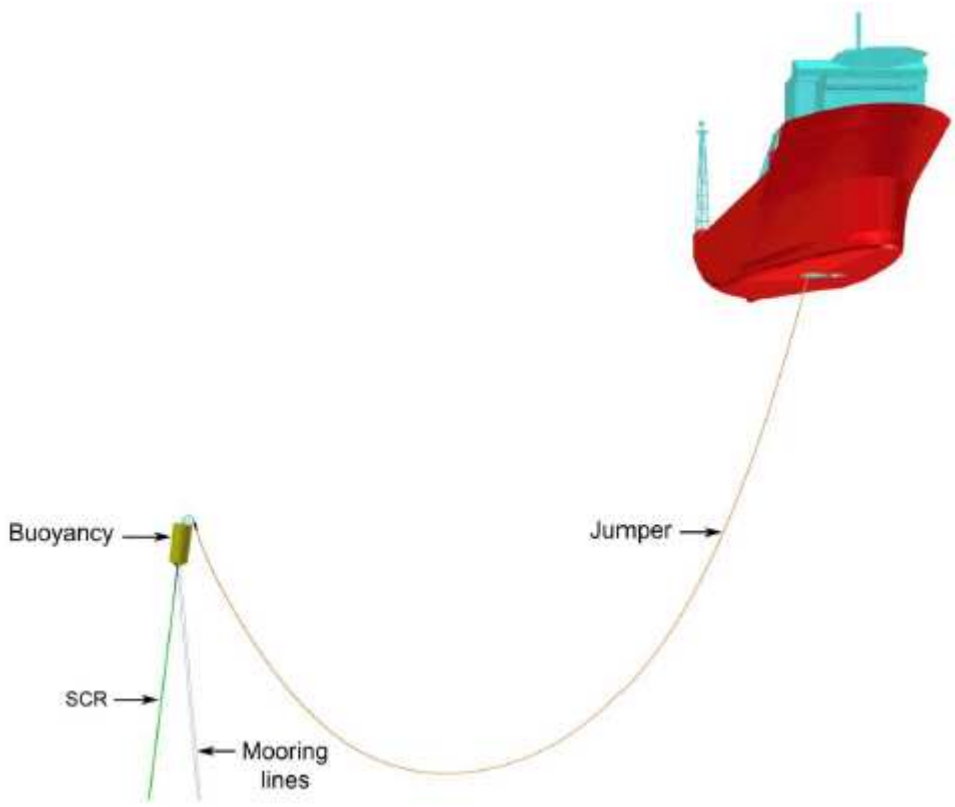

Figure 5.1 – COBRA riser arrangement (Karunakaran et al, 2011)

5.3 Design Parameter

The following sections provide detail design parameters that used in this thesis work.

5.3.1 Environmental Data

Sea water

The water depth considered in this thesis work is 2200 m. The sea water density is 1025 kg/m^3.

Waves

The wave and current data are taken from the metocean data on Central Cluster of Santos Basin, located at Sao Paulo Plateau, southern Brazilian oceanic region.

The extreme sea-state is modelled by irregular waves, using modified JONSWAP spectrum taken from the metocean data. The following table provides the extreme wave data for 10-year and 100-year return period.

	10-year	100-year
Significant wave height, H_s (m)	9.3	11.6
Corresponding wave peak period, T_p (s)	14.5	16.3

Table 5.1 – Wave Data

Current

The current flow direction is assumed to be in the same direction as vessel offset. However, according to Vogel et al. (2010), there were some events identified that the current direction was abruptly change in the Santos Basin area. The number of events was greatly identified at the 0-150 m layer and at 250-400 m layer during Fall 2006, and at the 150-250 m layer during Winter 2008. In general, all these events were identified among the 0-400 m layer, and they might related to the meanders or eddy on the unstable Rossby wave trains region.

The most extreme current profiles for 10-year and 100-year period are considered and presented in the following table.

Water depth (m)	10-year current		100-year current	
	Surface profile (m/s)	Mid-Level Profile (m/s)	Surface profile (m/s)	Mid-Level Profile (m/s)
At surface	0.92	0.36	1.05	0.42
-50	0.90	0.42	1.03	0.48
-100	0.77	0.42	0.89	0.45
-150	0.77	0.39	0.89	0.44
-200	0.76	0.37	0.89	0.46
-250	0.69	0.39	0.81	0.46
-300	0.62	0.39	0.73	0.53
-350	0.55	0.47	0.65	0.53
-375	0.48	0.47	0.59	0.54
-800	0.36	0.42	0.43	0.47
-1200	0.27	0.43	0.32	0.48
-1600	0.25	0.38	0.29	0.44
-2000	0.29	0.33	0.32	0.38
-2200	0.24	0.4	0.27	0.46

Table 5.2 – Current Profiles

The sudden change phenomenon on the current direction is considered by conservatively assuming two-directions of current profile occur at the same time at water depth 250 m. This assumption applies for both surface profile and mid-level profile current. Figures below show the comparison between typical one direction current profile and two directions current profile.

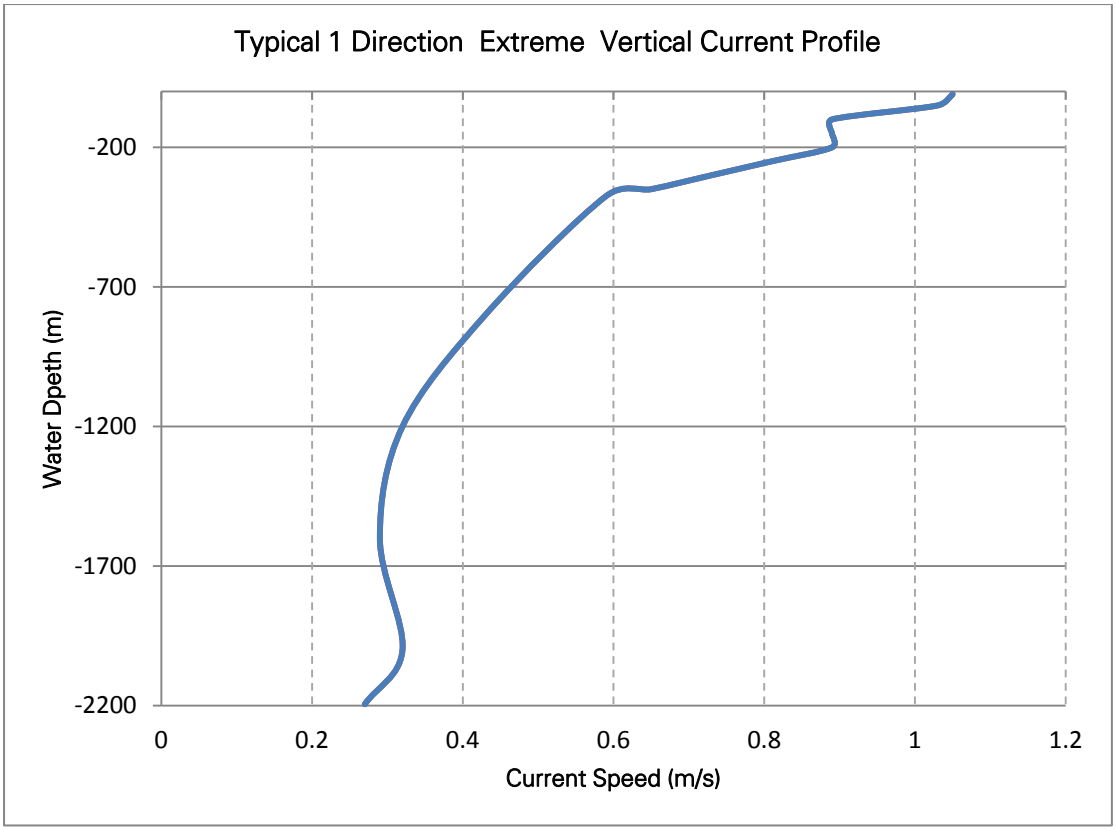

Figure 5.2 – Typical Unidirectional (1-Direction) Current Profile

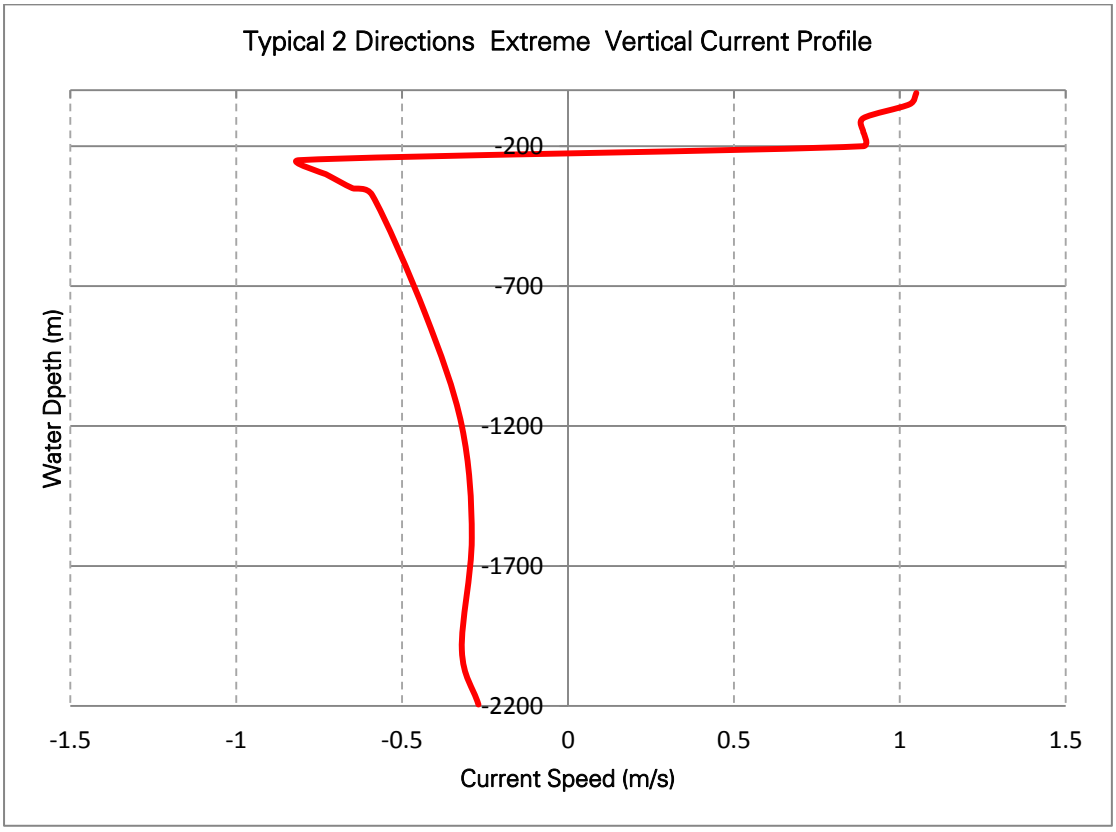

Figure 5.3 – Typical Bidirectional (2-Directions) Current Profile

Marine Growth

Marine growth is considered for the flexible jumper section. The following marine growth thickness is used in this thesis work:

Water Depth (m)	Marine Growth Thickness (mm)
+2 to -40	60
Below -40	30

Table 5.3 – Marine Growth Thickness

Hydrodynamic Coefficients

The following hydrodynamic coefficients are used in this thesis work:

Parameter	Coefficient
C_D, flexible jumpers	0.8
C_D, SCRs	1.1
C_M, flexible jumpers and SCRs	1.0

Table 5.4 – Hydrodynamic Coefficients

The axial directions on drag and inertia forces of the risers are not considered in this thesis work.

Soil-riser Interaction

The soil-riser interaction is modelled by linear soil stiffness and friction. The soil-riser parameters used in this thesis work are as follows:

- Lateral friction coefficient : 0.5
- Axial friction coefficient : 0.3
- Horizontal lateral/axial soil stiffness : 200 kN/m^2
- Vertical soil stiffness : 50 kN/m^2

5.3.2 Vessel Data

The response amplitude operators (RAO) of typical turret moored FPSO are used in this thesis work. The vessel will be considered in three positions, i.e. the zero mean offset position (nominal position), near offset position, and far offset position.

The following vessel offsets are used in the strength analysis:

Type of Analysis	Case	Vessel Offset
Static	10 year current	± 80 m
	100 year current	± 80 m
Dynamic	100 year sea-state / 10 year current	± 80 m
	10 year sea-state / 100 year current	± 80 m

Table 5.5 – Vessel Offset

Taut moored system is considered in this thesis. Hence, the vessel offsets are low. For a spread moored system, the offsets will be in order of 8% of water depth, which will require a slightly spread out system.

5.3.3 Riser & Jumper Data

Riser

Minimum riser wall thickness is estimated based on burst, collapse and combined loading criteria in accordance with DNV-OS-F201 and DNV-OS-F101. The estimation calculation is presented in Appendix A.

The riser has a 10 m tapered stress joint section with a maximum wall thickness of 2.5", connected towards the subsurface buoy. The following table provides the riser properties that are used in this thesis work.

Parameter	Value	Unit
Inner diameter (10" riser)	254	mm
Design pressure	500	bar
Density of internal fluid	500	kg/m^3
Wall thickness	26	mm
Riser material	Carbon Steel, grade X65	
Young's Modulus (E)	207000	MPa
Specified Minimum Yield Stress (SMYS)	448	MPa
Material Density	7850	kg/m^3
Thickness of coating	76.2	mm
Density of coating	700	kg/m^3
Mass including coating	244	kg/m
Safety Class	High	
Corrosion allowance	3	mm

Table 5.6 – Riser Properties

Jumper

The following table provides the flexible jumper properties that are used in this thesis work. The jumper sizing is based on internal diameter and limitation in minimum allowable tension.

Parameter	Value	Unit
Design Pressure	500	bar
10" Jumper above -40 m water depth		
Internal Diameter	254	mm
Outer diameter including marine growth	544	mm
Mass including marine growth	508	kg/mm
10" Jumper below -40 m water depth		
Internal Diameter	254	mm
Outer diameter including marine growth	484	mm
Mass including marine growth	444	kg/mm

Table 5.7 – Flexible Jumper Properties

5.3.4 Internal Fluid Data

The internal fluid condition that is considered in this thesis is oil fluid with density of 500 kg/m3 with correspondences internal pressure of 500 bar.

5.3.5 Subsurface Buoy Data

The concept of COBRA riser includes the usage of sub-surface buoy as the interface between the top section of flexible jumper and the bottom section of SCR. The sub-surface buoy that is considered in this thesis work is a single long slender cylinder buoy shape.

The following table provides the subsurface buoy data:

Parameter	Value	Unit
Outer Diameter	7.0	m
Length	14.0	m
Weight in water	-386	Te
Mass	165.7	Te
Ratio of weight in water and displacement	0.7	

Table 5.8 – Subsurface Buoy Properties

The figure below shows the sub-surface buoy configuration.

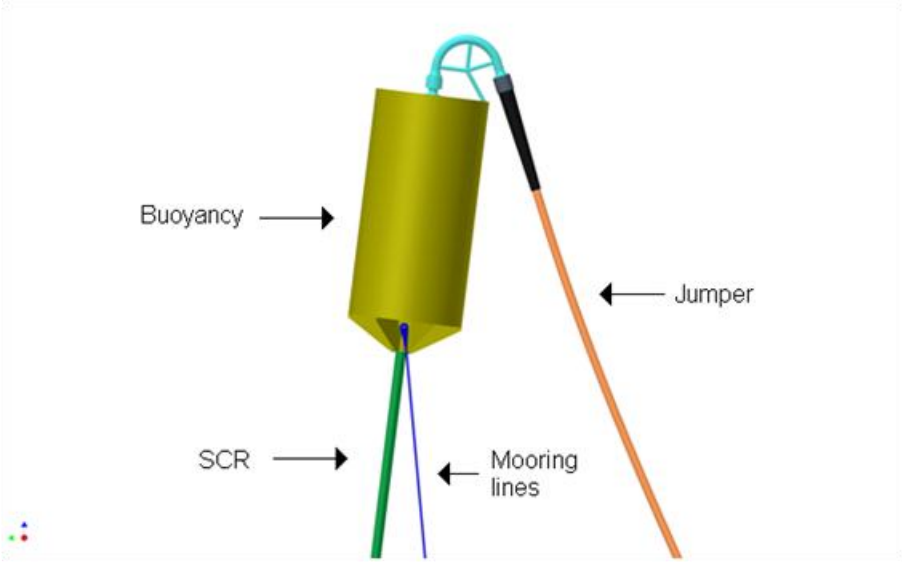

Figure 5.4 – Buoy Configuration Layout (Karunakaran et al, 2011)

In this thesis, sensitivity studies are performed in this buoy configuration, including setting up the buoy vertical position in deeper water depth, and putting the jumper connection below the buoy.

5.3.6 Buoy Mooring Line Data

The mooring lines connect the buoy and tethered it to the seabed. There are two mooring lines used in this COBRA riser concept. The lines are connected underneath the buoy, one to each side of SCR connection point, resulting in 3.0 m distance between each other.

The following figure shows the mooring lines connection configuration to the buoy.

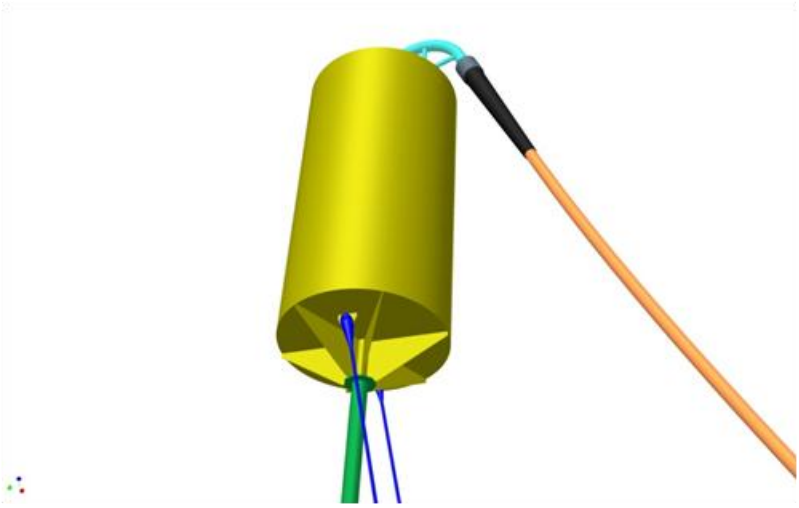

Figure 5.5 – Mooring lines connection points (Karunakaran et al, 2011)

The mooring line properties are provided in the table below.

Parameter	Value	Unit
Outer Diameter	135	mm
Mass in air	13	kg/m
Axial stiffness	400	MN
Torsional stiffness	80	$kN.m^2$

Table 5.9 – Mooring Line Properties

The Base Case in this thesis is using the anchor points which are spaced in the same distance as for the connection points at the buoy.

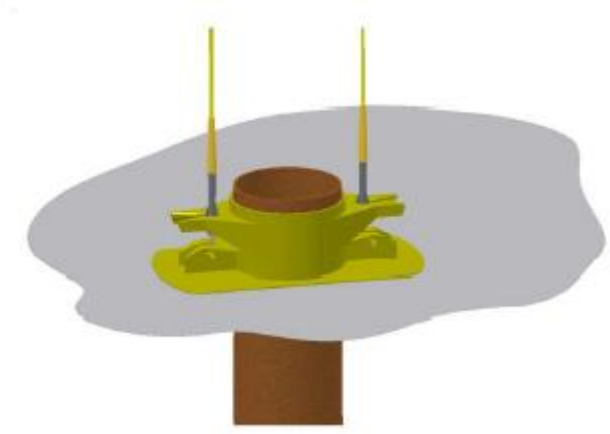

Figure 5.6 – Anchor points (Karunakaran et al, 2011)

Sensitivity studies are performed for this anchor points by setting up various set of parallel distance on the anchor point's position at the seabed.

5.4 Model Overview

In this thesis work, the OrcaFlex software is used as a tool for modeling and analysis. The COBRA riser model consists of 3D finite element model of a single flexible jumper, a slender sub-surface buoyancy module, and a single Steel Catenary Riser (SCR). In addition, representative FPSO geometry model is also used.

For Base Case model, the top end of flexible jumper is connected to the FPSO at -16 m below the surface level. The bottom end is connected to the sub-surface buoyancy module, located at -250 m below the surface. Two mooring lines connect the buoy and tethered it to the seabed. The lines are connected at the bottom of sub-surface buoy, one to each side of SCR connection point, resulting in 3.0 m distance between each other. The anchor points are spaced in the same distance as the connection point at the buoy. The SCR section is hanging at the sub-surface buoy, and laying to the seabed in simple catenary configuration.

The following figures show the Base Case model configuration.

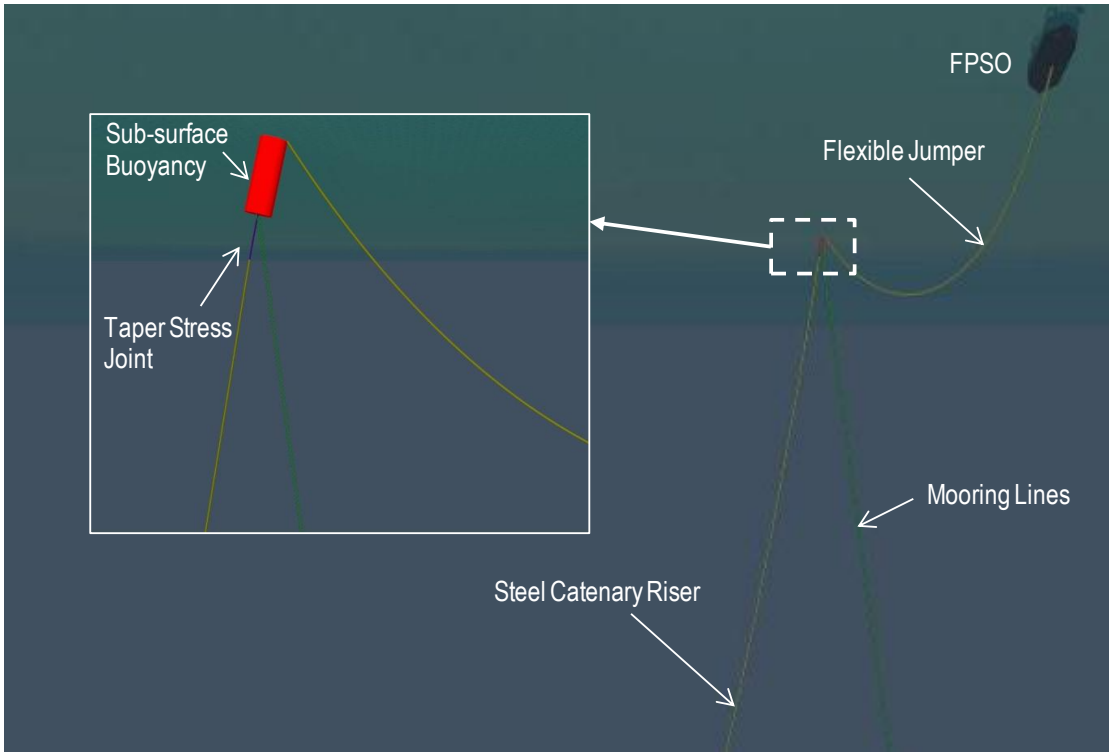

Figure 5.7 – Base case 3D OrcaFlex Model

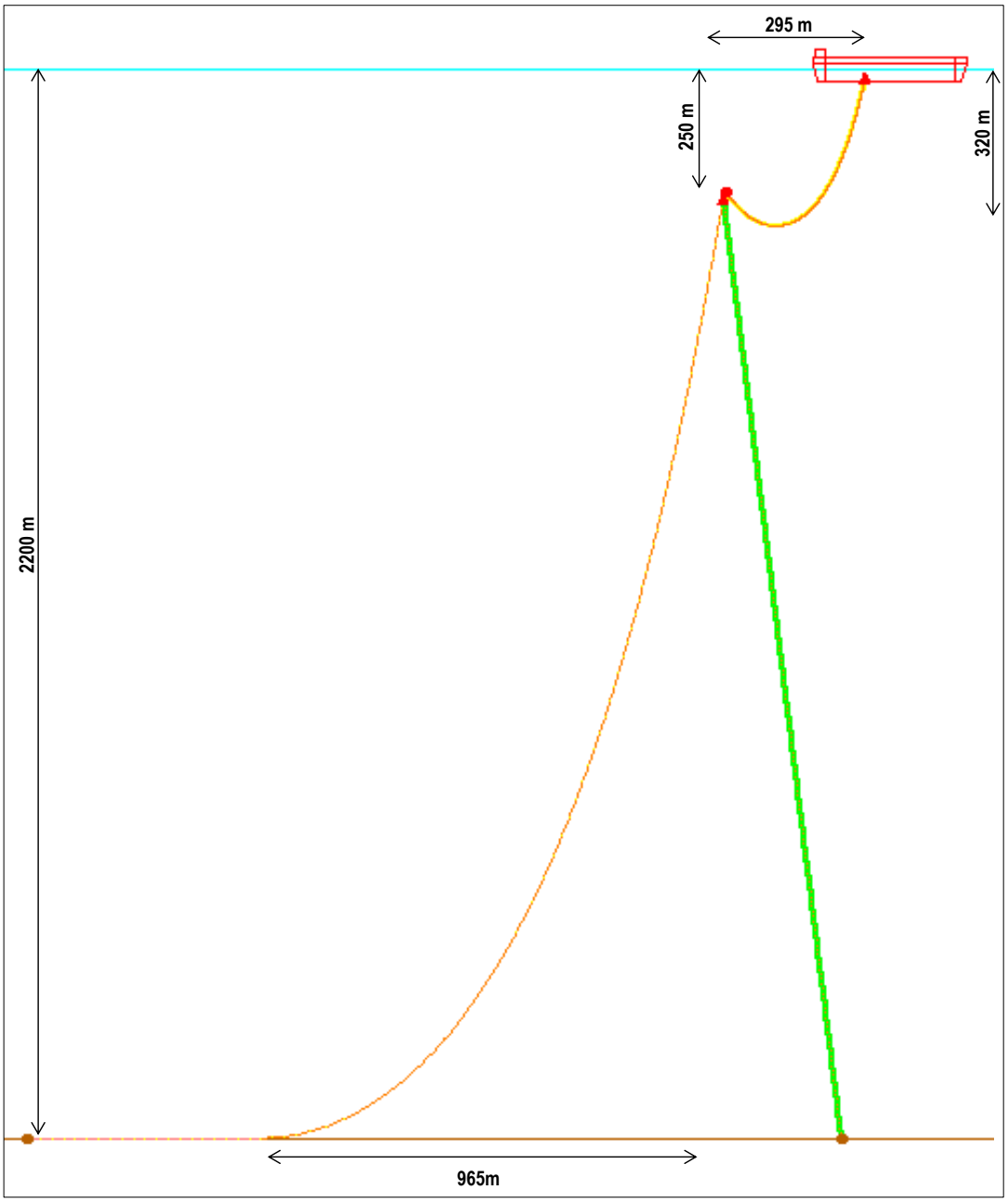

Figure 5.8 – Base Case Static Configuration (Elevation View)

The vessel and riser configuration is placed in the worst case scenario in conjunction with the extreme wave and current directions. The X axis in the following figure denotes the wave and current in 0 degree direction and the Y axis denotes the wave and current in 90 degree direction. However, only 0 and 180 degree directions of wave and current are considered in the analysis as these scenarios will give the worst impact to the riser.

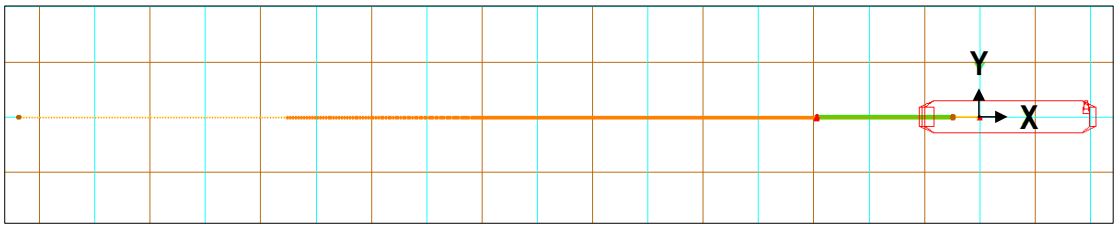

Figure 5.9 – Base Case (Plan View)

Riser and Mooring length

For Base Case study, the flexible jumper length is 535 m, and the SCR riser length is 2775 m. The mooring lines length is 1950 m for each line.

Riser segment

The riser model that is used in the finite element analysis is modelled using segmented model. Various segments length in the riser model is used in order to capture adequate representative riser response in particular critical section, e.g. top-end connection, sag-bend, touch-down area. The segment lengths that are considered in this thesis work are:

- Flexible jumper : 1 m
- Mooring line : 10 m
- SCR (tapered-stress-joint) : 0.1 m
- SCR (near tapered-stress-joint) : 1 m
- SCR (other section) : 5 m

For fatigue analysis, additional segment length is used in touch down area, i.e.:

- SCR (touch down zone) : 2.5 m

5.5 Analysis Cases

In this thesis work, the analyses are consist of two parts, i.e. Base Case model and Sensitivity Case model. The Base Case model arrangement is described in Section 5.4, and detail analysis result is presented in Chapter 6. The sensitivity models analyses result are presented in Chapter 7.

For both Base Case and sensitivity case model, the strength analyses include static and dynamic analysis in Ultimate Limit State (ULS) and Accidental Limit State (ALS) design condition. The accidental case condition is analyzed considering losing one of the mooring lines. Time-domain fatigue analysis is performed for Base Case model only, and it is based on Fatigue Limit State (FLS) design condition.

The sensitivity model consists of three cases, which include different case parameters. These cases are described in the following table.

Case	Parameter	Description	Design Condition
Case 1	Sub-surface buoy vertical depth	In Base Case study, the sub-surface buoy is located at -250 m below the surface. In this case, the sub-surface buoy will be located at -400 m.	Ultimate Limit State (ULS), Accidental Limit State (ALS)
Case 2	Flexible jumper end-connection point	In Base Case study, the jumper connection point is located at top of sub-surface buoy. In this case, the connection point will be placed at bottom of sub-surface buoy.	Ultimate Limit State (ULS), Accidental Limit State (ALS)
Case 3 Case 4 Case 5	Mooring line arrangements	In Base Case study, the anchor points are spaced in the same distance as for the connection points at bottom of the sub-surface buoy (3m). In this case, the anchor point will be spaced in various distances to study the effect on lateral displacement.	Ultimate Limit State (ULS)

Table 5.10 – Sensitivity Study Cases

General thesis work diagram is presented in Figure 5.10 below.

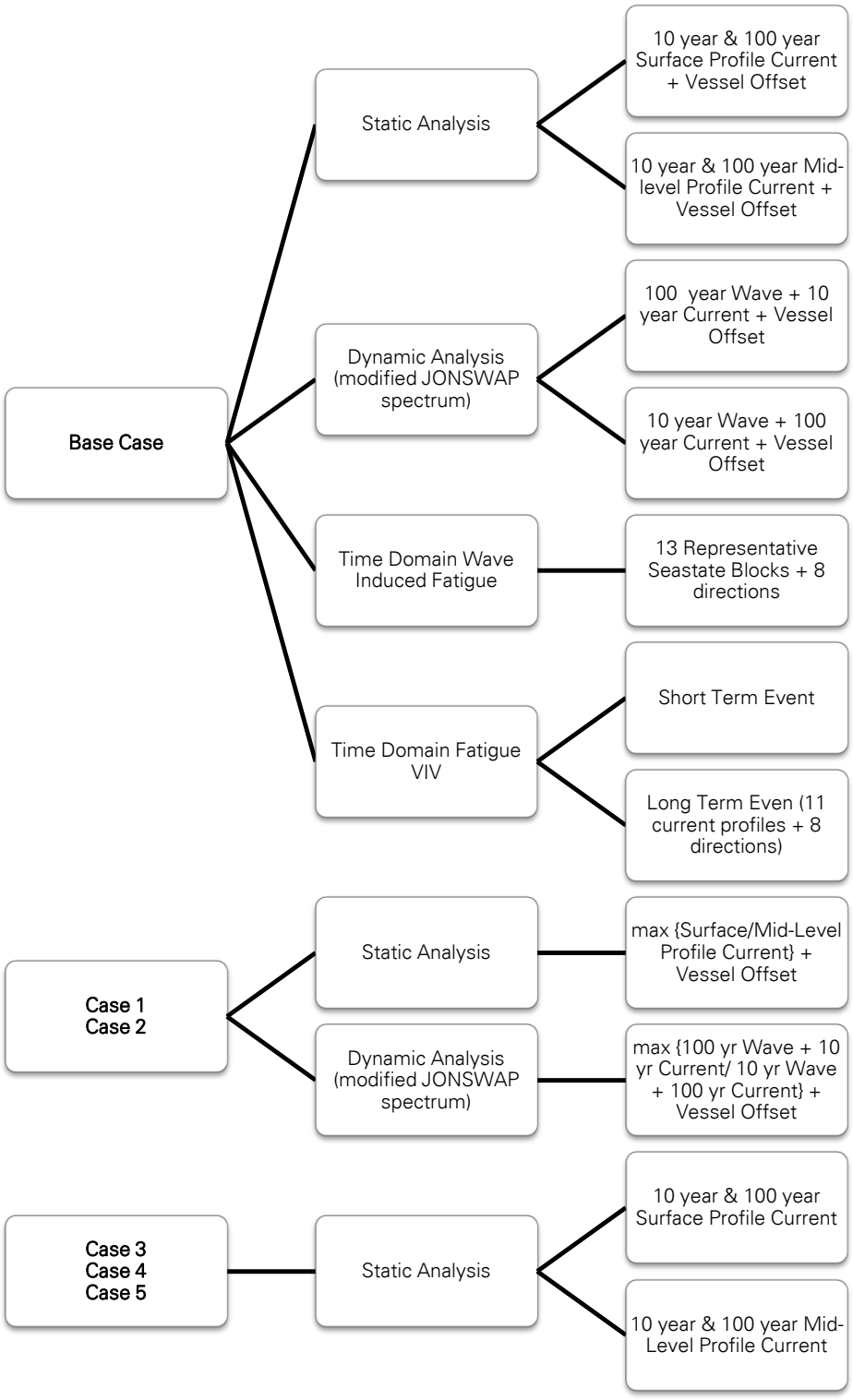

Figure 5.10 – Thesis Work Diagram

5.6 Design Acceptance Criteria

The design analysis result shall meet particular limiting criteria and requirements. The following points describe the criteria that need to be fulfilled in this thesis work:

- Maximum/min Top Tension of flexible jumper
  The catenary load is supported by the tensioner located at top section of product on the vessel. The wave and current motions create variations of tension load on the riser. The limiting capacity on the tensioner shall be reviewed with maximum tension load experienced by the flexible jumper. In addition, large range of variations on tension load should give more attention in the analysis.
- Compression
  No compression load is permitted along the flexible jumpers.
- Minimum Bend Radius (MBR) of flexible jumper
  Bending radius is the minimum radius of the riser can be bended without damaging it or making it buckle. The smaller the bend radius, the greater is the flexibility. Normally, the product shall not exceed the permissible bending radius that given by the manufacturer.
  In this thesis work, the minimum bend radius of the flexible jumper is given as 5 m. For static analysis at any vessel offset position, H_{min} (the distance between the lowest point of flexible jumper along the catenary configuration and its connection point at the sub-surface buoy) is fixed as 30 m.
- Buckling Utilization Factor
  A buckling utilization factor shall be less than 1.0 for various limit state design (ULS & ALS)

6. COBRA Concept Base Case Study

6.1 Introduction

This chapter presents the results for COBRA concept Base Case model as described in Chapter 5. The results are focused on riser strength analysis under static and dynamic behavior. In addition, fatigue responses due to wave and VIV (Vortex Induced Vibration) are also presented.

Initial riser wall thickness sizing is presented in Section 6.2. Detail case combination for Base Case study is presented in Section 6.3. Static and dynamic responses of riser for ULS (Ultimate Limit State) design are presented in Section 6.4 and 6.5. In Section 6.6, the ULS design results are compared with the ALS (Accidental Limit State) design results. Section 6.7 presents the result from fatigue responses due to wave and VIV. At the end, a discussion on overall Base Case analysis result is given in Section 6.8.

6.2 Wall Thickness Design

The first step of riser design comes from the wall thickness sizing. With reference to the previous chapter in Section 3.4.1, riser wall thickness shall be designed to withstand the internal overpressure from the fluid inside the riser which might cause bursting failure. In addition, it is also need to withstand external hydrostatic pressure which might cause collapse failure. In ultra deepwater environment, the hydrostatic pressure is extremely high at the sea bottom. In this condition, collapse resistance is normally the critical case.

Table below provides the minimum wall thickness requirement according to DNV-OS-F201. The riser internal diameter is 10", and carbon steel grade is X65. The design pressure is 500 bar and the total water depth is 2200 m.

Burst (operation) (mm)	Burst (system test) (mm)	Collapse (mm)
18	14.9	21.9

Table 6.1 – Minimum Wall Thickness Requirement

The result shows that the minimum wall thickness required is 21.9 mm based on collapse resistance criteria. Assessment on propagating buckling resulted in minimum wall thickness requirement of 27.7 mm. However, it is not common to design the riser wall thickness based on propagating buckling criteria as it will give inefficient and uneconomical design. Normally, propagating buckling can be simply avoided by using buckle arrestor on the particular critical location. For this thesis, minimum wall thickness of 26 mm is used.

Detail of wall thickness sizing calculation is provided in Appendix A.

6.3 Strength Analysis Case

In this Base Case study, the strength analysis is divided into two parts, i.e. Ultimate Limit State (ULS) design and Accidental Limit State (ALS) design. For both ULS and ALS design, various cases are created to consider the following design condition:

- Environmental load combination of 100 year wave and 10 year current load
- Environmental load combination of 10 year wave and 100 year current load
- Surface current profile and mid-level current profile (refer to Section 5.3.1 for details)

- One direction (unidirectional) current and 2-directions (bidirectional) current (refer to Section 5.3.1 for details)
- Near (-80 m), nominal, and far (+80 m) vessel offset with corresponding wave and current directions (i.e. 180 degree environmental loads are considered for near and nominal offset, and 0 degree environmental loads are considered for far and nominal offset).

There are 32 cases for each ULS and ALS design. The following table summarizes the case combination.

No	Wave & Current Return Period	Current Profile	Current Directional	Vessel Offset
1	100 year wave + 10 year current	Surface Profile	1-direction current (unidirectional)	Near (-80m) offset,180° current+wave
2				Nominal (0) offset, 180° current+wave
3				Nominal (0) offset, 0° current+wave
4				Far (+80m offset), 0° current+wave
5			2-directions current (bidirectional)	Near (-80m) offset,180° current+wave
6				Nominal (0) offset, 180° current+wave
7				Nominal (0) offset, 0° current+wave
8				Far (+80m offset), 0° current+wave
9		Mid-Level Profile	1-direction current (unidirectional)	Near (-80m) offset,180° current+wave
10				Nominal (0) offset, 180° current+wave
11				Nominal (0) offset, 0° current+wave
12				Far (+80m offset), 0° current+wave
13			2-directions current (bidirectional)	Near (-80m) offset,180° current+wave
14				Nominal (0) offset, 180° current+wave
15				Nominal (0) offset, 0° current+wave
16				Far (+80m offset), 0° current+wave
17	10 year wave + 100 year current	Surface Profile	1-direction current (unidirectional)	Near (-80m) offset,180° current+wave
18				Nominal (0) offset, 180° current+wave
19				Nominal (0) offset, 0° current+wave
20				Far (+80m offset), 0° current+wave
21			2-directions current (bidirectional)	Near (-80m) offset,180° current+wave
22				Nominal (0) offset, 180° current+wave
23				Nominal (0) offset, 0° current+wave
24				Far (+80m offset), 0° current+wave
25		Mid-Level Profile	1-direction current (unidirectional)	Near (-80m) offset,180° current+wave
26				Nominal (0) offset, 180° current+wave
27				Nominal (0) offset, 0° current+wave
28				Far (+80m offset), 0° current+wave
29			2-directions current (bidirectional)	Near (-80m) offset,180° current+wave
30				Nominal (0) offset, 180° current+wave
31				Nominal (0) offset, 0° current+wave
32				Far (+80m offset), 0° current+wave

Table 6.2 – Strength Analysis Cases

As described in earlier chapter (Section 5.5), the accidental case (ALS) condition is carried out by considering a condition if one of the two mooring lines fails. The same case combinations as shown in Table 6.2 are also used for this accidental case.

6.4 Static Response (ULS)

In static analysis, the static equilibrium configuration is achieved by considering only static loading (refer to Section 4.8.1 for the static loading description). To account for the variation of environmental loads and the corresponding vessel offset during operation, four static configurations are considered. The following figure shows the typical static configurations for the riser system.

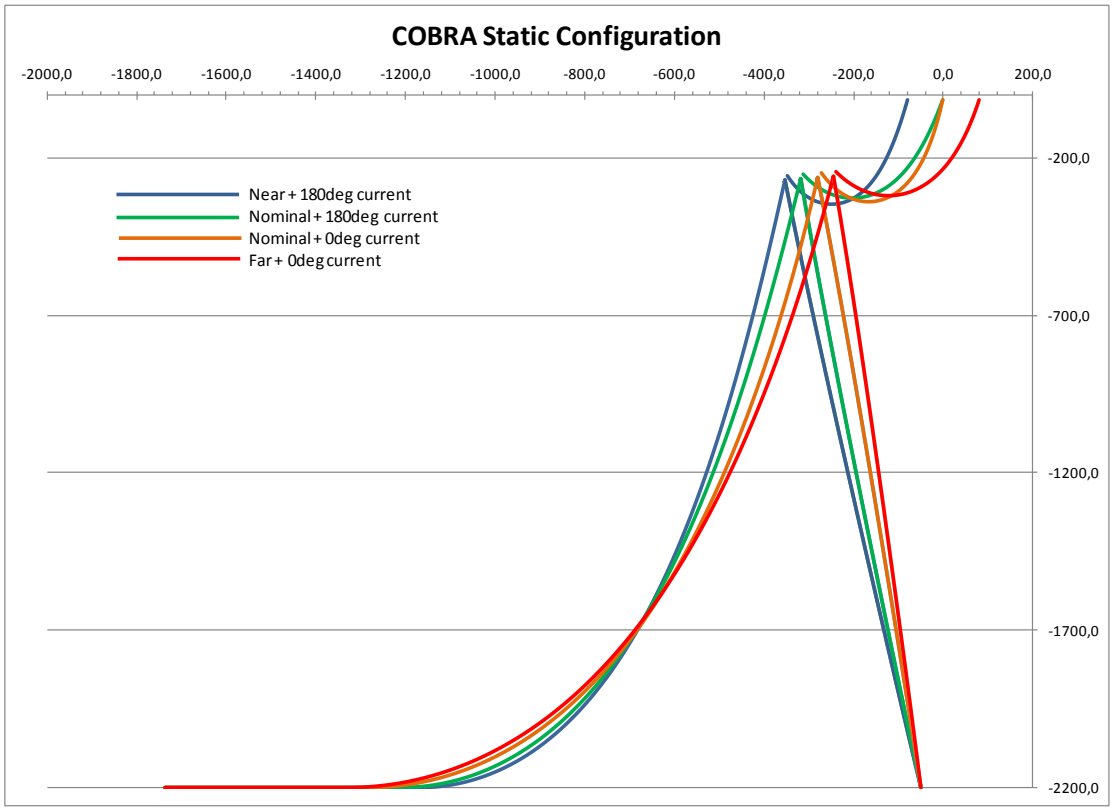

Figure 6.1 – Static Riser Configurations

Static responses for the flexible jumper, riser, and mooring line are presented in the following section.

6.4.1 Flexible Jumper

The total length of flexible jumper is 535 m. As described in Section 5.3.1, marine growth is included on the flexible jumper.

For flexible jumper, the design issues are minimum bending radius and compression load due to current, waves, and floater motions. Table 6.3 shows the summary result for static catenaries jumper configuration for near, nominal, and far vessel offset position. As described in Section 5.3.2, 80 m of vessel offset distance is considered for near and far position. Various current profiles based on case combination presented in Table 6.2 are also considered.

Static Result Summary - Jumper	Unidirectional current			Bidirectional current		
	Vessel Position			Vessel Position		
	Near	Nominal	Far	Near	Nominal	Far
Maximum Static angle at vessel (deg)[1]	12.3	15.6	13.9	8.1	13.2	17.2
Maximum Static angle at buoy (deg)[2]	25.8	34.1	35.0	19.1	34.6	43.2
Maximum Static tension at vessel (kN)	1102	1120	1114	1079	1125	1158
Maximum Static tension at buoy (kN)	432	464	484	428	468	515
Minimum Bending Radius (m)	66	69	95	45	66	122

Note:
[1] Static angle at vessel is relative to vertical
[2] Static angle at buoy is angle between buoy and jumper

Table 6.3 – Static Jumper Result (Base Case – ULS)

It is seen from the result that the jumper is in feasible static configuration. The minimum bending radius is 45 m for near vessel position, resulted in acceptable value (refer to Design Acceptance Criteria in Section 5.6). The maximum static angle at vessel and buoy are in accordance with the maximum static tension at vessel and buoy, where the highest tension comes from the far offset vessel position under bidirectional current load. High tension at top of sub-surface buoy might give significant impact on bending moment stress on top of riser hang-off connection which located at the bottom of the sub-surface buoy.

From the result, it can be observed that the effect of bidirectional (2-directions) current profile can increase the static tension load of the flexible jumper, in particular for far vessel offset case.

6.4.2 Riser

The riser is connected to the bottom of sub-surface buoy. As described in earlier chapter, it has a 10 m tapered stress joint section towards the sub-surface buoy. The maximum wall thickness of this tapered stress joint section is 2.5". The typical riser static configuration for near, nominal and far vessel positions are shown in Figure 6.1.

In static condition, it is important to see the initial catenary riser configuration. In shallow water depth, a small static top (hang-off) angle will give relatively short layback distance, while deeper water depth will give longer layback distance. Current load and corresponding vessel offset will also affect the layback distance, and various extreme current profiles might alters the location of touch down point (TDP) at the seabed. For seabed area with various soil conditions, alteration on touch down point location might give different dynamic response of the riser.

Short layback distance in shallow water depth might reduce the bend radius of the riser in touch down point (TDP). This will eventually resulted in higher bending stress. However, this is not a critical issue in ultra deepwater condition. For a steel catenary riser in ultra deepwater, large portion of the suspended riser that exposed to current load will also give significant impact on the initial riser configuration.

In COBRA riser arrangement, the steel catenary riser is hanging on the sub-surface buoyancy. In ultra deepwater field, a high payload for the riser requires a sufficient size of the sub-surface buoyancy.

Table 6.4 presents the summary result for static riser configuration for near, nominal and far vessel positions. The same various current profiles as for the flexible jumper are considered.

Static Result Summary - Riser	Unidirectional current Vessel Position			Bidirectional current Vessel Position		
	Near	Nominal	Far	Near	Nominal	Far
Maximum Static top angle (deg)	9.9	11.6	12.2	8.8	11.6	13.6
Maximum Static top tension (kN)	2186	2361	2413	2318	2360	2294
Minimum Static TDP tension (kN)	253	420	470	378	417	351

Table 6.4 – Static Riser Result (Base Case – ULS)

The result shows that the maximum static top angle of 13.6° comes from the far vessel position with bidirectional (2-directions) current profile. However, it is observed that the maximum top tension of 2413 kN comes from the far vessel position with unidirectional (1-direction) current profile. The lowest static TDP tension comes from the near vessel position with unidirectional current profile.

It is interesting to see the result from bidirectional (2-directions) current case, where the maximum static top angle comes from the far vessel position case, but near and nominal vessel position cases give higher static top tension and static TDP tension than far vessel position case. The results are in contrary with the result for unidirectional current case, where the maximum static top angle, top tension and TDP tension comes from the far vessel position.

Reference is made to the typical bidirectional (2-directions) current profile (presented in Figure 5.2) that is used in this thesis work. As described in Table 6.2 – Strength Analysis Cases, four typical vessel offset positions are considered in the analysis. For near and far offset cases with typical bidirectional current profile, the current direction in upper layer (from sea surface to -250 m depth) is analogous with the vessel offset direction. However, the direction of current in lower layer (from -250 m depth down to the seabed) is in the opposite direction with the vessel offset direction. With total water depth of 2200 m, the portion of lower layer current is almost 8 times larger than the upper layer. As also can be seen from Figure 5.8, the top of riser section is located below -250 m depth. For cases with typical bidirectional current profile, it can be seen that all of the riser sections are exposed to the lower layer current.

With regards to this condition, it can be concluded that for far vessel offset case, the lower layer current can reduce the suspended length of the riser. Eventually, this condition can reduces the static top tension of the riser, as can be seen from the summary result in Table 6.4.

Detail static riser results for all cases are presented in Appendix B.

6.4.3 Mooring Line

The general description of mooring lines configuration is presented in Section 5.3.6. The following table shows the summary of static analysis result of the mooring lines. The same various current profiles and vessel offset positions that are presented in Table 6.2 are also considered in this analysis.

Static Result Summary - Mooring Line	Unidirectional current Vessel Position			Bidirectional current Vessel Position		
	Near	Nominal	Far	Near	Nominal	Far
Maximum Static tension (kN)[1]	644	623	526	568	622	600

Note:
[1] The tension presented is the tension in each of the two mooring lines.

Table 6.5 – Static Mooring Line Result (Base Case – ULS)

The result shows that the maximum static tension in each of the mooring line comes from the near vessel offset position. Following the mooring line vertical configuration in Figure 6.1, for unidirectional (1-direction) current case, it is obvious that the tension load will start to reduce from near vessel position to far vessel position. However, for bidirectional current case, it can be seen that the highest tension comes from nominal vessel position, where near and far positions give lower tension.

6.5 Dynamic Response (ULS)

In dynamic analysis, nonlinear time domain analysis with irregular waves is considered. The combination of 10 year wave-100 year current and 100 year wave-10 year current are considered based on the wave and current data as described in Section 5.3.1 in Chapter 5.

To perform a design storm analysis (e.g. 100 year return period), the preferred method is normally by simulating a full three hours storm duration. In this thesis work, a sensitivity study to analyze the three hours storm duration with less time simulation duration is performed. A 0.02 second time step is considered for this study. The purpose for this sensitivity study is to capture the worst response within the full three hours storm duration in less simulation time. The following procedures are considered on the sensitivity study:

1. A simulation of random wave train for the full 3 hours storm duration is applied by applying the sea-state parameters and using modified JONSWAP spectrum from the metocean data.
2. Five highest waves are identified from the simulated wave train.
3. Simulations for each of these 5 waves are performed to get the response. Each simulation is 30 seconds before the wave peak and 30 seconds after the wave peak, resulted in 60 seconds simulation in total.
4. The worst response from the 5 simulations is taken as the worst response within the full storm duration.

The dynamic responses for flexible jumper, riser, and mooring lines are presented in the following section.

6.5.1 Flexible Jumper

The critical aspect in dynamic response of flexible jumper is the compression load that might occur due to waves and the vessel motions. The flexible jumper should be maintained in tensioned condition and no compression load is allowed. Minimum bending radius is also should be maintained in a certain limit due to high curvature and high bending stress. Dynamic vessel motion and near offset vessel position might significantly reduce the bend radius of jumper.

Large payload at vessel is another important aspect. The vessel type that considered in this thesis is a typical turret moored FPSO. Hence, the turret should have sufficient hang-off capacity with regards to the maximum tension load that might occur during operation. Large tension load at top of sub-surface buoy, as described in static response section, will give

significant impact on bending moment stress on top riser hang-off that is located at the bottom section of the sub-surface buoy. In dynamic condition, this bending stress might encounter various stress amplitude due to the vessel motion.

The following table shows the summary result from dynamic analysis of flexible jumper.

Dynamic Result Summary - Jumper	Unidirectional current Vessel Position			Bidirectional current Vessel Position		
	Near	Nominal	Far	Near	Nominal	Far
Minimum radius (m)	55	78	89	42	85	111
Hmin (m)	90	76	79	109	76	62
Minimum tension (kN)	148	209	216	111	198	265
Maximum tension at Vessel (kN)	1220	1311	1359	1209	1344	1399
Maximum tension at Buoy (kN)	454	501	555	453	524	606
Minimum angle at Vessel (deg)	7.7	11.9	4.7	4.9	8.5	9.0
Maximum angle at Vessel (deg)	15.3	18.8	17.2	12.1	17.1	20.4
Minimum angle at Buoy (deg)	23.2	30.8	33.4	17.8	30.8	38.5
Maximum angle at Buoy (deg)	26.1	34.7	37.7	19.7	35.7	44.8

Table 6.6 – Dynamic Jumper Result (Base Case – ULS)

The result shows that minimum radius of 42 m comes from near case under bidirectional current load and still in an acceptable limit. This result is in accordance with the minimum tension result of 111 kN, which means there is no compression load on the flexible jumper. The maximum tension at vessel and buoy from static and dynamic response are presented in the following figures.

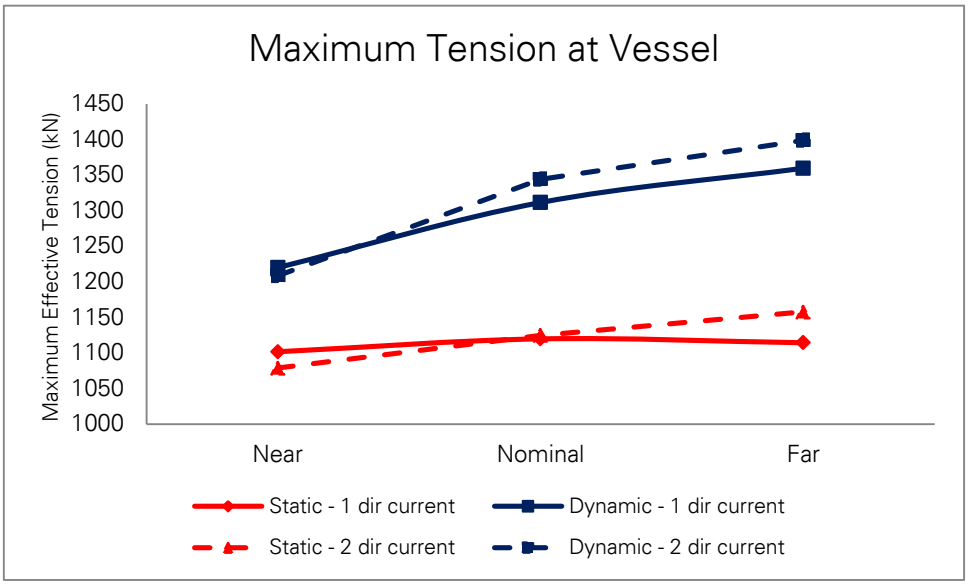

Figure 6.2 – Static and Dynamic Tension of Jumper at Vessel (Base Case)

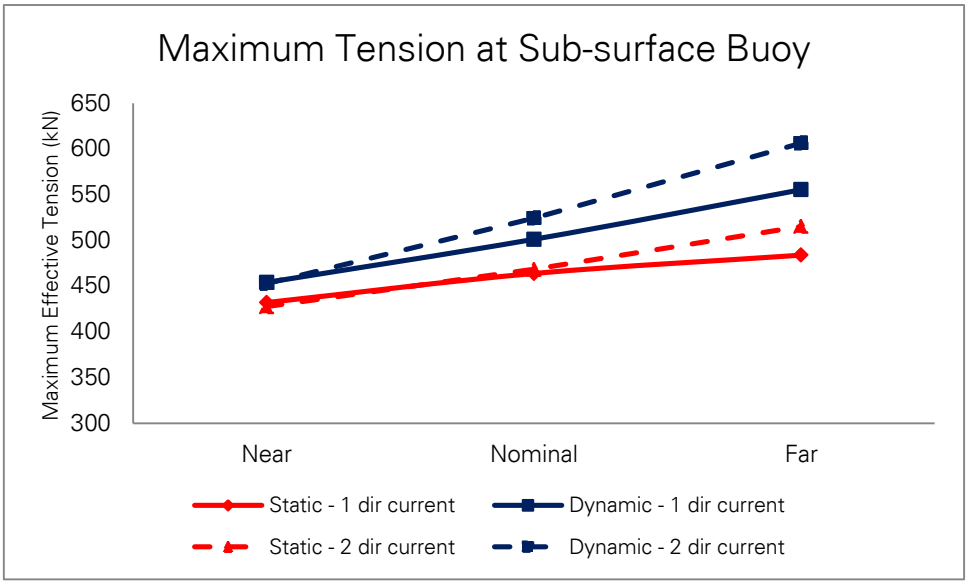

Figure 6.3 – Static and Dynamic Tension of Jumper at Sub-surface Buoy (Base Case)

From the figures above, it can be observed that bidirectional current profile has large impact for tension load in far vessel offset position. As seen from the result, the maximum tension load at vessel is increased by 240 kN due to dynamic motion effect. At sub-surface buoy, the maximum tension load is increased by 90 kN.

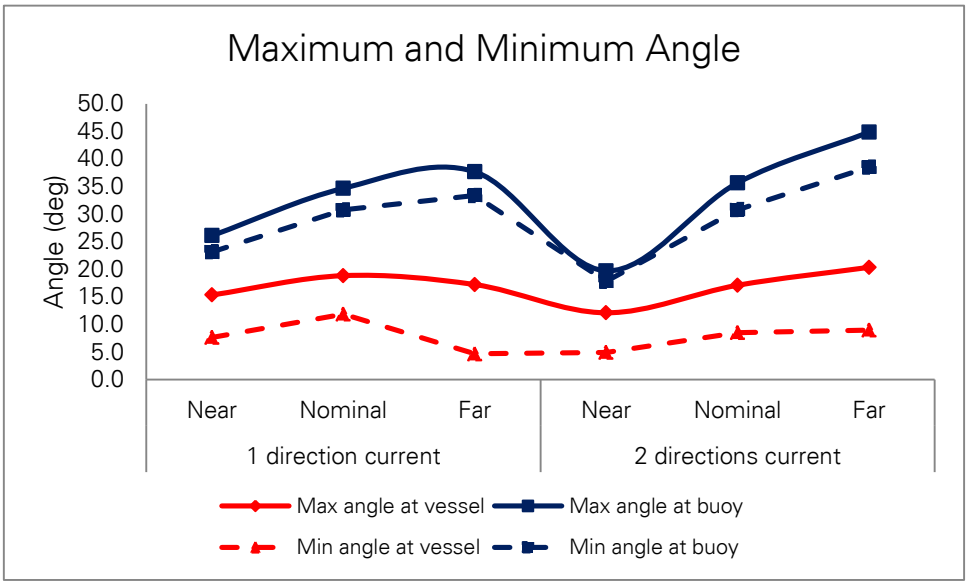

Figure 6.4 – Dynamic Angle of Jumper at Vessel and Sub-surface Buoy

Figure 6.4 shows the comparison of maximum and minimum angle at vessel and buoy from dynamic response result. The result shows that the differences between maximum and minimum angle at vessel are relatively higher than the differences between maximum and minimum angle at sub-surface buoy. This is in accordance with the result from maximum tension load at sub-surface buoy shown in Figure 6.3, where the escalation loads from static to dynamic response are relatively small. From these results, it can be seen that the dynamic effect at sub-surface buoy that located at 250 m below the sea surface is lower compared to the dynamic effect at vessel (sea surface).

6.5.2 Riser

In conventional SCR arrangement, large vertical heave motions at the vessel might result in severe dynamic riser response, including potential compression load and potential buckling at touch down point (TDP) area. In this COBRA riser arrangement, the vessel dynamic motions are absorbed by the flexible jumper. It is expected that the riser has no significant dynamic effect.

The following table summarizes the dynamic result of riser.

Dynamic Result Summary - Riser	Unidirectional current Vessel Position			Bidirectional current Vessel Position		
	Near	Nominal	Far	Near	Nominal	Far
Maximum Top Tension (kN)	2208	2435	2510	2350	2393	2389
Minimum TDP Tension (kN)	259	440	495	387	432	380
von Mises Stress - Top (MPa)	166	206	284	170	216	312
von Mises Stress - Below Stress Joint (MPa)	241	263	283	244	265	291
von Mises Stress - TDP (MPa)	261	265	266	264	264	264
Maximum Buckling Utilization - Top	0.37	0.37	0.40	0.37	0.37	0.50
Maximum Buckling Utilization - Below Stress Joint	0.67	0.67	0.67	0.67	0.67	0.67
Maximum Buckling Utilization - TDP	0.78	0.78	0.78	0.78	0.78	0.78

Table 6.7 – Dynamic Riser Result (Base Case – ULS)

From table above, the highest top tension load (2510 kN) and the lowest TDP tension (259 kN) resulted from far and near vessel offset position under unidirectional (1-direction) current load respectively. The same trend from static response is observed, where unidirectional current load drives the tension load responses. The comparison between static and dynamic top tension is presented in the figure below.

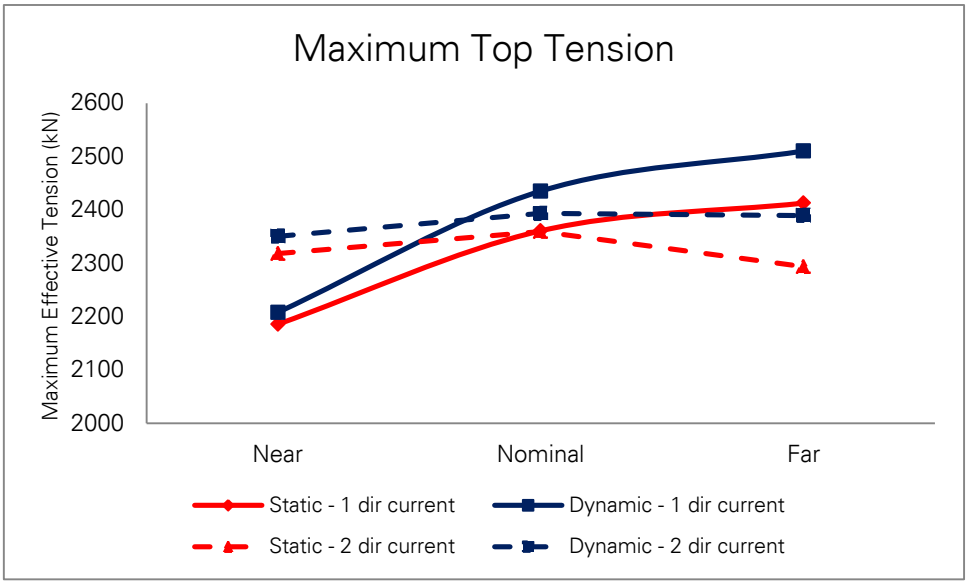

Figure 6.5 – Static and Dynamic Top Tension of Riser (Base Case)

From the figure above, it can be observed that there is significant result between unidirectional (1-direction) current load and bidirectional (2-directions) current load responses. In near vessel offset position case, bidirectional (2-directions) current load gives higher top tension, while unidirectional (1-direction) current load gives less top tension. The impact of this bidirectional current is explained in earlier in static response of riser (refer to Section 6.4.2). As seen from the result, the maximum static top tension is increased by 97 kN due to dynamic motions.

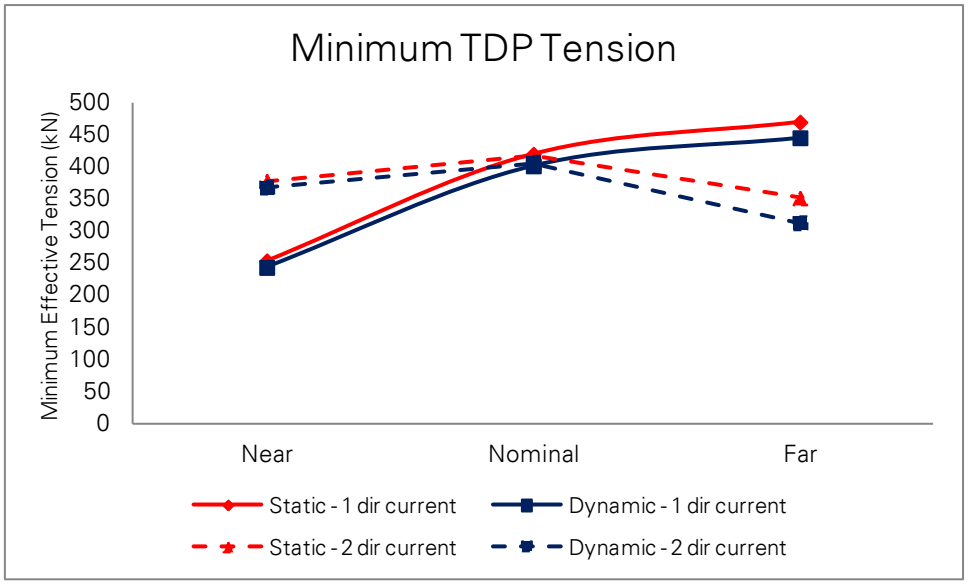

Figure 6.6 – Static and Dynamic TDP Tension of Riser (Base Case)

Minimum TDP tension shows the same trend with the maximum top tension result. However, it is interesting to see that the dynamic effect is not significant in the touch down area.

The following figures show the maximum static and dynamic von Mises stress result.

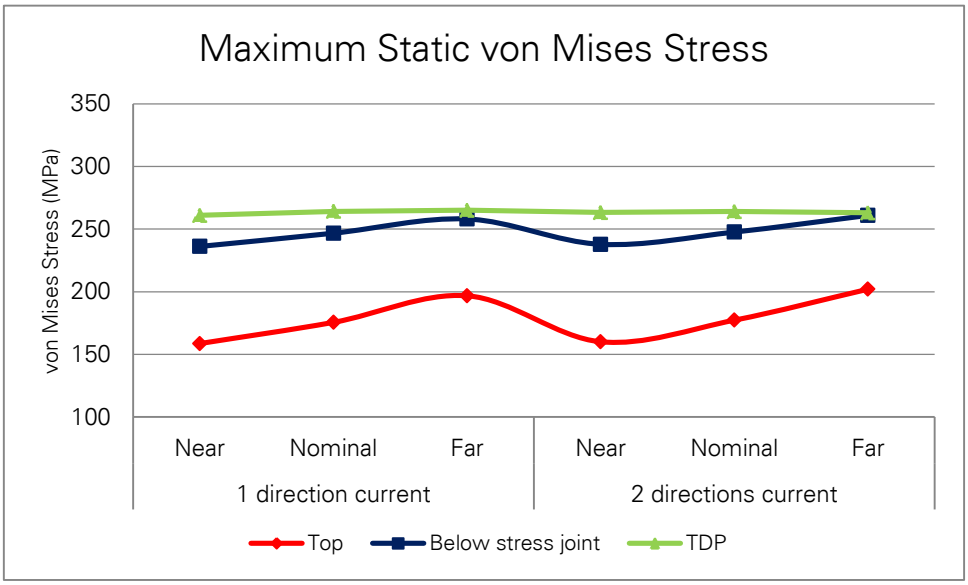

Figure 6.7 – Static von Mises Stress of Riser (Base Case)

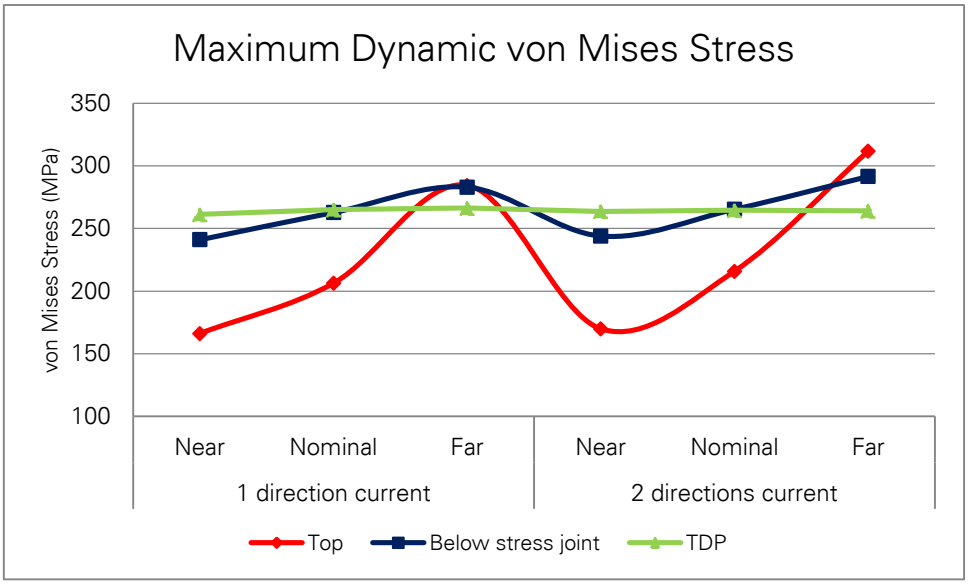

Figure 6.8 – Dynamic von Mises Stress of Riser (Base Case)

From Figure 6.7 and Figure 6.8, the result shows that the stresses at top hang-off section of riser, in particular for far vessel offset positions, are increased significantly due to the dynamic motion effect. The range of stress amplitude is lower at below stress joint section, and it almost constant at TDP section.

The highest von Mises stress (as shown in figures above and Table 6.7) comes from far vessel position with bidirectional (2-directions) current profile, located at top section of the riser. This result is in accordance with the result coming from the highest effective tension of jumper at sub-surface buoy (refer to Figure 6.3 – Static and Dynamic Tension of Jumper at Sub-surface Buoy). This proves the linear correlation between high tension load of jumper at sub-surface buoy and high bending stress of riser at top hang-off section, as described in Section 6.4.1.

Overall result of buckling utilization ratio is less than 1.0. The maximum buckling utilization ratio is 0.78 due to high hydrostatic pressure at 2200 m water depth. It can be seen that collapse resistance drives the buckling strength performance in this COBRA Base Case riser arrangement.

The detail results of dynamic response of riser are presented in Appendix B.

6.5.3 Mooring Line

The following table shows the summary result of dynamic mooring lines response.

Dynamic Result Summary - Mooring Line	Unidirectional current Vessel Position			Bidirectional current Vessel Position		
	Near	Nominal	Far	Near	Nominal	Far
Minimum tension (kN)[1]	599	458	424	513	497	493
Maximum tension (kN)[1]	681	664	599	602	697	695

Note:
[1] The tension presented is the tension in each of the two mooring lines.

Table 6.8 – Dynamic Result of Mooring Line (Base Case – ULS)

The following figure presents the summary result plot of minimum and maximum dynamic tension load on the mooring line, and the comparison with the static tension load.

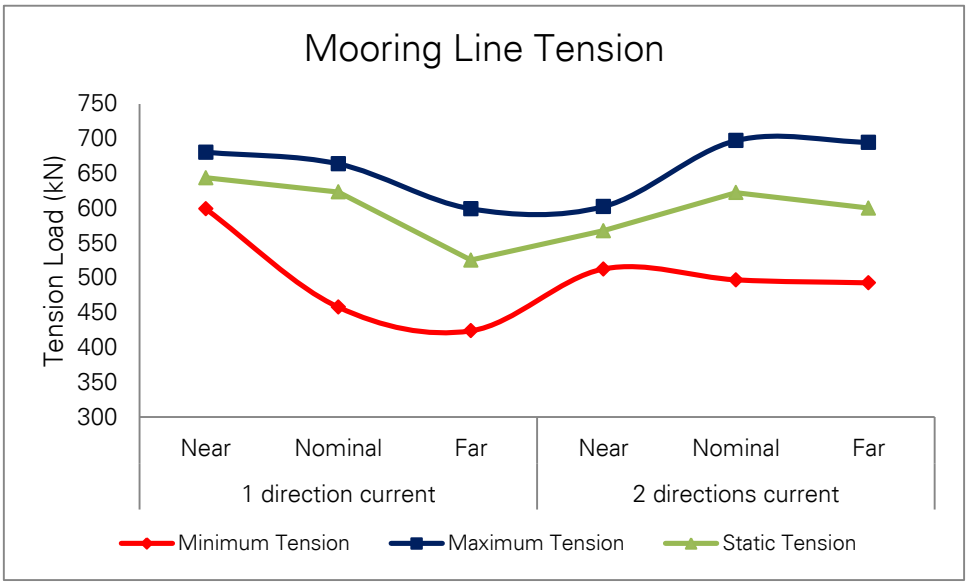

Figure 6.9 – Maximum and Minimum Mooring Line Tension (Base Case)

The maximum tension load is 697 kN, and the minimum tension load is 424 kN. As seen from the figure above, it can be seen that various range of tension loads might occurs in the mooring lines due to dynamic motion effect. When it comes to foundation anchor design, it is important to observe the maximum tension load on the mooring line. However, foundation anchor design is not included in this thesis scope of work.

6.6 Comparison with Accidental Case Result

As described in Section 6.3, the accidental case (ALS) condition is carried out by considering a condition if one of the two mooring lines fails. The same case combinations (as shown in Table 6.2) are used for this accidental case.

The following table summarizes the strength analysis result for normal and accidental cases.

	Case	
	Normal	Accidental
SCR		
Maximum Top Tension (kN)	2510	2526
Minimum TDP Tension (kN)	243	242
Maximum Buckling Utilization	0.78	0.78
Maximum von Mises Stress (MPa)	312	328
Jumper		
Minimum radius (m)	41.8	43.5
Minimum tension (kN)	111	117
Maximum tension at Vessel (kN)	1399	1382
Maximum tension at Buoy (kN)	606	584
Buoyancy mooring lines		
Minimum tension (kN)	424	895
Maximum tension (kN)	697	1365

Table 6.9 – Riser System Result Summary (Base Case)

From the results, it can be concluded that the COBRA Base Case riser system has sufficient strength capacity. The most critical section for buckling is located at the touch down area due to high hydrostatic collapse pressure. Maximum von Mises stress is observed at top of hang-off section due to harsh bidirectional (2-directions) current load. The result shows that the combination of 10-year wave - 100 year current with surface current profile is the most govern case (refer to Table 6.2 – Strength Analysis Cases for case combinations list). A complete analysis result is presented in Appendix B.

In overall comparison, accidental case does not give significant result in terms of the strength performance. However, a sufficient safety factor for each of the mooring line tension load capacity should be carefully anticipated if one of the mooring lines fails, as the tension load on the other line is increased double from the normal condition.

The detail analysis results for normal and accidental cases are presented in Appendix B.

6.7 Fatigue Analysis

Under normal operating condition, random waves and corresponding vessel movements create repeatedly cyclic stress on the riser system. These are typically the main source that caused fatigue damage in steel catenary riser. The damage in this type of riser is normally occurs due to oscillatory stress at metal weld joint connection between the pipes.

In addition to waves and vessel movement, fatigue damage might also occur due to Vortex Induced Vibration (VIV). The current that exposed to the riser creates various unsteady vortex flow patterns behind the cylinder section. This is normally called as vortex shedding. In such condition where the vortex shedding frequency and eigen frequency of riser are match, the structure will start to vibrate. This oscillatory vibration is the source for fatigue damage in VIV.

Insufficient fatigue life might cause fatigue failure on the riser system. This will eventually impacted on the overall field operation life. Hence, it is important to ensure that the riser system has sufficient fatigue life during operational period.

For this COBRA riser concept, a detailed time domain fatigue analysis for Base Case configuration is performed to capture the fatigue responses due to wave and VIV. The assessments for wave induced fatigue are carried out using OrcaFlex software. For VIV fatigue assessments, VIVANA software is used. As described in Chapter 2, this concept offers an excellent dynamic performance with less fatigue response. Thus, in this fatigue analysis study, it is expected that there is no significant fatigue response will occur.

6.7.1 Fatigue Analysis Parameter

Riser configuration

For fatigue analysis, the Base Case configuration with nominal (mean) vessel offset is considered.

Sea-state Data

For wave induced fatigue, 13 irregular sea states in 8 directions are performed. The sea states are taken from Santos Basin Central Cluster Region Metocean Data report. The wave data was tabulated at 3-hours interval with equivalent time exposure of 227136 hours. The sea states blocks used for each direction is presented in Table 6.10.

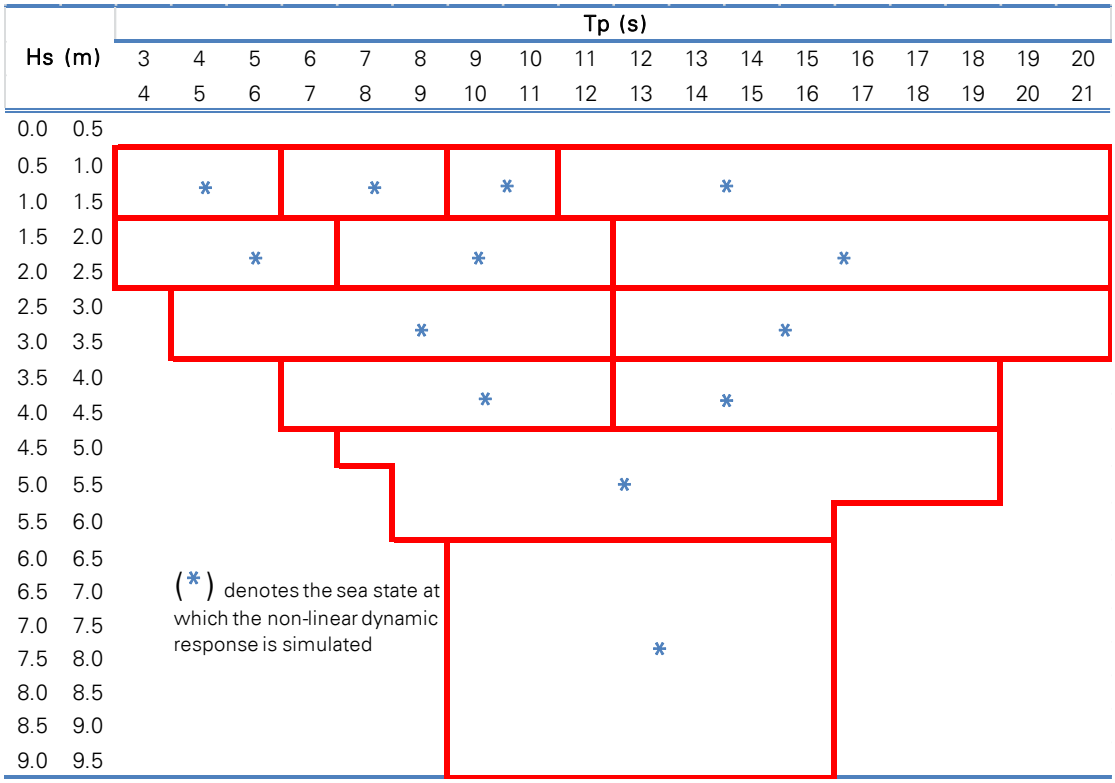

Table 6.10 – Sea state blocks used in fatigue wave analysis for all 8 directions

Table 6.11 provides fatigue probability for each direction.

No	Wave Direction (degree)	Fatigue Probability	Time Exposure (hour)
1	0	23.3%	52823
2	45	25.5%	57974
3	90	2.3%	5315
4	135	0.1%	326
5	180	0.6%	1413
6	225	8.7%	19706
7	270	21.1%	47873
8	315	18.4%	41709
	Total	100%	227136

Table 6.11 – Fatigue Wave Probability per Direction

For short term VIV fatigue event, the following current profiles are considered:

- 1 year unidirectional current profile with 2 x 24 hour time exposure in parallel and perpendicular direction
- 10 year unidirectional current profile with 2 x 12 hour time exposure in parallel and perpendicular direction
- 100 year current profile with 6 hour time exposure in parallel and perpendicular direction

The fatigue damage is calculated based on the following formula:

$$D_{VIV-ST} = D_{1-yr} \times \frac{2 \times 24hr}{219000hr} + D_{10-yr} \times \frac{2 \times 12hr}{219000hr} + D_{100-yr} \times \frac{6hr}{219000hr} \quad \textbf{(3.27)}$$

Where

$D_{1\text{-}yr}$: maximum fatigue damage from 1 year current

$D_{10\text{-}yr}$: maximum fatigue damage from 10 year current

$D_{100\text{-}yr}$: maximum fatigue damage from 100 year current

219000 hr : 25 year of operating life (in hours)

For long term VIV fatigue event, 11 current profiles in 8 directions with corresponding probabilities of occurrence are performed. The surface current velocities are ranging from 0.1 – 1.2 m/s, taken from the surface profile and the mid-level profile. The following table shows the fatigue probability in 8 directions of current.

No	Current Direction (degree)	Fatigue Probability	Time Exposure (hour)
1	0	11.68%	2917
2	45	12.93%	3230
3	90	12.95%	3233
4	135	13.00%	3248
5	180	11.67%	2914
6	225	11.72%	2928
7	270	12.68%	3168
8	315	13.37%	3336
	Total	100%	24974

Table 6.12 – Fatigue VIV Current Probability per Direction

S-N Curve and Stress Concentration Factor (SCF)

In this fatigue analysis, S-N curve in seawater with cathodic protection is used. Reference is made to DNV-RP-C203 (April, 2010) Table 2-2 and Figure 2-7. This S-N curve is shown in the following figure.

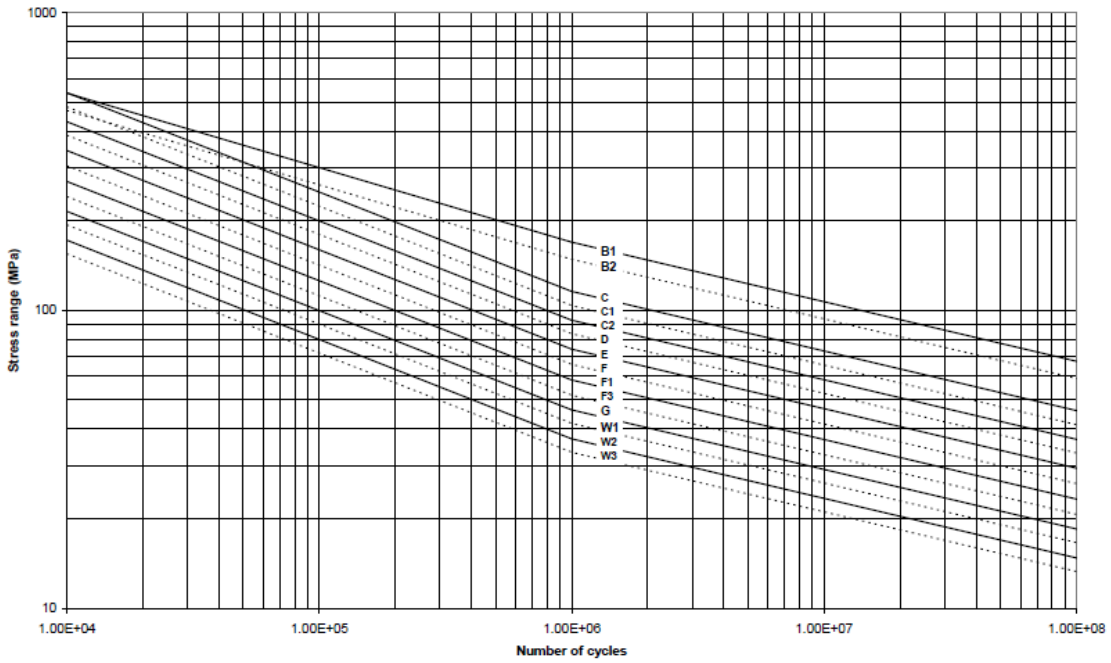

Figure 6.10 – S-N curve in seawater with cathodic protection (DNV, 2010)

For fatigue due to wave, the following curves and SCF factors are considered:

- Tapered stress joint section:
  - S-N curve : C-curve, D-curve, E-curve
  - Stress Concentration Factor : 1.0
- SCR section:
  - S-N curve : F1-curve
  - Stress Concentration Factor : 1.2

For fatigue due to VIV, the following curves and SCF factors are considered based on two different case, i.e.:

- Short term event:
  - S-N curve : D-curve, F1-curve
  - Stress Concentration Factor : 1.2
- Long term event:
  - S-N curve : D-curve, F1-curve
  - Stress Concentration Factor : 1.2

Design Fatigue Factor (DFF)

The Design Fatigue Factor (DFF) for this analysis is 10 (refer to Section 3.4.2 Fatigue Limit State), considering a high safety class for riser. A high safety class is also accounted to covers the difficulty to perform any repair or inspection activities in ultra deepwater condition.

6.7.2 Fatigue Response of Riser – Wave Induced

In this fatigue wave induced case, the analysis is carried out using OrcaFlex software. Two critical locations have been considered. They are at top hang-off point where tapered stress join section is placed, and touch-down-point (TDP) of the SCR. The tapered stress join is considered as a machined part which has high fatigue performance. Hence, C, D and E curves with SCF 1.0 are considered for this section. For the SCR part at TDP, a very conservative F-1 curve with SCF of 1.2 is considered. Thus, it is expected that a very robust fatigue design for this section can be achieved.

The following tables show the minimum fatigue life result for both critical locations.

Curve	Minimum Fatigue Life (years)
C	2407
D	487
E	281

Table 6.13 – Minimum Fatigue Life (Tapered Stress Joint)

Curve	Minimum Fatigue Life (years)
F1	> 10 000

Table 6.14 – Minimum Fatigue Life (Touch Down Point)

The following figures show the fatigue life plot from the results shown above.

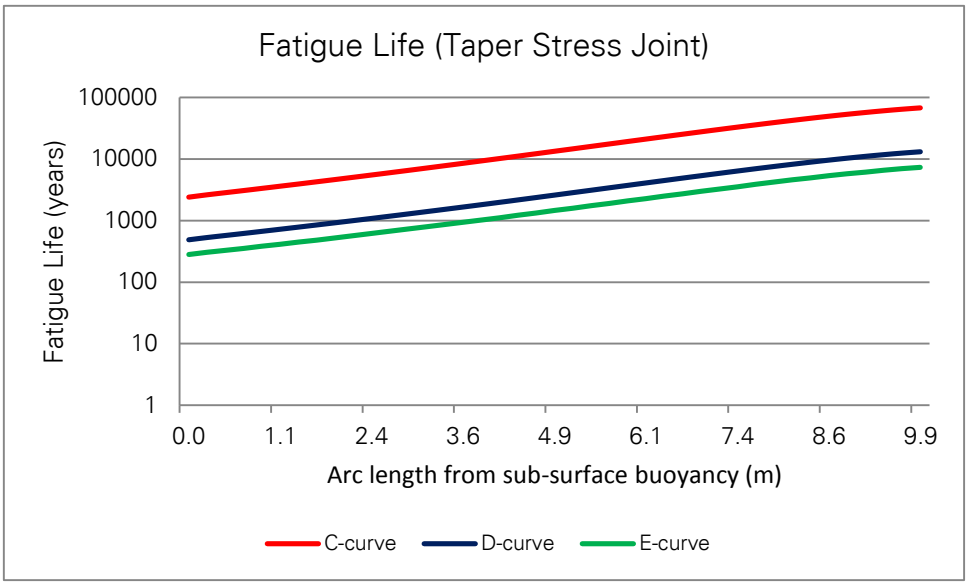

Figure 6.11 – Fatigue Life at Tapered Stress Joint

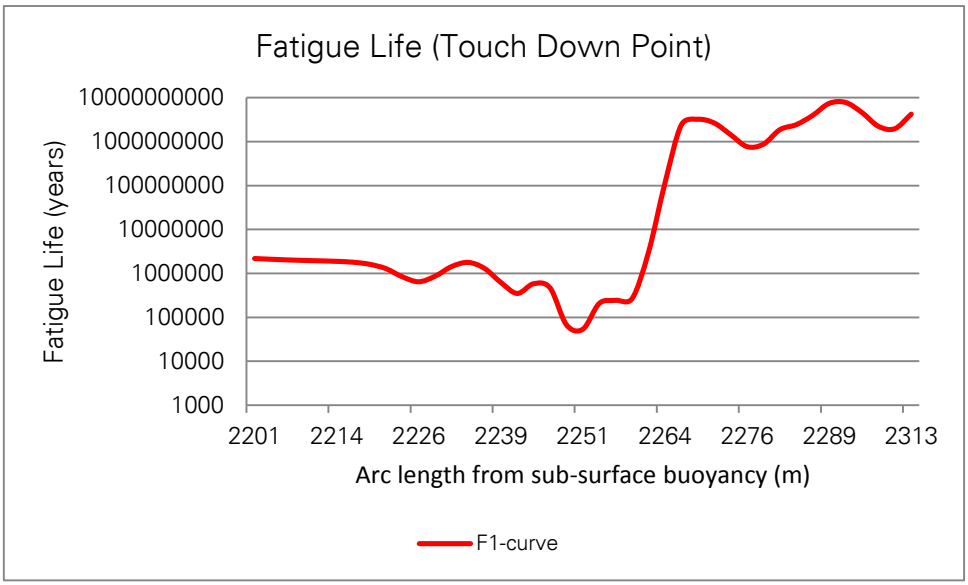

Figure 6.12 – Fatigue Life at Touch Down Point

From the result, it can be seen that the riser section has sufficient fatigue life. The fatigue result at tapered stress joint section with various S-N curve shows that even with lower E-curve, the minimum fatigue life of 281 years is still in an acceptable limit. The fatigue result at

TDP with fatigue life more than 10 000 years proves that there is no significant fatigue issues at this section, even when using onerous F1-curve with high SCF of 1.2. It can be concluded that the COBRA riser has very robust fatigue wave performance.

The detail analysis results of this fatigue analysis due to wave are presented in Appendix B

6.7.3 Fatigue Response of Riser – VIV

In this fatigue due to VIV case, the analysis was carried out using VIVANA software. As described earlier, two fatigue assessments are performed, i.e. short term event and long term event.

In long term event, 11 current profiles with corresponding probabilities of occurrences and various surface velocities are considered. The fatigue damage from the different current profiles is weighted and total accumulated damage is calculated.

For short term and long event, D-curve and F1-curve with SCF factor of 1.2 is considered.

The following tables present the result for short term and long term VIV events.

Curve	Minimum Fatigue Life (years)
D	36564
F1	6781

Table 6.15 – Short Term VIV Fatigue Life

Curve	Minimum Fatigue Life (years)
D	73577
F1	12352

Table 6.16 – Long Term VIV Fatigue Life

As seen from the result, the riser shows a very robust fatigue VIV performance. Short term event gives less fatigue life compared to long term event. Short term event is normally used as preliminary fatigue analysis review. As expected, the result shows that short term event has more conservative result.

It can be seen from the result of long term event, that even with onerous F1-curve, the riser shows sufficient fatigue life (more than 10 000 years). It can be concluded that the COBRA riser has very robust fatigue performance with regards to the particular ultra deepwater current environment in Santos Basin Central Cluster region, and no further fatigue improvement is needed.

6.8 Discussion

6.8.1 Strength Analysis

- As seen from Section 6.6 Comparison with Accidental Case Result, the COBRA riser Base Case system has sufficient strength capacity for both normal (ULS) extreme case and accidental (ALS) extreme case. The results show in acceptable result with reference to the design acceptance criteria as mentioned in Section 5.6.
- From the overall analyses result, it can be concluded that COBRA Base Case riser system has low dynamic effect. It can be seen from the static and dynamic result comparisons, as presented in Section 6.5. Low dynamic effect on the riser system is a good indication for a robust fatigue performance design.

- In this ultra deepwater condition, the effect of bidirectional (2-directions) current load is significant. As explained in Section 6.4.2, the upper and lower layer of this bidirectional current can reduces the static tension load of the riser. However, the result presented in Section 6.4.1 shows that this bidirectional current load can increase the effective tension of flexible jumper at sub-surface buoy. This result is also reflected in Section 6.5.2 where the highest von Mises stress in riser occurs at top of tapered stress joint section under bidirectional current load. The following figure shows the interaction between these loads.

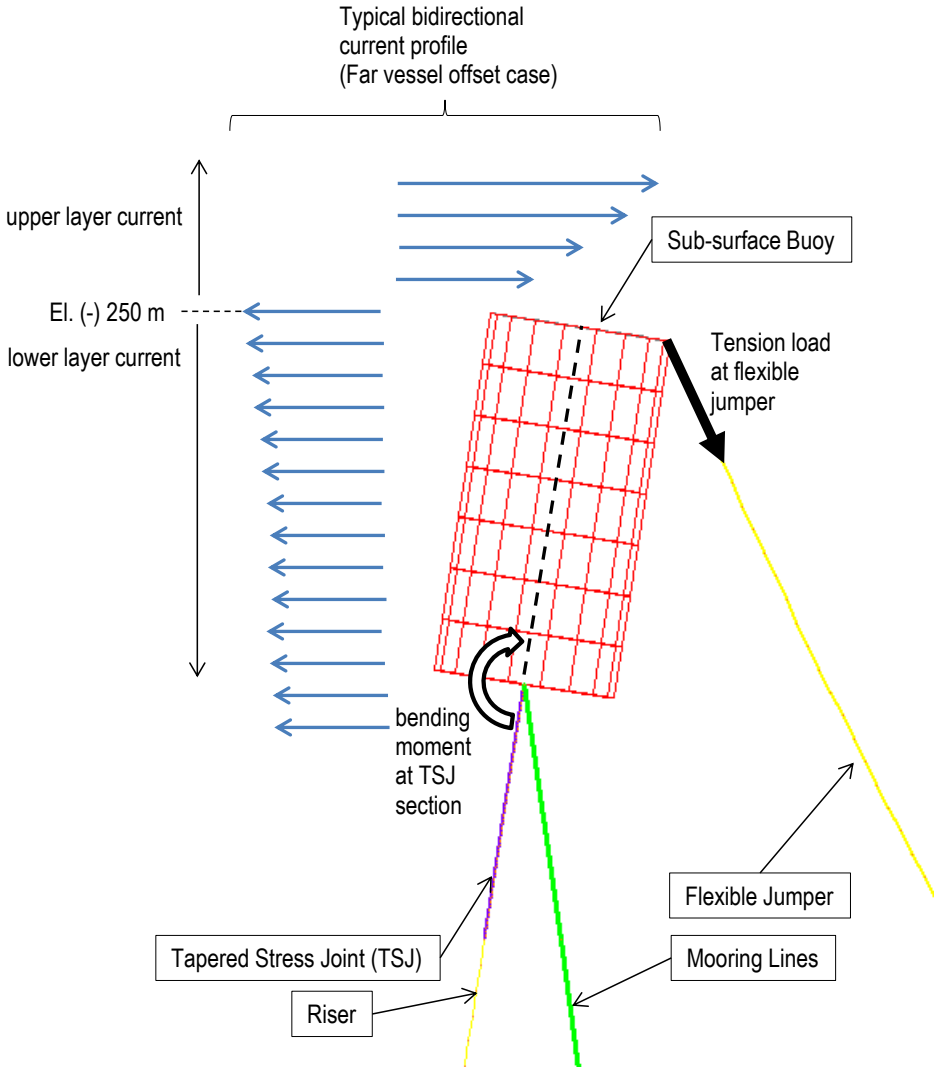

Figure 6.13 – Interaction between tension load on jumper and bending moment at top section of riser

From figure above, it is shown that the cross section point between upper and lower layer current is considered at -250 m below the sea surface, located at the interface connection between flexible jumper and top section of sub-surface buoy. High tension load at flexible jumper due to current load and corresponding far vessel offset position resulted in high bending moment at top of tapered stress joint section. The combination of this bending stress and high tension stress contributes to the high von Mises stress at top of tapered stress joint section. However, for this COBRA Base Case configuration, this result is still considered as acceptable.

- As mentioned in Section 6.6, the worst case combination comes from the combination of 10 year wave and 100 year surface profile current. It can be concluded that in ultra

deepwater condition, particularly in Santos Basin Central Cluster region, extreme current load has more significant effect on the riser strength performance.

6.8.2 Fatigue Analysis

- As seen from the result of fatigue analysis due to wave, the top of hang-off point section has lower fatigue life than the touch down point (TDP) section. This result indicates higher cyclic load occurs at top of the riser system compare. This result also proves that no significant dynamic load occurs at touch down area.
- In accordance with the result shown in Figure 6.12 – Fatigue Life at Touch Down Point, the critical fatigue life resulted in only short span of the riser. Even though that the result had shown sufficient fatigue life, but this is a good indication to improve the fatigue performance at touch down point, in case there is insufficient fatigue life for other case, e.g. harsher environment, different soil conditions, etc.
- There is a possibility of more robust fatigue performance if the sub-surface buoy is located in deeper water depth, where the dynamic effect might be lower than the current Base Case configuration.
- From fatigue due to VIV result, it can be concluded that there is no significant fatigue VIV issues with regards to the Santos Basin Central Cluster region metocean data. However, further investigation might be needed for fatigue VIV with bidirectional currents profile.

7. COBRA Concept Sensitivity Study

7.1 Introduction

This chapter presents sensitivity study for COBRA Base Case configuration as presented in Chapter 6. The method which presented here is based on alternative geometry arrangement of the riser system with regards to the strength performances. The results are focused only on strength analysis under static and dynamic behavior.

Three main sensitivity cases are performed. The descriptions of these cases are presented in Section 7.2. The result for Case 1, Case 2, and Case 3 are presented in Section 7.3, 7.4, and 7.5 respectively. The analysis result comparison with the Base Case result is presented in each section. At the end, discussions on overall sensitivity studies are given in Section 7.6.

7.2 Sensitivity Cases

The COBRA Base Case configuration results that are presented in Chapter 6 show sufficient strength capacity for both normal (ULS) and accidental (ALS) cases. However, based on the results and discussions, it is interesting to study the effect of bidirectional (2-directions) current profile for possible alternative riser arrangements. The purpose of this sensitivity study is to assess the robustness of COBRA Base Case riser concept if alternative riser arrangements are used. In this sensitivity study, the assessment is limited to the strength analysis design only.

Two sensitivity cases are performed to assess the strength performances of the riser system. The following table describes these two alternative cases (as also mentioned in Table 5.11 – Sensitivity Study Cases):

Case	Parameter	Case Description
Case 1	Sub-surface buoy	In Base Case study, the sub-surface buoy is located at -250 m below the surface. In this case (Case 1), the sub-surface buoy will be located at -400 m below the surface.
Case 2	Flexible jumper	In Base Case study, the flexible jumper connection point is located at top of sub-surface buoy. In this case (Case 2), the connection point will be placed at bottom of sub-surface buoy.

Table 7.1 – Strength Sensitivity Cases

According to the Base Case analysis result, the worst case combination comes from the combination of 10 year wave and 100 year surface profile current. Hence, for this sensitivity study, the case combination is only performed for 10 year wave and 100 year surface profile current.

A total of 8 cases are considered for each ULS and ALS design. The following table shows the details of case combination for this strength sensitivity study (as also can be seen in Table 6.2 – Strength Analysis Case):

No	Wave & Current Return Period	Current Profile	Current Directional	Vessel Offset
1	10 year wave + 100 year current	Surface Profile	1-direction current (unidirectional)	Near (-80m) offset,180° current+wave
2				Nominal (0) offset, 180° current+wave
3				Nominal (0) offset, 0° current+wave
4				Far (+80m offset), 0° current+wave
5			2-directions current (bidirectional)	Near (-80m) offset,180° current+wave
6				Nominal (0) offset, 180° current+wave
7				Nominal (0) offset, 0° current+wave
8				Far (+80m offset), 0° current+wave

Table 7.2 – Strength Sensitivity Case Combination

In addition to the strength sensitivity cases, another sensitivity case is also performed to assess the maximum lateral displacement of the Base Case riser system under perpendicular current load. Here, sensitivity case is performed to reduce the maximum lateral displacement of the riser system by looking into the possibility of alternative anchor point arrangement. It is important to check the lateral displacement of the riser system, mainly to avoid line clashing when there is other line component adjacent to the riser system (e.g. FPSO mooring line, other risers from other platform or vessel, etc.).

The analysis is performed under static current load for both surface current profile and mid-level current profile. Both 10 year and 100 year current return period are considered in this study. The vessel offset is limited to the nominal (mean) vessel offset position only.

The following table shows the case combinations for this lateral displacement assessment.

Case	Parameter	Current
Base Case	θ_1 = 0° (distance between mooring line = 3 m)[1]	10 year - Surface Profile (90 deg) 100 year - Surface Profile (90 deg) 10 year - Mid-level Profile (90 deg) 100 year - Mid-level Profile (90 deg)
Case 3	θ_1 = 5° (distance between mooring line = 46 m) [1]	10 year - Surface Profile (90 deg) 100 year - Surface Profile (90 deg) 10 year - Mid-level Profile (90 deg) 100 year - Mid-level Profile (90 deg)
Case 4	θ_1 = 10° (distance between mooring line = 89.4 m) [1]	10 year - Surface Profile (90 deg) 100 year - Surface Profile (90 deg) 10 year - Mid-level Profile (90 deg) 100 year - Mid-level Profile (90 deg)
Case 5	θ_1 = 15° (distance between mooring line = 134.2 m) [1]	10 year - Surface Profile (90 deg) 100 year - Surface Profile (90 deg) 10 year - Mid-level Profile (90 deg) 100 year - Mid-level Profile (90 deg)

Note:
[1] Refer to Figure 7.1 and Figure 7.2 for case parameter details

Table 7.3 – Lateral Displacement Case Combination

The following figures show the sketch for Case 3, Case 4, and Case 5 as mentioned in Table 7.3.

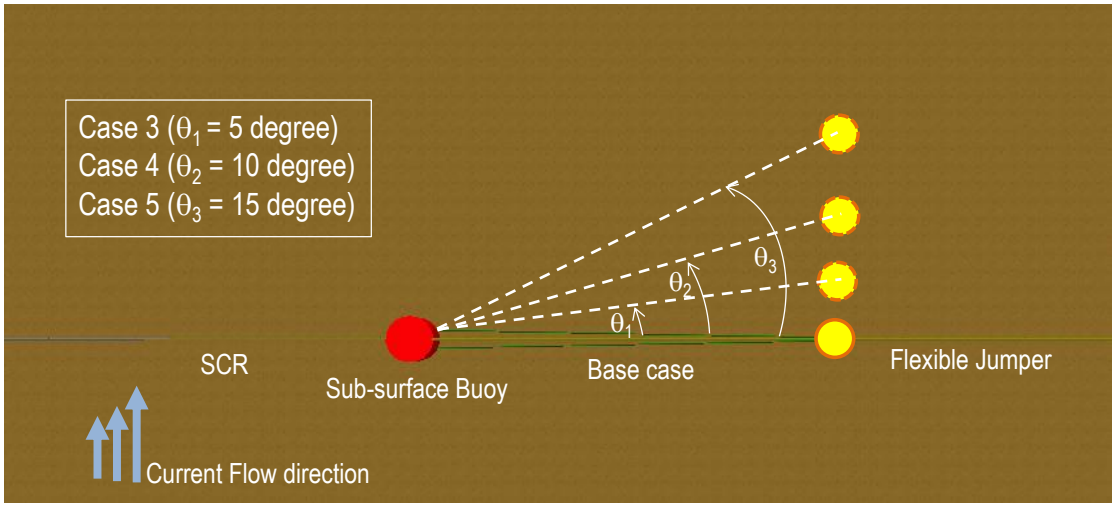

Figure 7.1 – Anchor Point Case Study (Plan View)

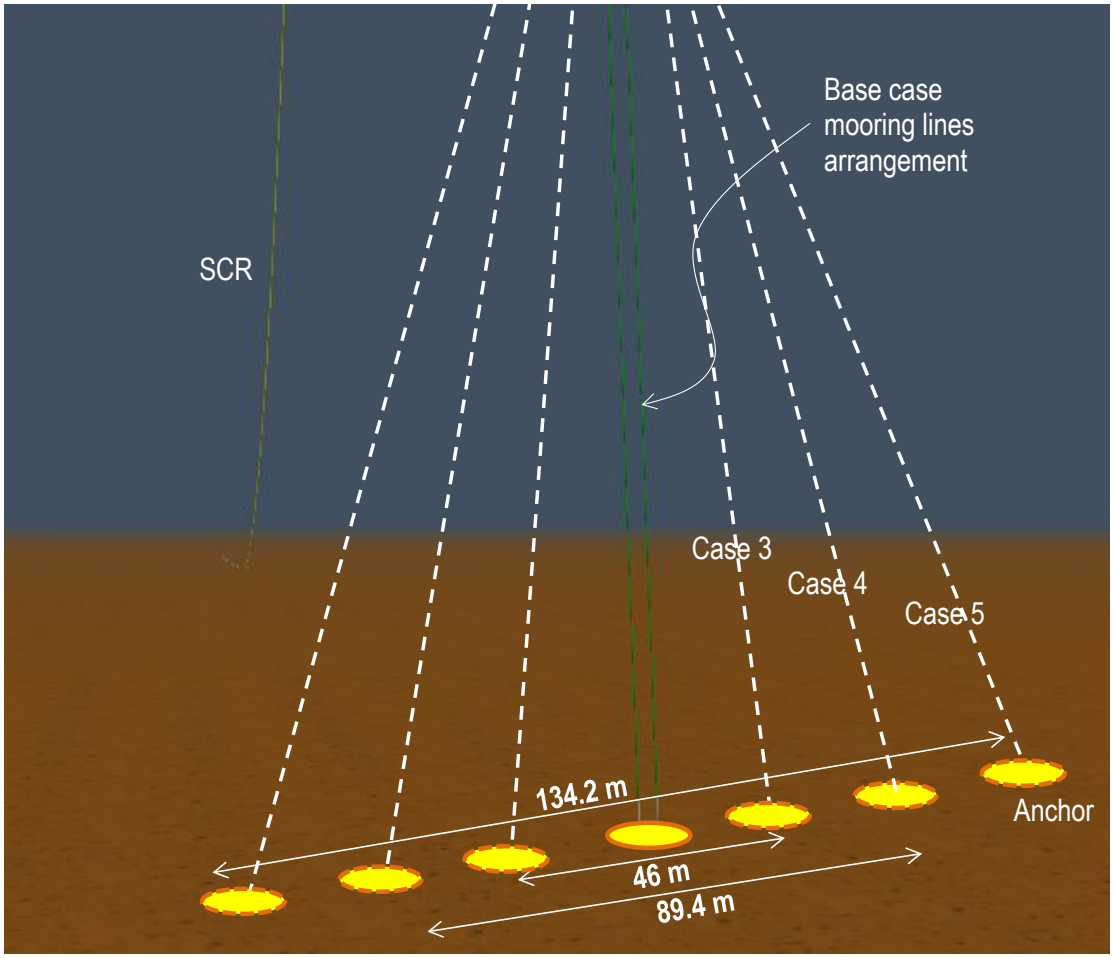

Figure 7.2 – Anchor Point Case Study (Isometric View)

7.3 Case 1 – Deeper Sub-surface Buoy

As explained in Section 7.2, in this case, the sub-surface buoy is placed at 400 m below the sea surface. The following figure show the riser system arrangement for Case 1.

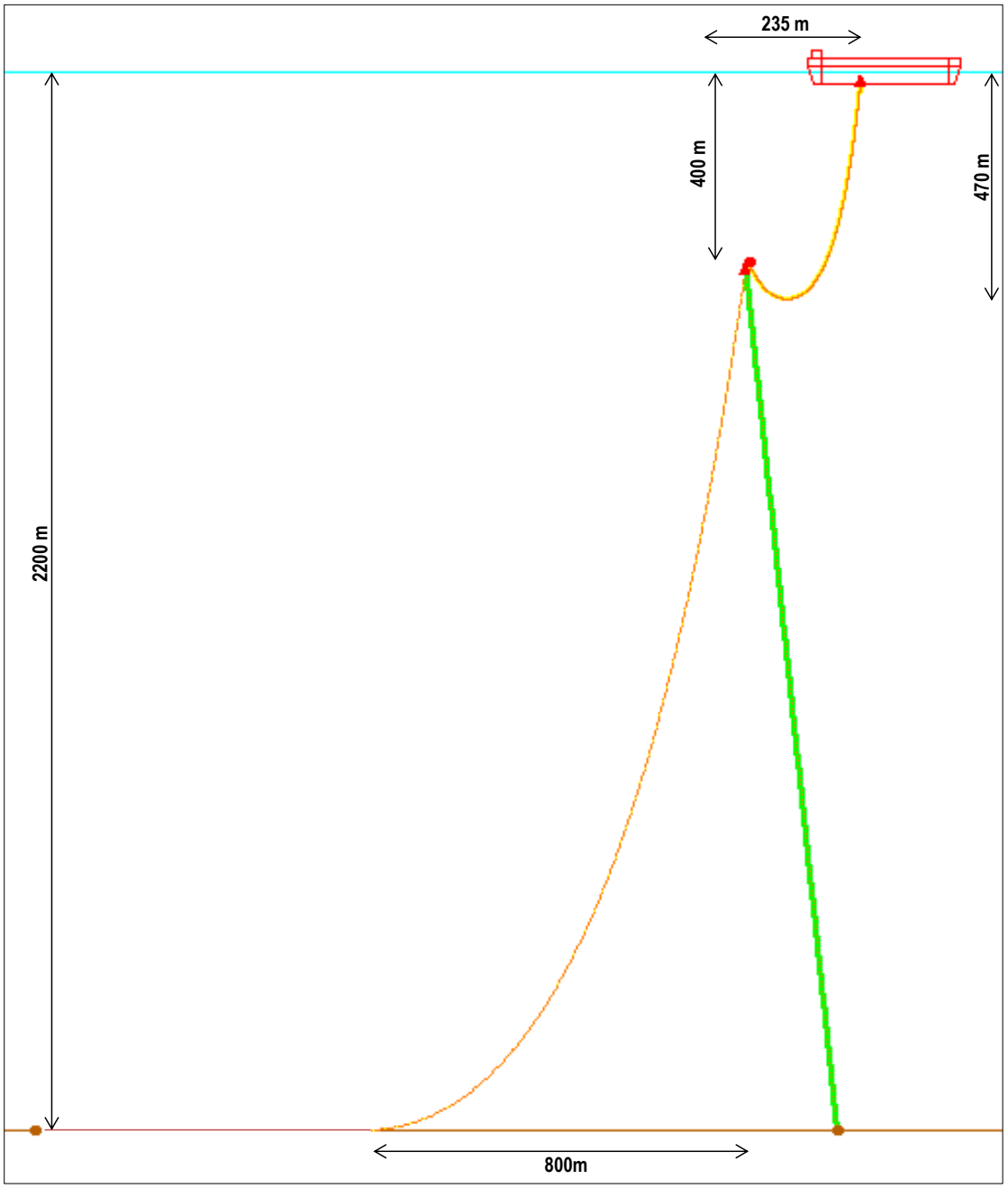

Figure 7.3 – Case 1 Static Configuration (Elevation View)

The same finite element modeling as the Base Case model is used. The overview of the riser system modeling is given earlier in Section 5.4 Model Overview. However, as the sub-surface buoy is located in deeper area, the flexible jumper length is modelled longer than the Base Case model. In addition, the mooring line length is modelled shorter than the Base Case model. For this case, the flexible jumper length is 650 m, and the mooring line length is 1800 m for each lines.

The following sections present the static and dynamic responses for this case.

7.3.1 Static Response (ULS)

In static analysis, the static equilibrium configuration is achieved by considering only static loading (refer to Section 4.8.1 for the static loading description). The same typical four static configurations as Base Case model are also considered (refer to Figure 6.1 – Static Riser Configuration).

Static responses for the flexible jumper, riser, and mooring lines are presented below.

Flexible Jumper

Table 7.4 shows the summary result for static catenaries jumper configuration for near, nominal, far vessel offset position. Various current profiles based on case combination presented in Table 7.2 have been considered.

Static Result Summary - Jumper	Unidirectional current Vessel Position			Bidirectional current Vessel Position		
	Near	Nominal	Far	Near	Nominal	Far
Maximum Static angle at vessel (deg)[1]	6.6	8.5	5.0	3.6	5.8	8.2
Maximum Static angle at buoy (deg)[2]	15.9	23.6	26.8	12.3	24.1	32.5
Maximum Static tension at vessel (kN)	1433	1440	1440	1422	1442	1456
Maximum Static tension at buoy (kN)	373	392	410	380	391	415
Minimum Bending Radius (m)	39	45	66	27	44	82

Note:
[1] Static angle at vessel is relative to vertical
[2] Static angle at buoy is angle between buoy and jumper

Table 7.4 – Static Jumper Result (Case 1 – ULS)

The following table shows the comparison of static jumper result between Base Case and Case 1 configuration.

Comparison between Base Case - Case 1	Base Case	Case 1
Maximum Static angle at vessel (deg)	17.2	8.5
Maximum Static angle at buoy (deg)	43.2	32.5
Maximum Static tension at vessel (kN)	1158	1456
Maximum Static tension at buoy (kN)	515	415
Minimum Bending Radius (m)	45	27

Table 7.5 – Comparison Static Jumper Result (Base Case – Case 1)

From the result, it can be seen that the jumper is still in feasible static configuration. The minimum bending radius is reduced to 27 m due to deeper sub-surface buoy location. This result is still in an acceptable result (refer to Design Acceptance Criteria in Section 5.6).

It is interesting to see that for Case 1 configuration, the maximum tension at vessel is increased significantly to 1456 kN, but the maximum tension at sub-surface buoy is reduced to 415 kN. With lower tension load at sub-surface buoy, it is expected that the von Mises stress on top of the riser hang-off connection will also be reduced.

Riser

Table 7.6 presents the summary result for static riser configuration for near, nominal, and far vessel position. The same various current profiles as for the flexible jumper are also have been considered.

Static Result Summary - Riser	Unidirectional current Vessel Position			Bidirectional current Vessel Position		
	Near	Nominal	Far	Near	Nominal	Far
Maximum Static top angle (deg)	7.2	8.6	9.5	6.9	8.7	10.3
Maximum Static top tension (kN)	1975	2116	2152	2086	2114	2047
Minimum Static TDP tension (kN)	212	346	379	318	344	278

Table 7.6 –Static Riser Result (Case 1 – ULS)

The following table shows the comparison of static riser result between Base Case and Case 1 configuration.

Comparison between Base Case - Case 1	Base Case	Case 1
Maximum Static top angle (deg)	13.6	10.3
Maximum Static top tension (kN)	2413	2152
Minimum Static TDP tension (kN)	253	212

Table 7.7 – Comparison Static Riser Result (Base Case – Case 1)

From Table 7.6, it can be observed that the static tension load variation in Case 1 riser configuration is typical with the Base Case configuration result (refer to Table 6.4). Maximum static top angle of 10.3° comes from far vessel position case with bidirectional current profile, maximum top tension of 2152 kN comes from the far vessel position case with unidirectional current profile, and minimum static TDP tension comes from the near vessel position case with unidirectional current profile. From the result, it can also be concluded that lower layer current from bidirectional current profile can reduce the static top tension of the riser as explained earlier in Section 6.4.2.

The comparison between Base Case and Case 1 result shows that the maximum static top angle is slightly reduced. The maximum static top tension is also reduced from Base Case result, as the static tension force is simply the function of suspended riser length. In Case 1 configuration with deeper sub-surface buoy, the suspended length is shorter than the Base Case configuration. The minimum static tension at TDP is still positive, which means no compression load occurs.

Mooring Line

The following table shows the static result summary for mooring lines.

Static Result Summary - Mooring Line	Unidirectional current Vessel Position			Bidirectional current Vessel Position		
	Near	Nominal	Far	Near	Nominal	Far
Maximum Static tension (kN)[1]	744	730	651	680	729	714

Note:
[1] The tension presented is the tension in each of the two mooring lines.

Table 7.8 – Static Mooring Lines Result (Case 1 – ULS)

The following table shows the comparison of static mooring lines result between Base Case and Case 1 configuration.

Comparison between Base Case - Case 1	Base Case	Case 1
Maximum Static tension (kN)	644	744

Table 7.9 – Comparison Static Mooring Lines Result (Base Case – Case 1)

From the result shown in Table 7.8, typical static tension result is observed with the Base Case result. However, it is interesting to see that Case 1 configuration has higher static tension load compare to Base Case. Case 1 configuration is using the same sub-surface buoyancy module with the Base Case configuration. Hence, both cases have similar uplift force from the buoyancy module. However, higher static tension load at mooring line occurs since Case 1 configuration has lower flexible jumper tension at sub-surface buoy, as can be seen in Table 7.5. This higher tension load might impact the foundation anchor design, which is not included in the scope of this thesis work.

7.3.2 Dynamic Response (ULS)

In the dynamic analysis, the same nonlinear time domain analysis with the Base Case model is considered. However, only case combination of 10 year wave/100 year current is considered, as this the worst case combination based from the result captured from Base Case result in Chapter 6. This case combination can be seen in Table 7.2 as presented in earlier section.

Dynamic response for the flexible jumper, riser, and mooring lines are presented below.

Flexible Jumper

The following table shows the summary result of flexible jumper in Case 1 configuration.

Dynamic Result Summary - Jumper	Unidirectional current Vessel Position			Bidirectional current Vessel Position		
	Near	Nominal	Far	Near	Nominal	Far
Minimum radius (m)	33	52	65	27	57	77
Hmin (m)	100	87	86	113	87	73
Minimum tension (kN)	88	134	147	66	119	173
Maximum tension at Vessel (kN)	1598	1746	1785	1591	1756	1795
Maximum tension at Buoy (kN)	385	428	463	394	423	469
Minimum angle at Vessel (deg)	5.3	6.9	0.1	2.4	3.9	2.7
Maximum angle at Vessel (deg)	9.1	11.2	7.2	6.0	8.3	10.6
Minimum angle at Buoy (deg)	14.3	21.8	26.5	12.2	22.1	30.1
Maximum angle at Buoy (deg)	16.0	23.7	29.0	13.2	24.4	33.4

Table 7.10 – Dynamic Jumper Result (Case 1 – ULS)

From table above, the result shows that minimum radius and Hmin resulted in acceptable limit. Minimum tension of 66 kN shows that there is no compression load on the flexible jumper.

The following figures show the comparison between static and dynamic response of maximum tension at vessel and sub-surface buoy.

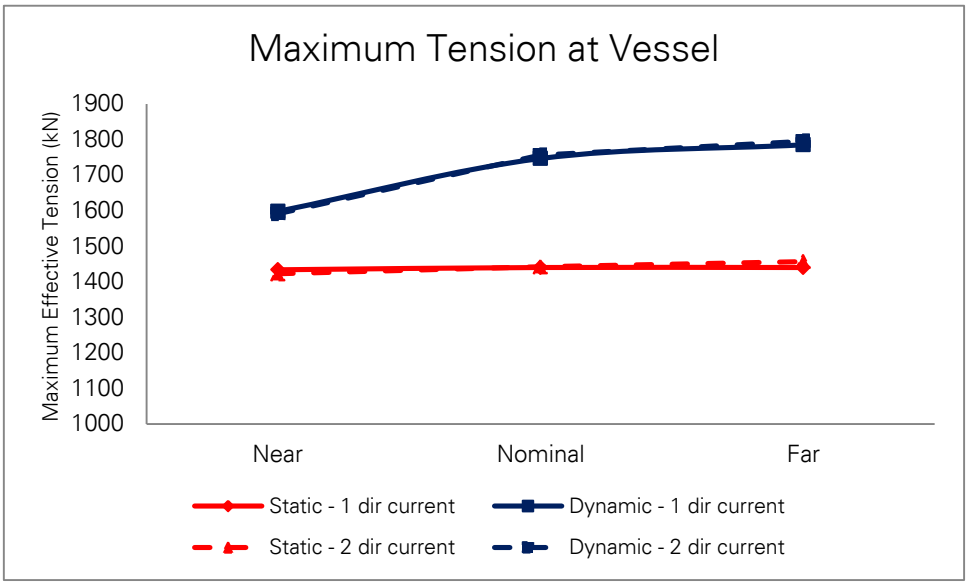

Figure 7.4 – Static and Dynamic Tension of Jumper at Vessel (Case 1)

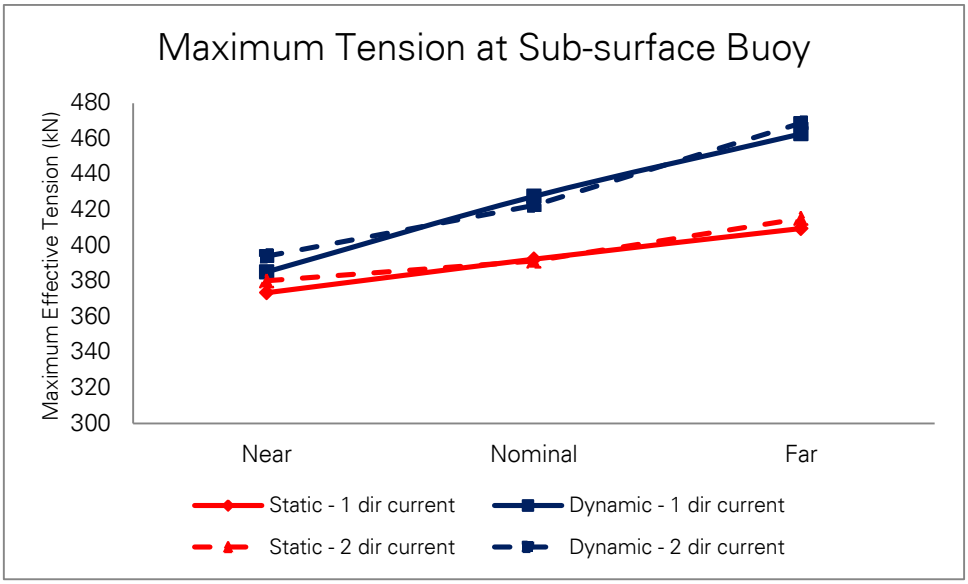

Figure 7.5 – Static and Dynamic Tension of Jumper at Sub-surface Buoy (Case 1)

From the figures above, it can be seen that similar response from Base Case result is occurs. Unidirectional and bidirectional current profiles have no significant impact for tension load in flexible jumper. However, the maximum tension load at vessel is increased by 340 kN due to dynamic motion. This result is higher than the Base Case configuration result because Case 1 configuration has longer flexible jumper length.

It is interesting to see that with longer flexible jumper length, Case 1 configuration has smaller tension load at sub-surface buoy compared to Base Case configuration. The maximum tension at sub-surface buoy in Case 1 configuration is 469 kN, while the Base Case configuration result is 606 kN. In Case 1 configuration, this maximum dynamic tension load is increased by 54 kN from the maximum static tension response, while Base Case configuration has higher increment of 90 kN.

The following table shows the comparison of dynamic jumper result between Base Case and Case 1.

Comparison between Base Case - Case 1	Base Case	Case 1
Minimum radius (m)	42	27
Hmin (m)	62	73
Minimum tension (kN)	111	66
Maximum tension at Vessel (kN)	1399	1795
Maximum tension at Buoy (kN)	606	469
Minimum angle at Vessel (deg)	4.7	0.1
Maximum angle at Vessel (deg)	20.4	11.2
Minimum angle at Buoy (deg)	17.8	12.2
Maximum angle at Buoy (deg)	44.8	33.4

Table 7.11 – Comparison Dynamic Jumper Result (Base Case – Case 1)

From the comparison result shown above, it can be observed that Case 1 flexible jumper has more advantage in lower tension load at sub-surface buoy. This result might improve the tapered stress joint design. However, it should be noted that the payload at vessel is increased significantly. Hence, in this configuration, the vessel's hang-off capacity should be reviewed to make sure that it has sufficient capacity.

Riser

The following table summarizes the dynamic result of riser.

Dynamic Result Summary - Riser	Unidirectional current Vessel Position			Bidirectional current Vessel Position		
	Near	Nominal	Far	Near	Nominal	Far
Maximum Top Tension (kN)	1990	2157	2199	2102	2139	2096
Minimum TDP Tension (kN)	208	336	364	313	338	261
von Mises Stress - Top (MPa)	160	160	179	154	154	175
von Mises Stress - Below Stress Joint (MPa)	233	233	244	230	230	242
von Mises Stress - Sagbend (MPa)	251	253	254	253	253	252
Maximum Buckling Utilization - Top	0.37	0.37	0.37	0.37	0.37	0.37
Maximum Buckling Utilization - Below Stress Joint	0.67	0.67	0.67	0.67	0.67	0.67
Maximum Buckling Utilization - Sagbend	0.78	0.78	0.78	0.78	0.78	0.78

Table 7.12 – Dynamic Riser Result (Case 1 – ULS)

For the top tension and TDP tension results, it can be seen that the same trend is observed from the static response. The maximum top tension and minimum TDP tension drives by unidirectional current profile. This trend is also observed from the Base Case configuration.

The following figures present the comparison of static and dynamic response at top and TDP tension.

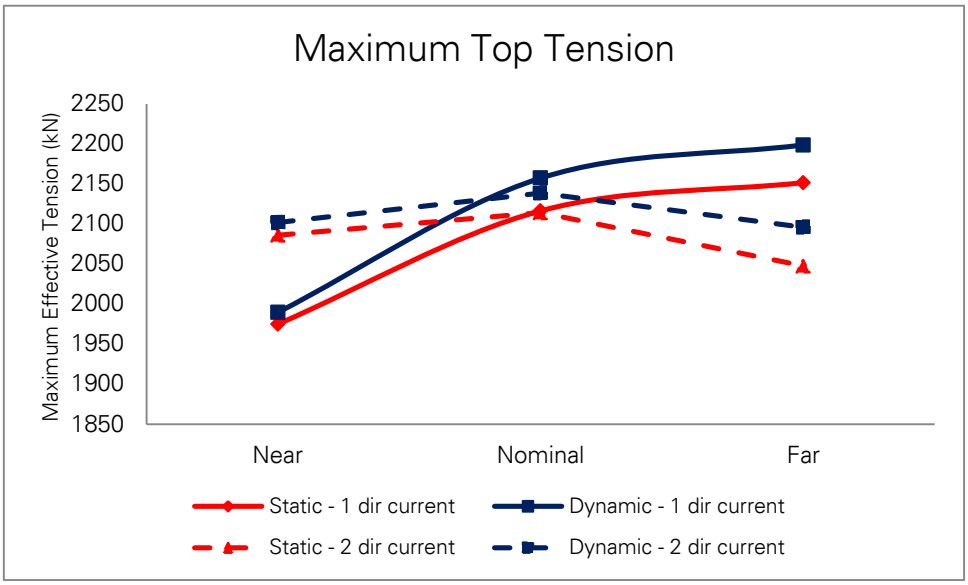

Figure 7.6 – Static and Dynamic Top Tension of Riser (Case 1)

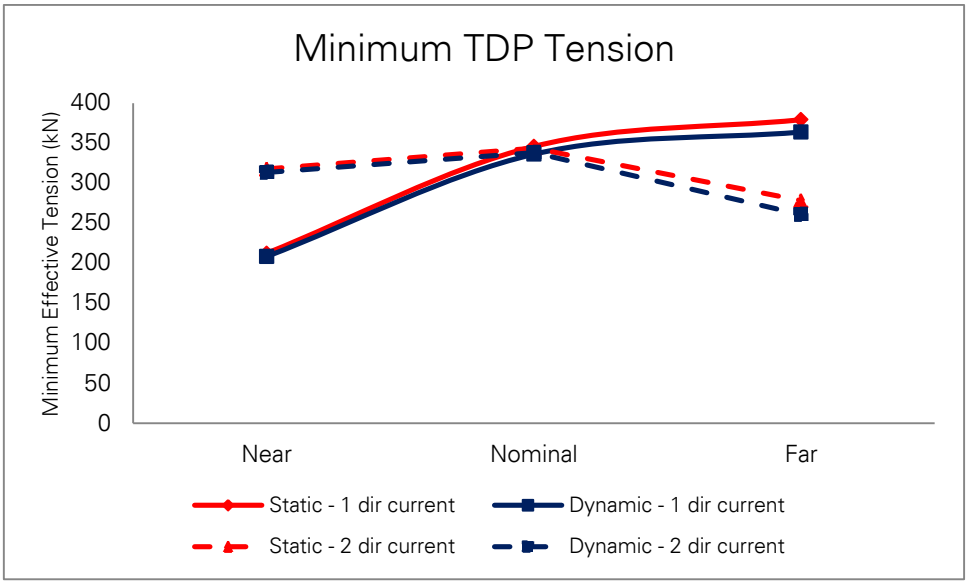

Figure 7.7 – Static and Dynamic TDP Tension of Riser (Case 1)

From the figures above, it can be seen that for this Case 1 configuration, bidirectional (2-directions) current profile is also gives significant effect in terms of tension load. As seen from Figure 7.6, for various vessel offset positions, the maximum static top tension load is magnified by 47 kN due to dynamic motion. This result is smaller compared to Base Case configuration, where static top tension load is magnified by 97 kN. From Figure 7.7, it can be seen that almost no significant dynamic effect at TDP tension.

The following figures show the maximum static and dynamic von Mises stress result for Case 1 riser configuration.

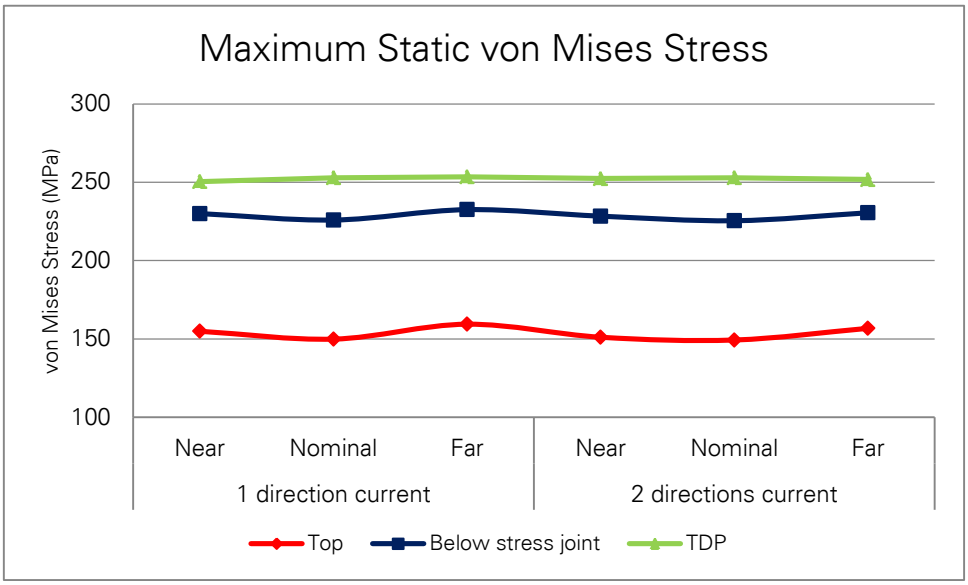

Figure 7.8 – Static von Mises Stress of Riser (Case 1)

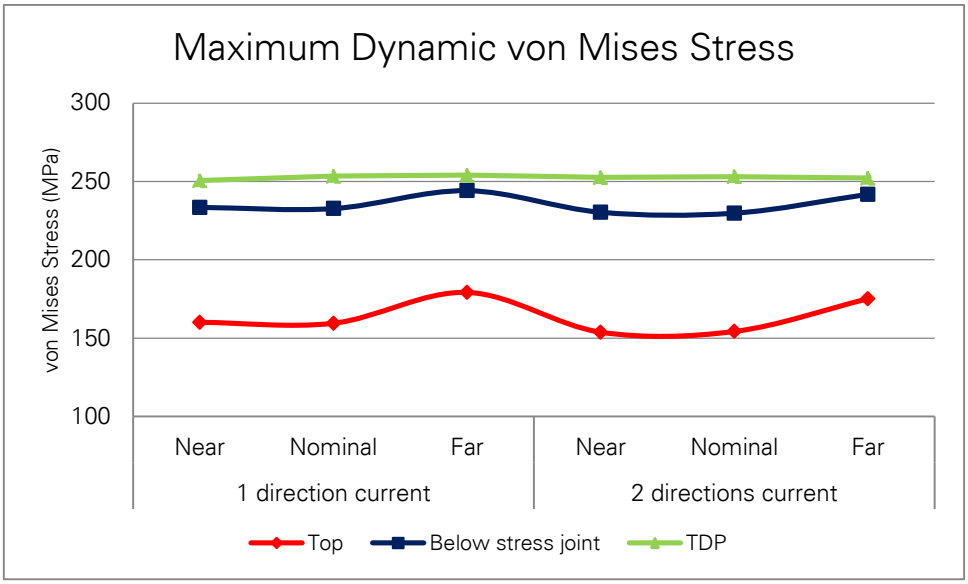

Figure 7.9 – Dynamic von Mises Stress of Riser (Case 1)

Figure 7.7 and Figure 7.8 show the von Mises stress at top, below stress joint, and TDP section for various vessel offset positions. As seen from that figures, the result shows that the von Mises stresses from static and dynamic response are almost similar. Slightly higher stress amplitude is observed on top and below stress joint section due to the dynamic effect. At TDP, the variation of stress amplitude is almost constant.

From Figure 7.9, it can be seen that the highest von Mises stress located at TDP section. This result is different compared to Base Case result, where the highest von Mises stress located at top section. It can be concluded that Case 1 configuration gives more robust performance. Moreover, it can also be concluded that Case 1 riser configuration has less dynamic effect compared to Base Case riser configuration.

From the static and dynamic response of flexible jumper tension load at sub-surface buoy, it can be seen that Case 1 configuration has less tension than the Base Case configuration.

Again, this proves the linear correlation between tension load of jumper at sub-surface buoy and high bending stress at top hang-off section of riser.

The following table shows the comparison between Base Case and Case 1 dynamic riser result.

Comparison between Base Case - Case 1	Base Case	Case 1
Maximum Top Tension (kN)	2510	2199
Minimum Sagbend Tension (kN)	243	208
von Mises Stress - Top (MPa)	312	179
von Mises Stress - Below Stress Joint (MPa)	291	244
von Mises Stress - Sagbend (MPa)	266	254
Maximum Buckling Utilization - Top	0.50	0.37
Maximum Buckling Utilization - Below Stress Joint	0.67	0.67
Maximum Buckling Utilization - Sagbend	0.78	0.78

Table 7.13 – Comparison Dynamic Riser Result (Base Case – Case 1)

From the result above, Case 1 riser configuration shows better result compared to Base case configuration. The most significant result in this comparison appears to be the von Mises stress at top section of the riser, where the stress reduced from 312 MPa into 179 MPa. It can be concluded that the riser in Case 1 configuration gives more robust result.

Mooring Line

The following table presents the dynamic mooring lines result.

Dynamic Result Summary - Mooring Line	Unidirectional current Vessel Position			Bidirectional current Vessel Position		
	Near	Nominal	Far	Near	Nominal	Far
Minimum tension (kN)[1]	723	618	596	659	638	656
Maximum tension (kN)[1]	765	756	703	697	770	773

Note:
[1] The tension presented is the tension in each of the two mooring lines.

Table 7.14 – Dynamic Mooring Lines Result (Case 1 – ULS)

Figure 7.10 presents the plot of minimum and maximum tension in mooring line, and the comparison with the static tension load.

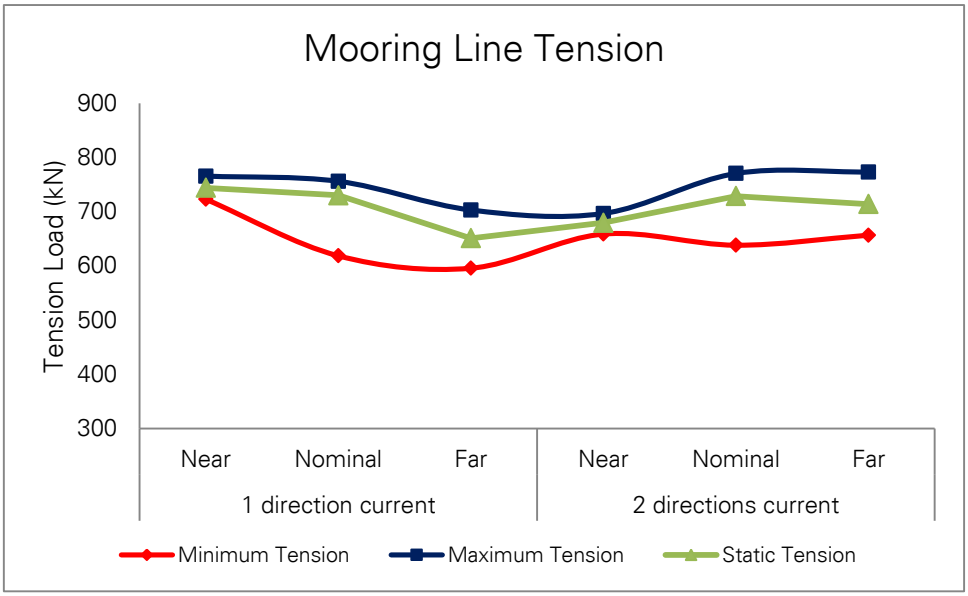

Figure 7.10 – Maximum and Minimum Mooring Line Tension (Case 1)

In this Case 1 configuration, it can be seen that the range between minimum and maximum tension load in the mooring line is relatively smaller compared to the Base Case configuration result. In Case 1 configuration, the maximum tension load is 773 kN and the minimum tension load is 596 kN, resulted in range of tension load of 177 kN. In Base Case configuration, the maximum tension load is 697 kN, and the minimum tension load is 424 kN, resulted in range of tension load of 273 kN. The following table shows the comparison between maximum and minimum tension load of Base Case and Case 1 configurations.

Comparison between Base Case - Case 1	Base Case	Case 1
Minimum tension (kN)	424	596
Maximum tension (kN)	697	773

Table 7.15 – Comparison Dynamic Mooring Lines Result (Base Case – Case 1)

From the result shown above, it can be concluded that Case 1 configuration has higher tension load. However, it can be seen that the dynamic effect in Case 1 configuration is lower compared to Base Case configuration. Less dynamic effect should give more robust design, in particular for the anchor foundation's design.

7.3.3 Comparison with Accidental Case Result

The accidental case (ALS) condition for Case 1 configuration is also carried out by considering a condition if one of the two mooring lines fails. In this configuration, only the worst case combinations are performed, as shown in Table 7.2.

The following table shows the comparison summary of the strength analysis result between normal (ULS) and accidental (ALS) case for Case 1 configuration.

	Case 1	
	Normal	Accidental
SCR		
Top Tension (kN)	2199	2241
TDP Tension (kN)	208	211
Buckling Utilization	0.78	0.78
von Mises Stress (MPa)	254	268
Jumper		
Minimum radius (m)	26.7	28.3
Minimum tension (kN)	66	70
Maximum tension at Vessel (kN)	1795	1784
Maximum tension at Buoy (kN)	469	464
Buoyancy mooring lines		
Minimum tension (kN)	596	1165
Maximum tension (kN)	773	1570

Table 7.16 – Riser System Result Summary (Case 1)

As seen from table above, it can be concluded that the riser system in Case 1 configuration is also has sufficient strength capacity. It is obvious that the tension load in one of the mooring line becomes approximately twice higher due to the failure. Hence, for the mooring line design, a sufficient safety factor should be carefully anticipated.

Detail analysis results for Case 1 are presented in Appendix C.

7.4 Case 2 – Flexible Jumper End Connection

In Case 2 configuration, Base Case model configuration is used as shown in Figure 5.8 – Base Case Static Configuration (Elevation View). However, as explained in Section 7.2, in this configuration, the connection point of flexible jumper to the sub-surface buoy is located at the bottom of the sub-surface buoy. Normally, a universal ball joint connection will be placed at top of the riser assembly for this type of configuration.

The following figure shows the Case 2 riser system configuration.

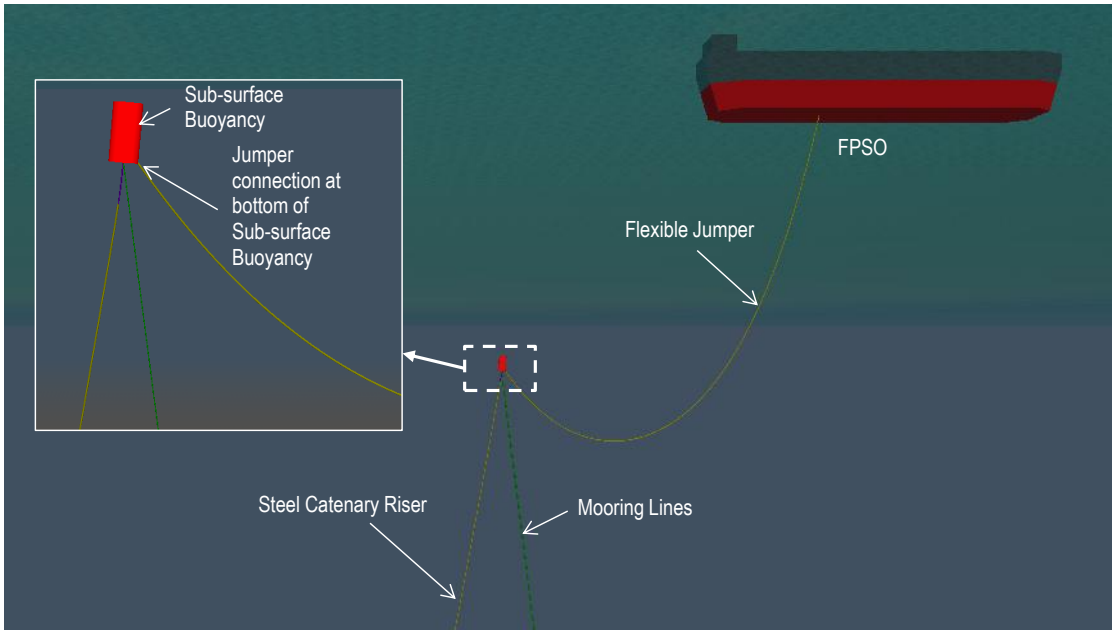

Figure 7.11 – Case 2 Riser System Configurations

The same finite element modeling as the Base Case model is used. The overview of the riser system modeling is given earlier in Section 5.4 Model Overview. The total length of flexible jumper section is the same as Base Case model.

The following sections present the static and dynamic responses for this case.

7.4.1 Static Response (ULS)

The same analysis method as Base Case and Case 1 configuration is also performed in Case-2 configuration. Typical four static configurations as Base Case model are also considered (refer to Figure 6.1 – Static Riser Configuration).

Static responses for the flexible jumper, riser, and mooring lines are presented below.

Flexible Jumper

Table 7.17 presents the summary result for static catenaries jumper configuration for near, nominal, far vessel offset position. Various current profiles based on case combination presented in Table 7.2 are considered.

Static Result Summary - Jumper	Unidirectional current Vessel Position			Bidirectional current Vessel Position		
	Near	Nominal	Far	Near	Nominal	Far
Maximum Static angle at vessel (deg)	12.2	15.6	11.6	7.8	12.5	16.6
Maximum Static angle at buoy (deg)	27.3	36.2	35.6	19.0	36.7	45.7
Maximum Static tension at vessel (kN)	1121	1141	1130	1093	1146	1181
Maximum Static tension at buoy (kN)	413	448	466	410	454	504
Minimum Bending Radius (m)	71	70	97	46	68	131

Note:
[1] Static angle at vessel is relative to vertical
[2] Static angle at buoy is angle between buoy and jumper

Table 7.17– Static Jumper Result (Case 2 – ULS)

The following table shows the comparison of static jumper result between Base Case and Case 2 configuration.

Comparison between Base Case - Case 2	Base Case	Case 2
Maximum Static angle at vessel (deg)	17.2	16.6
Maximum Static angle at buoy (deg)	43.2	45.7
Maximum Static tension at vessel (kN)	1158	1181
Maximum Static tension at buoy (kN)	515	504
Minimum Bending Radius (m)	45	46

Table 7.18 – Comparison Static Jumper Result (Base Case – Case 2)

As seen from the comparison above, Case 2 configuration has slightly higher static tension load at vessel and slightly lower tension load at sub-surface buoy. This lower tension load, however, might not significantly change the stress result at top of tapered stress joint section from the Base Case result.

Riser

Table 7.19 below shows the summary result of static riser configuration for near, nominal, and far vessel position.

Static Result Summary - Riser	Unidirectional current Vessel Position			Bidirectional current Vessel Position		
	Near	Nominal	Far	Near	Nominal	Far
Maximum Static top angle (deg)	4.9	5.4	5.8	5.1	5.4	5.6
Maximum Static top tension (kN)	2165	2351	2403	2307	2347	2275
Minimum Static TDP tension (kN)	270	444	494	401	440	374

Table 7.19– Static Riser Result (Case 2 – ULS)

The following table shows the comparison of static riser result between Base Case and Case-2 configuration.

Comparison between Base Case - Case 2	Base Case	Case 2
Maximum Static top angle (deg)	13.6	5.8
Maximum Static top tension (kN)	2413	2403
Minimum Static TDP tension (kN)	253	270

Table 7.20 – Comparison Static Riser Result (Base Case – Case 2)

From the result shown in Table 7.19, it can be seen that the tension load variation in Case 2 riser configuration is typical with the Base Case configuration result (refer to Table 6.4). It can

also be seen from this result that lower layer current from bidirectional current profile can reduce the static top tension of the riser as explained earlier in Section 6.4.2.

The comparison between Base Case and Case 2 result shows that the maximum static top angle in Case 2 configuration is reduced by half of the maximum static top angle in Base Case configuration. The reduction of hang-off angle will alter the touch-down-point (TDP) location. As mentioned in Section 6.4.2, alteration on touch down point location might give different dynamic response of the riser, in particular for seabed area with various soil conditions. This condition will also give different fatigue response at the TDP area.

Compared to Base Case result, the maximum static top tension in Case 2 is just slightly reduced. The minimum static tension at TDP is still positive, which means no compression load occurs.

Mooring Line

The following table presents the static result summary for mooring line in Case 2 configuration.

Static Result Summary - Mooring Line	Unidirectional current Vessel Position			Bidirectional current Vessel Position		
	Near	Nominal	Far	Near	Nominal	Far
Maximum Static tension (kN)	647	626	522	564	623	601

Note:
[1] The tension presented is the tension in each of the two mooring lines.

Table 7.21– Static Mooring Lines Result (Case 2 – ULS)

The following table shows the comparison of static mooring lines result between Base Case and Case 2 configuration.

Comparison between Base Case - Case 2	Base Case	Case 2
Maximum Static tension (kN)	644	647

Table 7.22 – Comparison Static Riser Result (Base Case – Case 2)

From the result shown above, it can be seen that the result for static mooring lines are almost similar with the Base Case configuration result.

7.4.2 Dynamic Response (ULS)

In the dynamic analysis, the same nonlinear time domain analysis with the Base Case and Case 1 model is considered. Overall case combinations for this dynamic analysis can be seen in Table 7.2.

The dynamic response for the flexible jumper, riser, and mooring lines are presented in the following part.

Flexible Jumper

The following table presents the summary result of flexible jumper in Case 2 configuration.

Dynamic Result Summary - Jumper	Unidirectional current Vessel Position			Bidirectional current Vessel Position		
	Near	Nominal	Far	Near	Nominal	Far
Minimum radius (m)	63	88	91	43	93	120
Hmin (m)	83	69	75	105	69	56
Minimum tension (kN)	164	228	218	112	204	282
Maximum tension at Vessel (kN)	1238	1336	1384	1214	1369	1428
Maximum tension at Buoy (kN)	432	484	544	430	510	601
Minimum angle at Vessel (deg)	10.7	13.5	4.8	6.4	9.0	10.0
Maximum angle at Vessel (deg)	15.2	18.8	14.1	10.8	15.3	19.3
Minimum angle at Buoy (deg)	26.2	34.9	35.1	18.8	34.1	42.7
Maximum angle at Buoy (deg)	27.5	36.7	38.3	19.5	37.8	47.7

Table 7.23 – Dynamic Jumper Result (Case 2 – ULS)

From table above, the result shows that minimum radius and Hmin resulted in acceptable limit. Almost similar result with Base Case configuration is observed. Minimum tension of 112 kN shows that there is no compression load on the flexible jumper. The following figures show the comparison between static and dynamic response of maximum tension at vessel and sub-surface buoy.

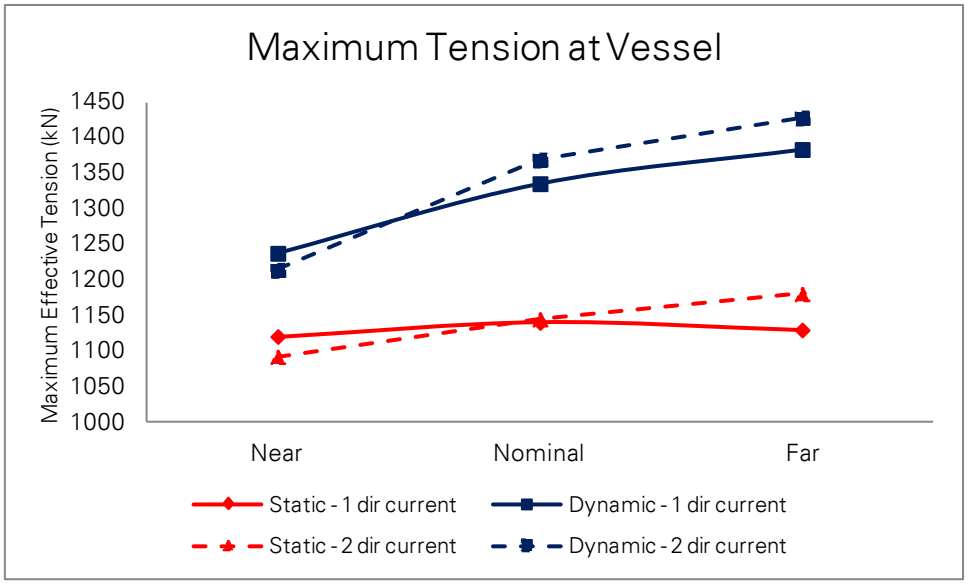

Figure 7.12 – Static and Dynamic Tension of Jumper at Vessel (Case 2)

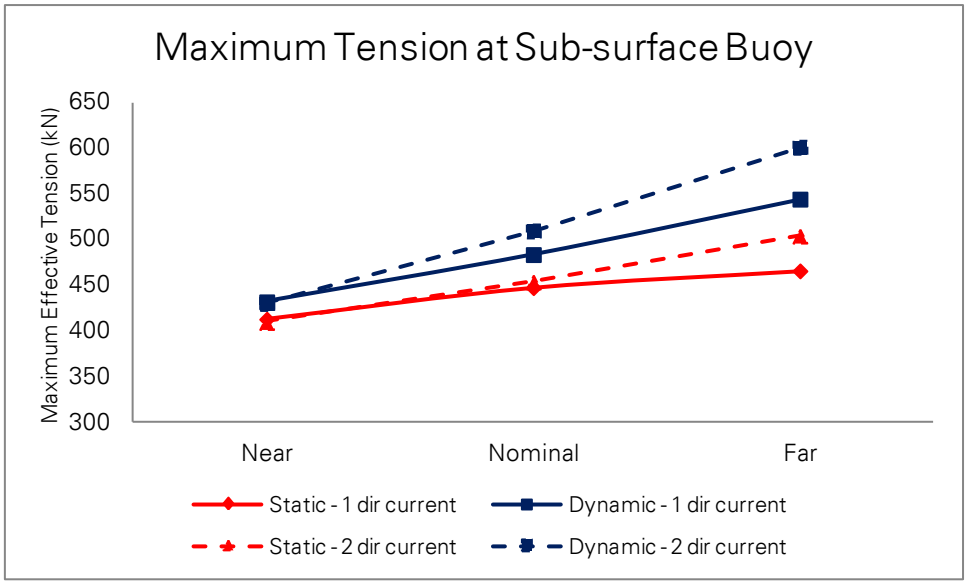

Figure 7.13 – Static and Dynamic Tension of Jumper at Sub-surface Buoy (Case 2)

From Figure 7.12 and Figure 7.13 above, it can be seen Case 2 jumper configuration has similar tension load with Base Case jumper configuration. The effect of bidirectional (2-directions) current profile is also has higher impact on far vessel position case.

The following figure shows the comparison of maximum and minimum angle at vessel and sub-surface buoy in Case 2 configuration. In this configuration, the angle of flexible jumper at sub-surface buoy is measured from the bottom section of the sub-surface buoy.

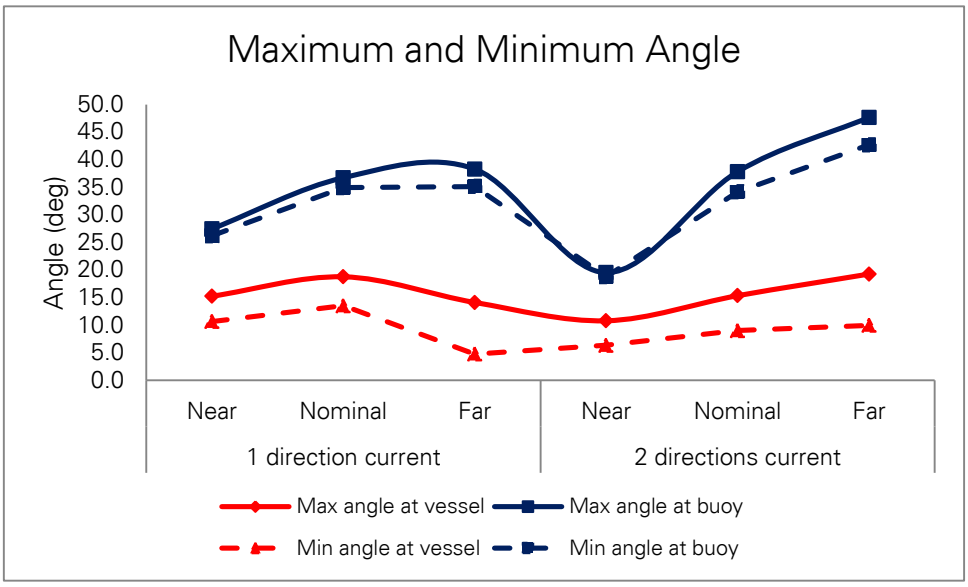

Figure 7.14 – Dynamic Angle of Jumper at Vessel and Sub-surface Buoy

As seen from the figure above, the maximum and minimum angle of flexible jumper in Case-2 configuration also shows similar result with the Base Case configuration result. Table 7.24 shows the comparison of dynamic jumper result between Base Case and Case 2 configuration.

Comparison between Base Case - Case 2	Base Case	Case 2
Minimum radius (m)	42	43
Hmin (m)	62	56
Minimum tension (kN)	111	112
Maximum tension at Vessel (kN)	1399	1428
Maximum tension at Buoy (kN)	606	601
Minimum angle at Vessel (deg)	4.7	4.8
Maximum angle at Vessel (deg)	20.4	19.3
Minimum angle at Buoy (deg)	17.8	18.8
Maximum angle at Buoy (deg)	44.8	47.7

Table 7.24 – Comparison Dynamic Jumper Result (Base Case – Case 2)

From the comparison result in Table 7.24 above, it can be concluded that there is no significant change in Case 2 flexible jumper configuration result.

Riser

The following table summarizes the dynamic result of riser in Case 2 configuration.

Dynamic Result Summary - Riser	Unidirectional current Vessel Position			Bidirectional current Vessel Position		
	Near	Nominal	Far	Near	Nominal	Far
Maximum Top Tension (kN)	2193	2419	2487	2334	2379	2362
Minimum Sagbend Tension (kN)	262	426	467	393	431	342
von Mises Stress - Top (MPa)	314	362	362	261	368	437
von Mises Stress - Below Stress Joint (MPa)	294	310	310	280	311	332
von Mises Stress - Sagbend (MPa)	261	265	266	264	264	264
Maximum Buckling Utilization - Top	0.56	0.76	0.72	0.37	0.78	1.10
Maximum Buckling Utilization - Below Stress Joint	0.67	0.67	0.67	0.67	0.67	0.67
Maximum Buckling Utilization - Sagbend	0.78	0.78	0.78	0.78	0.78	0.78

Table 7.25– Dynamic Riser Result (Case 2 – ULS)

As seen from Base Case and Case 1 configurations for maximum top tension and minimum TDP tension results, the same trend is observed from the static response. The maximum top tension and minimum TDP tension drives by unidirectional (1-direction) current profile.

The following figures present the comparison of static and dynamic response at top and TDP.

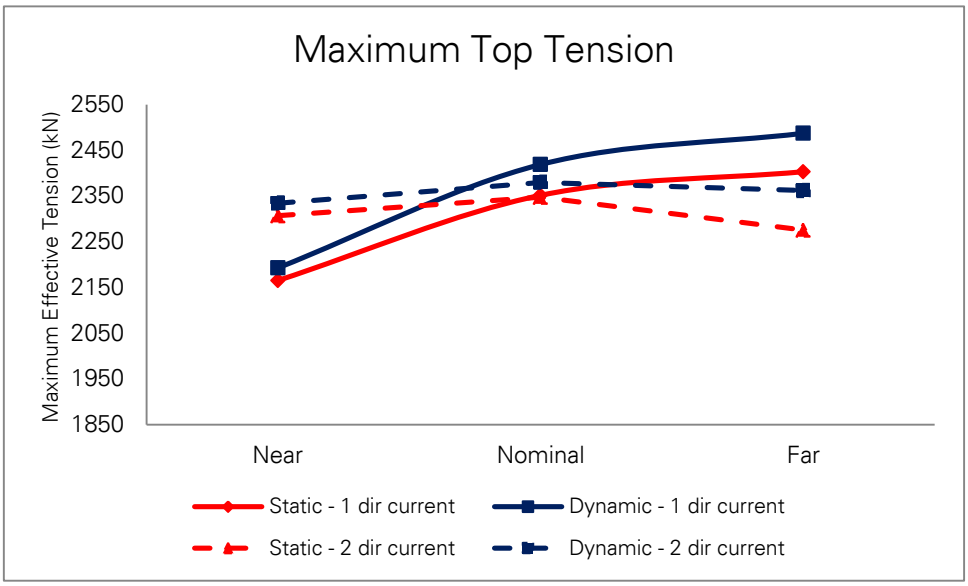

Figure 7.15 – Static and Dynamic Top Tension of Riser (Case 2)

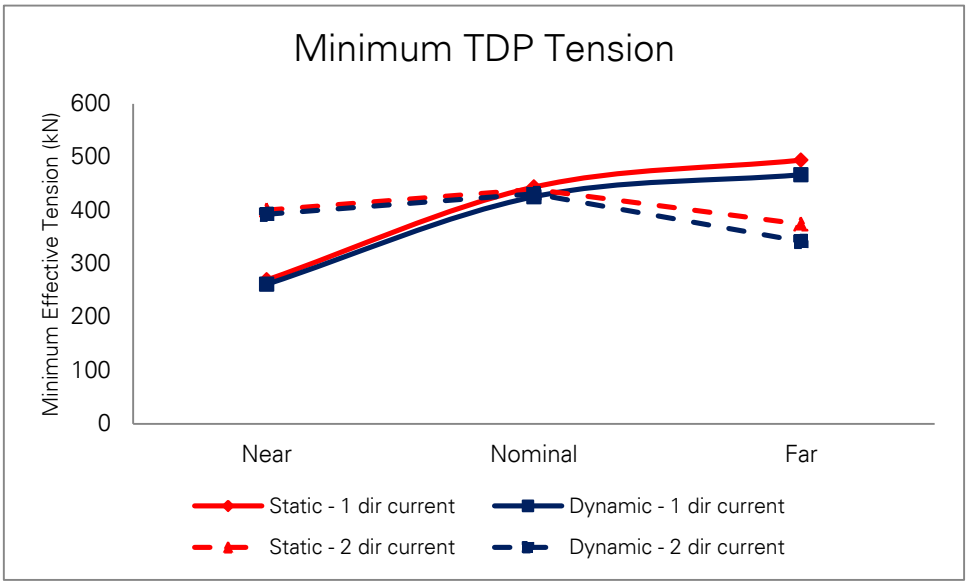

Figure 7.16 – Static and Dynamic TDP Tension of Riser (Case 2)

As seen from figures above, bidirectional (2-directions) current profile in Case 2 configuration is also gives significant effect for the tension load of riser. As seen from Figure 7.15, for various vessel offset positions, the maximum static top tension load of 2487 kN is magnified by 84 kN due to dynamic motion. This result is just slightly smaller than the Base Case configuration, where the maximum static top tension load of riser is increased by 97 kN due to the dynamic motion. From Figure 7.16, it can be seen that almost no significant dynamic effect occurs at TDP tension.

The following figures show the maximum static and dynamic von Mises stress result for Case 2 riser configuration.

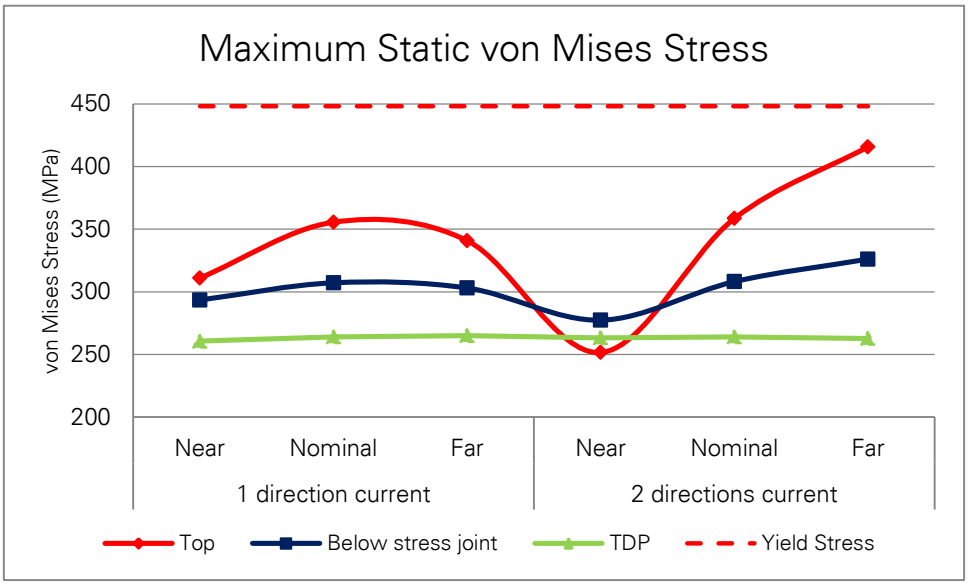

Figure 7.17 – Static von Mises Stress of Riser (Case 2)

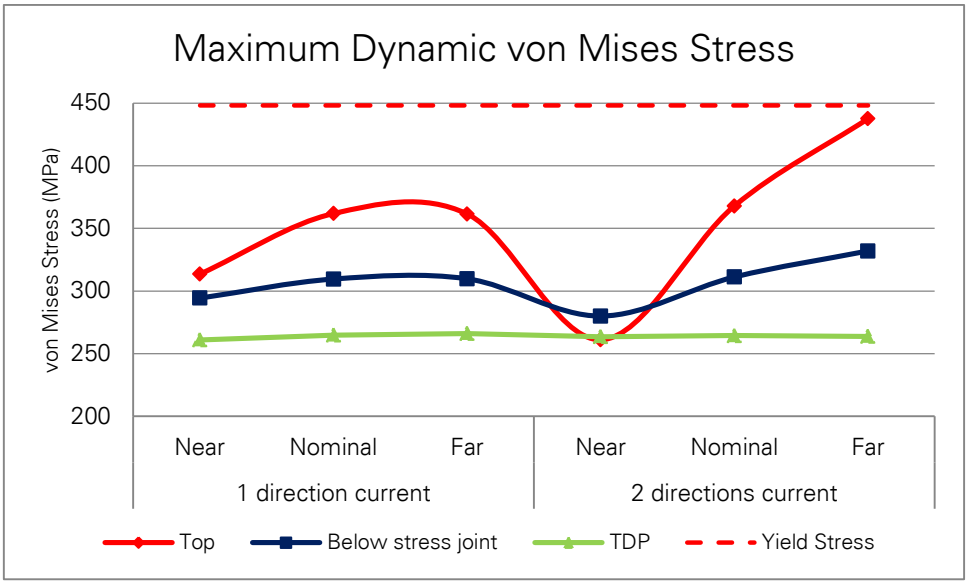

Figure 7.18 – Dynamic von Mises Stress of Riser (Case 2)

The von Mises stresses for various vessel offset positions are presented in Figure 7.17 and Figure 7.18 . As seen from the figures, the bidirectional (2-directions) current profile affects significantly to the von Mises stress result.

Earlier analyses result in Case 2 configuration shows that the static and dynamic tension load of flexible jumper is almost similar with the Base Case configuration result. In this case, the linear correlation between high tension load of flexible jumper at sub-surface buoy and high bending stress (which composed the von Mises stress) at top hang-off section of riser is not valid for this Case 2 configuration.

The following table shows the comparison between Base Case and Case 1 dynamic riser result.

Comparison between Base Case - Case 2	Base Case	Case 2
Maximum Top Tension (kN)	2510	2487
Minimum Sagbend Tension (kN)	243	262
von Mises Stress - Top (MPa)	312	437
von Mises Stress - Below Stress Joint (MPa)	291	332
von Mises Stress - Sagbend (MPa)	266	266
Maximum Buckling Utilization - Top	0.50	1.10
Maximum Buckling Utilization - Below Stress Joint	0.67	0.67
Maximum Buckling Utilization - Sagbend	0.78	0.78

Table 7.26 – Comparison Dynamic Riser Result (Base Case – Case 2)

From the comparison shown above, it can be concluded that locating the end-connection point of the flexible jumper at the bottom of the sub-surface buoy could give changes to the strength performance result of the riser.

Mooring Line

The following table presents the dynamic mooring lines result.

Dynamic Result Summary - Mooring Line	Unidirectional current Vessel Position			Bidirectional current Vessel Position		
	Near	Nominal	Far	Near	Nominal	Far
Minimum tension (kN)[1]	614	477	444	530	511	515
Maximum tension (kN)[1]	680	663	593	591	692	681

Note:
[1] The tension presented is the tension in each of the two mooring lines.

Table 7.27– Dynamic Mooring Lines Result (Case 2 – ULS)

Plots of minimum and maximum tension in mooring line, and the comparison with the static tension load, are presented in Figure 7.19.

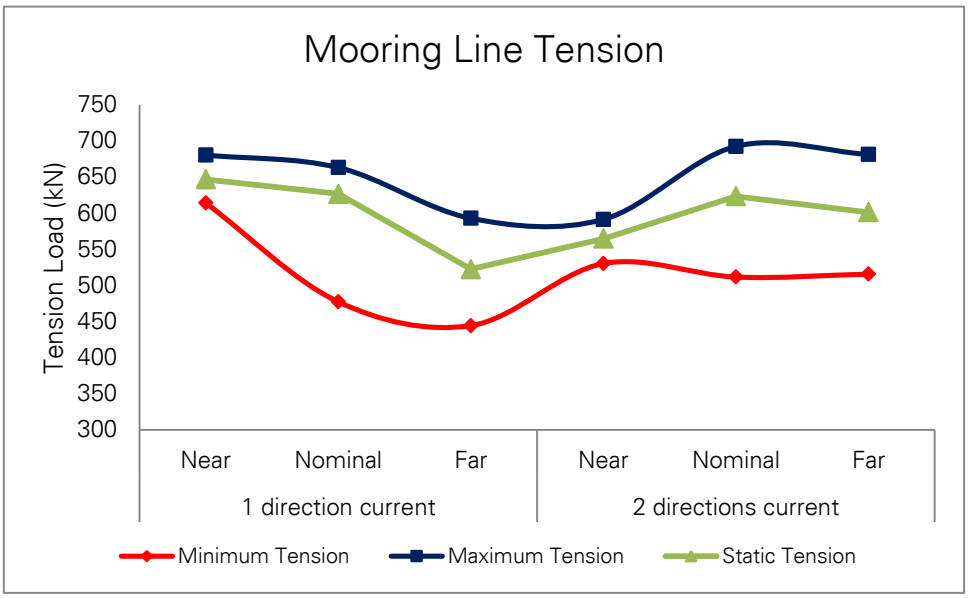

Figure 7.19 – Maximum and Minimum Mooring Line Tension (Case 2)

The following table shows the comparison of maximum and minimum tension load in the mooring lines between Base Case and Case 2.

Comparison between Base Case - Case 1	Base Case	Case 2
Minimum tension (kN)	424	444
Maximum tension (kN)	697	692

Table 7.28 – Comparison Dynamic Mooring Lines Result (Base Case – Case 2)

As seen from Figure 7.19 and Table 7.28, the minimum tension load and maximum tension in the mooring lines for Case 2 configuration has no significant impact compared to the Base Case configuration result.

7.4.3 Comparison with Accidental Case Result

The accidental case (ALS) condition for Case 2 configuration is also carried out by considering a condition if one of the two mooring lines fails. In this configuration, the same case combinations as shown in Table 7.2 are performed.

The following table shows the comparison summary of the strength analysis result between normal (ULS) and accidental (ALS) case for Case 2 configuration.

	Case 2	
	Normal	Accidental
SCR		
Top Tension (kN)	2487	2524
TDP Tension (kN)	262	261
Buckling Utilization	1.10	1.08
von Mises Stress (MPa)	437	435
Jumper		
Minimum radius (m)	43.0	44.8
Minimum tension (kN)	112	119
Maximum tension at Vessel (kN)	1428	1411
Maximum tension at Buoy (kN)	601	584
Buoyancy mooring lines		
Minimum tension (kN)	444	915
Maximum tension (kN)	692	1372

Table 7.29 – Riser System Result Summary (Case 2)

As seen from the table above, it can be seen that higher stresses are observed compared to Base Case configuration. More comprehensive analysis might give better result when the universal ball joint is modelled in more detail.

Detail analysis results for Case 2 are presented in Appendix C.

7.5 Case 3 – Assessment on Lateral Displacement

In this section, the assessment on lateral displacement of the riser is performed. As explained in earlier section of this chapter, the first assessment is carried out by analyzing the maximum lateral displacement of the Base Case riser configuration under perpendicular static current load. The next step is to find the alternative riser configurations in order to reduce the lateral displacement that has been observed from the first assessment. In this step, three alternative mooring line configurations are considered. These cases are listed in Table 7.3 – Lateral Displacement Case Combination and the explanations are sketched in Figure 7.1 and Figure 7.2. As mentioned earlier in Section 7.2, this assessment is important for checking any obstruction or clashing between adjacent lines (e.g. FPSO mooring lines, other hanging risers from different FPSO or platform, etc.) and to avoid any damage on the riser.

For this assessment, only static analysis is performed based on normal (10 year return period) and extreme (100 year return period) of surface and mid-level current profiles.

The following tables show the Base Case lateral displacement result.

Base Case (Distance between mooring line anchor = 3 m)	Surface Current Profile		Mid-level Current Profile	
	10 year	100 year	10 year	100 year
Buoy Lateral Displacement (m)	60.7	84.9	62.8	83.6
Riser Lateral Displacement (m)	63.4	88.8	74.1	98.7

Table 7.30 – Base Case Lateral Displacement Result

From the result, it can be seen that the relative maximum lateral displacement is 98.7 m. Figure 7.20 shows this displacement under 100 year mid-level current profile.

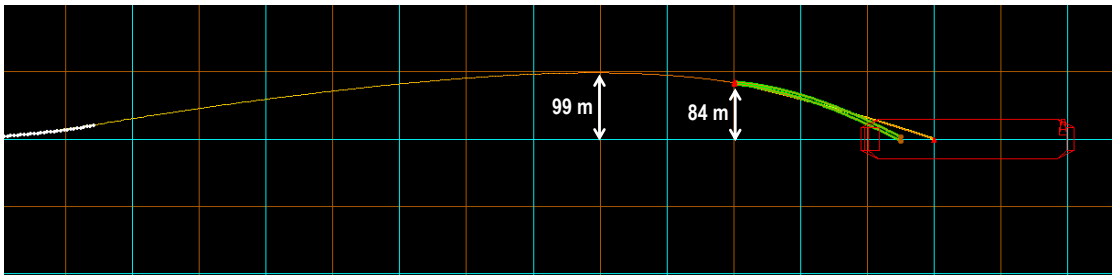

Figure 7.20 – Base Case Maximum Lateral Displacement (Plan View)

Table 7.31 shows the lateral displacement result from the alternative mooring line configurations.

Case 3 (Distance between mooring line anchor = 46 m)	Surface Current Profile		Mid-level Current Profile	
	10 year	100 year	10 year	100 year
Buoy Lateral Displacement (m)	59.0	82.7	61.2	81.6
Riser Lateral Displacement (m)	61.9	86.8	72.8	97.1

Case 4 (Distance between mooring line anchor = 89.4 m)	Surface Current Profile		Mid-level Current Profile	
	10 year	100 year	10 year	100 year
Buoy Lateral Displacement (m)	54.8	77.2	57.1	76.8
Riser Lateral Displacement (m)	58.0	81.9	69.5	93.2

Case 5 (Distance between mooring line anchor = 134.2 m)	Surface Current Profile		Mid-level Current Profile	
	10 year	100 year	10 year	100 year
Buoy Lateral Displacement (m)	48.9	70.0	51.4	70.4
Riser Lateral Displacement (m)	52.7	75.4	65.0	88.0

Table 7.31 – Optimization Cases Lateral Displacement Results

As seen from the result, Case 5 mooring line configuration can reduce the maximum lateral displacement from the Base Case result up to 10.7 m, resulting in 88 m of riser lateral displacement. This result is shown in Figure 7.21.

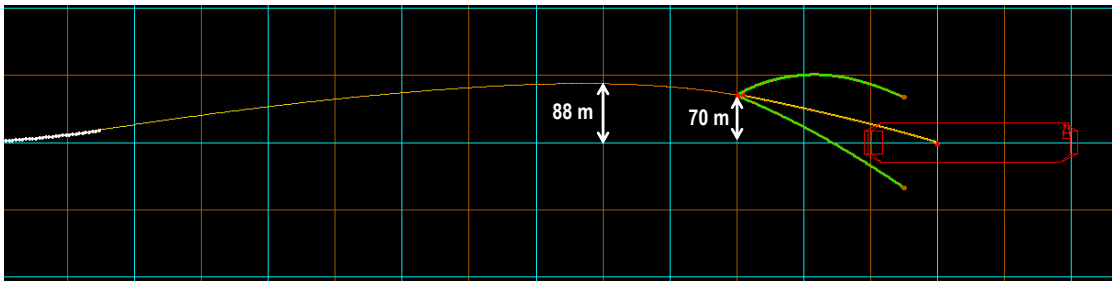

Figure 7.21 – Optimization Case Maximum Lateral Displacement (Plan View)

The following table shows the comparison summary between Base Case and Optimization Case result.

Lateral Displacement Summary	Base Case	Optimization Case
Maximum Buoy Lateral Displacement (m)	84.9	70.0
Maximum Riser Lateral Displacement (m)	98.7	88.0

Table 7.32 – Lateral Displacement Summary

From the assessment result, it is shown that the alternative mooring line configurations can reduce the lateral displacement of the riser system, in particular due to perpendicular extreme current load. From the analysis, it can be seen that there is a linear correlation between Case 3, Case 4 and Case 5 result as shown in Figure 7.22.

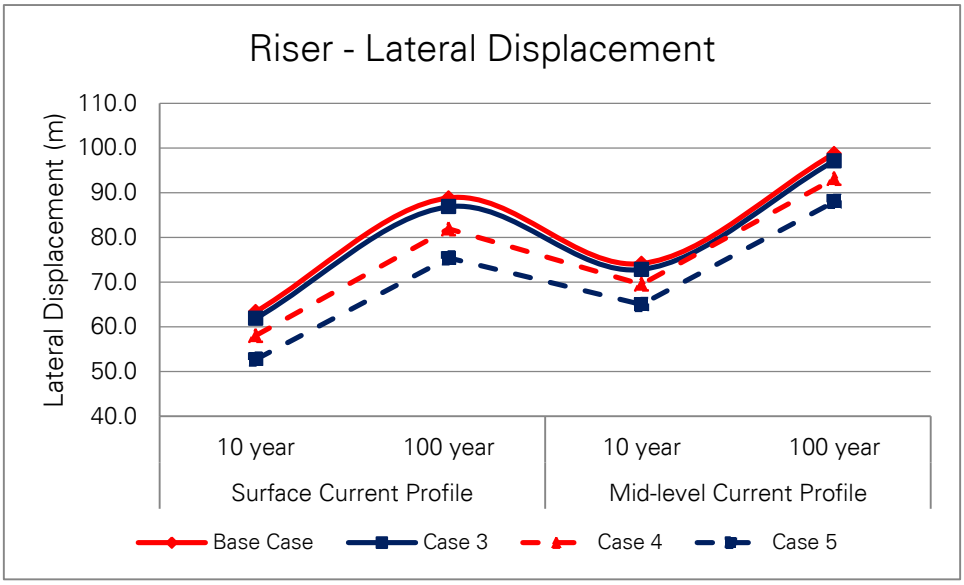

Figure 7.22 – Linear Correlation between Alternative Cases

As a result, it can be concluded that for particular COBRA riser Base Case arrangement under perpendicular static current load, the wider anchor point spacing between the mooring lines will further reduce the lateral displacement of the riser.

7.6 Discussion

The following section provides analyses discussions for each case presented in this chapter.

Case 1

- Static and dynamic response on flexible jumper shows that the maximum tension at sub-surface buoy is reduced. Less tension force at top of sub-surface buoy improves the strength design of the tapered stress joint section located at top of hang-off riser.
- Higher payload at vessel is observed due to longer flexible jumper length. In this case, it is important to review the vessel's hang-off capacity for Case 1 riser configuration.
- It is observed that bidirectional (2-directions) current profile (refer to Figure 5.3 – Typical Bidirectional (2-Directions) Current Profile) gives significant effect for the tension load on the riser. From the analysis result, it is shown that this current profile, in particular for far vessel offset case, can reduce the riser's tension load. Hence, it is important to consider the bidirectional current phenomena.
- Locating the sub-surface buoy in deeper area (400 m below sea-surface) gives less dynamic effect on the riser. This is reflected from the comparison between static and dynamic von Mises stress of Base Case configuration and Case 1 configuration. As a result, Case 1 configuration gives less von Mises stress than the Base Case configuration. This shows that Case 1 riser configuration has more robust strength performance.
- The tension load at each of the mooring lines is higher in Case 1 configuration. This is as the result of locating the sub-surface buoy in deeper area, where the span of the suspended riser is less compared to the Base Case configuration. Thus, the top hanging tension of the riser is becoming less. In other hand, the same size of sub-surface buoyancy module is considered for both Base Case and Case 1 configuration. Hence,

with the same uplift force from the submerged buoy, Case 1 resulted in higher tension load at each of the mooring lines.

Case 2

- In Case 2 configuration, the flexible jumper result from static and dynamic analyses are almost similar with the Base Case result that presented in Chapter 6.
- As seen from Base Case and Case 1 configuration result, in Case 2 configuration result, the bidirectional current profile is also has significant effect to the riser response, in particular for the tension load. Case 2 configuration also reflects the importance of considering bidirectional current profile phenomena.
- From the static response of the riser, it is observed that locating the flexible jumper end-connection at bottom of the sub-surface buoy can reduce by half of the maximum static top angle of the riser in Base Case configuration. As mentioned earlier that reduction of hang-off angle might change the location of the touch-down-point (TDP) of the riser. Alteration on TDP location might give different dynamic response of the riser, in particular for seabed area with various soil conditions. It is also important to see that different TDP area will resulted in different fatigue response.
- From Case 2 analysis result, it can be concluded that for COBRA riser arrangement, locating the end-connection point of the flexible jumper at the bottom of the sub-surface buoy could give different effect to the strength performance result of the riser.

Case 3

- Extreme current load that exposed the Base Case riser configuration gives maximum lateral displacement of 99 m. However, this lateral displacement can be reduced by using alternative mooring lines arrangement as presented in Section 7.5. It is shown that Case 5 configuration with 134.2 m distance between the mooring line's anchor point reduces the displacement by 11 m, resulted in maximum lateral displacement of 88 m.
- From the assessment result, it can be seen that there is a linear correlation between Case 3, Case 4 and Case 5 result as shown earlier in Figure 7.22. It can be concluded that for particular COBRA riser Base Case arrangement, wider anchor point spacing between the mooring lines will further reduce the lateral displacement of the riser under perpendicular current load.

8. Conclusion and Recommendation

8.1 Conclusion

The emerging oil and gas prospects in ultra deepwater field, in particular for Brazilian offshore area, have called for an alternative riser concept. It demands for a robust riser performance, while also expected to have a cost effective solution. In water depth of more than 2000 m, selecting appropriate riser system will have significant impact for overall project cost and schedule. Therefore, it is very important to select the best riser concept based on well proven technology for ultra deepwater field.

The most prominent riser concept needs to overcome the challenges in ultra deepwater condition. For particular field with floating production platform system, the floater complex motion will have significant effect on the riser long-life performance. In harsh environment condition, loads coming from wind, waves, and current will magnify this motion. During service life, long suspended length of the riser section will increase the floater payload. The riser section near the seabed will be exposed to high external hydrostatic pressure, in which it will require sufficient collapse resistance mechanism. At touch-down point (TDP), large dynamic heave and surge motion might lead to buckling issues and also fatigue problems.

Recent riser system developments have been technically proven to decoupling the motion effects. Most of the concepts are developed for hybrid riser system with complex design and expensive fabrication cost. Among of these concepts, Catenary Offset Buoyant Riser Assembly (COBRA) as newly developed hybrid riser concept presents cost effective and efficient design solution.

The concept of COBRA riser shows a robust and efficient design to overcome the challenges posed in ultra deepwater condition, in particular for Santos Basin Central Cluster region. The COBRA Base Case configuration shows sufficient strength capacity for extreme cases. It has low dynamic effect and also robust fatigue performance design for wave induced fatigue and fatigue due to Vortex Induced Vibration (VIV).

In Santos Basin area, it is observed that there is common sudden change phenomenon on the current direction. In this thesis, this effect is considered by conservatively assuming two-directions of current profile occur at the same time. The study in COBRA riser system shows that it has significant effect in terms of the strength performance of the riser. Under COBRA Base Case configuration, it affects significantly on the von Mises stress result at the tapered stress joint section which located at top of hang-off point.

The analyses results of COBRA Base Case configuration show that worst case combination comes from the environmental load combination of 10 year wave and 100 year surface current profile. This result shows that extreme dynamic load effect from wave has less impact compared to extreme static current load, which include the effect of bidirectional current. This result also shows that the flexible jumper in COBRA can effectively absorbs the floater motions and therefore improves both strength and fatigue performance on the overall riser system.

COBRA Base Case configuration gives very robust fatigue performance for both wave and VIV induced. For fatigue due to wave, minimum fatigue life of 281 years is observed at the tapered stress joint section. The result at touch-down point (TDP) with fatigue life more than 10 000 years shows that there is no significant fatigue issues at this section, even when

using onerous F1-curve with high SCF of 1.2. For fatigue due to VIV, the same F1 curve with high SCF of 1.2 shows the minimum fatigue life of 6781 years from the short term VIV event, and long term VIV gives the minimum fatigue life of more than 10 000 years. These results clearly indicate that COBRA riser has a very robust fatigue performance.

Sensitivity studies on alternative riser arrangements have been performed based on the same strength design conditions with COBRA Base Case configuration. The results show that locating the subsurface buoyancy in deeper area gives strength improvement as the dynamic effect on the riser is reduced. The results also show that locating the end-connection of the flexible jumper at the bottom section of the subsurface buoyancy gives some effects on the riser strength performance. When it comes to the lateral displacement, sensitivity studies results show that wider anchor point spacing between the mooring lines will further reduce the lateral displacement of the riser under perpendicular extreme current load.

In summary, based on detailed strength and fatigue response analyses, it is found that COBRA riser concept is feasible for 2200 m water depth, in particular for Santos Basin Cluster Region area. It is also shows that COBRA riser concept has sufficient strength performance even for extreme bidirectional (2-directions) current.

8.2 Recommendation

- To get more comprehensive and detail global analyses results, different number of current profiles from each of individual omni-directional current data may be used, as the bidirectional current profile may vary from one direction to another. Different upper and lower layer heights from each bidirectional current profile may give different analyses results.
- Fatigue analysis may be performed for different alternative COBRA riser configurations, for example in deeper subsurface buoyancy arrangement. From the strength analysis result, it is shows that locating subsurface buoyancy in deeper area gives less dynamic effect on the riser. The behavior of fatigue performance for various vessel offsets is also interesting to be studied.
- The sensitivity studies for additional parameters may be considered in order to study more detail behavior of COBRA riser concept. These parameters may include various numbers of riser sizes, various internal design pressures, and various subsurface buoyancy sizes.
- Detail installation analysis of COBRA riser is recommended to be performed. During installation, riser section may be exposed to different kind of loads, and it will depend on the installation procedure and installation method.

9. References

1. Alliot, V., Legras, J.L. , Perinet, D. (2005). Ultra-deepwater riser choice requires careful analysis. Available at: < http://www.offshore-mag.com/articles/print/volume-65/issue-6.html > [accessed on 11th March 2012]
2. Alliot, V., Legras, J.L. (2005). Lessons Learned From the Evolution and Development of Multiple-Lines Hybrid Riser Towers for Deep Water Production Applications. In: Offshore Technology Conference. Houston, TX, USA, 2-5 May 2005. Houston: Stolt Offshore S.A.
3. API. (2009). Specification for Unbonded Flexible Pipe – ANSI/API Specification 17J. Washington D.C., USA: American Petroleum Institute.
4. Barltrop, N.D.P. (1998). Floating Structures: A Guide for Design and Analysis / Volume 1 and 2 (Publication 101/98). London: The Centre for Marine and Petroleum Technology
5. Cao, J. (2011). Design of Deepwater Tower Riser for West of Africa Application. In: Offshore Technology Conference. Houston, Texas, USA, 2-5 May 2011. Houston: CNOOC Research Institute.
6. Chakrabarti, S.K. (1994). Hydrodynamics of Offshore Structures. Southampton: Computational Mechanics Publications.
7. Chakrabarti, S.K. (2005). Handbook of Offshore Engineering Volume II. UK: Elsevier Ltd.
8. Chapin, G. (2005). Inspection and Monitoring of Girassol Hybrid Riser Towers. In: Offshore Technology Conference. Houston, TX, USA, 2-5 May 2005. Houston: Total E&P Angola.
9. Clausen, T. and D'Souza, R. (2001). Dynamic riser key component for deepwater drilling, floating production. Available at: <http://www.offshore-mag.com/articles/print/volume-61/issue-5/news/deepwater-ep-dynamic-risers-key-component-for-deepwater-drilling-floating-production._printArticle.html> [accessed on 8th March 2012].
10. Cruz, D., Zimmermann, C., Neveux, P., Louvety, F. (2009). The Greater Plutonio Riser Tower. In: Offshore Technology Conference. Houston, Texas, 4-7 May 2009. Houston: BP, Acergy.
11. DNV. (2010). Offshore Standard DNV-OS-F201 Dynamic Risers, October 2010. Høvik, Norway: Det Norske Veritas.
12. DNV. (2010). Recommended Practice DNV-RP-C203 Fatigue Design of Offshore Steel Structures, April 2010. Høvik, Norway: Det Norske Veritas.
13. DNV. (2010). Recommended Practice DNV-RP-F204 Riser Fatigue, October 2010. Høvik, Norway: Det Norske Veritas.
14. Felista, A. (2009). Development of Method for Umbilical Installation Analysis Using Irregular Wave Spectra. Master Thesis. University of Stavanger.
15. Franciss, R. (2005). Subsurface Buoy Configuration for Rigid Risers in Ultradeep Water. In: SPE Latin American and Caribbean Petroleum Engineering Conference. Rio de Janeiro, Brazil, 20-23 June 2005. Rio de Janeiro: Petrobras.
16. GBI Research. (2010) The Future of the Offshore Drilling Industry to 2015 – Market Analysis, Capital Expenditure and Competitive Landscape. As retrieved from: <http://www.investorideas.com/Research/PDFs/Offshore_Drilling.pdf> [accessed on 19 February 2012]

17. Gudmestad, O.T. (2011). Lecture notes in Marine Operations (MOM-490), Fall 2011. Stavanger, Norway: University of Stavanger.

18. Hatton, S., Lim, F.,Dr. (1999). Third Generation Deepwater Hybrid Risers. In: World Wide Deepwater Technologies, IBC. London, UK, June 1999. London: 2H Offshore Engineering Limited, Woking, Surrey, UK

19. Howells, H., Dr., Hatton, S.A. (1997). Challenges for Ultra-Deep Water Riser Systems. In: Floating Production Systems IIR. London, UK, April 1997. London: 2H Offshore Engineering Limited.

20. Journée, J.M.J. and W.W. Massie (2001). Introduction In Offshore Hydromechanics (OT3600). Delft, Netherland: Delft University of Technology.

21. Karunakaran, D. (2010). Weight Distributed Steel Catenary Riser. In: Pipeline and Risers Conference by Norwegian Petroleum Forening. Trondheim, October 2010. Trondheim: Subsea 7.

22. Karunakaran, D. (2011). Lecture notes in Pipeline & Riser (MOK-160), Fall 2011. Stavanger, Norway: University of Stavanger.

23. Karunakaran, D., Aasen, H., Baarholm, R. (2011). New Un-coupled Deepwater Riser Concept for Harsh Environment – Catenary Offset Buoyant Riser Assembly (COBRA). In: Deepwater Offshore Technology Conference. New Orleans, USA, 11-13 October 2011. New Orleans: Subsea 7, Statoil.

24. Karunakaran, D., Dale, N., Hatton, S. (2007). The Grouped SLOR – Design & Implementation. In: 26th International Conference on Offshore Mechanics and Arctic Engineering. San Diego, California, USA, 10-15 June 2007. San Diego: OMAE2007

25. Karunakaran, D., Meling, T.S., Kristoffersen, S., Lund, K.M. (2005). Weight-optimized SCRs for Deepwater Harsh Environments. In: Offshore Technology Conference. Houston, Texas, 2-5 May 2005. Houson: Subsea 7, Statoil.

26. Larsen, C.M. and Passano, E. (1987). Fatigue Life Analysis of Production Riser. In: Offshore Technology Conference. Houston, Texas, 27-30 April 1987. Houston: Norwegian Inst. of Technology and SINTEF

27. Lien, T. (2010) Riser System. As retrieved from: <http://subsea1.com/index/page?keyword=riser_system> [accessed on 26 February 2012]

28. Lim, Frank. (2006). Installation of Riser in Deep Waters. In: 4th PetroMin Deepwater & Subsea Technology Conference & Exhibition. Kuala Lumpur, Malaysia, 20 – 21 June 2006. Kuala Lumpur: 2H Offshore Engineering Limited, United Kingdom.

29. Marintek Report. (2005). VIVANA - Theory Manual Version 3.4. Trondheim, Norway: Norwegian Marine Technology Research Institute (MARINTEK).

30. Menglan, D., Chen, J., Li, Z. (2011). Mechanics of Deepwater Steel Catenary Riser. Available at: < http://cdn.intechopen.com/pdfs/19441/InTech-Mechanics_of_deepwater_steel_catenary_riser.pdf > [accessed on 11th March 2012]

31. MercoPress. (2011). Petrobras confirms ultra-deep water Sergipe-Alagolas oil and gas province. As retrieved from: <http://en.mercopress.com/2011/09/22/petrobras-confirms-ultra-deep-water-sergipe-alagoas-oil-and-gas-province> [accessed on 19th February 2012]

32. Orcina Ltd. (2010). OrcaFlex Manual (Version 9.4a). Cumbria, UK: Orcina Ltd.

33. Palmer, A.C. and King, R.A. (2004) Subsea Pipeline Engineering. US: Penwell Corporation

34. Petrobras. (2011). Santos Basin Central Cluster Region Metocean Data (I-ET-3A26.00-1000-941-PPC-001 – Rev. C). Brazil: Petrobras.

35. Roveri, F. E., Velten Filho, A.G., Mello, V.C., Marques, L.F. (2008). The Roncador P-52 Oil Export System – Hybrid Riser at a 1800 m Water Depth. In: Offshore Technology Conference. Houston, Texas, 5-8 May 2008. Houston: Petrobras.

36. Saliés, J.B. (2005) Technological Challenges for the Development of Ultradeep Water Fields. In: SPE Latin American and Caribean Petroleum Engineering Conference. Rio de Janiero, Brazil, 20-23 June 2005. Rio de Janiero: Petrobras.

37. Shell Press Release. (2010) Perdido. [image online] As retrieved from: http://www-static.shell.com/static/aboutshell/imgs/544_wide/perdido_deepwater_milestones_2.jpg [accessed on 18th February 2012]

38. Shell US Media Line. (2011). Shell Sets World Record for Deepest Subsea Oil and Gas Well. As retrieved from: <http://www.shell.us/home/content/usa/aboutshell/media_center/news_and_press_releases/2011/11172011_perdido.html> [accessed on 18 February 2012]

39. Shotbolt, K. (2011). Lazy-S risers offer advantages in the ultra deep. As retrieved from: <http://www.offshore-mag.com/articles/print/volume-68/issue-9/subsea/lazy-s-risers-offer-advantages-in-the-ultra-deep.html> [accessed on 23th February 2012]

40. Shu, S., Seehausen, R., Bledsoe, S., Powell, T. (2011). Reviewing the state of deepwater production risers. As retrieved from: <http://www.offshore-mag.com/articles/print/volume-70/issue-11/subsea/reviewing-the-state-of-deepwater-production-risers.html> [accessed on 19 February 2012]

41. Smith, N.S. (2012). Subsea 7 Riser Technology. As retrieved from: <http://www.subsea7.com/files/docs/Datasheets/Technology/4_Pg_Leaflet_Riser_Technology__Reference.pdf> [accessed on 29th May 2012]

42. Stewart, Robert H. (2008). Introduction To Physical Oceanography. [pdf] Department of Oceanography, Texas A & M University. Available at:<http://oceanworld.tamu.edu/resources/ocng_textbook/PDF_files/book.pdf> [Accessed 14 November 2011].

43. Vogel, M., Silveira, I.C.A., Castro, B.M., Lima, J.A.M., Pereira, A.F., Hidromares, Williams, P. (2010). Metocean Measurement at Northern Santos Basin – Brazil. In: Offshore Technology Conference. Houston, Texas, 3-6 May 2010. Houston: OTC.

44. Walter, D. (2005) Freestanding Risers in Ultra Deepwater. In: Subsea Tieback Forum. Galveston, February 2005. Galveston: 2H Offshore.

Appendix A - Wall Thickness Sizing

A.1 Minimum Wall Thickness Design (DNV-OS-F201)

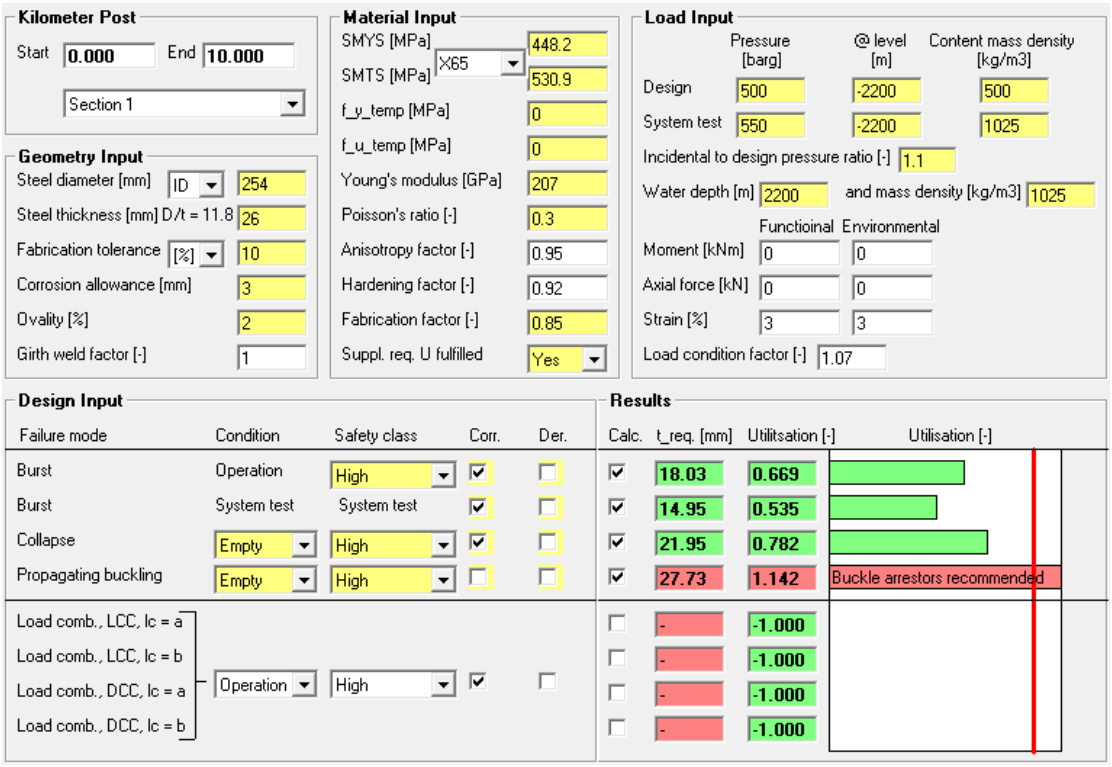

Appendix B - Base Case Result

B.1 Static Response (ULS)

B.1.1 Flexible Jumper

10 year current - surface profile	Unidirectional current			Bidirectional current		
	Vessel Position			Vessel Position		
	Near	Nominal	Far	Near	Nominal	Far
Static angle at vessel (deg)	11	15	13	8	12	16
Static angle at buoy (deg)	24	33	35	19	33	42
Static tension at vessel (kN)	1097	1114	1114	1077	1117	1148
Static tension at buoy (kN)	429	459	484	427	464	508
Minimum Bending Radius (m)	66	72	100	49	71	123

10 year current - mid-level profile	Unidirectional current			Bidirectional current		
	Vessel Position			Vessel Position		
	Near	Nominal	Far	Near	Nominal	Far
Static angle at vessel (deg)	10	13	14	7	13	17
Static angle at buoy (deg)	25	33	35	19	33	41
Static tension at vessel (kN)	1098	1115	1114	1079	1116	1145
Static tension at buoy (kN)	431	461	482	428	463	506
Minimum Bending Radius (m)	66	72	100	50	72	122

100 year current - surface profile	Unidirectional current			Bidirectional current		
	Vessel Position			Vessel Position		
	Near	Nominal	Far	Near	Nominal	Far
Static angle at vessel (deg)	12	16	12	8	13	17
Static angle at buoy (deg)	26	34	34	18	35	43
Static tension at vessel (kN)	1101	1120	1109	1074	1125	1158
Static tension at buoy (kN)	430	462	480	427	468	515
Minimum Bending Radius (m)	69	69	95	45	66	129

100 year current - mid-level profile	Unidirectional current			Bidirectional current		
	Vessel Position			Vessel Position		
	Near	Nominal	Far	Near	Nominal	Far
Static angle at vessel (deg)	11	14	13	7	13	17
Static angle at buoy (deg)	26	34	34	18	34	42
Static tension at vessel (kN)	1102	1119	1110	1076	1121	1152
Static tension at buoy (kN)	432	464	479	427	465	510
Minimum Bending Radius (m)	69	70	97	47	69	125

Table B.1 – Jumper Static Result (Base Case – ULS)

B.1.2 Riser

10 year current - surface profile	Unidirectional current			Bidirectional current		
	Vessel Position			Vessel Position		
	Near	Nominal	Far	Near	Nominal	Far
Static top angle (deg)	9	11	12	9	11	13
Static top tension (kN)	2186	2330	2383	2286	2327	2294
Static TDP tension (kN)	283	420	470	378	417	383

10 year current - mid-level profile	Unidirectional current			Bidirectional current		
	Vessel Position			Vessel Position		
	Near	Nominal	Far	Near	Nominal	Far
Static top angle (deg)	10	11	12	9	11	13
Static top tension (kN)	2174	2341	2394	2298	2340	2279
Static TDP tension (kN)	271	431	481	391	430	368

100 year current - surface profile	Unidirectional current			Bidirectional current		
	Vessel Position			Vessel Position		
	Near	Nominal	Far	Near	Nominal	Far
Static top angle (deg)	10	11	12	9	12	14
Static top tension (kN)	2167	2351	2403	2307	2347	2278
Static TDP tension (kN)	266	440	489	398	436	368

100 year current - mid-level profile	Unidirectional current			Bidirectional current		
	Vessel Position			Vessel Position		
	Near	Nominal	Far	Near	Nominal	Far
Static top angle (deg)	10	12	12	8	12	14
Static top tension (kN)	2155	2361	2413	2318	2360	2262
Static TDP tension (kN)	253	450	500	410	449	351

Table B.2 – Riser Static Result (Base Case – ULS)

B.1.3 Mooring Line

10 year current - surface profile	Unidirectional current			Bidirectional current		
	Vessel Position			Vessel Position		
	Near	Nominal	Far	Near	Nominal	Far
Static tension (kN)	627	607	526	568	605	583

10 year current - mid-level profile	Unidirectional current			Bidirectional current		
	Vessel Position			Vessel Position		
	Near	Nominal	Far	Near	Nominal	Far
Static tension (kN)	633	612	521	562	612	590

100 year current - surface profile	Unidirectional current			Bidirectional current		
	Vessel Position			Vessel Position		
	Near	Nominal	Far	Near	Nominal	Far
Static tension (kN)	639	619	514	556	616	594

100 year current - mid-level profile	Unidirectional current			Bidirectional current		
	Vessel Position			Vessel Position		
	Near	Nominal	Far	Near	Nominal	Far
Static tension (kN)	644	623	511	551	622	600

Table B.3 – Mooring Line Static Result (Base Case – ULS)

B.2 Dynamic Response (ULS)

B.2.1 Flexible Jumper

10 year current - surface profile + 100 year wave	Unidirectional current Vessel Position			Bidirectional current Vessel Position		
	Near	Nominal	Far	Near	Nominal	Far
Minimum radius (m)	55	78	96	44	87	112
Hmin (m)	94	80	80	110	79	66
Minimum tension (kN)	148	209	219	118	198	265
Maximum tension at Vessel (kN)	1209	1293	1341	1204	1312	1368
Maximum tension at Buoy (kN)	447	499	554	451	521	590
Minimum angle at Vessel (deg)	9.1	12.7	5.1	5.9	9.4	9.0
Maximum angle at Vessel (deg)	15.3	18.7	15.8	12.1	15.9	19.4
Minimum angle at Buoy (deg)	23.2	30.8	34.3	18.7	30.8	38.6
Maximum angle at Buoy (deg)	24.8	33.1	37.6	19.7	34.6	43.6

Table B.4 – Jumper Dynamic Result (10 yr surface profile current + 100 yr wave)

10 year current - mid-level profile + 100 year wave	Unidirectional current Vessel Position			Bidirectional current Vessel Position		
	Near	Nominal	Far	Near	Nominal	Far
Minimum radius (m)	56	78	95	43	85	111
Hmin (m)	95	81	79	109	80	66
Minimum tension (kN)	150	211	220	121	199	265
Maximum tension at Vessel (kN)	1216	1292	1341	1209	1311	1370
Maximum tension at Buoy (kN)	451	496	548	453	518	584
Minimum angle at Vessel (deg)	7.7	11.9	7.3	4.9	9.0	10.5
Maximum angle at Vessel (deg)	13.2	17.1	17.2	10.5	17.1	20.4
Minimum angle at Buoy (deg)	23.6	31.2	33.8	18.5	30.9	38.5
Maximum angle at Buoy (deg)	25.4	33.6	37.7	19.7	34.7	43.7

Table B.5 – Jumper Dynamic Result (10 yr mid-level profile current + 100 yr wave)

100 year current - surface profile + 10 year wave	Unidirectional current Vessel Position			Bidirectional current Vessel Position		
	Near	Nominal	Far	Near	Nominal	Far
Minimum radius (m)	62	86	89	42	93	120
Hmin (m)	90	76	82	113	76	62
Minimum tension (kN)	163	225	216	111	204	282
Maximum tension at Vessel (kN)	1216	1310	1356	1192	1344	1399
Maximum tension at Buoy (kN)	450	501	555	449	524	606
Minimum angle at Vessel (deg)	10.7	13.6	4.7	6.4	9.1	9.9
Maximum angle at Vessel (deg)	15.3	18.8	14.1	10.9	15.4	19.2
Minimum angle at Buoy (deg)	24.7	33.0	33.4	17.8	32.3	40.5
Maximum angle at Buoy (deg)	25.8	34.6	36.2	18.6	35.7	44.8

Table B.6 – Jumper Dynamic Result (100 yr surface profile current + 10 yr wave)

100 year current - mid-level profile + 10 year wave	Unidirectional current Vessel Position			Bidirectional current Vessel Position		
	Near	Nominal	Far	Near	Nominal	Far
Minimum radius (m)	60	82	90	42	90	117
Hmin (m)	91	77	81	111	78	64
Minimum tension (kN)	161	223	220	117	201	279
Maximum tension at Vessel (kN)	1220	1311	1359	1199	1341	1398
Maximum tension at Buoy (kN)	454	497	549	450	517	594
Minimum angle at Vessel (deg)	9.0	12.1	7.5	5.4	8.5	11.6
Maximum angle at Vessel (deg)	13.2	16.8	15.9	9.7	16.3	20.1
Minimum angle at Buoy (deg)	24.6	32.8	33.4	17.8	32.0	39.9
Maximum angle at Buoy (deg)	26.1	34.7	36.5	19.0	35.6	44.2

Table B.7 – Jumper Dynamic Result (100 yr mid-level profile current + 10 yr wave)

B.2.2 Riser

10 year current - surface profile + 100 year wave	Unidirectional current Vessel Position			Bidirectional current Vessel Position		
	Near	Nominal	Far	Near	Nominal	Far
Top Tension (kN)	2208	2391	2442	2307	2369	2355
TDP Tension (kN)	289	440	495	387	432	402
von Mises Stress - Top (MPa)	163	202	268	167	202	286
von Mises Stress - Below Stress Joint (MPa)	239	261	278	242	261	284
von Mises Stress - TDP (MPa)	261	264	265	263	264	264
Maximum Buckling Utilization - Top	0.37	0.37	0.37	0.37	0.37	0.40
Maximum Buckling Utilization - Below Stress Joint	0.67	0.67	0.67	0.67	0.67	0.67
Maximum Buckling Utilization - Sagbend	0.78	0.78	0.78	0.78	0.78	0.78

Table B.8 – Riser Dynamic Result (10 year surface profile current + 100 year wave)

10 year current - mid-level profile + 100 year wave	Unidirectional current Vessel Position			Bidirectional current Vessel Position		
	Near	Nominal	Far	Near	Nominal	Far
Top Tension (kN)	2196	2400	2452	2320	2381	2338
TDP Tension (kN)	276	452	508	402	447	386
von Mises Stress - Top (MPa)	164	200	263	168	199	276
von Mises Stress - Below Stress Joint (MPa)	239	260	277	243	259	281
von Mises Stress - TDP (MPa)	261	264	265	263	264	263
Maximum Buckling Utilization - Top	0.37	0.37	0.37	0.37	0.37	0.37
Maximum Buckling Utilization - Below Stress Joint	0.67	0.67	0.67	0.67	0.67	0.67
Maximum Buckling Utilization - Sagbend	0.78	0.78	0.78	0.78	0.78	0.78

Table B.9 – Riser Dynamic Result (10 year mid-level profile current + 100 year wave)

100 year current - surface profile + 10 year wave	Unidirectional current Vessel Position			Bidirectional current Vessel Position		
	Near	Nominal	Far	Near	Nominal	Far
Top Tension (kN)	2203	2432	2504	2340	2382	2389
TDP Tension (kN)	273	468	534	407	448	403
von Mises Stress - Top (MPa)	166	206	284	169	216	312
von Mises Stress - Below Stress Joint (MPa)	241	263	283	243	265	291
von Mises Stress - TDP (MPa)	261	265	266	264	264	264
Maximum Buckling Utilization - Top	0.37	0.37	0.40	0.37	0.37	0.50
Maximum Buckling Utilization - Below Stress Joint	0.67	0.67	0.67	0.67	0.67	0.67
Maximum Buckling Utilization - Sagbend	0.78	0.78	0.78	0.78	0.78	0.78

Table B.10 – Riser Dynamic Result (100 year surface profile current + 10 year wave)

100 year current - mid-level profile + 10 year wave	Unidirectional current Vessel Position			Bidirectional current Vessel Position		
	Near	Nominal	Far	Near	Nominal	Far
Top Tension (kN)	2189	2435	2510	2350	2393	2363
TDP Tension (kN)	259	477	546	421	462	380
von Mises Stress - Top (MPa)	166	203	277	170	204	293
von Mises Stress - Below Stress Joint (MPa)	241	262	281	244	261	286
von Mises Stress - TDP (MPa)	261	265	266	264	264	264
Maximum Buckling Utilization - Top	0.37	0.37	0.37	0.37	0.37	0.43
Maximum Buckling Utilization - Below Stress Joint	0.67	0.67	0.67	0.67	0.67	0.67
Maximum Buckling Utilization - Sagbend	0.78	0.78	0.78	0.78	0.78	0.78

Table B.11 – Riser Dynamic Result (100 year mid-level profile current + 10 year wave)

B.2.3 Mooring Line

10 year current - surface profile	Unidirectional current			Bidirectional current		
+	Vessel Position			Vessel Position		
100 year wave	Near	Nominal	Far	Near	Nominal	Far
Minimum tension (kN)	601	482	460	540	507	516
Maximum tension (kN)	668	652	594	602	663	658

10 year current - mid-level profile	Unidirectional current			Bidirectional current		
+	Vessel Position			Vessel Position		
100 year wave	Near	Nominal	Far	Near	Nominal	Far
Minimum tension (kN)	606	481	458	534	500	526
Maximum tension (kN)	673	658	586	597	668	662

100 year current - surface profile	Unidirectional current			Bidirectional current		
+	Vessel Position			Vessel Position		
10 year wave	Near	Nominal	Far	Near	Nominal	Far
Minimum tension (kN)	599	458	424	517	501	493
Maximum tension (kN)	676	660	599	585	697	695

100 year current - mid-level profile	Unidirectional current			Bidirectional current		
+	Vessel Position			Vessel Position		
10 year wave	Near	Nominal	Far	Near	Nominal	Far
Minimum tension (kN)	605	461	427	513	497	508
Maximum tension (kN)	681	664	589	580	696	694

Table B.12 – Mooring Line Dynamic Result (Base Case – ULS)

B.3 Static Response (ALS)

B.3.1 Flexible Jumper

10 year current - surface profile	Unidirectional current			Bidirectional current		
	Vessel Position			Vessel Position		
	Near	Nominal	Far	Near	Nominal	Far
Static angle at vessel (deg)	11	14	13	8	12	16
Static angle at buoy (deg)	24	32	35	20	32	41
Static tension at vessel (kN)	1091	1108	1113	1075	1111	1141
Static tension at buoy (kN)	433	463	490	432	467	510
Minimum Bending Radius (m)	65	75	102	50	73	122

10 year current - mid-level profile	Unidirectional current			Bidirectional current		
	Vessel Position			Vessel Position		
	Near	Nominal	Far	Near	Nominal	Far
Static angle at vessel (deg)	10	13	14	8	13	17
Static angle at buoy (deg)	24	32	36	20	32	40
Static tension at vessel (kN)	1091	1108	1114	1077	1109	1138
Static tension at buoy (kN)	435	464	488	432	465	507
Minimum Bending Radius (m)	65	75	103	52	75	120

100 year current - surface profile	Unidirectional current			Bidirectional current		
	Vessel Position			Vessel Position		
	Near	Nominal	Far	Near	Nominal	Far
Static angle at vessel (deg)	12	15	12	8	12	16
Static angle at buoy (deg)	25	33	34	19	34	42
Static tension at vessel (kN)	1095	1112	1109	1072	1117	1149
Static tension at buoy (kN)	434	465	487	431	471	516
Minimum Bending Radius (m)	68	71	98	47	69	127

100 year current - mid-level profile	Unidirectional current			Bidirectional current		
	Vessel Position			Vessel Position		
	Near	Nominal	Far	Near	Nominal	Far
Static angle at vessel (deg)	10	14	14	8	13	17
Static angle at buoy (deg)	25	33	35	19	33	41
Static tension at vessel (kN)	1094	1111	1111	1075	1112	1142
Static tension at buoy (kN)	436	466	486	432	468	511
Minimum Bending Radius (m)	67	73	100	50	72	123

Table B.13 – Jumper Static Results (Base Case – ALS)

B.3.2 Riser

10 year current - surface profile	Unidirectional current			Bidirectional current		
	Vessel Position			Vessel Position		
	Near	Nominal	Far	Near	Nominal	Far
Static top angle (deg)	11	12	13	10	12	14
Static top tension (kN)	2192	2328	2380	2283	2325	2299
Static TDP tension (kN)	288	416	467	374	413	388

10 year current - mid-level profile	Unidirectional current			Bidirectional current		
	Vessel Position			Vessel Position		
	Near	Nominal	Far	Near	Nominal	Far
Static top angle (deg)	11	12	13	10	12	14
Static top tension (kN)	2182	2338	2391	2295	2337	2285
Static TDP tension (kN)	276	427	478	386	426	373

100 year current - surface profile	Unidirectional current			Bidirectional current		
	Vessel Position			Vessel Position		
	Near	Nominal	Far	Near	Nominal	Far
Static top angle (deg)	11	12	13	10	13	14
Static top tension (kN)	2175	2347	2398	2302	2342	2285
Static TDP tension (kN)	272	435	484	392	431	374

100 year current - mid-level profile	Unidirectional current			Bidirectional current		
	Vessel Position			Vessel Position		
	Near	Nominal	Far	Near	Nominal	Far
Static top angle (deg)	11	13	13	10	13	14
Static top tension (kN)	2164	2355	2407	2313	2354	2269
Static TDP tension (kN)	260	444	495	404	443	358

Table B.14 – Riser Static Result (Base Case – ALS)

B.3.3 Mooring Line

10 year current - surface profile	Unidirectional current			Bidirectional current		
	Vessel Position			Vessel Position		
	Near	Nominal	Far	Near	Nominal	Far
Static tension (kN)	1243	1203	1047	1131	1198	1154

10 year current - mid-level profile	Unidirectional current			Bidirectional current		
	Vessel Position			Vessel Position		
	Near	Nominal	Far	Near	Nominal	Far
Static tension (kN)	1252	1212	1039	1121	1210	1166

100 year current - surface profile	Unidirectional current			Bidirectional current		
	Vessel Position			Vessel Position		
	Near	Nominal	Far	Near	Nominal	Far
Static tension (kN)	1265	1225	1025	1109	1218	1174

100 year current - mid-level profile	Unidirectional current			Bidirectional current		
	Vessel Position			Vessel Position		
	Near	Nominal	Far	Near	Nominal	Far
Static tension (kN)	1273	1232	1020	1101	1230	1186

Table B.15 – Mooring Line Static Result (Base Case – ALS)

B.4 Dynamic Response (ALS)

B.4.1 Flexible Jumper

10 year current - surface profile + 100 year wave	Unidirectional current Vessel Position			Bidirectional current Vessel Position		
	Near	Nominal	Far	Near	Nominal	Far
Minimum radius (m)	54	76	98	45	87	112
Hmin (m)	97	83	79	110	82	67
Minimum tension (kN)	147	206	230	123	201	271
Maximum tension at Vessel (kN)	1203	1287	1335	1201	1300	1354
Maximum tension at Buoy (kN)	454	502	551	460	519	579
Minimum angle at Vessel (deg)	9.0	12.6	5.4	6.2	9.7	8.8
Maximum angle at Vessel (deg)	15.3	18.6	16.2	12.4	15.8	19.3
Minimum angle at Buoy (deg)	22.6	30.1	34.6	19.3	30.2	37.9
Maximum angle at Buoy (deg)	24.1	32.3	38.1	20.2	33.9	42.8

Table B.16 – Jumper Dynamic Result (10 year surface profile current + 100 year wave)

10 year current - mid-level profile + 100 year wave	Unidirectional current Vessel Position			Bidirectional current Vessel Position		
	Near	Nominal	Far	Near	Nominal	Far
Minimum radius (m)	55	77	97	44	84	110
Hmin (m)	97	84	79	109	83	69
Minimum tension (kN)	148	207	231	126	201	269
Maximum tension at Vessel (kN)	1210	1286	1337	1206	1298	1356
Maximum tension at Buoy (kN)	457	497	545	462	515	572
Minimum angle at Vessel (deg)	7.5	11.7	7.7	5.3	9.4	10.3
Maximum angle at Vessel (deg)	13.1	17.0	17.7	10.8	17.0	20.2
Minimum angle at Buoy (deg)	22.9	30.4	34.2	19.2	30.1	37.6
Maximum angle at Buoy (deg)	24.6	32.6	38.3	20.4	33.9	42.7

Table B.17 – Jumper Dynamic Result (10 year mid-level profile current + 100 year wave)

100 year current - surface profile + 10 year wave	Unidirectional current Vessel Position			Bidirectional current Vessel Position		
	Near	Nominal	Far	Near	Nominal	Far
Minimum radius (m)	60	83	91	44	91	119
Hmin (m)	93	78	81	112	78	64
Minimum tension (kN)	161	224	226	117	206	284
Maximum tension at Vessel (kN)	1207	1306	1354	1188	1331	1382
Maximum tension at Buoy (kN)	451	496	548	451	512	584
Minimum angle at Vessel (deg)	10.6	13.4	5.1	6.8	9.5	9.6
Maximum angle at Vessel (deg)	15.2	18.7	14.6	11.3	15.2	19.1
Minimum angle at Buoy (deg)	23.8	32.0	34.1	18.6	31.6	39.6
Maximum angle at Buoy (deg)	24.9	33.6	36.8	19.3	34.5	43.9

Table B.18 – Jumper Dynamic Result (100 year surface profile current + 10 year wave)

100 year current - mid-level profile + 10 year wave	Unidirectional current Vessel Position			Bidirectional current Vessel Position		
	Near	Nominal	Far	Near	Nominal	Far
Minimum radius (m)	57	79	92	44	88	114
Hmin (m)	95	80	79	110	80	66
Minimum tension (kN)	159	221	231	124	202	280
Maximum tension at Vessel (kN)	1210	1308	1357	1195	1327	1381
Maximum tension at Buoy (kN)	454	494	543	453	506	573
Minimum angle at Vessel (deg)	8.8	11.9	7.9	5.8	9.0	11.3
Maximum angle at Vessel (deg)	13.1	16.6	16.5	10.1	16.0	19.9
Minimum angle at Buoy (deg)	23.7	31.7	34.2	18.7	31.1	38.9
Maximum angle at Buoy (deg)	25.1	33.5	37.2	19.8	34.2	43.1

Table B.19 – Jumper Dynamic Result (100 year mid-level profile current + 10 year wave)

B.4.2 Riser

10 year current - surface profile + 100 year wave	Unidirectional current Vessel Position			Bidirectional current Vessel Position		
	Near	Nominal	Far	Near	Nominal	Far
Top Tension (kN)	2231	2419	2497	2332	2404	2424
TDP Tension (kN)	298	452	518	396	447	430
von Mises Stress - Top (MPa)	198	255	317	204	256	328
von Mises Stress - Below Stress Joint (MPa)	259	275	292	262	276	296
von Mises Stress - TDP (MPa)	262	265	266	263	265	265
Maximum Buckling Utilization - Top	0.37	0.37	0.49	0.37	0.37	0.54
Maximum Buckling Utilization - Below Stress Joint	0.67	0.67	0.67	0.67	0.67	0.67
Maximum Buckling Utilization - TDP	0.78	0.78	0.78	0.78	0.78	0.78

Table B.20 – Riser Dynamic Result (10 year surface profile current + 100 year wave)

10 year current - mid-level profile + 100 year wave	Unidirectional current Vessel Position			Bidirectional current Vessel Position		
	Near	Nominal	Far	Near	Nominal	Far
Top Tension (kN)	2221	2423	2502	2346	2418	2403
TDP Tension (kN)	288	462	528	412	463	412
von Mises Stress - Top (MPa)	199	251	314	205	253	319
von Mises Stress - Below Stress Joint (MPa)	259	274	291	263	275	293
von Mises Stress - TDP (MPa)	261	265	266	264	265	264
Maximum Buckling Utilization - Top	0.37	0.37	0.48	0.37	0.37	0.50
Maximum Buckling Utilization - Below Stress Joint	0.67	0.67	0.67	0.67	0.67	0.67
Maximum Buckling Utilization - TDP	0.78	0.78	0.78	0.78	0.78	0.78

Table B.21 – Riser Dynamic Result (10 year mid-level profile current + 100 year wave)

100 year current - surface profile + 10 year wave	Unidirectional current Vessel Position			Bidirectional current Vessel Position		
	Near	Nominal	Far	Near	Nominal	Far
Top Tension (kN)	2228	2434	2522	2369	2411	2425
TDP Tension (kN)	284	468	535	417	456	420
von Mises Stress - Top (MPa)	196	251	311	202	255	326
von Mises Stress - Below Stress Joint (MPa)	258	274	290	260	276	296
von Mises Stress - TDP (MPa)	261	265	267	264	265	265
Maximum Buckling Utilization - Top	0.37	0.37	0.47	0.37	0.37	0.53
Maximum Buckling Utilization - Below Stress Joint	0.67	0.67	0.67	0.67	0.67	0.67
Maximum Buckling Utilization - TDP	0.78	0.78	0.78	0.78	0.78	0.78

Table B.22 – Riser Dynamic Result (100 year surface profile current + 10 year wave)

100 year current - mid-level profile + 10 year wave	Unidirectional current Vessel Position			Bidirectional current Vessel Position		
	Near	Nominal	Far	Near	Nominal	Far
Top Tension (kN)	2216	2437	2526	2378	2420	2398
TDP Tension (kN)	271	478	545	430	470	399
von Mises Stress - Top (MPa)	196	248	308	203	247	314
von Mises Stress - Below Stress Joint (MPa)	258	274	290	261	273	292
von Mises Stress - TDP (MPa)	261	265	267	264	265	264
Maximum Buckling Utilization - Top	0.37	0.37	0.46	0.37	0.37	0.48
Maximum Buckling Utilization - Below Stress Joint	0.67	0.67	0.67	0.67	0.67	0.67
Maximum Buckling Utilization - TDP	0.78	0.78	0.78	0.78	0.78	0.78

Table B.23 – Riser Dynamic Result (100 year mid-level profile current + 10 year wave)

B.4.3 Mooring Line

10 year current - surface profile	Unidirectional current			Bidirectional current		
+	Vessel Position			Vessel Position		
100 year wave	Near	Nominal	Far	Near	Nominal	Far
Minimum tension (kN)	1157	961	914	1038	971	1006
Maximum tension (kN)	1355	1329	1171	1234	1332	1309

10 year current - mid-level profile	Unidirectional current			Bidirectional current		
+	Vessel Position			Vessel Position		
100 year wave	Near	Nominal	Far	Near	Nominal	Far
Minimum tension (kN)	1166	962	915	1027	960	1030
Maximum tension (kN)	1365	1340	1151	1223	1339	1311

100 year current - surface profile	Unidirectional current			Bidirectional current		
+	Vessel Position			Vessel Position		
10 year wave	Near	Nominal	Far	Near	Nominal	Far
Minimum tension (kN)	1174	957	895	1009	970	1012
Maximum tension (kN)	1355	1318	1134	1191	1355	1339

100 year current - mid-level profile	Unidirectional current			Bidirectional current		
+	Vessel Position			Vessel Position		
10 year wave	Near	Nominal	Far	Near	Nominal	Far
Minimum tension (kN)	1183	963	898	1003	964	1041
Maximum tension (kN)	1362	1325	1117	1175	1354	1335

Table B.24 – Mooring Line Dynamic Result (Base Case – ALS)

B.5 Buckling Utilization Ratio

B.5.1 Base Case (ULS)

Base Case - ULS

	TOP					BELOW STRESS JOINT					SAGBEND				
	Functional		Environmental		Max Buckling Ratio	Functional		Environmental		Max Buckling Ratio	Functional		Environmental		Max Buckling Ratio
	Moment	Axial	Moment	Axial		Moment	Axial	Moment	Axial		Moment	Axial	Moment	Axial	
	kN-m	kN	kN-m	kN		kN-m	kN	kN-m	kN		kN-m	kN	kN-m	kN	
LC001	144	2186	71	22	0.372	33	2163	18	22	0.666	155	283	2	5	0.782
LC002	375	2232	170	35	0.372	90	2211	42	36	0.666	136	326	4	8	0.782
LC003	373	2330	278	61	0.372	84	2308	66	61	0.666	107	420	5	20	0.782
LC004	596	2383	362	59	0.372	137	2362	85	61	0.666	96	470	6	25	0.782
LC005	155	2286	113	22	0.372	32	2263	28	22	0.666	119	378	2	9	0.782
LC006	353	2327	185	41	0.372	79	2305	45	41	0.666	108	417	2	16	0.782
LC007	397	2236	263	69	0.372	96	2214	63	70	0.666	135	329	7	17	0.782
LC008	645	2294	400	62	0.404	155	2273	96	64	0.666	117	383	9	18	0.782
LC009	148	2174	86	22	0.372	33	2151	22	22	0.666	162	271	3	6	0.782
LC010	376	2220	183	34	0.372	90	2198	46	35	0.666	141	313	5	8	0.782
LC011	365	2341	260	59	0.372	84	2319	62	59	0.666	104	431	4	21	0.782
LC012	592	2394	343	58	0.372	136	2373	80	60	0.666	94	481	5	26	0.782
LC013	158	2298	122	22	0.372	34	2276	30	22	0.666	115	391	3	11	0.782
LC014	360	2340	189	41	0.372	82	2318	46	41	0.666	105	430	2	17	0.782
LC015	382	2221	249	65	0.372	91	2199	60	66	0.666	141	314	8	16	0.782
LC016	626	2279	376	59	0.372	150	2258	91	61	0.666	121	368	8	18	0.782
LC017	139	2167	121	36	0.372	33	2145	31	36	0.666	164	266	5	7	0.782
LC018	375	2215	139	36	0.372	91	2193	34	36	0.666	143	309	4	8	0.782
LC019	368	2351	313	81	0.372	82	2330	73	82	0.666	102	440	6	28	0.782
LC020	586	2403	442	101	0.398	133	2382	101	104	0.666	92	489	7	46	0.782
LC021	152	2307	135	33	0.372	30	2284	33	33	0.666	113	398	3	9	0.782
LC022	342	2347	154	35	0.372	76	2325	37	35	0.666	103	436	3	12	0.782
LC023	406	2219	328	95	0.372	99	2197	78	96	0.666	141	313	14	23	0.782
LC024	658	2278	499	111	0.495	160	2258	117	114	0.666	121	368	15	34	0.782
LC025	142	2155	126	34	0.372	32	2132	32	34	0.666	172	253	6	6	0.782
LC026	374	2202	140	35	0.372	90	2180	35	35	0.666	149	296	5	8	0.782
LC027	361	2361	293	74	0.372	82	2339	69	75	0.666	100	450	5	27	0.782
LC028	584	2413	409	98	0.372	134	2391	93	100	0.666	91	500	7	46	0.782
LC029	156	2318	143	32	0.372	33	2296	35	32	0.666	110	410	3	11	0.782
LC030	354	2360	158	34	0.372	80	2337	38	34	0.666	100	449	2	13	0.782
LC031	382	2203	292	86	0.372	92	2182	70	87	0.666	149	297	12	19	0.782
LC032	629	2262	449	101	0.431	151	2241	106	103	0.666	127	351	14	29	0.782

B.5.2 Base Case (ALS)

Base Case - ALS

	TOP					BELOW STRESS JOINT					SAGBEND				
	Functional		Environmental		Max Buckling Ratio	Functional		Environmental		Max Buckling Ratio	Functional		Environmental		Max Buckling Ratio
	Moment	Axial	Moment	Axial		Moment	Axial	Moment	Axial		Moment	Axial	Moment	Axial	
	kN-m	kN	kN-m	kN		kN-m	kN	kN-m	kN		kN-m	kN	kN-m	kN	
LCA001	564	2192	58	39	0.372	141	2171	13	39	0.666	153	288	7	11	0.782
LCA002	759	2238	108	60	0.372	188	2218	25	60	0.666	134	330	10	18	0.782
LCA003	759	2328	145	91	0.372	180	2308	33	91	0.666	108	416	6	36	0.782
LCA004	946	2380	233	117	0.493	222	2361	52	117	0.666	97	467	6	51	0.782
LCA005	566	2283	107	49	0.372	135	2262	25	49	0.666	120	374	4	22	0.782
LCA006	745	2325	143	79	0.372	177	2304	32	79	0.666	109	413	7	34	0.782
LCA007	777	2241	142	94	0.372	192	2221	36	94	0.666	133	333	13	27	0.782
LCA008	976	2299	257	125	0.536	237	2280	59	125	0.666	116	388	13	43	0.782
LCA009	568	2182	65	39	0.372	141	2160	15	39	0.666	159	276	8	11	0.782
LCA010	759	2227	114	62	0.372	187	2207	26	62	0.666	139	319	11	19	0.782
LCA011	755	2338	130	86	0.372	180	2317	29	86	0.666	105	427	6	35	0.782
LCA012	946	2391	218	112	0.480	223	2372	49	112	0.666	95	478	6	50	0.782
LCA013	568	2295	114	51	0.372	136	2273	26	52	0.666	116	386	4	25	0.782
LCA014	752	2337	142	81	0.372	179	2316	33	81	0.666	106	426	7	37	0.782
LCA015	764	2228	136	88	0.372	188	2208	35	88	0.666	139	319	13	25	0.782
LCA016	958	2285	236	118	0.503	233	2266	54	118	0.666	120	373	13	39	0.782
LCA017	563	2175	42	52	0.372	142	2154	10	52	0.666	161	272	9	12	0.782
LCA018	760	2222	64	54	0.372	189	2202	14	55	0.666	141	315	9	13	0.782
LCA019	757	2347	132	87	0.372	178	2326	31	87	0.666	104	435	6	34	0.782
LCA020	941	2398	211	124	0.471	220	2379	50	124	0.666	93	484	7	51	0.782
LCA021	563	2302	84	66	0.372	133	2281	18	66	0.666	114	392	5	25	0.782
LCA022	738	2342	91	68	0.372	174	2322	20	68	0.666	105	431	5	26	0.782
LCA023	783	2227	127	103	0.372	195	2206	29	103	0.666	139	319	15	29	0.782
LCA024	984	2285	238	140	0.526	241	2266	56	139	0.666	120	374	17	45	0.782
LCA025	566	2164	49	51	0.372	142	2143	12	51	0.666	168	260	10	12	0.782
LCA026	758	2211	63	53	0.372	188	2191	14	53	0.666	146	303	11	13	0.782
LCA027	753	2355	120	82	0.372	178	2335	28	82	0.666	101	444	5	33	0.782
LCA028	943	2407	193	119	0.458	221	2388	45	118	0.666	91	495	6	51	0.782
LCA029	567	2313	88	65	0.372	135	2291	20	65	0.666	111	404	6	26	0.782
LCA030	748	2354	94	66	0.372	177	2334	21	66	0.666	102	443	6	26	0.782
LCA031	764	2212	113	92	0.372	189	2192	26	92	0.666	145	304	15	25	0.782
LCA032	959	2269	213	128	0.484	234	2251	50	128	0.666	125	358	16	41	0.782

B.6 Fatigue due to Wave Induced

B.6.1 Fatigue Data

JONSWAP Wave Spectrum

5.3 JONSWAP Wave Spectrum for Santos/Campos Basins and Relation TZ / TP

The JONSWAP Wave Spectrum, adjusted for Santos/Campos Basins wave conditions, is:

$$S(f) = \frac{5}{16} * Hs^2 * Tp * \left(f_p / f\right)^5 * (1 - 0.287 * \ln\gamma) * \exp\left[-1{,}25 * \left(\frac{f}{f_p}\right)^{-4}\right] * \gamma^{\exp\left[-(f-f_p)^2/(2*\sigma^2*f_p^2)\right]}$$

$$\sigma = \begin{cases} \sigma_a = 0{,}07, & \text{for} \quad f \le f_p \\ \sigma_b = 0{,}09, & \text{for} \quad f > f_p \end{cases}$$

f

where: α - form parameter or Phillips constant

f_p - frequency (Hz)

- peak frequency (Hz)

γ - peakedness parameter or peak enhancement factor

σ - shape parameter or peak width

The gamma parameter is adjusted by the expression below:

$$\gamma = 6.4 \times \mathrm{Tp}^{(-0.491)}$$

Relation between Tz and Tp.

Mean Zero-crossing period : $T_z = \frac{1}{f_p}\sqrt{\frac{5+\gamma}{10.89+\gamma}}$ or $T_z = T_p\sqrt{\frac{5+\gamma}{10.89+\gamma}}$

where: $f_p = \frac{1}{T_p}$ and T_p - peak period.

Reference: Santos Basin Central Cluster Region Metocean Data (I-ET-3A26.00-1000-941-PPC-001- Rev. C, page 29 of 106)

Distribution of Total Significant Wave Heights and Primary Spectral Peak Directions

5.4.1 Distribution of Total Significant Wave Heights and Primary Spectral Peak Directions*

Hs(m)		DIRECTION(°)																Freq	%	Mean Dir
		N	NNE	NE	ENE	E	ESE	SE	SSE	S	SSW	SW	WSW	W	WNW	NW	NNW			
0.0	0.5	0	0	0	1	1	1	0	2	3	0	0	0	0	0	0	0	8	0.01	145.6
0.5	1.0	19	51	266	342	146	135	93	104	138	143	49	6	5	4	3	8	1512	2	99.2
1.0	1.5	55	370	1622	2303	2314	1826	1303	784	577	505	105	26	8	11	9	24	11842	15.64	97
1.5	2.0	100	882	4137	4266	3161	3089	2799	2516	2291	1330	169	49	24	3	4	16	24836	32.8	103.3
2.0	2.5	68	840	3481	2557	1530	1404	1654	1965	2753	2367	348	85	27	15	8	19	19121	25.25	117.1
2.5	3.0	37	482	1722	1169	709	552	556	944	1519	1928	360	136	35	10	8	8	10175	13.44	131.9
3.0	3.5	22	170	721	428	288	212	211	365	651	1039	361	93	27	10	4	6	4608	6.09	149.2
3.5	4.0	3	41	222	134	101	108	90	115	229	555	199	53	10	4	3	0	1867	2.47	168.1
4.0	4.5	0	15	69	34	22	33	33	63	74	265	146	40	15	1	0	0	810	1.07	189.2
4.5	5.0	0	2	24	12	17	10	18	30	36	127	97	30	7	0	0	0	410	0.54	196.6
5.0	5.5	0	1	5	8	5	0	8	12	17	68	74	29	2	0	0	0	229	0.3	208.4
5.5	6.0	0	0	0	3	0	0	0	6	12	28	58	17	0	0	0	0	124	0.16	215
6.0	6.5	0	0	0	0	0	0	0	0	3	20	43	0	0	0	0	0	66	0.09	223.2
6.5	7.0	0	0	0	0	0	0	0	0	3	4	32	0	0	0	0	0	39	0.05	222.2
7.0	7.5	0	0	0	0	0	0	0	0	3	7	19	0	0	0	0	0	29	0.04	219
7.5	8.0	0	0	0	0	0	0	0	0	0	1	10	0	0	0	0	0	11	0.01	226.9
8.0	8.5	0	0	0	0	0	0	0	0	0	1	8	0	0	0	0	0	9	0.01	226.6
8.5	9.0	0	0	0	0	0	0	0	0	0	0	10	0	0	0	0	0	10	0.01	231.4
9.0	9.5	0	0	0	0	0	0	0	0	0	1	3	0	0	0	0	0	4	0.01	227.2
9.5	10.0	0	0	0	0	0	0	0	0	0	2	0	0	0	0	0	0	2	0	207.8
10.0	10.5	0	0	0	0	0	0	0	0	0	0	0	0	0	0	0	0	0	0	NaN
10.5	11.0	0	0	0	0	0	0	0	0	0	0	0	0	0	0	0	0	0	0	NaN
Freq		304	2854	12269	11257	8294	7370	6765	6906	8309	8391	2091	564	160	58	39	81	75712		
%		0.4	3.77	16.2	14.87	10.95	9.73	8.94	9.12	10.97	11.08	2.76	0.74	0.21	0.08	0.05	0.11			
Mean Hs		1.98	2.12	2.1	1.94	1.86	1.87	1.95	2.12	2.28	2.58	3.28	3.13	2.8	2.33	2.19	1.85			

(*) The Total Significant Wave Height (Hst) is obtained as Hst=4*sqrt(m_0), where m_o is the integrated area of the total wave power spectrum (sea and swell partitions). The Primary Spectral Peak Direction is the approaching direction associated with the spectral peak period.

SOURCE: Modeled wave data - JIP BOMOSHU (Brazil Offshore Metocean Storm Hindcast Update - Grid Point 8139) and GROW Fine SAB, OceanWeather Inc., evaluated with in-situ wave measured data. The wave data was tabulated at 3-hour intervals, providing information equivalent to 227136 hours (=75712 * 3 hours).

Reference: Santos Basin Central Cluster Region Metocean Data (I-ET-3A26.00-1000-941-PPC-001- Rev. C, page 30 of 106)

Distribution of Total Significant Wave Heights and Primary Spectral Peak Periods

5.4.2 Distribution of Total Significant Wave Heights and Primary Spectral Peak Periods*

Hs(m)		Tp(s)																		Freq	%	Mean Tp
		3 4	4 5	5 6	6 7	7 8	8 9	9 10	10 11	11 12	12 13	13 14	14 15	15 16	16 17	17 18	18 19	19 20	20 21			
0.0	0.5	1	0	0	1	2	2	1	0	0	0	0	1	0	0	0	0	0	0	8	0.01	8.24
0.5	1.0	107	113	205	256	273	159	112	74	68	50	41	38	12	4	0	0	0	0	1512	2	7.73
1.0	1.5	15	938	1115	1792	3608	2505	692	373	283	260	108	103	31	11	3	0	2	3	11842	15.64	7.7
1.5	2.0	1	349	3682	3524	4602	6028	2948	1626	993	534	251	174	69	26	18	8	1	2	24836	32.8	8.12
2.0	2.5	0	13	1265	4995	2430	2755	2041	1870	1806	982	523	284	105	32	10	8	2	0	19121	25.25	8.74
2.5	3.0	0	6	109	2114	2404	1040	858	798	879	1021	514	288	108	20	8	6	1	1	10175	13.44	9.27
3.0	3.5	0	1	4	403	1240	856	277	292	294	424	431	280	77	18	8	1	1	1	4608	6.09	9.82
3.5	4.0	0	0	0	43	268	550	189	91	140	141	139	209	75	16	5	1	0	0	1867	2.47	10.45
4.0	4.5	0	0	0	3	31	207	161	48	47	63	68	89	73	17	3	0	0	0	810	1.07	11.16
4.5	5.0	0	0	0	0	4	48	116	48	15	21	41	57	35	19	6	0	0	0	410	0.54	11.75
5.0	5.5	0	0	0	0	0	16	45	60	19	15	16	22	20	7	8	1	0	0	229	0.3	11.88
5.5	6.0	0	0	0	0	0	2	22	44	19	7	6	15	9	0	0	0	0	0	124	0.16	11.5
6.0	6.5	0	0	0	0	0	0	10	18	22	0	3	11	2	0	0	0	0	0	66	0.09	11.55
6.5	7.0	0	0	0	0	0	0	3	12	12	2	0	7	3	0	0	0	0	0	39	0.05	11.99
7.0	7.5	0	0	0	0	0	0	4	4	14	1	0	1	5	0	0	0	0	0	29	0.04	11.99
7.5	8.0	0	0	0	0	0	0	2	1	1	4	0	0	3	0	0	0	0	0	11	0.01	12.51
8.0	8.5	0	0	0	0	0	0	0	5	0	1	0	1	2	0	0	0	0	0	9	0.01	12.47
8.5	9.0	0	0	0	0	0	0	1	6	3	0	0	0	0	0	0	0	0	0	10	0.01	10.82
9.0	9.5	0	0	0	0	0	0	0	1	1	1	0	0	0	1	0	0	0	0	4	0.01	12.88
9.5	10.0	0	0	0	0	0	0	0	0	0	0	0	0	0	2	0	0	0	0	2	0	16.95
10.0	10.5	0	0	0	0	0	0	0	0	0	0	0	0	0	0	0	0	0	0	0	0	0
10.5	11.0	0	0	0	0	0	0	0	0	0	0	0	0	0	0	0	0	0	0	0	0	0
Freq		124	1420	6380	13131	14862	14168	7482	5371	4616	3527	2141	1580	629	173	69	25	7	7	75712		
%		0.16	1.88	8.43	17.34	19.63	18.71	9.88	7.09	6.1	4.66	2.83	2.09	0.83	0.23	0.09	0.03	0.01	0.01			
Mean Hs		0.86	1.35	1.75	2.07	2.03	2.04	2.2	2.31	2.38	2.49	2.69	2.9	3.14	3.12	3.05	2.43	2.07	1.96			

(*) The Total Significant Wave Height (Hst) is obtained as Hst=4*sqrt(m_0), where m_o is the integrated area of the total wave power spectrum (sea and swell partitions). The Primary Spectral Peak is the period associated with maximum spectral energy.

SOURCE: Modeled wave data - JIP BOMOSHU (Brazil Offshore Metocean Storm Hindcast Update - Grid Point 8139) and GROW Fine SAB, OceanWeather Inc., evaluated with in-situ wave measured data. The wave data was tabulated at 3-hour intervals, providing information equivalent to 227136 hours (=75712 * 3 hours).

Reference: Santos Basin Central Cluster Region Metocean Data (I-ET-3A26.00-1000-941-PPC-001- Rev. C, page 31 of 106)

Seastate Probability Distribution

No	Direction (deg)	Percentage (%)	Exposure Time (hours)
1	0	23.26	52823
2	45	25.52	57973.5
3	90	2.34	5314.5
4	135	0.14	325.5
5	180	0.62	1413
6	225	8.68	19705.5
7	270	21.08	47872.5
8	315	18.36	41709
		100.00	227136

0° Direction

Seastate	Hs (m)	Tp (s)	rep (%)	Total Percentage	Exposure Time (hours)
1	1.25	4.5	3.29		1,739
2	1.25	7.5	11.35		5,995
3	1.25	10	1.65		873
4	1.25	14	1.34		710
5	2.25	5.5	18.27		9,648
6	2.25	9.5	35.79		18,906
7	2.25	16	4.00	23.26	2,113
8	3.25	8.5	15.29		8,076
9	3.25	15	4.24		2,238
10	4.25	9.5	2.35		1,240
11	4.25	14	1.19		627
12	5	12.5	1.01		532
13	7.5	13	0.22		119

45° Direction

Seastate	Hs (m)	Tp (s)	rep (%)	Total Percentage	Exposure Time (hours)
1	1.25	4.5	3.29		1,909
2	1.25	7.5	11.35		6,580
3	1.25	10	1.65		958
4	1.25	14	1.34		779
5	2.25	5.5	18.27		10,589
6	2.25	9.5	35.79		20,750
7	2.25	16	4.00	25.52	2,319
8	3.25	8.5	15.29		8,863
9	3.25	15	4.24		2,456
10	4.25	9.5	2.35		1,361
11	4.25	14	1.19		688
12	5	12.5	1.01		584
13	7.5	13	0.22		130

90° Direction

Seastate	Hs (m)	Tp (s)	rep (%)	Total Percentage	Exposure Time (hours)
1	1.25	4.5	3.29		175
2	1.25	7.5	11.35		603
3	1.25	10	1.65		88
4	1.25	14	1.34		71
5	2.25	5.5	18.27		971
6	2.25	9.5	35.79		1,902
7	2.25	16	4.00	2.34	213
8	3.25	8.5	15.29		812
9	3.25	15	4.24		225
10	4.25	9.5	2.35		125
11	4.25	14	1.19		63
12	5	12.5	1.01		54
13	7.5	13	0.22		12

135° Direction

Seastate	Hs (m)	Tp (s)	rep (%)	Total Percentage	Exposure Time (hours)
1	1.25	4.5	3.29	0.14	11
2	1.25	7.5	11.35		37
3	1.25	10	1.65		5
4	1.25	14	1.34		4
5	2.25	5.5	18.27		59
6	2.25	9.5	35.79		117
7	2.25	16	4.00		13
8	3.25	8.5	15.29		50
9	3.25	15	4.24		14
10	4.25	9.5	2.35		8
11	4.25	14	1.19		4
12	5	12.5	1.01		3
13	7.5	13	0.22		1

180° Direction

Seastate	Hs (m)	Tp (s)	rep (%)	Total Percentage	Exposure Time (hours)
1	1.25	4.5	3.29	0.62	47
2	1.25	7.5	11.35		160
3	1.25	10	1.65		23
4	1.25	14	1.34		19
5	2.25	5.5	18.27		258
6	2.25	9.5	35.79		506
7	2.25	16	4.00		57
8	3.25	8.5	15.29		216
9	3.25	15	4.24		60
10	4.25	9.5	2.35		33
11	4.25	14	1.19		17
12	5	12.5	1.01		14
13	7.5	13	0.22		3

225° Direction

Seastate	Hs (m)	Tp (s)	rep (%)	Total Percentage	Exposure Time (hours)
1	1.25	4.5	3.29	8.68	649
2	1.25	7.5	11.35		2,236
3	1.25	10	1.65		326
4	1.25	14	1.34		265
5	2.25	5.5	18.27		3,599
6	2.25	9.5	35.79		7,053
7	2.25	16	4.00		788
8	3.25	8.5	15.29		3,013
9	3.25	15	4.24		835
10	4.25	9.5	2.35		463
11	4.25	14	1.19		234
12	5	12.5	1.01		199
13	7.5	13	0.22		44

270° Direction

Seastate	Hs (m)	Tp (s)	rep (%)	Total Percentage	Exposure Time (hours)
1	1.25	4.5	3.29	21.08	1,576
2	1.25	7.5	11.35		5,433
3	1.25	10	1.65		791
4	1.25	14	1.34		643
5	2.25	5.5	18.27		8,744
6	2.25	9.5	35.79		17,135
7	2.25	16	4.00		1,915
8	3.25	8.5	15.29		7,319
9	3.25	15	4.24		2,028
10	4.25	9.5	2.35		1,124
11	4.25	14	1.19		568
12	5	12.5	1.01		482
13	7.5	13	0.22		107

315° Direction

Seastate	Hs (m)	Tp (s)	rep (%)	Total Percentage	Exposure Time (hours)
1	1.25	4.5	3.29		1,373
2	1.25	7.5	11.35		4,734
3	1.25	10	1.65		689
4	1.25	14	1.34		560
5	2.25	5.5	18.27		7,618
6	2.25	9.5	35.79		14,929
7	2.25	16	4.00	18.36	1,669
8	3.25	8.5	15.29		6,377
9	3.25	15	4.24		1,767
10	4.25	9.5	2.35		979
11	4.25	14	1.19		495
12	5	12.5	1.01		420
13	7.5	13	0.22		94

B.6.2 Fatigue Response

Tapered Stress Joint Section – C-curve; SCF 1.0

Fatigue Damage Tables

OrcaFlex 9.4f: base case - 8 directions_rev1.ftg (modified 13:13 on 03.05.2012 by OrcaFlex 9.4f)

Title: COBRA 2200 m - Fatigue Analysis - 8 directions

Damage Calculation: Homogeneous pipe stress

Analysis Type: Rainflow

Radial Position: Outer

Worst Damage	
Damage over total exposure	0.010732783
Total exposure time (years)	25.8346
Life (years)	2407.0726
Arc Length (m)	0.0
Theta (deg)	180.0

	Excessive Damage (> 0,1)	
Arc Length (m)	**Theta (deg)**	**Total**
(none)	(none)	(none)

	ZZ Stress (kPa)
Min	-117465.2818
Max	286653.1446

Fatigue Life Plot

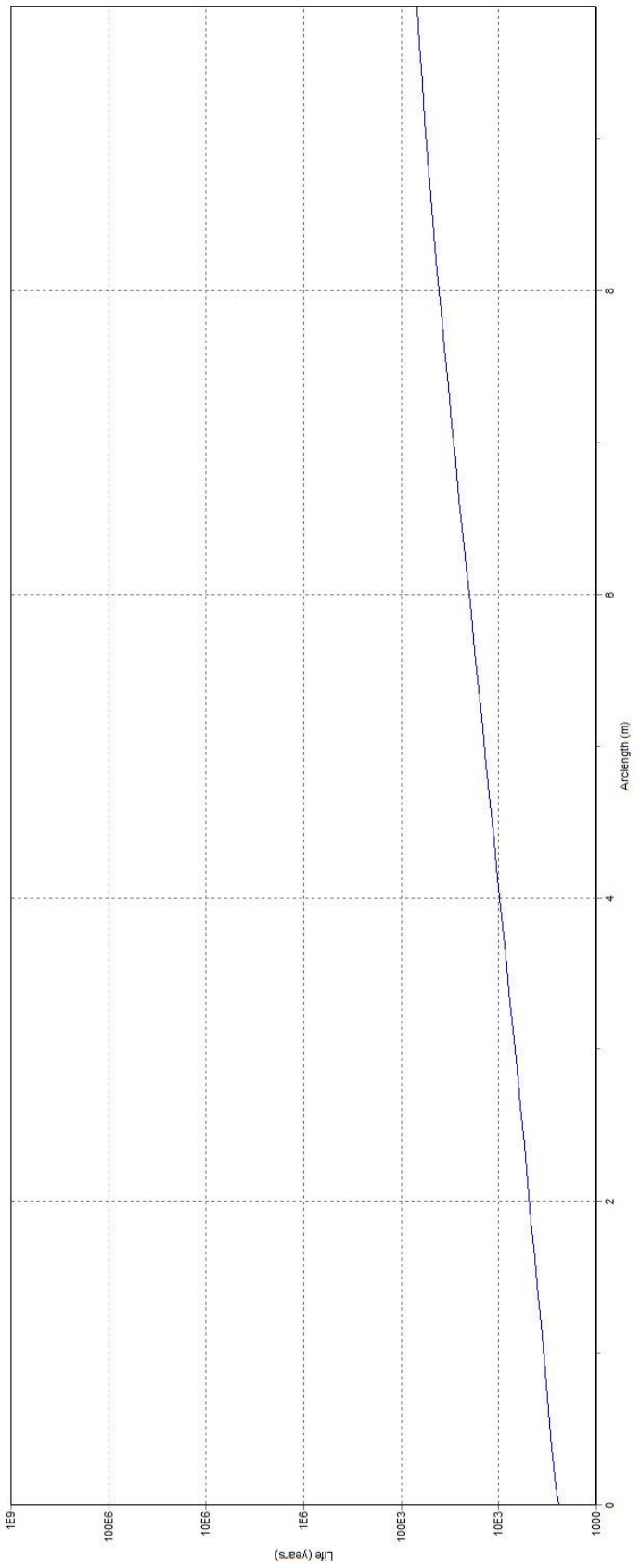

Tapered Stress Joint Section – D-curve; SCF 1.0

Fatigue Damage Tables

OrcaFlex 9.4f: base case - 8 directions - D curve_rev1.ftg (modified 13:29 on 03.05.2012 by OrcaFlex 9.4f)
Title: COBRA 2200 m - Fatigue Analysis - 8 directions (D Curve)
Damage Calculation: Homogeneous pipe stress
Analysis Type: Rainflow
Radial Position: Outer

Worst Damage	
Damage over total exposure	0.052954266
Total exposure time (years)	25.8346
Life (years)	487.866
Arc Length (m)	0.0
Theta (deg)	180.0

	Excessive Damage (> 0,1)	
Arc Length (m)	**Theta (deg)**	**Total**
(none)	(none)	(none)

	ZZ Stress (kPa)
Min	-117465.2818
Max	286653.1446

Fatigue Life Plot

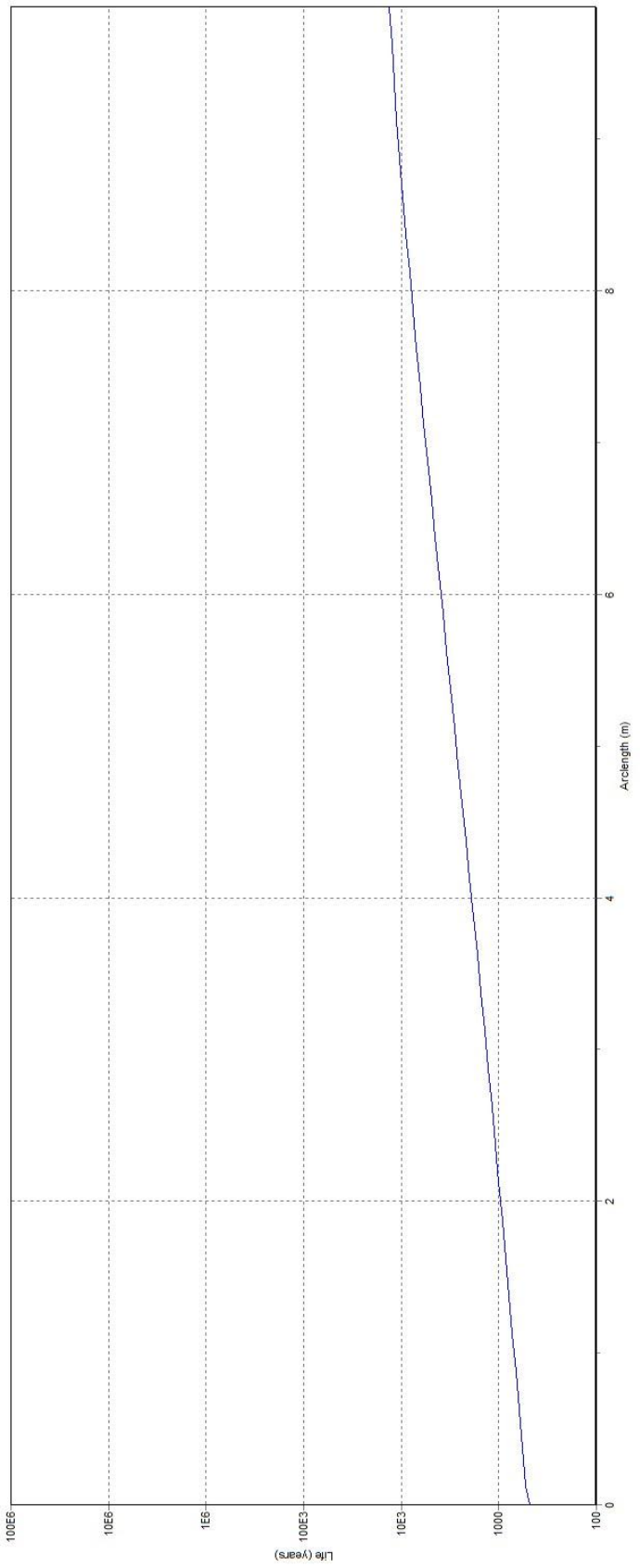

Tapered Stress Joint Section – E-curve; SCF 1.0

Fatigue Damage Tables

OrcaFlex 9.4f: base case - 8 directions - E curve_rev1.ftg (modified 14:14 on 03.05.2012 by OrcaFlex 9.4f)
Title: COBRA 2200 m - Fatigue Analysis - 8 directions (E Curve)
Damage Calculation: Homogeneous pipe stress
Analysis Type: Rainflow
Radial Position: Outer

Worst Damage	
Damage over total exposure	0.091932574
Total exposure time (years)	25.8346
Life (years)	281.0167
Arc Length (m)	0.0
Theta (deg)	180.0

	Excessive Damage (> 0,1)	
Arc Length (m)	**Theta (deg)**	**Total**
(none)	(none)	(none)

	ZZ Stress (kPa)
Min	-117465.2818
Max	286653.1446

Fatigue Life Plot

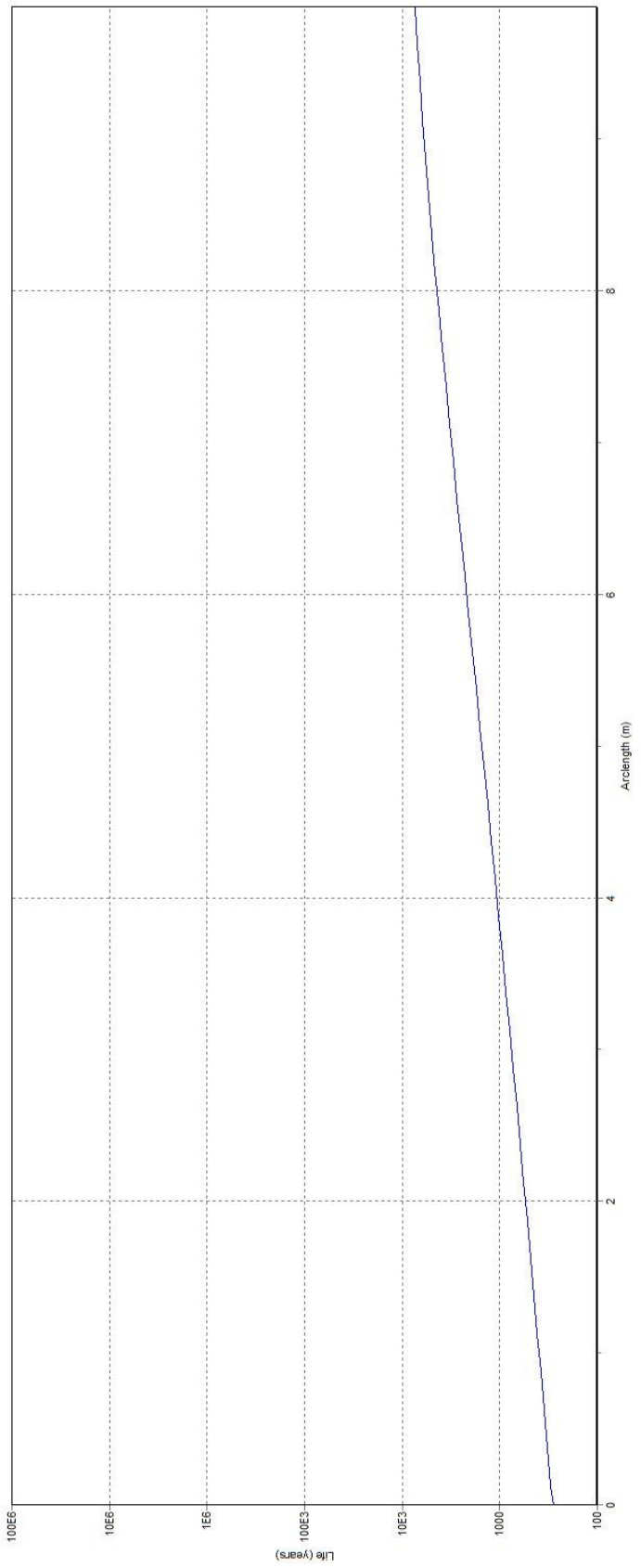

Touch Down Point – F1-curve; SCF 1.2

Fatigue Damage Tables

OrcaFlex 9.4f: base case - 8 directions_rev1 - TDZ longer.ftg (modified 15:27 on 03.05.2012 by OrcaFlex 9.4f)

Title: COBRA 2200 m - Fatigue Analysis - 8 directions - longer TDZ

Damage Calculation: Homogeneous pipe stress

Analysis Type: Rainflow

Radial Position: Outer

Worst Damage	
Damage over total exposure	0.000480166
Total exposure time (years)	25.8346
Life (years)	53803.4541
Arc Length (m)	2307.5
Theta (deg)	180.0

	Excessive Damage (> 0,1)	
Arc Length (m)	**Theta (deg)**	**Total**
(none)	(none)	(none)

	ZZ Stress (kPa)
Min	-15233.62519
Max	166667.5646

Fatigue Life Plot

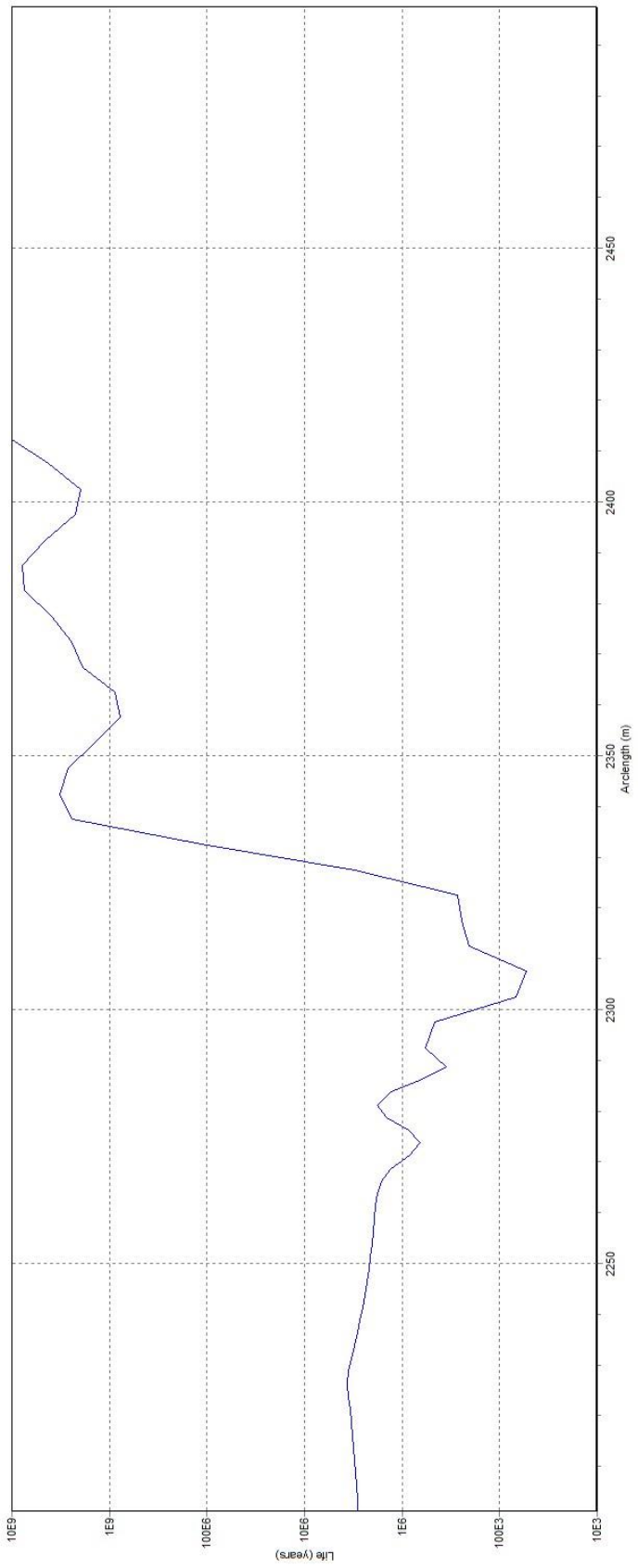

B.7 Fatigue due to VIV

B.7.1 Fatigue Data for Long Term Event

The following current profiles are taken from Santos Basin Central Cluster Region Metocean Data (I-ET-3A26.00-1000-941-PPC-001- Rev. C, Section 6.3 Current Profiles for Fatigue Analysis)

6.3.1 Current Profile (m/s) for Fatigue Analysis with N Direction at surface

	0.00		0.10		0.20		0.30	
	0.10		0.20		0.30		0.40	
Depth	Int.	Dir.	Int.	Dir.	Int.	Dir.	Int.	Dir.
0	0.06	360	0.15	0	0.24	1	0.34	1
50	0.06	359	0.15	360	0.23	0	0.32	1
100	0.05	355	0.13	357	0.20	1	0.26	2
150	0.05	344	0.12	355	0.17	1	0.21	4
200	0.04	341	0.10	354	0.16	359	0.19	2
250	0.04	346	0.09	350	0.14	354	0.17	1
300	0.03	330	0.08	349	0.12	352	0.14	359
350	0.03	316	0.07	348	0.11	351	0.13	359
375	0.03	320	0.06	347	0.10	350	0.12	358
800	0.02	277	0.02	324	0.04	334	0.05	339
1200	0.01	305	0.01	342	0.03	354	0.03	6
1600	0.00	352	0.01	296	0.01	352	0.03	2
2000	0.01	68	0.00	18	0.01	62	0.03	52
2200	0.04	88	0.03	77	0.05	72	0.06	67
Freq.	484		1122		943		359	

	0.40		0.50		0.60		
	0.50		0.60		0.70		
Depth	Int.	Dir.	Int.	Dir.	Int.	Dir.	
0	0.44	9	0.53	13	0.60	18	
50	0.43	9	0.52	12	0.59	16	
100	0.36	10	0.42	16	0.45	9	
150	0.29	11	0.32	14	0.27	11	
200	0.25	9	0.26	9	0.26	15	
250	0.22	8	0.19	8	0.23	11	
300	0.17	8	0.16	9	0.20	22	
350	0.15	7	0.13	8	0.20	7	
375	0.13	7	0.11	5	0.23	1	
800	0.07	359	0.06	345	0.12	1	
1200	0.05	13	0.03	13	0.05	15	
1600	0.03	25	0.02	29	0.06	77	
2000	0.05	56	0.04	44	0.09	60	
2200	0.08	61	0.06	67	0.10	89	
Freq.	151		56		1		**3116**
							12.48%

SOURCE: PETROBRAS Metocean Database (Engineering measurement program - mooring P1).

6.3.2 Current Profile (m/s) for Fatigue Analysis with NE Direction at surface

	0.00		0.10		0.20		0.30	
	0.10		0.20		0.30		0.40	
Depth	Int.	Dir.	Int.	Dir.	Int.	Dir.	Int.	Dir.
0	0.07	45	0.15	45	0.24	45	0.34	44
50	0.07	42	0.15	41	0.24	42	0.32	42
100	0.06	38	0.13	37	0.21	39	0.26	38
150	0.05	29	0.12	33	0.17	33	0.22	37
200	0.03	23	0.09	29	0.14	31	0.17	34
250	0.03	28	0.07	26	0.12	31	0.15	32
300	0.02	16	0.06	24	0.10	29	0.12	32
350	0.02	354	0.06	19	0.09	30	0.10	33
375	0.02	349	0.05	15	0.08	27	0.09	32
800	0.02	264	0.01	315	0.03	7	0.03	25
1200	0.01	323	0.01	339	0.01	3	0.01	29
1600	0.00	36	0.00	120	0.01	7	0.02	43
2000	0.01	83	0.01	80	0.02	68	0.03	73
2200	0.04	87	0.04	88	0.04	78	0.05	78
Freq.	511		988		802		528	

	0.40		0.50		0.60		
	0.50		0.60		0.70		
Depth	Int.	Dir.	Int.	Dir.	Int.	Dir.	
0	0.43	44	0.52	42	0.63	32	
50	0.41	42	0.48	39	0.49	31	
100	0.29	38	0.33	37	0.23	24	
150	0.23	37	0.26	36	0.16	22	
200	0.19	36	0.20	39	0.16	20	
250	0.16	33	0.17	37	0.22	34	
300	0.12	32	0.14	38	0.14	34	
350	0.10	30	0.11	26	0.12	41	
375	0.09	29	0.09	29	0.09	23	
800	0.04	37	0.06	44	0.10	60	
1200	0.01	94	0.02	65	0.06	139	
1600	0.02	40	0.03	27	0.06	354	
2000	0.04	69	0.05	54	0.02	17	
2200	0.06	81	0.08	71	0.10	52	
Freq.	247		57		1		**3134**
							12.55%

SOURCE: PETROBRAS Metocean Database (Engineering measurement program - mooring P1).

6.3.3 Current Profile (m/s) for Fatigue Analysis with E Direction at surface

	0.00		0.10		0.20		0.30	
	0.10		0.20		0.30		0.40	
Depth	Int.	Dir.	Int.	Dir.	Int.	Dir.	Int.	Dir.
0	0.06	91	0.15	91	0.24	90	0.33	90
50	0.06	88	0.14	90	0.23	89	0.31	88
100	0.06	85	0.11	91	0.17	90	0.20	88
150	0.05	81	0.09	87	0.14	90	0.15	91
200	0.04	86	0.07	88	0.11	90	0.11	96
250	0.03	92	0.06	85	0.10	93	0.09	92
300	0.02	76	0.04	91	0.09	96	0.06	93
350	0.01	66	0.03	91	0.07	94	0.06	90
375	0.01	44	0.03	86	0.06	93	0.05	91
800	0.02	252	0.01	212	0.02	135	0.02	144
1200	0.00	88	0.00	36	0.01	78	0.01	107
1600	0.01	94	0.01	121	0.02	100	0.02	79
2000	0.02	77	0.02	114	0.03	73	0.03	77
2200	0.04	95	0.04	101	0.05	93	0.05	91
Freq.	494		953		712		386	

	0.40		0.50		0.60		
	0.50		0.60		0.70		
Depth	Int.	Dir.	Int.	Dir.	Int.	Dir.	
0	0.43	86	0.53	86	0.64	89	
50	0.39	83	0.48	85	0.56	89	
100	0.21	82	0.29	86	0.35	92	
150	0.15	80	0.21	82	0.27	85	
200	0.09	87	0.14	79	0.19	95	
250	0.08	95	0.09	81	0.17	88	
300	0.06	94	0.09	86	0.14	82	
350	0.06	83	0.06	84	0.11	84	
375	0.05	79	0.05	89	0.10	79	
800	0.02	128	0.02	121	0.02	26	
1200	0.01	161	0.01	74	0.01	20	
1600	0.03	70	0.03	56	0.04	20	
2000	0.04	59	0.04	44	0.04	40	
2200	0.06	83	0.06	71	0.07	61	
Freq.	145		59		13		**2762**
							11.06%

SOURCE: PETROBRAS Metocean Database (Engineering measurement program - mooring P1).

6.3.4 Current Profile (m/s) for Fatigue Analysis with SE Direction at surface

	0.00		0.10		0.20		0.30	
	0.10		0.20		0.30		0.40	
Depth	Int.	Dir.	Int.	Dir.	Int.	Dir.	Int.	Dir.
0	0.07	135	0.15	135	0.24	135	0.34	134
50	0.06	135	0.14	136	0.23	134	0.32	134
100	0.05	151	0.12	139	0.19	135	0.23	134
150	0.04	148	0.10	139	0.14	137	0.17	141
200	0.03	163	0.07	146	0.11	144	0.13	149
250	0.02	155	0.06	149	0.09	150	0.11	153
300	0.02	197	0.05	151	0.08	150	0.09	157
350	0.02	196	0.05	157	0.07	156	0.06	161
375	0.02	191	0.04	158	0.06	157	0.06	166
800	0.02	233	0.02	197	0.03	191	0.03	188
1200	0.01	183	0.01	199	0.01	179	0.02	192
1600	0.01	106	0.02	121	0.02	152	0.02	129
2000	0.03	84	0.04	101	0.04	110	0.03	101
2200	0.05	90	0.05	95	0.05	102	0.05	101
Freq.	485		1040		741		446	

	0.40		0.50		0.60		0.70		
	0.50		0.60		0.70		0.80		
Depth	Int.	Dir.	Int.	Dir.	Int.	Dir.	Int.	Dir.	
0	0.43	132	0.52	132	0.59	128	0.74	156	
50	0.40	131	0.47	132	0.50	133	0.71	156	
100	0.26	133	0.23	138	0.37	146	0.61	174	
150	0.18	137	0.17	146	0.27	150	0.50	174	
200	0.12	143	0.13	135	0.25	164	0.47	175	
250	0.10	147	0.11	141	0.23	153	0.44	174	
300	0.07	153	0.10	147	0.14	173	0.37	180	
350	0.06	155	0.08	149	0.16	170	0.28	179	
375	0.05	158	0.07	147	0.15	161	0.24	180	
800	0.04	179	0.06	206	0.04	157	0.10	200	
1200	0.03	190	0.03	192	0.03	130	0.10	168	
1600	0.02	149	0.00	250	0.05	90	0.07	164	
2000	0.02	103	0.01	174	0.03	90	0.02	193	
2200	0.04	114	0.04	123	0.05	76	0.05	181	
Freq.	197		24		3		4		**2940**
									11.78%

SOURCE: PETROBRAS Metocean Database (Engineering measurement program - mooring P1).

6.3.5 Current Profile (m/s) for Fatigue Analysis with S Direction at surface

	0.00		0.10		0.20		0.30		0.40		0.50	
	0.10		0.20		0.30		0.40		0.50		0.60	
Depth	Int.	Dir.	Int.	Dir.	Int.	Dir.	Int.	Dir.	Int.	Dir.	Int.	Dir.
0	0.06	180	0.15	180	0.24	180	0.33	181	0.43	182	0.54	182
50	0.06	177	0.14	180	0.24	180	0.32	181	0.42	183	0.53	182
100	0.06	188	0.12	183	0.18	181	0.25	182	0.30	183	0.49	181
150	0.06	194	0.10	191	0.14	184	0.21	187	0.25	186	0.42	181
200	0.05	203	0.09	194	0.13	192	0.18	190	0.23	193	0.36	179
250	0.04	205	0.07	200	0.12	194	0.16	190	0.22	195	0.30	179
300	0.03	214	0.07	201	0.11	192	0.14	192	0.20	195	0.27	174
350	0.03	215	0.06	203	0.09	195	0.12	194	0.17	195	0.24	175
375	0.03	218	0.05	204	0.08	196	0.11	195	0.16	196	0.23	174
800	0.02	231	0.03	229	0.05	207	0.07	191	0.09	203	0.13	154
1200	0.01	248	0.02	226	0.03	199	0.05	199	0.05	185	0.09	116
1600	0.01	127	0.01	134	0.01	168	0.02	185	0.03	156	0.07	120
2000	0.03	92	0.03	91	0.03	129	0.03	146	0.04	128	0.09	89
2200	0.05	87	0.05	93	0.05	112	0.05	122	0.06	108	0.15	97
Freq.	501		972		762		378		126		85	

	0.60		0.70		0.80		0.90		1.00		1.10		
	0.70		0.80		0.90		1.00		1.10		1.20		
Depth	Int.	Dir.	Int.	Dir.	Int.	Dir.	Int.	Dir.	Int.	Dir.	Int.	Dir.	
0	0.63	179	0.73	173	0.84	174	0.95	173	1.03	173	1.17	174	
50	0.62	178	0.70	173	0.84	173	0.96	174	1.02	173	1.04	171	
100	0.58	183	0.61	174	0.77	169	0.89	174	0.93	173	1.04	172	
150	0.52	181	0.56	175	0.66	173	0.71	172	0.74	174	0.80	177	
200	0.42	179	0.49	177	0.57	172	0.60	172	0.59	174	0.67	174	
250	0.37	174	0.45	173	0.50	172	0.50	173	0.53	171	0.55	173	
300	0.31	173	0.37	172	0.42	169	0.43	172	0.47	172	0.49	178	
350	0.29	178	0.32	174	0.37	172	0.37	172	0.41	175	0.37	174	
375	0.27	174	0.29	175	0.32	173	0.34	174	0.37	177	0.38	171	
800	0.12	164	0.13	187	0.15	192	0.17	188	0.15	175	0.22	170	
1200	0.08	139	0.09	164	0.07	182	0.08	158	0.08	181	0.09	174	
1600	0.06	112	0.04	128	0.05	172	0.04	167	0.04	143	0.10	164	
2000	0.07	104	0.04	89	0.04	112	0.04	112	0.04	160	0.05	13	
2200	0.13	107	0.09	109	0.06	120	0.07	109	0.08	127	0.03	100	
Freq.	38		40		24		38		15		3		**2982**
													11.94%

SOURCE: PETROBRAS Metocean Database (Engineering measurement program - mooring P1).

6.3.6 Current Profile (m/s) for Fatigue Analysis with SW Direction at surface

	0.00		0.10		0.20		0.30	
	0.10		0.20		0.30		0.40	
Depth	Int.	Dir.	Int.	Dir.	Int.	Dir.	Int.	Dir.
0	0.06	225	0.15	225	0.24	225	0.34	226
50	0.06	224	0.14	225	0.24	225	0.34	226
100	0.06	231	0.13	230	0.20	225	0.27	224
150	0.06	235	0.11	230	0.16	226	0.20	224
200	0.05	247	0.09	238	0.14	231	0.17	224
250	0.05	241	0.09	233	0.12	228	0.15	226
300	0.05	240	0.08	235	0.11	228	0.14	230
350	0.04	243	0.07	239	0.10	231	0.12	227
375	0.04	246	0.07	240	0.09	235	0.11	230
800	0.03	252	0.04	241	0.06	240	0.07	243
1200	0.01	248	0.02	243	0.04	236	0.04	238
1600	0.00	65	0.01	223	0.02	230	0.01	223
2000	0.02	92	0.01	85	0.02	145	0.02	75
2200	0.05	93	0.04	96	0.05	122	0.05	96
Freq.	477		894		743		383	

	0.40		0.50		0.60		
	0.50		0.60		0.70		
Depth	Int.	Dir.	Int.	Dir.	Int.	Dir.	
0	0.43	227	0.53	227	0.61	225	
50	0.44	227	0.54	227	0.62	221	
100	0.31	229	0.39	225	0.43	213	
150	0.25	231	0.33	224	0.36	211	
200	0.22	234	0.30	232	0.30	219	
250	0.21	233	0.25	227	0.26	220	
300	0.17	235	0.21	227	0.18	214	
350	0.15	238	0.19	233	0.18	224	
375	0.15	238	0.18	233	0.17	229	
800	0.09	240	0.09	219	0.04	135	
1200	0.05	238	0.07	233	0.08	221	
1600	0.02	204	0.04	183	0.06	163	
2000	0.02	120	0.04	107	0.09	98	
2200	0.04	96	0.06	120	0.08	166	
Freq.	186		90		20		**2793**
							11.18%

SOURCE: PETROBRAS Metocean Database (Engineering measurement program - mooring P1).

6.3.7 Current Profile (m/s) for Fatigue Analysis with W Direction at surface

	0.00		0.10		0.20		0.30		0.40	
	0.10		0.20		0.30		0.40		0.50	
Depth	Int.	Dir.	Int.	Dir.	Int.	Dir.	Int.	Dir.	Int.	Dir.
0	0.06	315	0.15	314	0.24	315	0.33	315	0.43	311
50	0.06	315	0.14	313	0.23	315	0.32	315	0.41	310
100	0.05	304	0.12	309	0.18	315	0.24	313	0.30	310
150	0.05	297	0.11	308	0.15	317	0.20	312	0.26	308
200	0.05	295	0.09	306	0.13	316	0.16	310	0.20	299
250	0.04	297	0.08	303	0.12	317	0.13	316	0.16	298
300	0.03	295	0.07	306	0.11	317	0.13	317	0.16	301
350	0.03	292	0.06	306	0.10	315	0.11	315	0.12	304
375	0.03	290	0.06	305	0.09	316	0.11	316	0.12	303
800	0.02	265	0.03	288	0.04	302	0.04	301	0.05	288
1200	0.01	253	0.02	295	0.03	316	0.03	341	0.03	334
1600	0.01	18	0.01	288	0.02	300	0.02	309	0.02	307
2000	0.01	70	0.00	139	0.01	231	0.00	177	0.01	251
2200	0.04	86	0.04	90	0.05	80	0.06	79	0.06	84
Freq.	540		1123		724		283		98	

	0.50		0.60		0.80		0.90		
	0.60		0.70		0.90		1.00		
Depth	Int.	Dir.	Int.	Dir.	Int.	Dir.	Int.	Dir.	
0	0.54	307	0.60	320	0.84	295	0.90	293	
50	0.52	307	0.57	318	0.85	295	0.92	294	
100	0.43	309	0.46	319	0.61	287	0.56	284	
150	0.39	307	0.32	322	0.49	288	0.50	291	
200	0.28	308	0.25	316	0.37	295	0.35	295	
250	0.24	302	0.18	318	0.33	288	0.33	280	
300	0.20	304	0.18	327	0.25	288	0.26	285	
350	0.18	305	0.11	318	0.28	294	0.21	311	
375	0.15	305	0.12	347	0.29	296	0.25	306	
800	0.04	309	0.05	343	0.16	296	0.15	314	
1200	0.03	330	0.09	6	0.07	236	0.06	264	
1600	0.02	337	0.07	23	0.08	233	0.06	270	
2000	0.02	28	0.05	26	0.07	210	0.07	234	
2200	0.05	80	0.07	43	0.06	179	0.01	159	
Freq.	34		4		3		1		**3035**
									12.15%

SOURCE: PETROBRAS Metocean Database (Engineering measurement program - mooring P1).

6.3.8 Current Profile (m/s) for Fatigue Analysis with NW Direction at surface

	0.00		0.10		0.20		0.30		0.40	
	0.10		0.20		0.30		0.40		0.50	
Depth	Int.	Dir.	Int.	Dir.	Int.	Dir.	Int.	Dir.	Int.	Dir.
0	0.06	270	0.15	271	0.24	270	0.33	270	0.43	272
50	0.06	271	0.15	271	0.24	270	0.34	269	0.43	271
100	0.07	268	0.13	271	0.19	267	0.27	266	0.36	270
150	0.06	266	0.11	271	0.15	263	0.22	262	0.27	269
200	0.06	273	0.09	269	0.13	265	0.18	263	0.22	267
250	0.06	272	0.08	265	0.11	267	0.15	264	0.18	271
300	0.05	262	0.07	266	0.10	268	0.13	262	0.16	266
350	0.04	260	0.07	265	0.09	267	0.12	265	0.14	265
375	0.04	261	0.06	267	0.08	268	0.11	264	0.13	264
800	0.02	257	0.04	267	0.05	265	0.07	267	0.07	273
1200	0.01	234	0.02	266	0.03	268	0.04	272	0.06	289
1600	0.00	353	0.01	267	0.02	252	0.02	261	0.02	232
2000	0.02	110	0.01	104	0.01	153	0.01	131	0.01	208
2200	0.04	97	0.04	100	0.04	102	0.04	95	0.03	97
Freq.	476		997		810		384		168	

	0.50		0.60		0.70		0.80		0.90		
	0.60		0.70		0.80		0.90		1.00		
Depth	Int.	Dir.	Int.	Dir.	Int.	Dir.	Int.	Dir.	Int.	Dir.	
0	0.52	273	0.64	274	0.74	274	0.82	273	0.92	271	
50	0.52	273	0.64	274	0.74	273	0.82	273	0.91	271	
100	0.43	272	0.59	273	0.66	273	0.69	271	0.72	269	
150	0.37	272	0.48	273	0.53	273	0.51	271	0.53	268	
200	0.29	272	0.37	275	0.43	273	0.41	269	0.39	266	
250	0.26	271	0.36	277	0.37	274	0.36	270	0.34	262	
300	0.23	271	0.31	269	0.33	272	0.32	274	0.30	265	
350	0.20	270	0.25	274	0.29	270	0.29	268	0.25	266	
375	0.18	273	0.24	274	0.26	268	0.26	269	0.23	268	
800	0.10	272	0.12	254	0.11	254	0.11	273	0.06	304	
1200	0.07	253	0.06	266	0.06	261	0.07	239	0.09	245	
1600	0.03	244	0.04	240	0.04	243	0.05	237	0.05	215	
2000	0.03	229	0.02	255	0.02	209	0.05	205	0.03	204	
2200	0.05	138	0.04	164	0.04	158	0.06	143	0.04	108	
Freq.	78		44		44		27		7		**2810**
											11.25%

SOURCE: PETROBRAS Metocean Database (Engineering measurement program - mooring P1).

6.3.9 Current Profile (m/s) for Fatigue Analysis with N Direction at 800m

	0.00		0.10		0.20		0.30		
	0.10		0.20		0.30		0.40		
Depth	Int.	Dir.	Int.	Dir.	Int.	Dir.	Int.	Dir.	
0	0.15	13	0.07	194	0.08	173	0.10	320	
50	0.16	16	0.06	194	0.08	172	0.08	330	
100	0.17	23	0.04	182	0.10	165	0.09	14	
150	0.16	23	0.05	194	0.09	166	0.08	339	
200	0.13	16	0.04	178	0.08	148	0.04	112	
250	0.10	356	0.03	177	0.03	152	0.09	336	
300	0.09	11	0.01	143	0.04	166	0.05	37	
350	0.08	17	0.03	93	0.03	160	0.15	37	
375	0.07	33	0.03	73	0.02	153	0.13	32	
800	0.06	360	0.15	360	0.22	2	0.31	354	
1200	0.13	62	0.08	64	0.02	63	0.19	88	
1600	0.06	67	0.06	46	0.06	87	0.11	28	
2000	0.06	92	0.10	78	0.13	83	0.09	42	
2200	0.10	87	0.11	86	0.08	93	0.19	83	
Freq.	10		35		68		4		**117**
									0.47%

6.3.10 Current Profile (m/s) for Fatigue Analysis with NE Direction at 800m

	0.00		0.10		0.20		0.30		
	0.10		0.20		0.30		0.40		
Depth	Int.	Dir.	Int.	Dir.	Int.	Dir.	Int.	Dir.	
0	0.04	193	0.09	240	0.04	240	0.08	194	
50	0.04	205	0.09	226	0.04	231	0.11	183	
100	0.09	215	0.10	197	0.08	206	0.05	153	
150	0.09	201	0.10	190	0.08	201	0.04	170	
200	0.08	221	0.10	176	0.07	184	0.04	215	
250	0.05	216	0.06	139	0.05	151	0.03	103	
300	0.02	204	0.03	144	0.05	161	0.07	221	
350	0.02	270	0.02	126	0.05	163	0.04	172	
375	0.01	252	0.01	98	0.04	163	0.04	103	
800	0.06	46	0.13	43	0.22	45	0.31	38	
1200	0.12	57	0.11	109	0.05	66	0.17	110	
1600	0.05	72	0.06	58	0.04	108	0.11	57	
2000	0.06	74	0.10	93	0.11	126	0.09	53	
2200	0.09	83	0.11	89	0.08	93	0.18	85	
Freq.	23		17		54		2		**96**
									0.38%

SOURCE: PETROBRAS Metocean Database (Engineering measurement program - mooring P1).

6.3.11 Current Profile (m/s) for Fatigue Analysis with E Direction at 800m

	0.00		0.10		0.20		0.30		
	0.10		0.20		0.30		0.40		
Depth	Int.	Dir.	Int.	Dir.	Int.	Dir.	Int.	Dir.	
0	0.12	267	0.10	190	0.07	146	0.22	217	
50	0.11	257	0.10	185	0.07	152	0.18	206	
100	0.09	238	0.11	176	0.09	179	0.18	228	
150	0.09	225	0.08	186	0.09	184	0.12	192	
200	0.08	222	0.11	185	0.07	198	0.08	149	
250	0.03	247	0.10	187	0.07	173	0.08	172	
300	0.06	321	0.11	169	0.08	172	0.15	206	
350	0.03	312	0.08	175	0.08	167	0.13	196	
375	0.03	309	0.09	167	0.09	166	0.13	193	
800	0.06	91	0.15	96	0.23	95	0.30	85	
1200	0.09	43	0.10	99	0.06	84	0.06	160	
1600	0.08	43	0.07	47	0.04	97	0.13	86	
2000	0.06	354	0.05	76	0.05	86	0.09	52	
2200	0.14	76	0.13	94	0.09	94	0.14	107	
Freq.	23		19		110		3		**155**
									0.62%

6.3.12 Current Profile (m/s) for Fatigue Analysis with SE Direction at 800m

	0.00		0.10		0.20		0.30		
	0.10		0.20		0.30		0.40		
Depth	Int.	Dir.	Int.	Dir.	Int.	Dir.	Int.	Dir.	
0	0.10	241	0.18	203	0.09	173	0.33	189	
50	0.13	230	0.18	205	0.09	173	0.31	191	
100	0.09	230	0.21	199	0.09	182	0.29	190	
150	0.10	217	0.18	210	0.10	192	0.27	187	
200	0.07	221	0.18	196	0.09	191	0.23	171	
250	0.03	219	0.14	188	0.08	193	0.23	165	
300	0.04	306	0.12	192	0.07	190	0.20	178	
350	0.01	200	0.11	195	0.06	192	0.14	182	
375	0.01	190	0.11	193	0.06	191	0.15	176	
800	0.05	132	0.17	130	0.23	133	0.31	123	
1200	0.05	20	0.07	82	0.06	71	0.05	111	
1600	0.05	70	0.08	94	0.03	136	0.06	125	
2000	0.05	42	0.09	92	0.05	155	0.09	114	
2200	0.11	82	0.15	93	0.08	98	0.11	99	
Freq.	23		24		344		5		**396**
									1.59%

SOURCE: PETROBRAS Metocean Database (Engineering measurement program - mooring P1).

6.3.13 Current Profile (m/s) for Fatigue Analysis with S Direction at 800m

	0.00		0.10		0.20		
	0.10		0.20		0.30		
Depth	Int.	Dir.	Int.	Dir.	Int.	Dir.	
0	0.08	210	0.08	193	0.05	335	
50	0.08	211	0.07	197	0.06	335	
100	0.05	193	0.08	187	0.06	345	
150	0.07	194	0.06	176	0.08	327	
200	0.04	185	0.05	219	0.07	314	
250	0.05	268	0.05	176	0.06	331	
300	0.03	219	0.04	192	0.05	316	
350	0.02	197	0.04	202	0.05	307	
375	0.03	251	0.05	206	0.05	307	
800	0.06	179	0.16	179	0.23	177	
1200	0.10	43	0.02	156	0.08	61	
1600	0.05	87	0.02	138	0.03	266	
2000	0.04	92	0.05	181	0.12	234	
2200	0.12	89	0.05	100	0.05	100	
Freq.	10		17		159		**186**
							0.74%

6.3.14 Current Profile (m/s) for Fatigue Analysis with SW Direction at 800m

	0.00		0.10		0.20		
	0.10		0.20		0.30		
Depth	Int.	Dir.	Int.	Dir.	Int.	Dir.	
0	0.11	174	0.16	187	0.07	256	
50	0.12	165	0.15	181	0.07	261	
100	0.10	183	0.13	192	0.05	275	
150	0.14	190	0.17	196	0.04	291	
200	0.10	194	0.16	212	0.04	310	
250	0.06	198	0.14	227	0.03	295	
300	0.04	176	0.11	225	0.03	303	
350	0.03	191	0.05	206	0.03	294	
375	0.04	192	0.04	224	0.03	297	
800	0.05	237	0.17	231	0.23	224	
1200	0.04	359	0.07	33	0.06	100	
1600	0.04	41	0.09	44	0.03	324	
2000	0.08	79	0.05	0	0.08	299	
2200	0.08	81	0.13	85	0.03	110	
Freq.	15		8		112		**135**
							0.54%

SOURCE: PETROBRAS Metocean Database (Engineering measurement program - mooring P1).

6.3.15 Current Profile (m/s) for Fatigue Analysis with W Direction at 800m

	0.00		0.10		0.20		0.30		
	0.10		0.20		0.30		0.40		
Depth	Int.	Dir.	Int.	Dir.	Int.	Dir.	Int.	Dir.	
0	0.04	206	0.15	237	0.08	248	0.22	220	
50	0.06	195	0.17	232	0.08	242	0.25	219	
100	0.10	180	0.15	236	0.07	232	0.29	226	
150	0.12	190	0.18	224	0.07	225	0.34	233	
200	0.08	186	0.16	225	0.06	221	0.34	219	
250	0.08	155	0.14	225	0.05	230	0.20	261	
300	0.05	131	0.12	238	0.02	254	0.25	258	
350	0.02	101	0.12	250	0.04	301	0.17	267	
375	0.02	103	0.11	259	0.04	289	0.19	257	
800	0.05	267	0.16	282	0.22	271	0.31	291	
1200	0.13	48	0.13	328	0.03	22	0.18	298	
1600	0.06	51	0.09	336	0.05	5	0.11	308	
2000	0.13	83	0.10	355	0.08	5	0.13	340	
2200	0.12	78	0.12	52	0.07	74	0.12	334	
Freq.	14		21		68		1		**104**
									0.42%

SOURCE: PETROBRAS Metocean Database (Engineering measurement program - mooring P1).

6.3.16 Current Profile (m/s) for Fatigue Analysis with NW Direction at 800m

	0.00		0.10		0.20		0.30		
	0.10		0.20		0.30		0.40		
Depth	Int.	Dir.	Int.	Dir.	Int.	Dir.	Int.	Dir.	
0	0.07	275	0.10	213	0.12	234	0.16	235	
50	0.06	273	0.09	220	0.12	237	0.17	236	
100	0.04	340	0.07	224	0.11	236	0.21	238	
150	0.04	329	0.09	218	0.12	228	0.16	250	
200	0.03	328	0.08	208	0.11	234	0.13	246	
250	0.04	265	0.06	222	0.10	246	0.16	254	
300	0.04	311	0.05	214	0.10	264	0.18	269	
350	0.06	7	0.01	286	0.09	283	0.18	280	
375	0.05	7	0.02	324	0.09	287	0.18	277	
800	0.07	313	0.15	312	0.23	313	0.31	312	
1200	0.07	23	0.10	42	0.09	340	0.18	314	
1600	0.03	54	0.06	16	0.07	5	0.09	349	
2000	0.05	86	0.06	36	0.10	28	0.10	27	
2200	0.11	90	0.13	77	0.12	65	0.13	49	
Freq.	16		59		120		18		**213**
									0.85%

SOURCE: PETROBRAS Metocean Database (Engineering measurement program - mooring P1).

B.7.2 Fatigue Response for Long Term Event

D-Curve; SCF 1.2

Fatigue VIV - D Curve							
Direction	Surface	Overall Freq	Midlevel	Overall Freq		Surface + Midlevel	Overall Freq
N	3116	12.48%	117	0.47%		3233	12.95%
NE	3134	12.55%	96	0.38%		3230	12.93%
E	2762	11.06%	155	0.62%		2917	11.68%
SE	2940	11.78%	396	1.59%		3336	13.37%
S	2982	11.94%	186	0.74%		3168	12.68%
SW	2793	11.18%	135	0.54%		2928	11.72%
W	2810	11.25%	104	0.42%		2914	11.67%
NW	3035	12.15%	213	0.85%		3248	13.00%
Total	23572	94.39%	1402	5.61%		24974	100%

N	Freq	Max Damage	Freq * Max Damage			
1	484	4.54E-13	6.79696E-14			
2	1122	1.32E-11	4.56921E-12			
3	943	2.94E-07	8.56692E-08			
4	359	2.10E-07	2.32712E-08			
5	151	2.16E-05	1.00927E-06			
6	56	6.71E-07	1.16301E-08			
7	1	1.28E-03	3.9601E-07			
8	10	1.36E-04	4.22147E-07			
9	35	2.23E-04	2.41817E-06			
10	68	1.52E-06	3.19303E-08			
11	4	1.97E-03	2.43291E-06		Freq (%)	N Fatigue Damage
	3233	OK!	**6.83101E-06**		12.95%	**8.84616E-07**

NE	Freq	Max Damage	Freq * Max Damage			
1	511	0	0			
2	988	7.17E-14	2.19342E-14			
3	802	6.15E-10	1.52636E-10			
4	528	1.71E-07	2.79301E-08			
5	247	1.06E-07	8.112E-09			
6	57	7.98E-07	1.40866E-08			
7	1	9.92E-05	3.07155E-08			
8	23	5.74E-06	4.08424E-08			
9	17	9.11E-06	4.79505E-08			
10	54	1.35E-05	2.26482E-07			
11	2	2.28E-03	1.41356E-06		Freq (%)	NE Fatigue Damage
	3230	OK!	**1.80983E-06**		12.93%	**2.34011E-07**

E	Freq	Max Damage	Freq * Max Damage			
1	494	0	0			
2	953	3.93E-16	1.28281E-16			
3	712	5.67E-08	1.3829E-08			
4	386	5.73E-08	7.58079E-09			
5	145	1.09E-07	5.44011E-09			
6	59	1.09E-07	2.21296E-09			
7	13	1.81E-07	8.05893E-10			
8	23	8.47E-05	6.67465E-07			
9	19	1.48E-04	9.63027E-07			
10	110	7.22E-05	2.72093E-06			
11	3	9.83E-04	1.01144E-06		Freq (%)	E Fatigue Damage
	2917	OK!	**5.39273E-06**		11.68%	**6.29871E-07**

SE	Freq	Max Damage	Freq * Max Damage			
1	485	2.43E-10	3.53675E-11			
2	1040	2.90E-08	9.05448E-09			
3	741	4.11E-08	9.12367E-09			
4	446	1.60E-07	2.13735E-08			
5	197	1.21E-09	7.12412E-11			
6	24	2.33E-07	1.67964E-09			
7	3	1.62E-06	1.46106E-09			
8	4	8.13E-05	9.74652E-08			
9	23	2.37E-05	1.63275E-07			
10	24	1.16E-03	8.3518E-06			
11	344	4.59E-05	4.73144E-06			
12	5	1.69E-03	2.52983E-06	Freq (%)		**SE Fatigue Damage**
	3336	OK!	**1.59166E-05**	13.37%		**2.12805E-06**

S	Freq	Max Damage	Freq * Max Damage			
1	501	3.06E-10	4.84094E-11			
2	972	3.02E-09	9.27113E-10			
3	762	4.85E-07	1.16621E-07			
4	378	1.39E-05	1.6547E-06			
5	126	2.27E-05	9.01051E-07			
6	85	9.93E-05	2.66486E-06			
7	38	4.96E-04	5.94842E-06			
8	40	1.04E-04	1.31073E-06			
9	24	3.99E-04	3.01932E-06			
10	38	4.41E-04	5.28965E-06			
11	15	5.32E-04	2.51851E-06			
12	3	8.83E-04	8.36278E-07			
13	10	5.87E-06	1.85275E-08			
14	17	2.11E-06	1.13205E-08			
15	159	1.21E-05	6.095E-07	Freq (%)		**S Fatigue Damage**
	3168	OK!	**2.49005E-05**	12.68%		**3.15738E-06**

SW	Freq	Max Damage	Freq * Max Damage			
1	477	7.25E-12	1.18E-12			
2	894	2.64E-09	8.07E-10			
3	743	1.48E-06	3.76E-07			
4	383	4.55E-06	5.95E-07			
5	186	1.23E-05	7.80E-07			
6	90	9.22E-05	2.83E-06			
7	20	1.03E-05	7.02E-08			
8	15	1.31E-05	6.70E-08			
9	8	9.78E-06	2.67E-08			
10	112	3.84E-05	1.47E-06	Freq (%)		**SW Fatigue Damage**
	2928	OK!	**6.21694E-06**	11.72%		**7.28626E-07**

W	Freq	Max Damage	Freq * Max Damage			
1	540	3.23E-14	5.98E-15			
2	1123	3.63E-10	1.40E-10			
3	724	2.94E-08	7.30E-09			
4	283	1.51E-07	1.46E-08			
5	98	1.45E-07	4.87E-09			
6	34	2.97E-07	3.47E-09			
7	4	2.23E-05	3.06E-08			
8	3	1.21E-03	1.24E-06			
9	1	1.43E-03	4.89E-07			
10	14	6.20E-04	2.98E-06			
11	21	1.39E-03	1.00E-05			
12	68	1.19E-05	2.78E-07			
13	1	3.03E-03	1.04E-06	Freq (%)		**W Fatigue Damage**
	2914	OK!	**1.60938E-05**	11.67%		**1.87814E-06**

NW	Freq	Max Damage	Freq * Max Damage					
1	476	1.33E-13	1.94E-14					
2	997	1.55E-09	4.76E-10					
3	810	7.86E-08	1.96E-08					
4	384	5.53E-06	6.54E-07					
5	168	1.16E-05	6.00E-07					
6	78	3.01E-05	7.22E-07					
7	44	9.01E-06	1.22E-07					
8	44	1.09E-04	1.48E-06					
9	27	1.34E-04	1.12E-06					
10	7	9.43E-06	2.03E-08					
11	16	1.28E-05	6.31E-08					
12	59	2.03E-05	3.69E-07					
13	120	1.44E-04	5.34E-06					
14	18	3.59E-03	1.99E-05		Freq (%)		**NW Fatigue Damage**	
	3248	OK!	**3.03887E-05**		13.00%		**3.95053E-06**	
					100.00%			
						D_{VIV} =	**1.35912E-05**	
						Total exposure time =	24974	hours
							2.85	years
						Fatigue Life =	**73,576.9**	**years**

F1-Curve; SCF 1.2

Fatigue VIV - F1 Curve							
Direction	Surface	Overall Freq	Midlevel	Overall Freq		Surface + Midlevel	Overall Freq
N	3116	12.48%	117	0.47%		3233	12.95%
NE	3134	12.55%	96	0.38%		3230	12.93%
E	2762	11.06%	155	0.62%		2917	11.68%
SE	2940	11.78%	396	1.59%		3336	13.37%
S	2982	11.94%	186	0.74%		3168	12.68%
SW	2793	11.18%	135	0.54%		2928	11.72%
W	2810	11.25%	104	0.42%		2914	11.67%
NW	3035	12.15%	213	0.85%		3248	13.00%
Total	23572	94.39%	1402	5.61%		24974	100%

N	Freq	Max Damage	Freq * Max Damage			
1	484	2.70E-12	4.04865E-13			
2	1122	7.84E-11	2.72174E-11			
3	943	1.75E-06	5.10293E-07			
4	359	1.25E-06	1.38614E-07			
5	151	1.29E-04	6.01198E-06			
6	56	4.00E-06	6.92751E-08			
7	1	7.63E-03	2.35895E-06			
8	10	8.13E-04	2.51457E-06			
9	35	1.33E-03	1.44038E-05			
10	68	9.04E-06	1.90198E-07			
11	4	1.17E-02	1.44918E-05		Freq (%)	N Fatigue Damage
	3233		**4.06895E-05**		12.95%	**5.26929E-06**

NE	Freq	Max Damage	Freq * Max Damage			
1	511	0	0			
2	988	4.27E-13	1.30655E-13			
3	802	3.66E-09	9.0919E-10			
4	528	1.02E-06	1.66361E-07			
5	247	6.32E-07	4.83218E-08			
6	57	4.75E-06	8.39082E-08			
7	1	5.91E-04	1.82963E-07			
8	23	3.42E-05	2.4328E-07			
9	17	5.43E-05	2.85626E-07			
10	54	8.07E-05	1.34903E-06			
11	2	1.36E-02	8.41981E-06		Freq (%)	NE Fatigue Damage
	3230		**1.07802E-05**		12.93%	**1.39388E-06**

E	Freq	Max Damage	Freq * Max Damage			
1	494	0	0			
2	953	2.34E-15	7.64132E-16			
3	712	3.37E-07	8.23743E-08			
4	386	3.41E-07	4.51555E-08			
5	145	6.52E-07	3.2405E-08			
6	59	6.52E-07	1.31813E-08			
7	13	1.08E-06	4.80024E-09			
8	23	5.04E-04	3.97584E-06			
9	19	8.81E-04	5.73641E-06			
10	110	4.30E-04	1.62077E-05			
11	3	5.86E-03	6.02479E-06		Freq (%)	E Fatigue Damage
	2917		**3.21227E-05**		11.68%	**3.75193E-06**

SW	Freq	Max Damage	Freq * Max Damage			
1	477	4.32E-11	7.03E-12			
2	894	1.57E-08	4.81E-09			
3	743	8.83E-06	2.24E-06			
4	383	2.71E-05	3.54E-06			
5	186	7.31E-05	4.64E-06			
6	90	5.49E-04	1.69E-05			
7	20	6.12E-05	4.18E-07			
8	15	7.79E-05	3.99E-07			
9	8	5.82E-05	1.59E-07			
10	112	2.29E-04	8.75E-06	Freq (%)		**SW Fatigue Damage**
	2928		**3.70319E-05**	11.72%		**4.34014E-06**

W	Freq	Max Damage	Freq * Max Damage			
1	540	1.92E-13	3.56E-14			
2	1123	2.16E-09	8.32E-10			
3	724	1.75E-07	4.35E-08			
4	283	8.98E-07	8.72E-08			
5	98	8.62E-07	2.90E-08			
6	34	1.77E-06	2.07E-08			
7	4	1.33E-04	1.82E-07			
8	3	7.20E-03	7.41E-06			
9	1	8.49E-03	2.91E-06			
10	14	3.69E-03	1.77E-05			
11	21	8.27E-03	5.96E-05			
12	68	7.10E-05	1.66E-06			
13	1	1.80E-02	6.19E-06	Freq (%)		**W Fatigue Damage**
	2914		**9.5865E-05**	11.67%		**1.11874E-05**

NW	Freq	Max Damage	Freq * Max Damage				
1	476	7.89E-13	1.16E-13				
2	997	9.23E-09	2.83E-09				
3	810	4.68E-07	1.17E-07				
4	384	3.30E-05	3.90E-06				
5	168	6.91E-05	3.58E-06				
6	78	1.79E-04	4.30E-06				
7	44	5.37E-05	7.27E-07				
8	44	6.49E-04	8.80E-06				
9	27	8.01E-04	6.66E-06				
10	7	5.62E-05	1.21E-07				
11	16	7.63E-05	3.76E-07				
12	59	1.21E-04	2.20E-06				
13	120	8.60E-04	3.18E-05				
14	18	2.14E-02	1.18E-04	Freq (%)		**NW Fatigue Damage**	
	3248		**0.000181015**	13.00%		**2.3532E-05**	
				100.00%			
					D_{VIV} =	**8.09577E-05**	
					Total exposure time =	24974	hours
						2.85	years
					Fatigue Life =	**12,352.1**	**years**

B.7.3 Fatigue Data for Short Term Event

Current Profiles

Level	1 year (m/s)	10 year (m/s)	100 year (m/s)
0	0.76	0.92	1.05
-50	0.74	0.9	1.03
-100	0.61	0.77	0.89
-150	0.61	0.77	0.89
-200	0.61	0.76	0.89
-250	0.54	0.69	0.81
-300	0.47	0.62	0.73
-350	0.41	0.55	0.65
-375	0.35	0.48	0.59
-800	0.26	0.36	0.43
-1200	0.21	0.27	0.32
-1600	0.2	0.25	0.29
-2000	0.25	0.29	0.32
-2200	0.21	0.24	0.27

B.7.4 Fatigue Response for Short Term Event

D-Curve; SCF 1.2

VIV - Fatigue Damage (Short Term - D curve)				
1 year current				
Cross Flow - 90 deg			**Cross Flow - 180 deg**	
Maximum fatigue damage.			Maximum fatigue damage.	
----------			----------	
Element no.	76		Element no.	81
End no.	1		End no.	2
Point no. ..	12		Point no. ..	8
.....			.....	
Accumulated damage	**0.0308**		Accumulated damage	**0.0406**
Corresponding fatigue life (years)	**32.5**		Corresponding fatigue life (years)	**24.6**
10 year current				
Cross Flow - 90 deg			**Cross Flow - 180 deg**	
Maximum fatigue damage.			Maximum fatigue damage.	
----------			----------	
Element no.	76		Element no.	84
End no.	1		End no.	2
Point no. ..	12		Point no. ..	8
.....			.....	
Accumulated damage	**0.0826**		Accumulated damage	**0.0202**
Corresponding fatigue life (years)	**12.1**		Corresponding fatigue life (years)	**49.5**
100 year current				
Cross Flow - 90 deg			**Cross Flow - 180 deg**	
Maximum fatigue damage.			Maximum fatigue damage.	
----------			----------	
Element no.	76		Element no.	87
End no.	1		End no.	2
Point no. ..	12		Point no. ..	8
.....			.....	
Accumulated damage	**0.0331**		Accumulated damage	**0.0197**
Corresponding fatigue life (years)	**30.2**		Corresponding fatigue life (years)	**50.8**
D_{VIV} = D1 x 2 x 24hr/25yr + D2 x 2 x 12hr/25yr + D3 x 6hr/25yr				
25 year	227136	hour		
D_{VIV} 1 year	1.50915E-05		(2 x 24 hour)	
D_{VIV} 10 year	1.08646E-05		(2 x 12 hour)	
D_{VIV} 100 year	1.39331E-06		(6 hour)	
total	2.73495E-05			
Fatigue life (short term)	36564			

F1-Curve; SCF 1.2

VIV - Fatigue Damage (Short Term - F1 Curve)				
1 year current				
Cross Flow - 90 deg			**Cross Flow - 180 deg**	
Maximum fatigue damage.			Maximum fatigue damage.	
----------			----------	
Element no.	76		Element no.	81
End no.	1		End no.	2
Point no. ..	12		Point no. ..	8
.....			.....	
Accumulated damage	**0.1834**		Accumulated damage	**0.2137**
Corresponding fatigue life (years)	**5.5**		Corresponding fatigue life (years)	**4.7**
10 year current				
Cross Flow - 90 deg			**Cross Flow - 180 deg**	
Maximum fatigue damage.			Maximum fatigue damage.	
----------			----------	
Element no.	76		Element no.	84
End no.	1		End no.	2
Point no. ..	12		Point no. ..	8
.....			.....	
Accumulated damage	**0.4038**		Accumulated damage	**0.1192**
Corresponding fatigue life (years)	**2.5**		Corresponding fatigue life (years)	**8.4**
100 year current				
Cross Flow - 90 deg			**Cross Flow - 180 deg**	
Maximum fatigue damage.			Maximum fatigue damage.	
----------			----------	
Element no.	76		Element no.	87
End no.	1		End no.	2
Point no. ..	12		Point no. ..	8
.....			.....	
Accumulated damage	**0.1970**		Accumulated damage	**0.1172**
Corresponding fatigue life (years)	**5.1**		Corresponding fatigue life (years)	**8.5**
D_{VIV} = D1 x 2 x 24hr/25yr + D2 x 2 x 12hr/25yr + D3 x 6hr/25yr				
25 year	227136	hour		
D_{VIV} 1 year	8.39074E-05		(2 x 24 hour)	
D_{VIV} 10 year	5.52673E-05		(2 x 12 hour)	
D_{VIV} 100 year	8.29961E-06		(6 hour)	
total	0.000147474			
Fatigue life (short term)	6781			

Appendix C – Sensitivity Study Result

C.1 Case 1 – Deeper Sub-surface Buoyancy

C.1.1 Static Response (ULS)

Flexible Jumper

100 year current - surface profile	Unidirectional current			Bidirectional current		
	Vessel Position			Vessel Position		
	Near	Nominal	Far	Near	Nominal	Far
Static angle at vessel (deg)	6.6	8.5	5.0	3.6	5.8	8.2
Static angle at buoy (deg)	15.9	23.6	26.8	12.3	24.1	32.5
Static tension at vessel (kN)	1433	1440	1440	1422	1442	1456
Static tension at buoy (kN)	373	392	410	380	391	415
Minimum Bending Radius (m)	39	45	66	27	44	82

Table C.1 – Jumper Static Result (Case 1 – ULS)

Riser

100 year current - surface profile	Unidirectional current			Bidirectional current		
	Vessel Position			Vessel Position		
	Near	Nominal	Far	Near	Nominal	Far
Static top angle (deg)	7.2	8.6	9.5	6.9	8.7	10.3
Static top tension (kN)	1975	2116	2152	2086	2114	2047
Static TDP tension (kN)	212	346	379	318	344	278

Table C.2 – Riser Static Result (Case 1 – ULS)

Mooring Line

100 year current - surface profile	Unidirectional current			Bidirectional current		
	Vessel Position			Vessel Position		
	Near	Nominal	Far	Near	Nominal	Far
Static tension (kN)	744	730	651	680	729	714

Table C.3 – Mooring Lines Static Result (Case 1 – ULS)

C.1.2 Dynamic Response (ULS)

Flexible Jumper

100 year current - surface profile + 10 year wave	Unidirectional current Vessel Position			Bidirectional current Vessel Position		
	Near	Nominal	Far	Near	Nominal	Far
Minimum radius (m)	33	52	65	27	57	77
Hmin (m)	100	87	86	113	87	73
Minimum tension (kN)	88	134	147	66	119	173
Maximum tension at Vessel (kN)	1598	1746	1785	1591	1756	1795
Maximum tension at Buoy (kN)	385	428	463	394	423	469
Minimum angle at Vessel (deg)	5.3	6.9	0.0	2.4	3.9	2.7
Maximum angle at Vessel (deg)	9.1	11.2	7.2	6.0	8.3	10.6
Minimum angle at Buoy (deg)	14.3	21.8	26.5	12.2	22.1	30.1
Maximum angle at Buoy (deg)	16.0	23.7	29.0	13.2	24.4	33.4

Table C.4 – Jumper Dynamic Result (Case 1 – ULS)

Riser

100 year current - surface profile + 10 year wave	Unidirectional current Vessel Position			Bidirectional current Vessel Position		
	Near	Nominal	Far	Near	Nominal	Far
Top Tension (kN)	1990	2157	2199	2102	2139	2096
TDP Tension (kN)	215	357	394	322	351	288
von Mises Stress - Top (MPa)	160	160	179	154	154	175
von Mises Stress - Below Stress Joint (MPa)	233	233	244	230	230	242
von Mises Stress - TDP (MPa)	251	253	254	253	253	252
Maximum Buckling Utilization - Top	0.37	0.37	0.37	0.37	0.37	0.37
Maximum Buckling Utilization - Below Stress Joint	0.67	0.67	0.67	0.67	0.67	0.67
Maximum Buckling Utilization - TDP	0.78	0.78	0.78	0.78	0.78	0.78

Table C.5 – Riser Dynamic Result (Case 1 – ULS)

Mooring Line

100 year current - surface profile + 10 year wave	Unidirectional current Vessel Position			Bidirectional current Vessel Position		
	Near	Nominal	Far	Near	Nominal	Far
Minimum tension (kN)	723	618	596	659	638	656
Maximum tension (kN)	765	756	703	697	770	773

Table C.6 – Mooring Lines Dynamic Result (Case 1 – ULS)

C.1.3 Static Response (ALS)

Flexible Jumper

100 year current - surface profile	Unidirectional current			Bidirectional current		
	Vessel Position			Vessel Position		
	Near	Nominal	Far	Near	Nominal	Far
Static angle at vessel (deg)	6.5	8.4	5.3	3.8	5.7	8.1
Static angle at buoy (deg)	15.4	22.9	27.3	12.8	23.4	31.6
Static tension at vessel (kN)	1427	1434	1437	1419	1435	1450
Static tension at buoy (kN)	379	397	415	384	396	419
Minimum Bending Radius (m)	38	47	68	29	46	80

Table C.7 – Jumper Static Result (Case 1 – ALS)

Riser

100 year current - surface profile	Unidirectional current			Bidirectional current		
	Vessel Position			Vessel Position		
	Near	Nominal	Far	Near	Nominal	Far
Static top angle (deg)	9.2	10.3	10.9	8.6	10.4	11.7
Static top tension (kN)	1983	2114	2149	2084	2112	2054
Static TDP tension (kN)	217	342	376	314	340	283

Table C.8 –Riser Static Result (Case 1 – ALS)

Mooring Line

100 year current - surface profile	Unidirectional current			Bidirectional current		
	Vessel Position			Vessel Position		
	Near	Nominal	Far	Near	Nominal	Far
Static tension (kN)	1475	1447	1298	1355	1444	1415

Table C.9 – Mooring Line Static Result (Case 1 – ALS)

C.1.4 Dynamic Response (ALS)

Flexible Jumper

100 year current - surface profile + 10 year wave	Unidirectional current Vessel Position			Bidirectional current Vessel Position		
	Near	Nominal	Far	Near	Nominal	Far
Minimum radius (m)	33	51	66	28	56	76
Hmin (m)	102	89	86	113	89	76
Minimum tension (kN)	87	133	154	70	120	174
Maximum tension at Vessel (kN)	1591	1740	1779	1587	1746	1784
Maximum tension at Buoy (kN)	391	428	463	399	422	464
Minimum angle at Vessel (deg)	5.3	6.8	0.0	2.6	4.1	2.6
Maximum angle at Vessel (deg)	9.0	11.2	7.5	6.2	8.4	10.5
Minimum angle at Buoy (deg)	13.9	21.1	27.0	12.8	21.5	29.4
Maximum angle at Buoy (deg)	15.5	23.0	29.5	13.7	23.7	32.6

Table C.10 – Jumper Dynamic Result (Case 1 – ALS)

Riser

100 year current - surface profile + 10 year wave	Unidirectional current Vessel Position			Bidirectional current Vessel Position		
	Near	Nominal	Far	Near	Nominal	Far
Top Tension (kN)	2006	2187	2241	2111	2152	2145
Sagbend Tension (kN)	222	369	413	322	353	308
von Mises Stress - Top (MPa)	170	202	247	178	196	238
von Mises Stress - Below Stress Joint (MPa)	239	256	268	243	253	266
von Mises Stress - Sagbend (MPa)	251	254	255	253	253	253
Maximum Buckling Utilization - Top	0.37	0.37	0.37	0.37	0.37	0.37
Maximum Buckling Utilization - Below Stress Joint	0.67	0.67	0.67	0.67	0.67	0.67
Maximum Buckling Utilization - Sagbend	0.78	0.78	0.78	0.78	0.78	0.78

Table C.11 – Riser Dynamic Result (Case 1 – ALS)

Mooring Line

100 year current - surface profile + 10 year wave	Unidirectional current Vessel Position			Bidirectional current Vessel Position		
	Near	Nominal	Far	Near	Nominal	Far
Minimum tension (kN)	1427	1218	1165	1303	1258	1274
Maximum tension (kN)	1525	1518	1418	1403	1570	1566

Table C.12 – Mooring Line Dynamic Result (Case 1 – ALS)

C.2 Case 2 – Jumper Connection to Sub-surface Buoy

C.2.1 Static Response (ULS)

Flexible Jumper

100 year current - surface profile	Unidirectional current Vessel Position			Bidirectional current Vessel Position		
	Near	Nominal	Far	Near	Nominal	Far
Static angle at vessel (deg)	12.2	15.6	11.6	7.8	12.5	16.6
Static angle at buoy (deg)	27.3	36.2	35.6	19.0	36.7	45.7
Static tension at vessel (kN)	1121	1141	1130	1093	1146	1181
Static tension at buoy (kN)	413	448	466	410	454	504
Minimum Bending Radius (m)	70	70	97	46	68	131

Table C.13 – Jumper Static Result (Case 2 – ULS)

Riser

100 year current - surface profile	Unidirectional current Vessel Position			Bidirectional current Vessel Position		
	Near	Nominal	Far	Near	Nominal	Far
Static top angle (deg)	4.9	5.4	5.8	5.1	5.4	5.6
Static top tension (kN)	2165	2351	2403	2307	2347	2275
Static TDP tension (kN)	270	444	494	401	440	374

Table C.14 – Riser Static Result (Case 2 – ULS)

Mooring Line

100 year current - surface profile	Unidirectional current Vessel Position			Bidirectional current Vessel Position		
	Near	Nominal	Far	Near	Nominal	Far
Static tension (kN)	579	559	454	493	557	535

Table C.15 – Mooring Lines Static Result (Case 2 – ULS)

C.2.2 Dynamic Response (ULS)

Flexible Jumper

100 year current - surface profile + 10 year wave	Unidirectional current Vessel Position			Bidirectional current Vessel Position		
	Near	Nominal	Far	Near	Nominal	Far
Minimum radius (m)	63	88	91	43	93	120
Hmin (m)	83.1	68.9	75.5	105.5	69.3	55.7
Minimum tension (kN)	164	228	218	112	204	282
Maximum tension at Vessel (kN)	1238	1336	1384	1214	1369	1428
Maximum tension at Buoy (kN)	432	484	544	430	510	601
Minimum angle at Vessel (deg)	10.7	13.5	4.8	6.4	9.0	10.0
Maximum angle at Vessel (deg)	15.2	18.8	14.1	10.8	15.3	19.3
Minimum angle at Buoy (deg)	26.2	34.9	35.1	18.8	34.1	42.7
Maximum angle at Buoy (deg)	27.5	36.7	38.3	19.5	37.8	47.7

Table C.16 – Jumper Dynamic Result (Case 2 – ULS)

Riser

100 year current - surface profile + 10 year wave	Unidirectional current Vessel Position			Bidirectional current Vessel Position		
	Near	Nominal	Far	Near	Nominal	Far
Top Tension (kN)	2193	2419	2487	2334	2379	2362
TDP Tension (kN)	262	426	467	393	431	342
von Mises Stress - Top (MPa)	314	362	362	261	368	437
von Mises Stress - Below Stress Joint (MPa)	294	310	310	280	311	332
von Mises Stress - TDP (MPa)	261	265	266	264	264	264
Maximum Buckling Utilization - Top	0.56	0.76	0.72	0.37	0.78	1.10
Maximum Buckling Utilization - Below Stress Joint	0.67	0.67	0.67	0.67	0.67	0.67
Maximum Buckling Utilization - TDP	0.78	0.78	0.78	0.78	0.78	0.78

Table C.17– Riser Dynamic Result (Case 2 – ULS)

Mooring Line

100 year current - surface profile + 10 year wave	Unidirectional current Vessel Position			Bidirectional current Vessel Position		
	Near	Nominal	Far	Near	Nominal	Far
Minimum tension (kN)	614	477	444	530	511	515
Maximum tension (kN)	680	663	593	591	692	681

Table C.18 – Mooring Lines Dynamic Result (Case 2 – ULS)

C.2.3 Static Response (ALS)

Flexible Jumper

100 year current - surface profile	Unidirectional current			Bidirectional current		
	Vessel Position			Vessel Position		
	Near	Nominal	Far	Near	Nominal	Far
Static angle at vessel (deg)	12.1	15.4	12.1	8.2	12.3	16.3
Static angle at buoy (deg)	26.4	35.1	36.3	19.8	35.6	44.5
Static tension at vessel (kN)	1114	1133	1130	1091	1138	1172
Static tension at buoy (kN)	417	450	473	414	456	504
Minimum Bending Radius (m)	69	73	100	48	70	129

Table C.19 – Jumper Static Results (Case 2 – ALS)

Riser

100 year current - surface profile	Unidirectional current			Bidirectional current		
	Vessel Position			Vessel Position		
	Near	Nominal	Far	Near	Nominal	Far
Static top angle (deg)	6.1	6.2	6.4	6.0	6.2	6.4
Static top tension (kN)	2176	2350	2402	2305	2345	2284
Static TDP tension (kN)	275	439	490	395	435	380

Table C.20 – Riser Static Result (Case 2 – ALS)

Mooring Line

100 year current - surface profile	Unidirectional current			Bidirectional current		
	Vessel Position			Vessel Position		
	Near	Nominal	Far	Near	Nominal	Far
Static tension (kN)	1280	1240	1042	1126	1233	1189

Table C.21 – Mooring Line Static Result (Case 2 – ALS)

C.2.4 Dynamic Response (ALS)

Flexible Jumper

100 year current - surface profile + 10 year wave	Unidirectional current Vessel Position			Bidirectional current Vessel Position		
	Near	Nominal	Far	Near	Nominal	Far
Minimum radius (m)	61	85	92	45	91	118
Hmin (m)	86	72	75	105	72	58
Minimum tension (kN)	162	226	229	119	209	285
Maximum tension at Vessel (kN)	1229	1331	1380	1211	1355	1411
Maximum tension at Buoy (kN)	434	482	540	435	500	584
Minimum angle at Vessel (deg)	10.5	13.4	5.2	6.7	9.4	9.7
Maximum angle at Vessel (deg)	15.1	18.6	14.6	11.2	15.2	19.1
Minimum angle at Buoy (deg)	25.4	34.0	35.7	19.6	33.2	41.6
Maximum angle at Buoy (deg)	26.5	35.6	38.9	20.3	36.7	46.7

Table C.22 – Jumper Dynamic Result (Case 2 – ALS)

Riser

100 year current - surface profile + 10 year wave	Unidirectional current Vessel Position			Bidirectional current Vessel Position		
	Near	Nominal	Far	Near	Nominal	Far
Top Tension (kN)	2225	2435	2524	2368	2408	2426
TDP Tension (kN)	261	417	458	379	417	329
von Mises Stress - Top (MPa)	278	347	347	212	351	435
von Mises Stress - Below Stress Joint (MPa)	284	305	305	267	306	332
von Mises Stress - TDP (MPa)	261	265	267	264	265	265
Maximum Buckling Utilization - Top	0.42	0.68	0.65	0.37	0.70	1.08
Maximum Buckling Utilization - Below Stress Joint	0.67	0.67	0.67	0.67	0.67	0.67
Maximum Buckling Utilization - TDP	0.78	0.78	0.78	0.78	0.78	0.78

Table C.23 – Riser Dynamic Result (Case 2 – ALS)

Mooring Line

100 year current - surface profile + 10 year wave	Unidirectional current Vessel Position			Bidirectional current Vessel Position		
	Near	Nominal	Far	Near	Nominal	Far
Minimum tension (kN)	1197	977	915	1031	995	1028
Maximum tension (kN)	1364	1322	1155	1207	1372	1359

Table C.24 – Mooring Line Dynamic Result (Case 2 – ALS)

C.3 Case 3 – Assessment on Lateral Displacement

Base Case (Distance between mooring anchor = 3 m)	Surface Profile Current		Mid-level Profile Current	
	10 yr	100 yr	10 yr	100 yr
Buoy Lateral Displacement (m)	60.7	84.9	62.8	83.6
Maximum Riser Lateral Displacement (m)	63.4	88.8	74.1	98.7

Table C.25 – Base Case Result

Case 3 (Distance between mooring anchor = 46 m)	Surface Profile Current		Mid-level Profile Current	
	10 yr	100 yr	10 yr	100 yr
Buoy Lateral Displacement (m)	59.0	82.7	61.2	81.6
Maximum Riser Lateral Displacement (m)	61.9	86.8	72.8	97.1

Case 4 (Distance between mooring anchor = 89.4 m)	Surface Profile Current		Mid-level Profile Current	
	10 yr	100 yr	10 yr	100 yr
Buoy Lateral Displacement (m)	54.8	77.2	57.1	76.8
Maximum Riser Lateral Displacement (m)	58.0	81.9	69.5	93.2

Case 5 (Distance between mooring anchor = 134.2 m)	Surface Profile Current		Mid-level Profile Current	
	10 yr	100 yr	10 yr	100 yr
Buoy Lateral Displacement (m)	48.9	70.0	51.4	70.4
Maximum Riser Lateral Displacement (m)	52.7	75.4	65.0	88.0

Table C.26 – Sensitivity Study Result

C.4 Buckling Utilization Ratio

C.4.1 Case 1 (ULS)

Case 1 - ULS

	TOP					BELOW STRESS JOINT					SAGBEND				
	Functional		Environmental		Max Buckling Ratio	Functional		Environmental		Max Buckling Ratio	Functional		Environmental		Max Buckling Ratio
	Moment	Axial	Moment	Axial		Moment	Axial	Moment	Axial		Moment	Axial	Moment	Axial	
	kN-m	kN	kN-m	kN		kN-m	kN	kN-m	kN		kN-m	kN	kN-m	kN	
LC117	178	1975	84	15	0.372	52	1952	23	15	0.666	201	212	3	3	0.782
LC118	5	2006	118	27	0.372	5	1984	32	27	0.666	180	240	4	5	0.782
LC119	64	2116	167	41	0.372	10	2094	43	41	0.666	129	346	3	12	0.782
LC120	230	2152	242	47	0.372	52	2129	61	47	0.666	118	379	5	15	0.782
LC121	94	2086	54	16	0.372	31	2063	14	16	0.666	140	318	2	4	0.782
LC122	51	2114	91	24	0.372	7	2092	24	24	0.666	130	344	2	7	0.782
LC123	11	2009	155	42	0.372	1	1986	48	42	0.666	179	242	6	8	0.782
LC124	200	2047	238	48	0.372	48	2025	62	49	0.666	158	278	8	10	0.782

C.4.2 Case 1 (ALS)

Case 1 - ALS

	TOP					BELOW STRESS JOINT					SAGBEND				
	Functional		Environmental		Max Buckling Ratio	Functional		Environmental		Max Buckling Ratio	Functional		Environmental		Max Buckling Ratio
	Moment	Axial	Moment	Axial		Moment	Axial	Moment	Axial		Moment	Axial	Moment	Axial	
	kN-m	kN	kN-m	kN		kN-m	kN	kN-m	kN		kN-m	kN	kN-m	kN	
LCA117	373	1983	18	23	0.372	98	1961	4	22	0.666	197	217	4	4	0.782
LCA118	563	2014	27	36	0.372	148	1992	6	36	0.666	177	245	7	7	0.782
LCA119	606	2114	78	73	0.372	153	2093	18	73	0.666	130	342	7	27	0.782
LCA120	754	2149	130	92	0.372	189	2128	31	92	0.666	119	376	9	37	0.782
LCA121	434	2084	38	27	0.372	109	2062	9	27	0.666	141	314	2	8	0.782
LCA122	595	2112	49	41	0.372	150	2090	11	41	0.666	131	340	4	13	0.782
LCA123	578	2016	50	74	0.372	152	1995	10	74	0.666	176	247	15	17	0.782
LCA124	739	2054	112	91	0.372	193	2033	26	91	0.666	155	283	18	25	0.782

C.4.3 Case 2 (ULS)

Case 2 - ULS

	TOP					BELOW STRESS JOINT					SAGBEND				
	Functional		Environmental		Max Buckling Ratio	Functional		Environmental		Max Buckling Ratio	Functional		Environmental		Max Buckling Ratio
	Moment	Axial	Moment	Axial		Moment	Axial	Moment	Axial		Moment	Axial	Moment	Axial	
	kN-m	kN	kN-m	kN		kN-m	kN	kN-m	kN		kN-m	kN	kN-m	kN	
LC217	1170	2165	12	28	0.555	304	2148	6	27	0.666	162	270	4	5	0.782
LC218	1364	2212	30	36	0.756	349	2197	11	36	0.666	141	314	4	8	0.782
LC219	1072	2351	99	67	0.515	270	2333	29	67	0.666	102	444	4	23	0.782
LC220	1286	2403	97	84	0.719	318	2387	31	84	0.666	91	494	5	36	0.782
LC221	895	2307	45	27	0.372	229	2287	13	27	0.666	112	401	2	8	0.782
LC222	1059	2347	50	32	0.481	267	2329	14	32	0.666	102	440	2	11	0.782
LC223	1377	2217	42	76	0.777	352	2201	16	75	0.666	140	318	10	17	0.782
LC224	1625	2275	91	86	1.102	409	2263	22	87	0.666	120	374	10	25	0.782

C.4.4 Case 2 (ALS)

Case 2 - ALS

	TOP					BELOW STRESS JOINT					SAGBEND				
	Functional		Environmental		Max Buckling Ratio	Functional		Environmental		Max Buckling Ratio	Functional		Environmental		Max Buckling Ratio
	Moment	Axial	Moment	Axial		Moment	Axial	Moment	Axial		Moment	Axial	Moment	Axial	
	kN-m	kN	kN-m	kN		kN-m	kN	kN-m	kN		kN-m	kN	kN-m	kN	
LCA217	1000	2176	24	49	0.417	259	2157	8	48	0.666	159	275	8	10	0.782
LCA218	1279	2223	50	51	0.680	327	2206	15	50	0.666	139	319	7	12	0.782
LCA219	949	2350	57	85	0.396	239	2330	17	85	0.666	103	439	6	32	0.782
LCA220	1217	2402	98	122	0.651	301	2385	27	122	0.666	92	490	8	51	0.782
LCA221	684	2305	35	63	0.372	176	2284	11	63	0.666	114	395	5	23	0.782
LCA222	932	2345	46	63	0.379	235	2326	14	62	0.666	104	435	5	23	0.782
LCA223	1300	2227	45	105	0.699	331	2210	18	105	0.666	137	323	16	30	0.782
LCA224	1600	2284	109	142	1.084	401	2271	27	141	0.666	118	380	17	46	0.782

Appendix D – OrcaFlex Software General Description

D.1 Introduction

The following section will give the general description of the OrcaFlex software that is used in this thesis. The content of this section will be mainly based on the OrcaFlex Manual version 9.4a.

D.2 General Description about OrcaFlex

OrcaFlex is a marine dynamics program developed by Orcina for static and dynamic analysis of a wide range of offshore system, including all types of marine risers. The main analyses covered in this software are the global analysis, moorings, installation, and towed system analysis.

The software has several objects (i.e. Lines, Vessels, and Buoys) that can be built up and interconnected via special objects (i.e. Link, Winch, and Shape) to create a mathematical model of the system. Figure below shows the sample of 3D view capability and also the computer model in OrcaFlex.

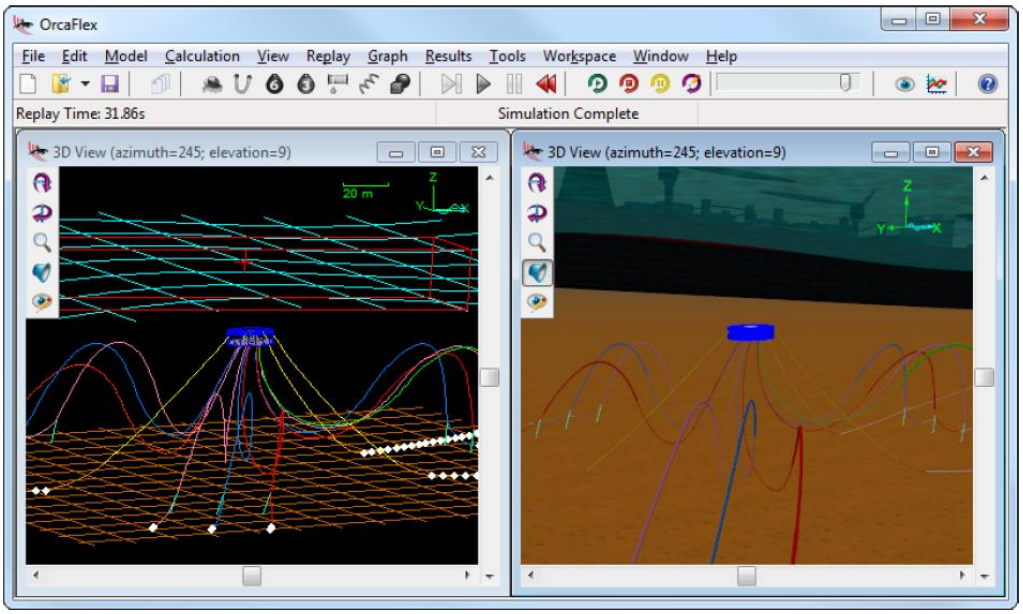

Figure D.1 – A 3D View OrcaFlex computer model (Orcina, 2010, page 52)

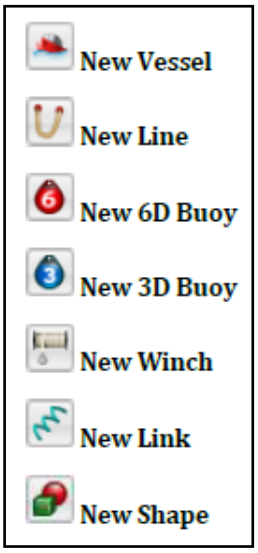

FigureD.2 – Object Menu (Orcina, 2010, page 46)

General sequence runs from static state, followed by dynamic simulation. The following diagram shows the sequence of states used and the actions.

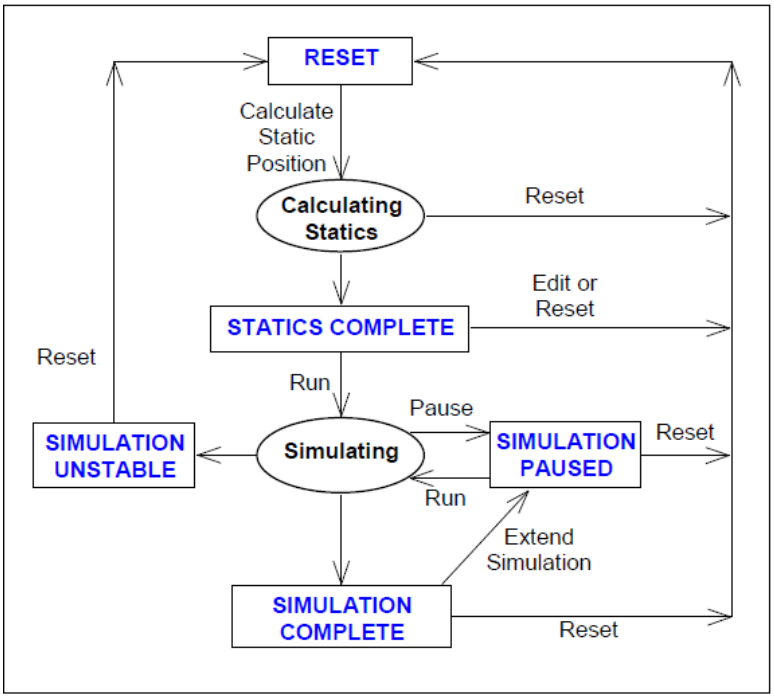

Figure D.3 – Sequential states of OrcaFlex (Orcina, 2010, page 26)

D.3 Coordinate System

There are two coordinate systems that used by OrcaFlex. They are global coordinate system (GX, GY, and GZ) and local coordinate system (x, y, and z). These coordinate systems are a right-handed system and normally its Z-axis is heading to the positive upwards.

The following figures show the description of the coordinate systems and the direction and heading conventions in OrcaFlex.

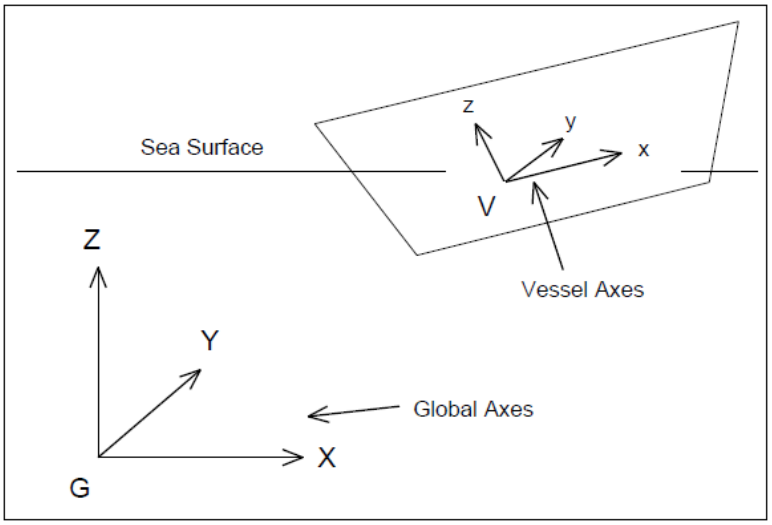

Figure D.4 – Coordinate system (Orcina, 2010, page 111)

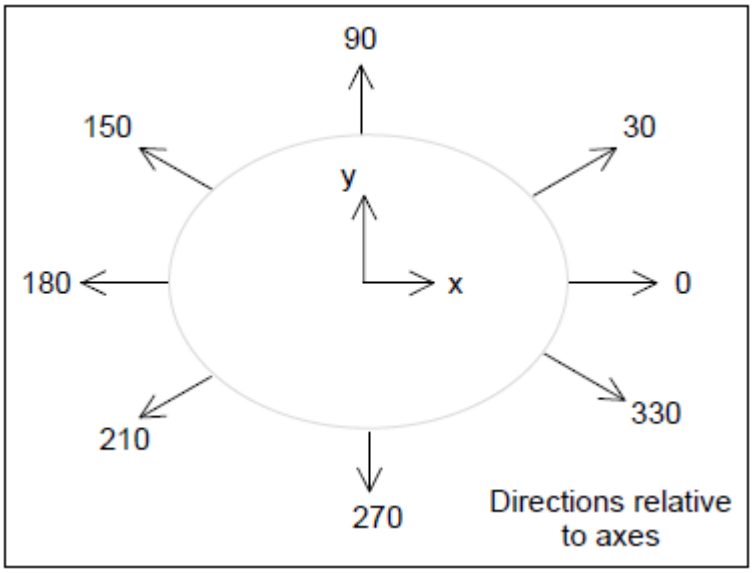

Figure D.5 – Directions and headings (Orcina, 2010, page 112)

D.3.1 Static and Dynamic Stage

D.3.2 Static Analysis

The static analysis provides the initial static equilibrium condition of the computer model, and it is used as a startup point for dynamic simulation. In summary, two objectives for a static analysis are:

1. To determine the equilibrium configuration of the system under weight, buoyancy, hydrodynamic drag, etc.
2. To provide a starting configuration for dynamic simulation

D.3.3 Dynamic Analysis

The dynamic analysis is a time simulation of the motions of the model over a specified period of time, starting from the position derived by the static analysis. The period of simulation is defined as a number of consecutive stages.

Before the main simulation stage, there is a build-up stage, during which the wave and vessel motions are smoothly ramped up from zero to their full size. This provides a gentle start and reduces the transients that are generated from static position to full dynamic motion. This build-up stage is numbered 0 and its length should normally be set to at least one wave period. Refer to below for details.

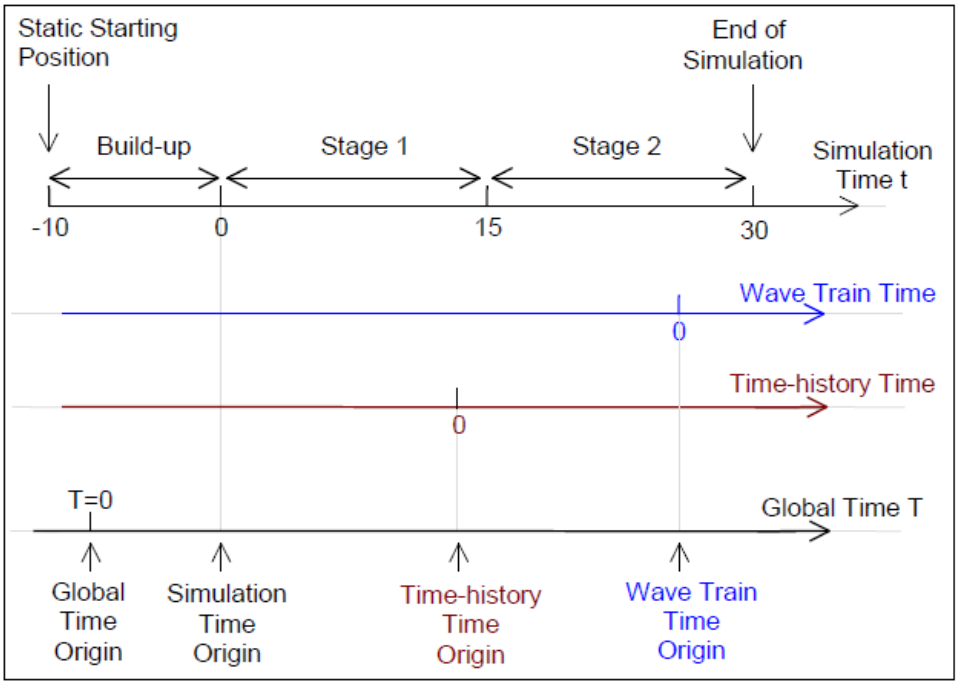

Figure D.6 – Time and simulation stages in dynamic analysis (Orcina, 2010, page 121)

D.4 Modeling

OrcaFlex uses a finite element model as the basic concept of modeling. For example, a single length of pipe can be discretized into several nodes and segments model. The following figure shows the general OrcaFlex line model.

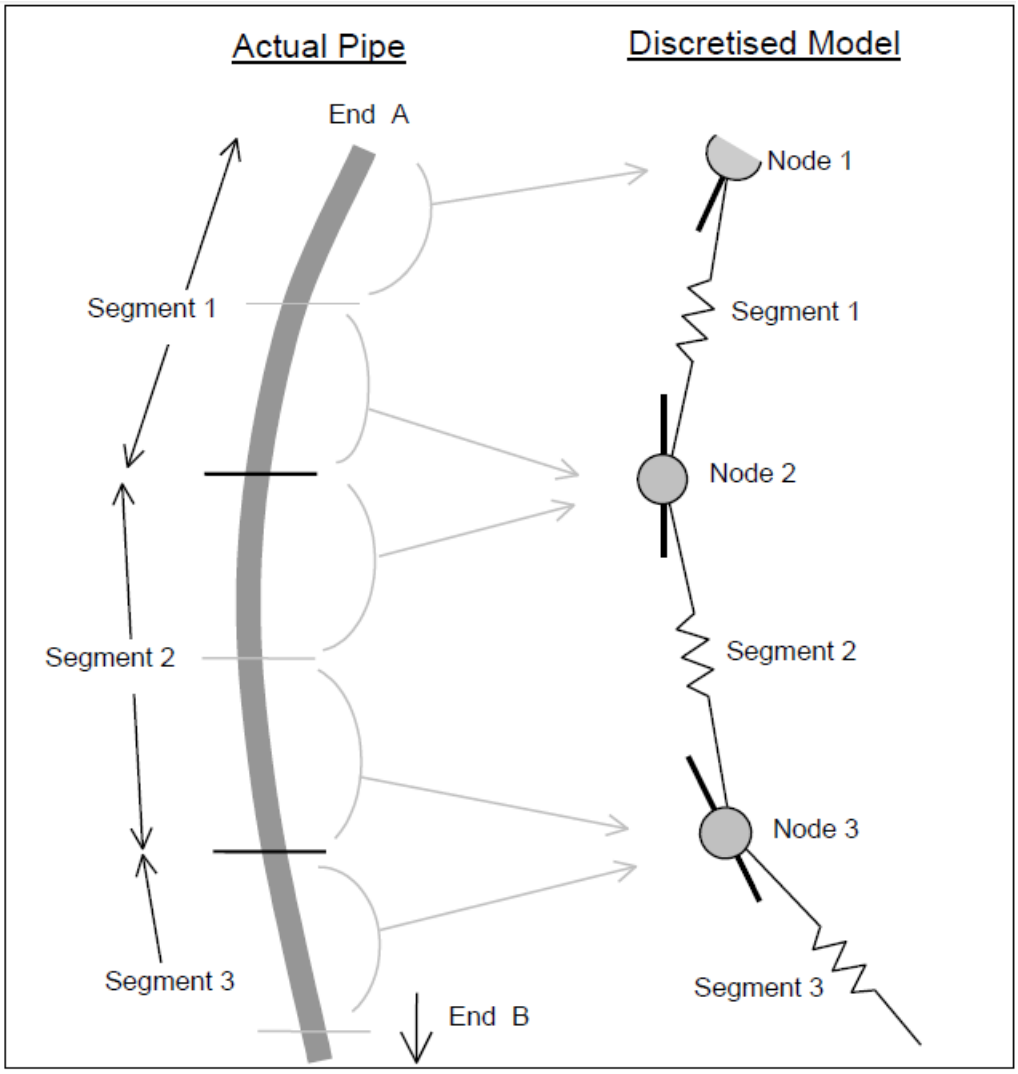

Figure D.7 – Line Model (Orcina, 2010, page 155)

Each node is effectively a short straight rod that represents the two segments either side of the node, except the end nodes, which have only half-segment next to them. Each line segment is divided into two halves and the properties (mass, weight, buoyancy, drag, etc.) of each half segment are lumped and assigned to the node at that end of the segment. Forces and moments are applied at the nodes.

Each segment is a straight massless element that models just the axial and torsional properties of the line. It can be thought as being made up by two co-axial telescoping rods that are connected by axial and torsional spring + dampers. The bending properties of the line are represented by rotational spring + dampers at each end of the segment.

The following figure shows structural detail of the line model.

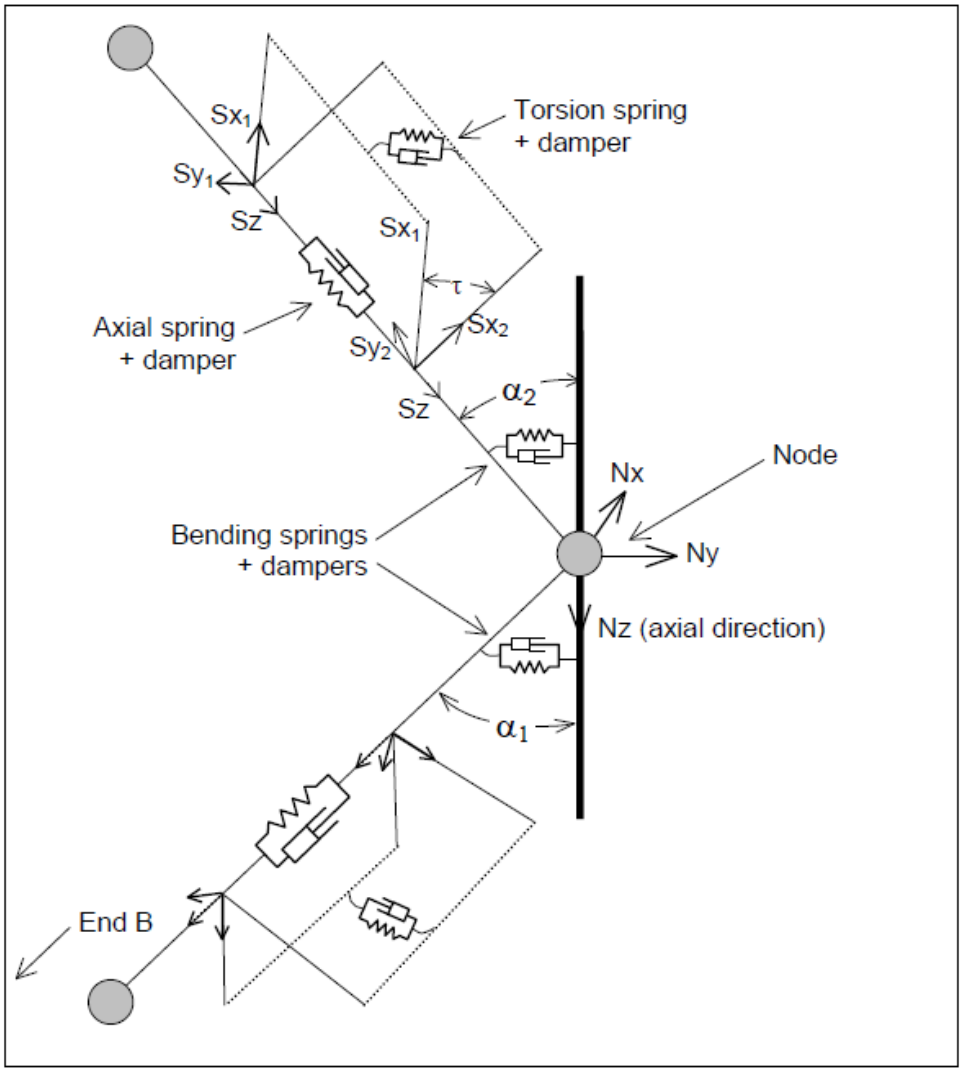

Figure D.8 – Detailed Representation of Line Model (Orcina, 2010, page 157)